

**Understanding the Functional
Involvement of ER α and Hypoxia in
the Pathophysiology of Breast
Cancers with Different Molecular
Subtypes**

Jodie Rebecca Malcolm

Ph.D.

University of York

Biology

September 2024

Abstract

Breast cancer is the leading cause of cancer-related mortality for women. Dysregulated RNA polymerase III (Pol III) transcription of tRNA is significantly implicated in cancer progression. Oestrogen receptor alpha ($ER\alpha$) potentiates ~75% of breast tumours, and resistance to endocrine therapies that target $ER\alpha$ activity is a major clinical problem urgently requiring significant advances in research to improve survival outcomes for women with endocrine-resistant disease. The $ER\alpha$ is a prolific transcription factor that upregulates many pro-tumorigenic genes, including tRNAs in response to hormone activation. This thesis sought to investigate the mechanism driving $ER\alpha$ -dependent tRNA expression. Analysis of public CHIP-seq data showed $ER\alpha$ was physically associated with ~50% of tRNA loci in breast cancer cells. $ER\alpha$ recruitment to tRNA genes was mediated by protein-protein interactions of $ER\alpha$ with Pol III-specific TFIIIC, determined by qPLEX-RIME and co-immunoprecipitation. FOXA1, a modulator of $ER\alpha$ activity, was enriched at tRNA promoters, suggesting FOXA1 may facilitate $ER\alpha$ recruitment to Pol III-transcribed genes and hormone-dependent activation of transcription. Further exploration of this $ER\alpha$ -FOXA1-Pol III axis could lead to novel and necessary developments in the treatment of advanced $ER\alpha$ -driven breast cancer

Altered Na^+ homeostasis is a critical determinant of breast cancer progression. Intratumoral hypoxia is linked to disruption of many cellular processes, including ion transport, which has significant implications in therapy resistance and advanced disease. This thesis aimed to delineate hypoxia-dependent changes in Na^+ transport. Optimisation of reference genes (RGs) for studying alterations in gene expression in hypoxic breast cancer cell lines by RT-qPCR identified *RPLP1* and *RPL27* as suitable RGs for such investigations. RNA-seq and RT-qPCR found hypoxia enhanced Na^+ transporter gene expression in $ER\alpha^+$ breast cancer cell lines, particularly by upregulating Na^+/K^+ -ATPase (NKA) and epithelial Na^+ channel (ENaC), highlighting a new mechanism by which hypoxia may contribute to breast cancer progression and therapy resistance. Conversely, voltage gated Na^+ channels (VGSCs) were not affected by low O_2 tension, but $ER\alpha$ was shown to mediate expression of some VGSC isoforms. Understanding changes in Na^+ handling in advanced breast cancer is imperative and may result in the development or repurposing of targeted therapies aimed at modulating Na^+ transport to improve breast cancer outcomes.

Table of Contents

Abbreviations.....	14
Acknowledgments.....	19
Declaration	21
1. Introduction.....	22
1.1 Overview of breast cancer.....	22
1.1.1 Studying molecular characteristics of different breast cancer subtypes..	22
1.2. Oestrogen receptor structure and activity.....	26
1.2.1. Regulators and co-factors of ER α activity	30
1.2.2 Therapeutic strategies and resistance in Luminal A and TNBC tumours	31
1.2 RNA Polymerase III and tRNA gene transcription.....	32
1.2.1 Class III transcription by Pol III.....	33
1.2.1.1 Post transcriptional processing of tRNA.....	36
1.2.2 Implications of dysregulated Pol III activity and aberrant tRNA in cancer	36
1.2.2.1 ER α regulation of tRNA expression in ER α + cancer.....	37
1.3 Hypoxia and hypoxia-inducible factors	39
1.3.1 Hypoxia in cancer	42
1.3.2 Implications of Hypoxia in ER α + breast cancers	43
1.3.3 Hypoxia, glycolysis and pathological transport of ions and solutes.....	45
1.4 Na ⁺ homeostasis and dysregulated Na ⁺ transport in cancer	46
1.4.1 Voltage gated Na ⁺ channels	46
1.4.1.1 Expression of VGSC subunits in cancer	50
1.4.1.2 Tumour progression and VGSC activity	55
1.4.2 NKA and ENaC	57
1.4.2.1 Evidence of NKA and ENaC in cancer	60
1.4.3. Tumour microenvironment and dysregulated Na ⁺ homeostasis.....	61
1.4.4 Hypoxia and Na ⁺ transport in solid tumours	62
1.4.5 The future of targeting dysregulated Na ⁺ transport in cancer.....	63
1.5 Project rationale, hypotheses and aims	65

2. Materials and Methods.....	66
2.1 Cell culture	66
2.1.1 Cell lines	66
2.1.2 Maintenance of cells	66
2.1.2.1 Cell counts and viability check	67
2.1.2.2 Hypoxic culture of breast cancer cell lines	67
2.1.2.3 Charcoal stripping Hormone-depletion of FBS	67
2.1.3 Freezing and thawing of breast cancer cells.....	68
2.1.4 <i>Mycoplasma</i> testing of cells	68
2.1.5 Pharmacology	69
2.2 Chromatin immunoprecipitation	71
2.3 Immunocytochemistry and confocal microscopy.....	76
2.4 Wound healing assay	76
2.4 RNA Extraction, cDNA synthesis and quantitative PCR	78
2.4.1 RNA extraction	78
2.4.2 Luminal A cell line sample preparation for RNA-sequencing.....	78
2.4.2 cDNA synthesis	79
2.4.3 qPCR for ChIP experiments	79
2.4.4 qPCR	79
2.4.5 qPCR analysis	80
2.5 Protein extraction and western blotting	81
2.5.1 Protein extraction	81
2.5.2 Co-immunoprecipitation	81
2.5.3 Western blot.....	81
2.5.2.1 Densitometry Analysis of HIF α and α -Tubulin bands	83
2.6 Bioinformatic approaches to investigate ER α association with tRNA genes in breast cancer cell lines and patient specimens.....	85
2.6.1 Acquiring MCF-7, MDA-MB-231 and clinical breast cancer ER α and FOXA1 ChIP-seq datasets	85

2.6.2 EaSeq for the quantification of transcription factor enrichment.....	87
2.6.3 Characterisation of ER α -bound tRNA genes based on their role in cellular processes	87
2.6.4 tRNA gene coordinate remapping	87
2.7 Motif analysis	88
2.8 Analysing public qPLEX-RIME data.....	88
2.9 Reference gene candidate selection and validation.....	88
2.9.1 Analysis of public RNA-seq data to identify reference genes.....	88
2.9.2 Stability score determination	90
2.9.3 RefFinder for RG selection.....	90
2.10 RNA-seq analysis of ER α + breast cancer cell lines	90
2.10.1 Preparation of RNA-seq datasets.....	91
2.10.2 Differential expression and gene set enrichment analysis	91
2.11 Statistical analysis	92
3. Investigating ER α localisation at tRNA genes in ER α + Breast Cancer Cell Lines and Patient Breast Tumours	93
3.1 Introduction	93
3.1.1 Aims and hypotheses.....	94
3.2 Results	95
3.2.1 Cellular localisation of ER α in MCF-7 breast cancer cells is responsive to hormone stimulation	95
3.2.2 The localisation of ER α at tRNA genes in ER α + cell lines is widespread	100
3.2.3 ER α -targeted tRNA genes are not preferentially implicated in proliferation or differentiation.....	105
3.2.4 The ER α does not utilise consensus ERE and half ERE motifs for recruitment to target tRNA genes.....	108
3.2.5 Exogenous ER α is not associated with tRNA genes in MDA-MB-231 cells	110

3.2.6 The ER α is localised at tDNA in primary and metastatic breast tumours	113
3.2.7. FOXA1 and ER α enhance Pol III loading at tRNA genes.....	122
3.2.8 The ER α associates with other Pol III transcribed genes.....	126
3.2.9 The ER α interacts with Pol III subunits in MCF-7 cells and human breast tumours.....	132
3.3 Discussion.....	135
3.3.1 Summary of main findings.....	135
3.3.2 Localisation of the ER α with tRNA and ncRNA genes <i>in vitro</i> and <i>in vivo</i>	136
3.3.3 Exploring ER α recruitment to target tRNA genes	137
3.3.4 Differential codon usage for tRNA isotypes and the implications in cellular processes and disease	143
3.3.5 Future work.....	143
3.4 Conclusion.....	146
4. Identification of Robust RT-qPCR Reference Genes for Studying Changes in Gene Expression in Response to Hypoxia in Breast Cancer Cell Lines	147
4.1 Introduction.....	147
4.1.1 Aims and objectives	148
4.2 Results	149
4.2.1 The HIF Switch in Hypoxic Breast Cancer Cell Lines Occurs between 8 and 48 Hours of O ₂ Deprivation.....	149
4.2.2 Analysis of public RNA-seq dataset identifies 10 RG candidates.....	152
4.2.3 Assessment of RG candidate mRNA expression confirms eight highly expressed genes.....	159
4.2.4 Evaluating RG expression in normoxic vs. hypoxic breast cancer cell lines filters out poor RG candidates and identifies robust RGs with the least variability in expression.....	162
4.2.5 <i>RPLP1</i> and <i>RPL27</i> are suitable RGs for normalising gene expression in normoxic vs. hypoxic ER α + and TNBC cell lines.....	169

4.2.6 Evaluation of RG shortlist in additional 28 breast epithelial or cancer cell lines	171
4.3 Discussion.....	173
4.3.1 Summary of main findings.....	173
4.3.2 The “HIF switch” in Luminal A and TNBC cell lines.....	173
4.3.3 Ribosomal constituents as stably expressed RGs for hypoxic breast cancer studies	174
4.3.4 Limitations and considerations of this study	175
4.4 Conclusion	177
4.5 Data Availability	177
5. Effect of Hypoxia and the ER α on Na ⁺ Transport in Breast Cancer Cells	178
5.1 Introduction	178
5.1.1 Aims and hypotheses.....	180
5.2 Results	182
5.2.1 mRNA expression of VGSCs is not regulated by hypoxia in TNBC or Luminal A breast cancer cell lines	182
5.2.2 RNA-seq datasets are of good quality and suitable to use for the exploration of ER α and hypoxia-mediated regulation of Na ⁺ transport in Luminal A cell lines	185
5.2.3 Breast cancer cell lines had expected transcriptional responses to hypoxic culture and ER α knockdown.....	188
5.2.4 Genome-wide expression alterations because of cell line perturbations include Na ⁺ transporter genes.....	191
5.2.5 ER α knockdown or hypoxia switches off biosynthetic and cell division processes in MCF-7 and T-47D breast cancer cell lines	199
5.2.6 Positive enrichment of Na ⁺ transport occurs in Luminal A cell lines cultured in hypoxia.....	216
5.2.7 METABRIC analysis reveals significant implications of hypoxia-regulated Na ⁺ transporter gene amplification in relapse-free and overall survival	222
5.2.8 Hypoxia does not significantly affect <i>ATP1A1</i> expression when measured by RT-qPCR	227

5.2.9 Ouabain inhibition of NKA does not affect normoxic or hypoxic breast cancer cell migration	229
5.2.10 Ion transporter genes are significantly affected by O ₂ and ER α perturbations in Luminal A cell lines	231
5.3 Discussion	238
5.3.1 Summary of main findings	238
5.3.2 Differential regulation of VGSC subunits in two models of Luminal A breast cancer	239
5.3.3 Hypoxia regulates Na ⁺ network <i>in vitro</i>	242
5.3.4 Limitations and Future work	246
5.4 Conclusion.....	248
6. General discussion.....	249
6.1 ER α regulation of tRNA expression in breast cancer	249
6.2 Role of hypoxia in progressing breast cancer development by modulating Na ⁺ transport	253
6.2.1 Potential role of ER α in mediating VGSC expression in breast cancer	254
6.3 Future directions.....	257
6.4 Conclusion.....	259
Appendix.....	261
References	278

List of Figures

Figure 1.1 Structure of Canonical Oestrogen Receptors.....	29
Figure 1.2 RNA Polymerase III Promoter Architecture and Initiation Assembly Factors	35
Figure 1.3 Domain Organisation of HIF Proteins	41
Figure 1.4 Schematic of VGSC Structure	49
Figure 1.5 Voltage Gated Sodium Channels in Solid Tumours.....	54
Figure 1.6 Schematic of NKA and ENaC Structures	59
Figure 2.1 Example Figure to Demonstrate how Measurements were Taken in Each Well to Calculate MI	77
Figure 3.1 The ER α is Localised in Cytosol and Nuclei of MCF-7 Cells.....	96
Figure 3.2 MCF-7 Breast Cancer Cells Proliferate in Response to Oestradiol ...	99
Figure 3.3 ER α is Enriched at tRNA Genes in ER α + Cell Lines.....	101
Figure 3.4 Identification of ER α at Individual tRNA Loci.....	104
Figure 3.5 Functional Stratification of tRNA Genes Targeted by ER α	107
Figure 3.6 ER α Localisation at tRNA Genes Does Not Require Consensus ERE Motifs	109
Figure 3.7 Exogenous ER α Does Not Associate at tRNA Genes in TNBC Cells	112
Figure 3.8 ER α is Enriched at tRNA Genes in Primary Breast Tumours	116
Figure 3.9 Breast Cancer Metastasis are Positive for ER α Enrichment at tRNA Genes	119
Figure 3.10 Quantification of ER α Enrichment in the MCF-7 Cell Line, Primary Breast Tumours and Metastatic Patient Samples	121
Figure 3.11 FOXA1 is Recruited to tRNA Genes by the ER α and is Required for RNA Polymerase III Loading at tDNA Promoters	125
Figure 3.12 ER α is not Found at an ERE in Proximity of the <i>BC200</i> Promoter	127
Figure 3.13 ER α is Localised at <i>RN7SL1</i> in MCF-7 Cells and Patient Metastasis	129

Figure 3.14 ER α is Localised at <i>RMRP</i> in MCF-7 Cells and Patient Metastasis	131
Figure 3.15 Pol III Subunits Physically Interact with ER α in MCF-7 Cells and ER α + Breast Tumours.....	134
Figure 3.16 Proposed mechanism of ER α recruitment to Type III promoters ...	142
Figure 4.1 Identifying the HIF Switch in Breast Cancer Cell Lines.....	151
Figure 4.2 Checking Responsiveness of Breast Cancer Cell Lines to Hypoxia in a Publicly Available RNA-seq Dataset	154
Figure 4.3 Members of the HIF Complex are Variable in their Expression in Normoxia and Hypoxia	156
Figure 4.4 Expression of RG Candidates in MCF-7, T-47D, MDA-MB-231 and MDA-MB-468 Breast Cancer Cell Lines Cultured in 20% O ₂	161
Figure 4.5 RG Stability in Breast Cancer Cell Lines Cultured in Normoxia or Hypoxia.	163
Figure 4.6 Geomean of Ranking Values for RG Candidates.	168
Figure 4.7 RG Expression Level Stability and Hypoxic Induction of <i>CA9</i>	170
Figure 5.1 Effect of Acute or Chronic Hypoxia on VGSC Subunit mRNA Expression in TNBC and Luminal A Cell Lines.....	184
Figure 5.2 Data Quality of RNA-seq from MCF-7 Breast Cancer Cells.....	187
Figure 5.3 Demonstrating Cell Line Response to Hypoxia	189
Figure 5.4 Luminal A Cell Line Response to ER α Knockdown	190
Figure 5.5 Transcriptome-Wide Expression Changes in Hypoxic Luminal A Cells	194
Figure 5.6 Fulvestrant-Induced Transcriptome-Wide Expression Changes MCF-7 and T-47D Cells.....	198
Figure 5.7 Most Enriched GO Terms in MCF-7 Cells Following ER α Knockdown	201
Figure 5.8 Most Enriched GO Terms in T-47D Cells Following ER α Knockdown	205
Figure 5.9 Most Enriched GO Terms in Hypoxic vs. Normoxic MCF-7 Cells.....	209
Figure 5.10 Most Enriched GO Terms in Hypoxic vs. Normoxic T-47D Cells....	213

Figure 5.11 GSEA Plot Showing Positive Enrichment of Na ⁺ Transporter Genes in Hypoxic vs. Normoxic MCF-7 Cells	217
Figure 5.12 GSEA Plot Showing Positive Enrichment of Na ⁺ Transporter Genes in Hypoxic vs. Normoxic T-47D Cells	219
Figure 5.13 Leading Edge and Differentially Expressed Na ⁺ Channel Genes in MCF-7 and T-47D Cells Cultured in Hypoxia vs. Normoxia	221
Figure 5.14 Overall and Relapse Free Survival Associated with Amplified <i>ATP1A1</i> in Breast Cancer Patients (a METABRIC Analysis)	224
Figure 5.15 RT-qPCR of <i>ATP1A1</i> in MCF-7 and T-47D Breast Cancer Cells Following Acute or Chronic Hypoxic Culture.....	228
Figure 5.16 Investigating NKA Inhibition on the Migratory Capacity of Normoxic or Hypoxic Breast Cancer Cells.....	230
Figure 5.17 RT-qPCR of Ion Transporters Differentially Expressed in All RNA-Seq Comparisons in MCF-7 Cells.....	235
Figure 5.18 RT-qPCR of Ion Transporters Differentially Expressed in All RNA-Seq Comparisons in T-47D Cells.....	237
Figure 6.1 Hypothetical Mechanism of ER α Activity in Luminal A Breast Cancer Cells Discussed in this Thesis	252
Figure 6.2 Proposed Model of Hypoxia-Driven Na ⁺ Transport.....	256
Appendix Figure I Effect of Acute or Chronic Hypoxia on VGSC Subunit mRNA Expression in T-47D Cells	261
Appendix Figure II Data Quality of RNA-seq from T-47D Breast Cancer Cells	262
Appendix Figure III Volcano Transcriptome-Wide Gene Expression Changes in MCF-7 Cells Following Different Oxygen and ER α Perturbations	263
Appendix Figure IV Volcano Transcriptome-Wide Gene Expression Changes in T-47D Cells Following Different Oxygen and ER α Perturbations	264
Appendix Figure V Heatmaps of Ion Channel Genes with Greatest Significant Log ₂ Fold Change in Expression Following 48 Hours of Hypoxic Culture	266
Appendix Figure VI Heatmaps of Ion Channel Genes with Greatest Significant Log ₂ Fold Change in Expression Following ER α Knockdown	268
Appendix Figure VII GSEA Plot Showing Positive Enrichment of Na ⁺ Transporter Genes in ER α - Hypoxic vs. Normoxic T-47D Cells	269

List of Tables

Table 1.1 Breast Cancer Cell Lines Commonly Used in Research	25
Table 1.2 Tissue Specificity of VGSCs and TTX Sensitivity	48
Table 2.1 Pharmacological agents and their properties	70
Table 2.2 Antibody Information and Experimental Application	73
Table 2.3 Sequence Information of Primers Used in ChIP-qPCR and RT-qPCR Studies	74
Table 2.4 Western blot polyacrylamide gel recipes	84
Table 2.5 Details of Public ChIP-Seq Datasets.....	86
Table 2.6 SRA Accession Numbers of Hypoxic and Normoxic Breast Cancer Cell Lines	89
Table 4.1 Similarity (s) Score between Hypoxic and Normoxic RNA-Sequencing Reads of RG Candidates.....	158
Table 4.2 Primer Efficiencies of RG Candidates	164
Table 4.3 Summaries of Ranked RG Stability According to RefFinder and Prerequisite Programs.....	167
Table 4.4 s scores of top five RG candidates in 28 breast cancer or normal mammary epithelial cell lines.....	172
Table 5.1 Details of Experimental Conditions	186
Table 5.2 Most Enriched BP Terms in MCF-7 Cells Treated with Fulvestrant or Vehicle.....	202
Table 5.3 Most Enriched MF Terms in MCF-7 Cells Treated with Fulvestrant Compared to Vehicle	203
Table 5.4 Most Enriched BP Terms in T-47D Cells Treated with Fulvestrant Compared to Vehicle	206
Table 5.5 Most Enriched MF Terms in T-47D Cells Treated with Fulvestrant Compared to Vehicle	207
Table 5.6 Most Enriched BP Terms in MCF-7 Cells Cultured in Hypoxia vs. Normoxia.....	210
Table 5.7 Most Enriched MF Terms in MCF-7 Cells Cultured in Hypoxia vs. Normoxia.....	211

Table 5.8 Most Enriched BP Terms in T-47D Cells Cultured in Hypoxia vs. Normoxia.....	214
Table 5.9 Most Enriched MF Terms in T-47D Cells Cultured in Hypoxia vs. Normoxia.....	215
Table 5.10 Overall and Relapse-Free Survival in the METABRIC Cohort with Alterations in Na ⁺ Transporter Gene Expression	225
Table 5.11 Median Overall and Relapse-Free Survival in the METABRIC Cohort	226
Table 5.12 Log ₂ FC in Shared Differentially Expressed Ion Transporter Genes.	233
Appendix Table I Most Upregulated Genes According to Log ₂ FC in Normoxic vs. Hypoxic MCF-7 Cells.....	270
Appendix Table II Most Downregulated Genes According to Log ₂ FC in Normoxic vs. Hypoxic MCF-7 Cells	271
Appendix Table III Most Upregulated Genes According to Log ₂ FC in Normoxic vs. Hypoxic T-47D Cells	272
Appendix Table IV Most Downregulated Genes According to Log ₂ FC in Normoxic vs. Hypoxic T-47D Cells	273
Appendix Table V Most Upregulated Genes According to Log ₂ FC in Vehicle vs. Fulvestrant Treated MCF-7 Cells.....	274
Appendix Table VI Most Downregulated Genes According to Log ₂ FC in Vehicle vs. Fulvestrant Treated MCF-7 Cells	275
Appendix Table VII Most Upregulated Genes According to Log ₂ FC in Vehicle vs. Fulvestrant Treated T-47D Cells	276
Appendix Table VIII Most Downregulated Genes According to Log ₂ FC in Vehicle vs. Fulvestrant Treated T-47D Cells	277

Abbreviations

5-aza-dC	5-Aza-2'-Deoxycytidine
AC	Adenocarcinoma
AF	Activating Function
AI	Aromatase Inhibitor
ANOVA	Analysis Of Variance
Ap1	Activator Protein-1
AR	Androgen Receptor
ASIC	Acid Sensing Ion Channel
A.U.	Arbitrary Units
BC	Breast Cancer
Bdp1	B Double Prime 1
bHLH	Basic-Helix-Loop-Helix
BRCA1	Breast Cancer Type 1 Susceptibility Protein
Brf	TFIIIB-Related Factor
Ca₂⁺	Calcium
CA9	Carbonic Anhydrase Ix
CAF	Cancer-Associated Fibroblast
CAM	Cell Adhesion Molecule
ChIP-seq	Chromatin Immunoprecipitation with Sequencing
Cl₂⁻	Chloride
CNS	Central Nervous System
CoCl₂	Cobalt Chloride
CRCa	Colorectal Carcinoma
C-TAD	Carboxy-Terminus Activation Domain
DBD	DNA Binding Domain
DGEA	Differential Gene Expression Analysis
DMOG	Dimethyloxalylglycine
DNMT	DNA Methyltransferase
DRG	Dorsal Root Ganglion
DSE	Distal Sequence Element
ECM	Extracellular Matrix
EF2K	Elongation Factor-2 Kinase
EGF	Epidermal Growth Factor
EMT	Epithelial-To-Mesenchymal Transition
ENaC	Epithelial Sodium Channel
ENCODE	Encyclopaedia Of DNA Elements
EPO	Erythropoietin
ER	Oestrogen Receptor
ERE	Oestrogen Response Element

ERα	Oestrogen Receptor Alpha
ERα+	Oestrogen Receptor Positive
ERα-	Oestrogen Receptor Negative
ERβ	Oestrogen Receptor Beta
ES	Enrichment Score
ETC	Electron Transport Chain
FDR	False Discovery Rate
FFPE	Formalin-Fixed Paraffin-Embedded
FIH	Factor Inhibiting HIF
FOXA1	Forkhead Box A1
GdO	Good Outcome
GLUT	Glucose Transporter
GO	Gene Ontology
GPER	G-Protein Coupled Oestrogen Receptor
GRO-seq	Global Run-On Sequencing
GSEA	Gene Set Enrichment Analysis
H⁺	Hydrogen
H₂O₂	Hydrogen Peroxide
HAT	Histone Acetyltransferase
HDAC	Histone Deacetylase
HER2	Human Epidermal Growth Factor Receptor 2
hESC	Human Embryonic Stem Cell
Hg	Mercury
HGNC	Human genome organisation gene nomenclature committee
HIF	Hypoxia-Inducible Factor
HNSCC	Head And Neck Squamous Cell Carcinoma
HRE	Hypoxia-Response Element
HSP90	Heat Shock Protein 90
Hypoxia	Less Than Physiological Levels of Oxygen
ICC	Immunocytochemistry
ICR	Internal Control Region
IDC	Invasive Ductal Carcinoma
Ig	Immunoglobulin
IHC	Immunohistochemistry
I_{Na}	Sodium Current
K⁺	Potassium
LBD	Ligand Binding Domain
lncRNA	Long Non-Coding Ribonucleic Acid
LPS	Lipopolysaccharide
LZ	Leucine Zipper
MACC1	Metastasis-Associated in Colon Cancer

MAPK	Mitogen-Activated Protein Kinases
mcm⁵s⁵U	5-Methoxycarbonyl-Methyl-2-Thiouridine
MCP	Monocyte Chemoattractant Protein
MCT	Monocarboxylate Transporter
MI	Migratory Index
miRNA	Micro Ribonucleic Acid
MMP	Matrix Metalloproteinases
Na⁺	Sodium
[Na⁺]_e	Extracellular Sodium Concentration
[Na⁺]_i	Intracellular Sodium Concentration
Na_v	Voltage Gate Sodium Channel, Alpha Isoform
NCOA	Nuclear Coactivator
NCOR	Nuclear Corepressor
NCX	Sodium Calcium Exchanger
NDBTs	Sodium Driven Bicarbonate Transporters
NHE	Sodium Hydrogen Exchanger
NKA	Sodium Potassium ATPase
nNa_v	Neonatal Voltage Gate Sodium Channel, Alpha Isoform
Normoxia	Atmospheric Levels of Oxygen
NSCLC	Non-Small Cell Lung Cancer
N-TAD	Amino-Terminus Activation Domain
NTD	Amino-Terminus Domain
NTME	Non-Tumorigenic Mammary Epithelium
O₂	Oxygen
ODDD	Oxygen Dependent Degradation Domain
OXPHOS	Oxidative Phosphorylation
PAS	Per Arnt Sim
PBS	Phosphate-Buffered Saline
PCA	Principal Component Analysis
PDK1	Pyruvate Dehydrogenase Kinase
PGK1	Phosphoglycerate Kinase
PHD	Prolyl Hydroxylase Domain
pHe	Extracellular Ph
pHi	Intracellular Ph
Physoxia	Physiological Levels of Oxygen
PIC	Pre-Initiation Complex
PNS	Peripheral Nervous System
PO	Poor Outcome
PO₂	Partial Pressure of Oxygen
Pol	Ribonucleic Acid Polymerase
Pol I	Ribonucleic Acid Polymerase I

PoI II	Ribonucleic Acid Polymerase II
PoI III	Ribonucleic Acid Polymerase III
PR	Progesterone Receptor
PSE	Proximal Sequence Element
PTC	Papillary Thyroid Cancer
PTEN	Phosphatase And Tensin Homolog
pVHL	Von Hippel-Lindau
Q-value / Q	Quantification Value
Rb	Retinoblastoma
RCC	Renal Cell Carcinoma
REST	Repressor Element Silencing Transcription
RG	Reference Gene
RNA	Ribonucleic Acid
ROS	Reactive Oxygen Species
rRNA	Ribosomal Ribonucleic Acid
RT-qPCR	Reverse Transcriptase – Quantitative Polymerase Chain Reaction
SCLC	Small Cell Lung Cancer
SERD	Selective Oestrogen Receptor Downregulator
SERM	Selective Oestrogen Receptor Modulator
SGLT	Na ⁺ /Glucose Cotransporter
SIK	Salt Inducible Kinase
SMRT	Silencing Mediator of Retinoic Acid and Thyroid Hormone Receptor
snoRNA	Small Nucleolar Ribonucleic Acid
snRNA	Small Non-Coding Ribonucleic Acid
Sp1	Specificity Protein-1
SRA	Sequence Read Archive
SRC	Steroid Receptor Coactivator
SRP	Signal Recognition Particle
TAM	Tumour-Associated Macrophage
TBP	Tata-Box Binding Protein
TCA	Tricarboxylic Acid
TDA	Topological Data Analysis
TGF	Transforming Growth Factor
TNBC	Triple Negative Breast Cancer
TNF	Tumour Necrosis Factor
TNM	Tumour-Node-Metastasis
TPM	Transcripts Per Million
tRNA	Transfer Ribonucleic Acid
TSS	Transcription Start Site
TTX	Tetrodotoxin
VEGF	Vascular Endothelial Growth Factor

VGSC

Voltage-Gated Sodium Channel

V_m

Membrane Potential

Acknowledgments

First, I would like to thank my fantastic supervisors who have provided exceptional support over the last few years. Thank you, Will Brackenbury, for welcoming me into your lab and ensuring that I could complete my PhD in a collaborative and supportive environment. Your guidance has allowed me to develop into a confident researcher, while being a part of a wonderful group. Thank you, Andy Holding, for being equally excellent and encouraging over the last two years and being a valuable source of knowledge in steroid receptor biology! I have particularly enjoyed our monthly catchups, which were always light-hearted, good fun and insightful. You have both been truly exceptional and I am very thankful to have been able to work under your supervision. A special thank you to Betsy Pownall, for providing invaluable support throughout my PhD, particularly during the tougher times. I'm incredibly grateful for your unwavering support.

I would also like to thank some of the wonderful friends I have made throughout my PhD journey. Thank you to Caroline Swan, for all your love and encouragement from day one. From our walks to the donks, trips to Beetle Bank Farm, and meanders around campus to feed the ducks, to always being there to listen during the lows and celebrate during the highs, your presence has been invaluable. Thank you to Lottie Plunkett-Jones, for the much-needed morning coffee chats to start the day off right, trips to the pub, and sharing the embarrassment of placing last in every pub quiz. Your good humour and kindness have been a great comfort, and I am excited to see you flourish during your own PhD journey in York! Thank you, Clare Steele-King, for opening the doors with enthusiasm and excitement into the world of EM and sustainable research, and for never failing to make me laugh. I would also like to thank the Brackenbury lab for welcoming me into their space without hesitation, for being incredibly kind and supportive, and for always being keen to celebrate every success, no matter how big or small, with a drink at the Deramore! Thank you to the Holding lab for also sharing your space, reagents, knowledge, and for always being so kind and encouraging. Thank you, Richard Ingram, for all your help and sharing your expertise.

Of course, this research would not have been possible without the exceptional support from across the department. From the BTF, a special thank you to Peter O'Toole for allowing me into your I&C lab to play with the ultramicrotomes and EMs, but for also running such a fantastic facility that has been of immense

importance and value to me and my research throughout my PhD. I'd also like to thank Sally James, Lesley Gilbert and Samantha Donninger from genomics who have provided a significant amount of expertise and guidance throughout my time at York. Thank you to all the fantastic staff in stores and in infrastructure who provide endless laughs and good chats, while ensuring research runs smoothly in the department!

I would like to thank my incredible family for their unshakable encouragement and support over the last four years and beyond. Thank you, mum, for always believing in me, and teaching me that nothing is out of reach if you work hard for it. Thank you, dad, for being an incredible role model, teaching me to live life to the fullest and have as much fun as possible along the way. I am looking forward to attending many more concerts with you in the future! Thank you, Kellie, for being the best stepmum I could have hoped for. I am grateful for the countless ways you have all shown your love, and I appreciate all you have done for me and sacrifices you have made to ensure I achieve my goals. Thank you, Gran, for your love and cherished weekends spent in your company and beautiful garden. A special thank you to my wonderful husband Mike. I am forever grateful to have you by my side and I'm glad you were with me at every step of this crazy journey. I would not be where I am today without your love and support, and I am excited for our next chapter together. I would also like to thank my lovely mother-in-law, Nettie, for your unconditional love, support and encouragement which have meant the world to me and have been an immense source of comfort and motivation. To my sisters Amelie and Freya, and my cheeky little brother William, thank you for being the absolute best siblings. I promise to spend more time with you once my Ph.D. is finished, and I am excited about all the fun adventures we will have together.

I would like to acknowledge the incredible women in my life who have faced breast cancer with unwavering strength and grace. My wonderfully bonkers nan, my dear friend Kath, and my spirited stepmum Kellie, who was diagnosed with breast cancer during the final year of my Ph.D. Despite the challenges, Kellie has continued to laugh through life, serving as an incredible role model and beacon of sunshine for me, dad and William.

Lastly, I acknowledge my little cousin Owen, who sadly passed away from cancer far too young. Owen is the reason I have chosen to peruse a career in cancer research, and this thesis is dedicated to his memory.

Declaration

I declare that this thesis is a presentation of original work, and I am the sole author. This work has not previously been submitted for an award at this, or any other University. All sources are acknowledged as references.

Five publications have arisen from this thesis:

Malcolm, Jodie R., Bridge KS, Holding AN, Brackenbury WJ. "Identification of robust RT-qPCR reference genes for studying changes in gene expression in response to hypoxia in breast cancer cell lines." *BMC Genomics* 26:59 (Malcolm et al., 2025)

Capatina, Alina L., Jodie R. Malcolm, Jack Stenning, Rachael L. Moore, Katherine S. Bridge, William J. Brackenbury, Andrew N. Holding. 2024 "Hypoxia-induced epigenetic regulation of breast cancer progression and the tumour microenvironment." *Frontiers Cell and Developmental Biology* 12 (August): 1421629 (Capatina et al., 2024)

Malcolm, Jodie R., Nattanan Sajjaboontawee, Serife Yerlikaya, Charlotte Plunkett Jones, Peter J. Boxall, and William J. Brackenbury. 2023. "Voltage-gated sodium channels, sodium transport and progression of solid tumours". *Current Topics in Membranes* 92 (October): 71-98 (Malcolm et al., 2023)

Malcolm, Jodie R., Natasha K. Leese, Philippa I. Lamond-Warner, William J. Brackenbury, and Robert J. White. 2022. "Widespread Association of ER α with RMRP and tRNA Genes in MCF-7 Cells and Breast Cancers." *Gene* 821 (February): 146280. (Malcolm et al., 2022)

Malcolm, Jodie R., and Robert J. White. 2022. "Alternative Isoforms of RNA Polymerase III Impact the Non-Coding RNA Transcriptome, Viability, Proliferation and Differentiation of Prostate Cancer Cells." *Journal of Translational Genetics and Genomics* 6 (1): 126–33. (Malcolm and White, 2022)

1. Introduction

1.1 Overview of breast cancer

Breast cancer is the second most common malignancy diagnosed worldwide after lung cancer, accounting for 11.6% of cancers diagnosed in 2022 (Bray et al., 2024). Due to improved health education, implementation of screening programmes for early detection and advancements in therapeutic strategies, overall survival for women diagnosed with breast cancer has greatly improved over the last few decades (Nardin et al., 2020). However, despite a favourable five-year relative survival of 91% when all breast cancer diagnoses are considered, approximately 30% of cases will ultimately result in death as a consequence of therapy resistance, metastasis, or delayed presentation of treatment toxicities (Darby et al., 2013; Anurag et al., 2018; Gote et al., 2021). 90% of metastatic cancers are incurable, and approximately 75% of primary breast tumours have already established micrometastases at the time of diagnosis (Nicolini et al., 2022; Pedersen et al., 2022). As such, metastatic breast cancer is the leading cause of cancer-related death in women and identifying novel molecular targets for therapeutic intervention is imperative (Bray et al., 2024). Many factors dictate breast cancer survival, including subtype and grade, age, race, obesity, family history and geographical location (Yedjou et al., 2019; Goodarzi et al., 2020; Johansson et al., 2021; Dehesh et al., 2023).

1.1.1 Studying molecular characteristics of different breast cancer subtypes

Breast cancers are highly heterogeneous with distinct subtypes that are characterised by immunohistochemistry (IHC) for oestrogen receptor alpha ($ER\alpha$), progesterone receptor (PgR), human epidermal growth factor receptor 2 (HER2), and Ki67 expressing cells (%) (Abubakar et al., 2019). In addition, intrinsic molecular subtypes are further defined by comparison of mRNA expression of 50 genes (PAM50) including *CDC6*, *EGFR*, *FOXA1*, *MELK*, *MYC* and *PGR*, which improves prognostication when compared to clinical factors (histological grade, tumour size, lymph node positivity, metastasis) and IHC (Parker et al., 2009; Nielsen et al., 2010). There are four universally recognised breast cancer subtypes: Luminal A ($ER\alpha+$, PgR+, HER2-, Ki67 26.9 %), Luminal B ($ER\alpha+$, PgR+/-, HER2+/-, Ki67 41.5 %), HER2-enriched ($ER\alpha-$, PgR-, HER2+, Ki67 61.1 %) and TNBC ($ER\alpha-$,

PgR⁻, HER2⁻, Ki67 68.6 %) (Husni Cangara et al., 2021). TNBC has been further deconstructed into basal-like or normal-like, and more recently basal-like claudin-low subtypes (Perou et al., 2000; Prat and Perou, 2011; Mathews et al., 2019). Luminal and TNBC constitute approximately 70% and 20% of total breast cancer diagnoses, respectively (Łukasiewicz et al., 2021). Since development of PAM50 for breast cancer classification, additional gene signatures have been suggested to further improve prognostic risk prediction and subtype classification, including incorporating a 13-gene hypoxia signature or implementing topological data analysis (TDA) which expands PAM50 intrinsic subtypes into seven classes based on activation or inactivation of gene groups specific to normal mammary cell types (Nicolau et al., 2011; Mathews et al., 2019; Pu et al., 2020). Accurate classification of breast cancer subtype is important, as gene expression and hormone status guide treatment strategies and provide valuable information about predicted overall or disease-free survival. Patients with ER α ⁺ tumours initially have a more favourable five-year outcome compared to patients with ER α negative (ER α ⁻) breast cancers. However ER α ⁺ patients have a constant long-term risk of relapse as a consequence of *de novo* and acquired resistance to conventional anti-oestrogen therapy, even several decades after the primary diagnosis (Pan et al., 2017; Lindström et al., 2018; Yu et al., 2019). In contrast, TNBC tumours are more aggressive and typically more advanced at the time of primary diagnoses, with an initial worse overall survival and disease-free survival when compared to all other subtypes of breast cancer (Onitilo et al., 2009). However, TNBC patients who have been disease free for five years have a low probability of disease recurrence over the following ten years (Reddy et al., 2018).

A significant amount of current knowledge surrounding breast cancer development and progression is derived from *in vitro* and *in vivo* studies utilising breast cancer cell lines. At least 92 breast cancer cell lines have been described in literature, but the number of cell lines routinely implemented is very small in comparison, where MCF-7, T-47D and MDA-MB-231 cells make up more than two-thirds of breast cancer cell lines used in such studies (Dai et al., 2017). For each breast cancer subtype, corresponding cell lines exist which can be used to investigate unique molecular characteristics and phenotypic properties driving a particular disease (Table 1.1). However, many issues surrounding use of cell lines for research into cancer progression have been described. Tumours are heterogeneous, where the proportion of cancer cells is low compared to abundance

of other cell types making up the tumour microenvironment (TME) (Nofech-Mozes et al., 2023). Furthermore, TME is hostile where cancer cells are subject to a significant number of challenges including nutrient starvation and oxygen (O₂) depletion, attack by infiltrating immune cells and extracellular acidification (Reshetnyak et al., 2011; Petrova et al., 2018; Galli et al., 2020; Vaziri-Gohar et al., 2022). As such, 2D culture of a single homogenous cell type in normal atmospheric O₂ (20 - 21% O₂; normoxia) is unable to completely recapitulate complex aberrations in metabolism as well as cell-cell and cell-stroma networks that significantly influence cancer cell growth and survival.

Table 1.1 Breast Cancer Cell Lines Commonly Used in Research. Four subtypes of breast cancer include Luminal A, Luminal B, HER2+ and triple negative breast cancer (TNBC). Characterisation of subtype is determined by immunohistology staining of ER α , PR and HER2 as either positive (+) or negative (-). Abbreviations: invasive ductal carcinoma (IDC), adenocarcinoma (AC) and metastasis (met). (Park et al., 2012; Vasconcelos et al., 2016; Dai et al., 2017).

Cell Line	Source	Tumour	Subtype	ER α	PR	HER2
MCF-7	Pleural effusion	IDC	Luminal A	+	+	-
T-47D	Pleural effusion	IDC	Luminal A	+	+	-
ZR-75-1	Mammary gland	IDC	Luminal A	+	+/-	-
BT474	Tumour	IDC	Luminal B	+	+	+
MDA-MB-361	Brain met	AC	Luminal B	+	+/-	+
ZR-75-27	Mammary gland	IDC	Luminal B	+	-	+
HCC1008	Lymph node met	IDC	HER2	+	+	-
MDA-MB-453	Pericardial effusion	AC	HER2	+	+	-
SKBR3	Pleural effusion	AC	HER2	+	+	-
BT549	Tumour	IDC	TNBC	-	-	-
MDA-MB-231	Pleural effusion	AC	TNBC	-	-	-
MDA-MB-468	Pleural effusion	AC	TNBC	-	-	-
MCF-10A	Mammary gland	N/A	"normal"	-	-	-

1.2. Oestrogen receptor structure and activity

Oestrogen receptors (ERs) include nuclear receptors ER α and ER β , and G-protein-coupled oestrogen receptor (GPER), which orchestrate biologic effects in response to steroid compounds (Walter et al., 1985; Kuiper et al., 1996; Carmeci et al., 1997; Kumar et al., 2011). To date, four steroid oestrogens have been identified in humans with similar chemical structure but different affinity for ERs: oestrone, oestradiol, oestriol and oestetrol (Kumar and Goyal, 2021). ER α is predominantly expressed in female reproductive tissues, white adipose tissue, and breast. ER β is expressed in male reproductive organs, the central nervous system (CNS) and the cardiovascular system (Jia et al., 2015). GPER is expressed in skeletal muscle, neurons and immune cells (Olde and Leeb-Lundberg, 2009). In Luminal breast cancers, ER α is the predominant driving force behind cancer cell survival and progression (Harvey et al., 1999; Perou et al., 2000; Sørli et al., 2001; Groenendijk et al., 2019).

GPER exists as a 42 kDa transmembrane protein of seven α -helices, whereas nuclear ER α and ER β are compartmentalised into distinct functional regions making up a 66 kDa and 59 kDa protein, respectively (Figure 1.1). Activating Function (AF) 1 and 2 are localised in the N terminal domain (NTD) or C Terminus next to the ligand binding domain (LBD) and are important for hormone receptor activity in a ligand-independent (AF1) or ligand-dependent (AF2) manner. AF1 and AF2 are necessary for maintaining protein-protein interactions with nuclear coregulators to facilitate transcription factor activity (Shiau et al., 1998; Wärnmark et al., 2003; Huang et al., 2018).

The DNA binding domain (DBD) of ERs associate with oestrogen response elements (EREs) at proximal promoters or distal enhancers of ER target genes (Klein-Hitpass et al., 1989; Kumar et al., 2011; Huang et al., 2018). The DBD is made up of two zinc-binding motifs, each of which contains α -helices that make phosphate contacts with the major groove of EREs (Schwabe et al., 1993; Chen et al., 2023a). The LBD contains 12 helices that make up a hormone binding pocket, a dimerization interface, and co-regulator interaction sites (Kumar et al., 2011; Chen et al., 2023a). Oestrogens and selective oestrogen receptor modulators (SERMs; see Chapter 1.1.3) compete for binding to ER α , where only one compound can occupy LBD with significant effects on ER α transcriptional activity (Hanker et al.,

2020). The AF2 pocket that sits proximal to the LBD preferentially binds coregulators that contain at least one LxxLL consensus motif, forming a stable α -helix within the AF2 binding groove. Conformational changes that occur with agonist binding to ER LBD exposes critical residues in the AF2 binding pocket for coregulator interactions, whereas antagonist association with the ERs LBD results in the AF2 coregulator pocket being blocked and significantly impedes ER transcriptional activity. The AF2 domain is therefore critical in ER activity and breast cancer progression (Foo et al., 2024).

Nuclear ERs were thought to be exclusively activated upon binding of oestrogens to LBD, otherwise steroid receptors would remain sequestered in the cytoplasm in association with heat shock protein 90 (HSP90) and unable to bind to chromatin to act as a transcription factor (Devin-Leclerc et al., 1998). However, ER α can associate with chromatin in the absence of steroids, occurring in particular by protein kinase A or mitogen-activated protein kinase (MAPK) phosphorylation of the hormone receptor, with genome-wide transcriptional activity that is independent of ligand (Patrone et al., 1998; Maggi, 2011; Caizzi et al., 2014). Many oestrogen-dependent and oestrogen-independent genes have been identified. Oestrogen-induced genes include *CCND1*, *CTSD*, and *MYC* which are important for cell proliferation and survival (Westley and May, 1987; Cavallès et al., 1993; Altucci et al., 1996; Prall et al., 1997; Wang et al., 2011; Clusan et al., 2023). In contrast, ligand-independent gene targets of ER α are associated with development, cell differentiation and morphogenesis (Caizzi et al., 2014). Two canonical mechanisms of nuclear ER-mediated transcriptional regulation are known: (i) ERs make direct contact with an ERE (GGTCAnnnTGACC) and mediate transcriptional responses through interactions with co-regulators (Ikeda et al., 2015). Or (ii) ERs associate with activator protein-1 (Ap1) and specificity protein-1 (Sp1) at promoters of target genes through a protein-protein interaction, and act to either stabilise transcription factor complexes, or recruit additional cofactors to facilitate transcription changes. In this instance, ER is not directly bound to DNA. GPER is responsible for mediating most of the rapid non-genomic effects of hormone, distinct from those of ER α and ER β and involving MAPKs Erk-1 and Erk-2 (Filardo et al., 2000; Revankar et al., 2005). ER α and ER β have high sequence similarity and share a significant number of DNA binding sites enriched for EREs as determined by CHIP-on-chip (Liu et al., 2008). The genome-wide binding of ER α has been extensively studied, at the chromatin and transcriptome level, revealing important activities of this hormone

receptor (Piryaei et al., 2023). However, while ER β associates with genomic loci distinct from ER α target genes, this ER isoform remains less well studied owing to critical differences in ER β expression and lack of sufficiently adapted ChIP protocols that can capture ER β chromatin dynamics (Zhao et al., 2010; Indukuri et al., 2022). It is known however that ER β can regulate ER α transcriptome, either enhancing or inhibiting ER α -regulated gene expression (Williams et al., 2008; Grober et al., 2011; Madak-Erdogan et al., 2013).

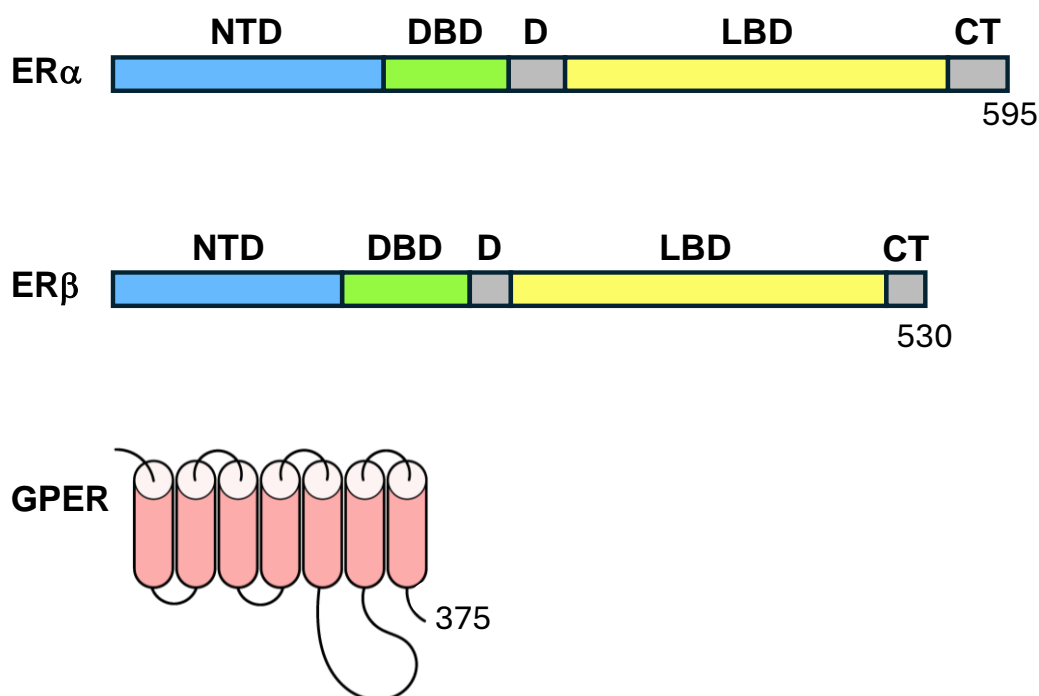


Figure 1.1 Structure of Canonical Oestrogen Receptors. Nuclear receptors ER α (595 aa) and ER β (530 aa) are compartmentalised into distinct functional regions. N-terminal domain (NTD) houses activation function (AF) domain 1 (AF1) and is the major compartment exhibiting divergence between ER α and ER β . DNA binding domain (DBD) interacts with oestrogen response elements (EREs) proximal to target genes. The hinge region (D) contains a nuclear localisation signal and acts as a flexible region between DBD and ligand binding domain (LBD). LBD contains a hormone binding pocket where oestradiol can associate with hormone receptors. LBD is therefore important for functional activity of ERs in response to hormone stimulation. AF2 is located in the C terminus (CT) next to the LBD, where it is responsible for regulating gene transcription in a ligand-specific manner. GPER (375 aa) consists of 7 transmembrane α -helical regions with 4 extracellular and 4 intracellular segments (Capatina et al., 2024).

1.2.1. Regulators and co-factors of ER α activity

Modulation of ER α activity is dependent on associated cofactors and regulatory proteins. P160 steroid receptor coactivator (SRC) family consists of three nuclear receptor coactivator (NCOA) members, SRC-1 (NCOA1), SRC-2 (NCOA2) and SRC-3 (NCOA3) (Varlakhanova et al., 2010). Three additional NCOA proteins exist, NCOA4, NCOA5 and NCOA6, which are distantly related to SRC transcription factors (Sun and Xu, 2020). Only one coregulator can occupy ER α regulatory binding sites, with differential transcriptional targets depending on identity of NCOA-ER α complex (Zwart et al., 2011). SRC proteins contain functional domains that enhance interactions with transcription factors to further fine tune regulation of ER α regulated genes, including histone acetyltransferases (HATs), p300 and CBP (Hanstein et al., 1996; Smith et al., 1996; Xu et al., 2009). ER α can also form complexes with corepressor proteins: silencing mediator of retinoic acid and thyroid hormone receptors (SMRT) and nuclear corepressors (NCOR). In contrast to recruitment of HATs and active transcription mediated by SRC-ER α , SMRT/NCOR-ER α represses gene transcription by recruitment of several members of the histone deacetylase (HDAC) family (Heinzel et al., 1997; Fischle et al., 2002). Thus, transcriptional regulation is strongly influenced by associated coregulator proteins which modulate chromatin landscape surrounding ER α target genes.

In addition to coregulatory SRC-HAT complex formation, pioneer factor Forkhead Box A1 (FOXA1) binds condensed chromatin to facilitate chromatin opening, providing transcription factors accessibility to target DNA elements that were previously obscured in heterochromatin domains. Downstream of FOXA1 binding to DNA is reduced cytosine methylation and enhanced H3K4 dimethylation, demonstrating FOXA1-mediated epigenetic modifications dictate chromatin accessibility (Sérandour et al., 2011). FOXA1 is essential for pancreatic and renal function, embryogenesis and postnatal development of mammary and prostate tissue (Bernardo and Keri, 2012). Thus, FOXA1 has been implicated in modulation of ER α and androgen receptor (AR) in breast and prostate cells under normal and malignant conditions, respectively (Gao et al., 2003; Mirosevich et al., 2005; Hurtado et al., 2011). Expression of FOXA1 and ER α are significantly positively correlated in breast cancer, and pioneer activity is essential for many ER α associations at target DNA (Carroll et al., 2005; Hurtado et al., 2011). However,

FOXA1 recruitment is dynamic and can also be influenced by activated DNA-bound ER α (Swinstead et al., 2016; Paakinaho et al., 2019).

1.2.2 Therapeutic strategies and resistance in Luminal A and TNBC tumours

Clinically, breast cancers of Luminal A subtype are low grade, slow growing and highly responsive to anti-oestrogen therapies (Orrantia-Borunda et al., 2022). Despite an initial favourable prognosis, Luminal A breast cancers have a long-term risk of disease recurrence, which is reduced by tamoxifen (Yu et al., 2019). Late local and distant recurrence remains a significant risk for at least 20 years from diagnoses, with more than 50% of recurrences occurring after the first five years of follow-up (Pistilli et al., 2022). Mainstay Luminal A breast cancer treatment is surgery in combination with oestrogen suppression or ER α antagonism. Aromatase inhibitors (AIs) including letrozole or anastrozole are used in post-menopausal patients to block aromatase conversion of androgens produced in ovaries, breast and adipose tissue, to oestrogens. ER α is activated by oestrogens, therefore use of AIs is one mechanism to attenuate ER α function (Smith and Dowsett, 2003). SERMs are used for pre-menopausal women and include tamoxifen and raloxifene, which compete with oestrogens for binding to ER α , and can both agonise and antagonise ER α transcriptional activities. In breast tissue, tamoxifen causes antiestrogenic and antitumour effects, whereas in bone and brain, tamoxifen stimulates ER α activity (Lee et al., 2008). Fulvestrant is a first generation selective oestrogen receptor downregulator (SERD) used to induce proteasomal degradation of ER α , and impair intra-nuclear mobility of the hormone receptor (Long and Nephew, 2006; Vergote and Abram, 2006). Endocrine resistance, referring to resistance to SERDs, SERMs or AIs, occurs in ER α + metastatic breast cancers. Mechanisms bestowing endocrine resistance to breast cancer cells include point mutations in *ESR1*, the gene encoding ER α , which promote hormone-independent ER α activity and decrease sensitivity to AIs and SERMs (Jeselsohn et al., 2015; Kinslow et al., 2022). Additionally, ER α + breast tumours shut off oestrogen signalling and activate alternative growth-stimulating pathways including HER2, in response to endocrine therapy which render AIs, SERDS and SERMS redundant (Creighton et al., 2008). Furthermore, due to the critical role the AF2 pocket plays in modulating ER α activity through coregulator recruitment, Deep Docking computational methods have been developed and implemented to identify novel

targets that may be able to block AF2 functionality in endocrine resistant breast cancer disease (Foo et al., 2024). TNBC accounts for 15-20 % of global breast cancer instances, and is particularly prevalent in women with mutations in the gene encoding breast cancer type 1 susceptibility protein (*BRCA1*) (Lee et al., 2011; Zagami and Carey, 2022). Surgery is a key part of TNBC treatment strategy. Breast-conserving lumpectomy or a mastectomy are performed depending on the stage of cancer at diagnosis (Obidiro et al., 2023). Because TNBC tumours lack targetable hormone and growth factor receptors, pharmacological treatment options are less specific than those available for patients with Luminal or HER2 subtype. As such, systemic chemotherapies that take advantage of the high proliferation of TNBC cells are used. Anthracyclines such as doxorubicin are potent topoisomerase inhibitors, preventing DNA replication, thus causing growth arrest and cell death (Tewey et al., 1984; Geisberg and Sawyer, 2010). Anthracyclines also activate CD8+ T cells of the immune system to further fine-tune anti-cancer responses (Denkert et al., 2010). Taxanes including paclitaxel disrupt cell cycle progression by stabilising microtubules and inducing apoptosis due to aberrations in spindle formation and mitosis (Abal et al., 2003). Despite initial promising responses to anthracycline and taxane chemotherapy, resistance to treatment and disease recurrence is significantly more likely for women with TNBC compared to other breast cancer subtypes (Nedeljković and Damjanović, 2019). *De novo* expression of Multidrug-resistant protein (MRP)-1 and MRP-8 are significantly elevated in TNBC tumours, and confers resistance to anthracyclines, taxanes and many other chemotherapy agents. Additionally, MRP-1 is upregulated in TNBC in response to treatment (Guestini et al., 2019). Recently, a ground-breaking clinical trial exploring therapeutic benefit of immune checkpoint inhibition for patients with advanced TNBC demonstrated significant improved overall survival when programmed cell death protein 1 (PD-1) is targeted by immunotherapy pembrolizumab (Cortes et al., 2022). Pembrolizumab (Keytruda) is now approved for treatment of PD-1 expressing early high-risk TNBC in combination with chemotherapy and surgery (Li et al., 2023).

1.2 RNA Polymerase III and tRNA gene transcription

Transcription of the human genome is mediated by three specialised RNA polymerase enzymes (Pol I, Pol II and Pol III), each of which are responsible for orchestrating expression of specific classes of genes (class I, class II and class III,

respectively) and share a 12-subunit core (Cramer, 2002). Pol I is restricted to the nucleolus, whereas Pol II and Pol III are localised to the nucleoplasm. Pol I is essential for transcribing 28S, 5.8S and 18S ribosomal RNA (rRNA) in equimolar amounts, accounting for more than 50% of all RNA synthesised in a cell (Russell and Zomerdijk, 2005). Pol II transcribes messenger RNA (mRNA), micro-RNA (miRNA), small nucleolar RNA (snoRNA) and small non-coding RNA (snRNA). Pol III contains 17 subunits, making it the largest of all three Pol enzymes (Ramsay et al., 2020). Expression of transfer RNA (tRNA), 5S rRNA, 7SL of the signal recognition particle, U6 spliceosome small nuclear RNA and other class III non-protein-coding genes is carried out by Pol III in eukaryotic cells (White, 2004). Thus, Pol III is crucial for expressing RNA with functions related to ribosomal biogenesis and protein synthesis.

1.2.1 Class III transcription by Pol III

Pre-initiation complex (PIC) assembly and Pol III transcription of target genes is dependent on internal and external regulatory elements, and corresponding organisation of transcription factors. There are three different promoter types that recruit Pol III to transcription start sites (TSS) of target genes (Type I, Type II and Type III) (Figure 1.2). A conserved feature of all three promoter types is binding of transcription factor TFIIIB, which positions Pol III at the TSS of target genes. TFIIIB is made up of a TATA box binding protein (TBP), B double prime 1 (Bdp1), and TFIIIB-related factor (Brf)1 or Brf2 which directly associate with Pol III (Gouge et al., 2017). TFIIIA is a 5S rRNA-specific transcription factor, thus unique to Type I promoters. Internal Control Regions (ICR) are recognised by TFIIIA, which initiates PIC assembly by sequential recruitment of TFIIIC, Brf1-containing TFIIIB and then Pol III. Type II promoters exist in tRNA genes. Here, internal A and B box sequences downstream of TSS are recognised by TFIIIC, a six-subunit complex that recruits Brf1-TFIIIB to promoters, and subsequent loading of Pol III (Kassavetis et al., 2001; Vorländer et al., 2020). Type III promoters are distinct from Type I and Type II as they contain exclusively gene-external elements. For complete PIC assembly at Type III genes, Brf2-TFIIIB-TBP associates with a TATA box located upstream of TSS and interacts with SNAPc positioned at a proximal sequence element (PSE). In addition to PSE, a distal sequence element (DSE) is occupied by transcription activators such as ZNF143 and POU2F1 that enhance Pol III PIC assembly (James Faresse et al., 2012).

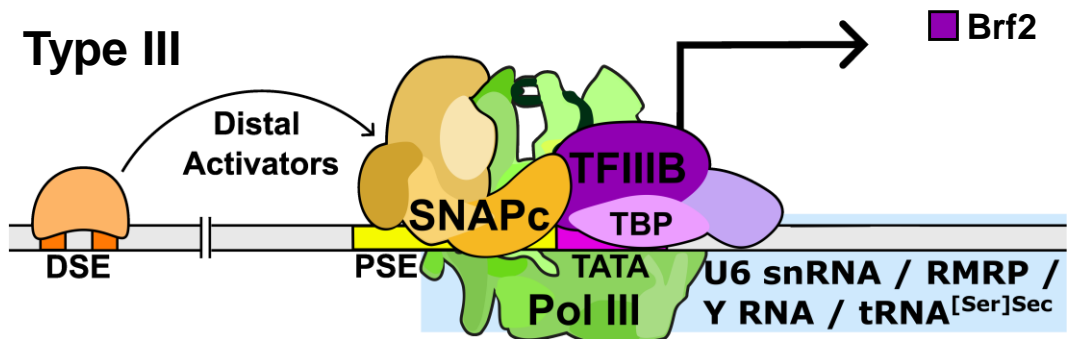
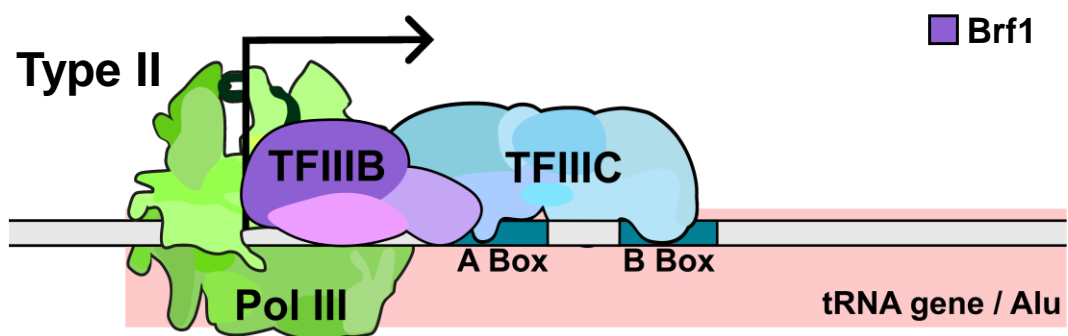
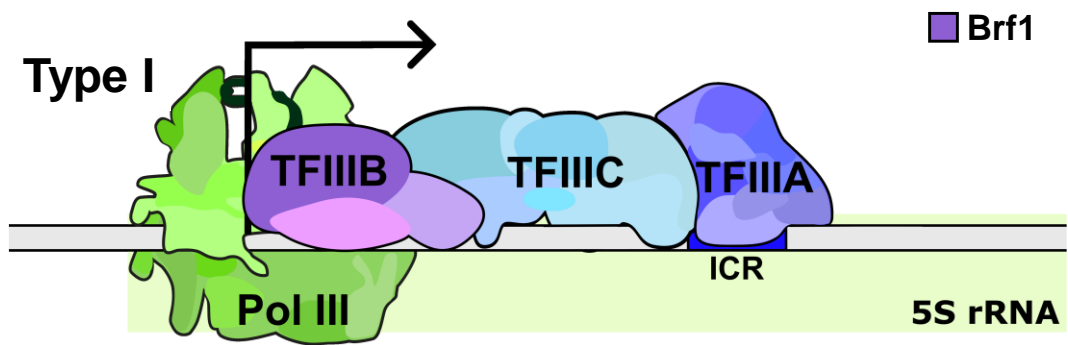


Figure 1.2 RNA Polymerase III Promoter Architecture and Initiation Assembly

Factors. Three different types of class III promoters exist (Type I, Type II and Type III). All types of class III promoters utilise TFIIIB trimer composed of TBP, BDP and Brf1 or Brf2. 5S rRNA genes uses a Type 1 promoter which includes an internal control region (ICR) recognised by 5S gene-specific TFIIIA, as well as Brf1-containing TFIIIB and TFIIIC. Type 2 promoters are used by tRNA genes and Alu elements. Type 2 requires TFIIIC which recognises A and B box internal promoter elements downstream of TSS, and recruits Brf1-containing TFIIIB. Type 3 promoters are used by U6 snRNA, RMRP, Y RNA and a specialised selenocysteine tRNA (tRNA^{[Ser]^{Sec}). Unlike Type 1 and Type 2 promoters, Type 3 promoters are external, made up of a proximal sequence element (PSE) recognised by SNAPc and a TATA box which is recognised by the TBP component of the Brf2-containing TFIIIB. Additionally, Type 3 promoters contain a distal sequence element (DSE) which are typically located around positions -210 and -240 and are occupied by transcriptional activators that assist Pol III in transcription. Adapted from (Arimbasseri and Maraia, 2016).}

1.2.1.1 Post transcriptional processing of tRNA

Canonical tRNA transcripts are relatively small, averaging between 76 to 90 nucleotides in length. Following transcription, pre-tRNA are immediately processed in the nucleus by ribonucleoprotein RNase P to remove ~10 bases from the 5' end of the transcript, and endonuclease RNase Z which cleaves the poly U tract at the 3' end of the transcript (Berg and Brandl, 2021). Addition of a 3'-terminal CCA modification is carried out by a tRNA nucleotidyltransferase prior to cytoplasmic localisation, and is essential for attachment of amino acid at the 3' terminus of tRNA molecules (Nagaike et al., 2001). A small subset of tRNA genes contain introns which are spliced by tRNA splicing Sen complex and a tRNA ligase (Greer et al., 1983; Paushkin et al., 2004). Export of processed tRNA out of the nucleus is carried out by the β -importin family member Xpot (Arts et al., 1998; Cook et al., 2009). Additional modification of tRNA is carried out in the cytoplasm by specialised enzymes and can be extensive, where ~12% of tRNA residues have some form of base modification such as methylation, thiolation, acetylation, hydroxylation, pseudouridylation or deamination (Phizicky and Alfonzo, 2010; Lei et al., 2023). The resulting complex is a cloverleaf structure of four helices with a single 3' CCA which carries a charged amino acid, and three functional hairpin loops: dihydrouracil (D), anticodon (AC) and thymine (T) loops. The D loop is important for aminoacyl-tRNA synthetase recognition, which is the enzyme involved in aminoacylation of the tRNA molecule at 3' CAA (Hardt et al., 1993). The AC loop decodes mRNA codons. Many modifications are centred around the AC loop and are therefore important for translation and translation fidelity (Urbonavicius et al., 2001; Murphy and Ramakrishnan, 2004; Johansson et al., 2008). Modifications that occur in the main body of tRNA and away from the AC are more important in stabilising tRNA structure and ensuring proper folding (Davanloo et al., 1979; Vermeulen et al., 2005; Ohira and Suzuki, 2024). The T loop recognises ribosome and is involved in formation of a tRNA-ribosome complex during protein synthesis (Chan et al., 2013).

1.2.2 Implications of dysregulated Pol III activity and aberrant tRNA in cancer

While induction of Pol III gene transcription is dependent on recruitment of necessary transcription machinery to promoters, synthesis of translational apparatus is energy intensive and subsequently tightly regulated to ensure Pol III activity is dampened in unfavourable conditions. MAF1 is the major general

negative regulator of Pol III activity in response to stress, by blocking Pol III interactions with TFIIIB and promoters and ensuring Pol III output is sensitive to growth factor signalling through the mTOR pathway (Desai et al., 2005; Kantidakis et al., 2010; Bonhoure et al., 2020). Mammalian cells contain two Pol III isoforms that differ in one subunit, either POLR3G or POLR3GL, which arose from a gene duplication event and share 49% protein sequence identity (Haurie et al., 2010; Renaud et al., 2014). POLR3G is selectively elevated by oncogenes and pluripotency factors that do not induce POLR3GL, including MYC, NANOG and OCT4A (Enver et al., 2005; Haurie et al., 2010; Wong et al., 2011; Durrieu-Gaillard et al., 2018; Wang et al., 2020; Van Bortle et al., 2021). Accordingly, POLR3G to POLR3GL ratio is significantly elevated in a variety of cancer types relative to matched healthy tissues, such as in lung and colorectal carcinomas (Van Bortle et al., 2021). High POLR3G levels correlate with a worse prognosis for patients with lung adenocarcinomas, oesophageal, bladder urothelial and transitional cell carcinomas (Liu et al., 2020; Van Bortle et al., 2021). Overexpression of POLR3G is observed in clinical TNBC specimens, but not breast cancers of other molecular subtypes and blocking POLR3G results in reduced tumour growth and suppressed metastasis *in vivo* (Lautré et al., 2022). Cryo-EM of POLR3G and POLR3GL paralogues in the Pol III complex revealed a more stable interaction of POLR3G with core Pol III subunits, blocking the specific site MAF1 occupies (Girbig et al., 2021). Thus, selective incorporation of POLR3G over POLR3GL impedes MAF1 repression of Pol III transcription and consequently promotes tumorigenicity. Ras and Myc oncogenes stimulate tRNA synthesis by phosphorylating and inhibiting MAF1, promoting Pol III function and enhancing cell and tissue growth (Srisanthadevan-Pirahas et al., 2018). Additionally, loss of key tumour suppressors: retinoblastoma protein (Rb), p54, phosphatase and tensin homolog (PTEN) and BRCA1 is linked to enhanced Pol III activity (White et al., 1996; Cairns and White, 1998; Woiwode et al., 2008; Veras et al., 2009). As such, Pol III activity is strongly connected to oncogenicity. Therefore, a large proportion of tRNAs are frequently induced in cancers. Overexpression of tRNAs correlates with a worse prognosis in breast cancer (Pavon-Eternod et al., 2009; Goodarzi et al., 2016).

1.2.2.1 ER α regulation of tRNA expression in ER α + cancer

ER α is implicated in regulating expression and modification of tRNA. Depletion of ER α in a PTEN-null mouse model of prostate cancer significantly

reduces *Elp3* mRNA in association with polysome, and further decreases ELP3 protein levels (Lorent et al., 2019). ELP3 is one enzyme responsible for a 5-methoxycarbonyl-methyl-2-thiouridine (mcm^5s^5U) modification at position 34 (U34) of the AC loop in tRNA, which is important for modulating codon recognition and therefore translation efficiency (Rafels-Ybern et al., 2018). Accordingly, mcm^5s^5U modification of tRNAs are decreased by 40% following steroid receptor knockdown (Lorent et al., 2019). In yeast, mcm^5s^5U modification of U34 is present on tRNA-Glu-UUC, tRNA-Lys-UUU and tRNA-Gln-UUG which decode GAA, AAA and CAA codons through U-G wobble decoding (Johansson et al., 2008). In breast tumours, oncoprotein DEK is elevated and associated with high histological grade, lymph node metastasis and high Ki67 (Yang et al., 2021a). Translation of *DeK* is dependent on U34 mcm^5s^5U modification (Delaunay et al., 2016). Thus, ER α drives breast cancer tumorigenesis by upregulating tRNA modifying enzymes, enhancing translation efficiency of oncogenes. In addition, ER α can directly influence tRNA expression in response to oestradiol. Global run-on (GRO)-sequencing (seq) used to measure nascent gene transcription as it occurs demonstrated significant induction of ~32% of tRNA genes in MCF-7 cells within 10 – 160 minutes of 100 nM oestradiol stimulation (Hah et al., 2011). The rapid nature of oestradiol-mediated induction of tRNA suggests ER α is directly targeting many tRNA genes, rather than secondary or tertiary effects of hormone stimulation elevating tRNA transcription. Alcohol consumption is significantly associated with risk of breast cancer, although the exact mechanism by which alcohol increases breast cancer development is still largely unknown (Jung et al., 2016). A link between alcohol and ER α + tumours has been suggested, but much disagreement surrounding ER α + breast cancer and a correlation with alcohol intake exists (Freudenheim, 2020). In MCF-7 cells, 5 nM oestradiol induced a ~2-fold increase in tRNA^{Leu} and 5S rRNA, which was increased 11- and 14-fold respectively by the addition of 25 mM ethanol in a Brf1-dependent mechanism, linking activated ER α and alcohol to aberrant Pol III activity (Zhang et al., 2013b). Conversely, Tamoxifen represses Pol III-dependent gene transcription in breast cancer cells by inhibiting expression of Brf1 and Pol III transcription of Type I and Type II genes (Zhong et al., 2014). Furthermore, ER α directly associates with Brf1, tRNA^{Leu} and 5S rRNA promoters in MCF-7 cells (Fang et al., 2017). Thus, oestradiol-dependent induction of tRNA transcription likely occurs because of direct ER α associations with tDNA. P300 is an intrinsic co-activator of TFIIC, with HAT activity being essential for activation of tRNA gene transcription (Mertens and Roeder, 2008). Active ER α may drive tRNA expression by recruiting necessary co-

activators to tRNA promoters. A tRNAome-wide study of ER α and related cofactor occupancy at tRNA loci has not been conducted but would provide valuable insight into non-coding ER α targets that may be therapeutically relevant for breast cancer patients.

1.3 Hypoxia and hypoxia-inducible factors

Hypoxia is a physiological term describing insufficient supply of O₂ to tissues or cells required for maintaining normal function and homeostasis. In particular, O₂ is vital in the electron transport chain (ETC), acting as a terminal electron acceptor during ATP synthesis (Hirota, 2020). If tissues and cells were maintained in hypoxic environments, they would be unable to survive. As such, adaptation to cellular hypoxia is driven by accumulation of transcription factors termed hypoxia-inducible factors (HIFs) which coordinate expression of a myriad of genes that impose survival advantages when O₂ is limited. HIFs were first described in 1992, when rapid upregulation of erythropoietin (*EPO*) mRNA levels in hypoxic Hep3B cells was studied (Semenza and Wang, 1992). A functional HIF is a heterodimer consisting of two basic-helix-loop-helix (bHLH) *Per Arnt Sim* (PAS) proteins of 120 kDa and 94 kDa, termed HIF-1 α and HIF-1 β (ARNT), respectively (Wang et al., 1995). Alternative HIF- α isoforms were discovered by homology screens for interaction partners of HIF-1 β , namely HIF-2 α (EPAS1) and HIF-3 α (Ema et al., 1997; Tian et al., 1997; Gu et al., 1998). HIFs regulate transcription of target genes through recognition and binding to a core pentanucleotide sequence (5'-RCGTG-3') referred to as the hypoxia response element (HRE) (Wang and Semenza, 1993). While HIF-1 β has roles outside of hypoxia response and is therefore constitutively expressed in normoxia, HIF- α are specific hypoxia-sensing molecules that accumulate when O₂ availability is limited. (Jewell et al., 2001).

HIF proteins are compartmentalised into discrete functional segments, with HIF-1 α and HIF-2 α sharing greatest domain organisation homology (Figure 1.3). All HIF proteins contain N-terminal bHLH and PAS domains. The bHLH domains are important for making contact with minor groove of target DNA, whereas PAS domains are important for correct heterodimerization of HIF- α with HIF-1 β (Wang et al., 1995). HIF- α are constitutively transcribed and translated. In the presence of physiological levels of O₂ (physoxia) or normoxia, prolyl hydroxylase domain (PHD) enzymes catalyse hydroxylation of two prolyl residues in oxygen-dependent

degradation domain (ODDD) of HIF- α , stabilising an association with E3 ubiquitin ligase member Von Hippel-Lindau (pVHL), leading to rapid polyubiquitination and proteasomal degradation (Maxwell et al., 1999). Therefore, HIF- α have a high turnover rate when O₂ is available, and a half-life of approximately five to ten minutes (Wang et al., 1995; Salceda and Caro, 1997). HIF-1 β is O₂-independent with distinct roles in cellular signalling pathways involved in xenobiotic and hypoxic responses, as well as regulating adaptive immunity and organ development (Fujisawa-Sehara et al., 1987; Walisser et al., 2005; Carreira et al., 2015; Neavin et al., 2018; Haidar et al., 2021). As such, HIF-1 β does not possess an ODDD and is stable in normoxia and hypoxia. An additional level of negative HIF- α regulation comes in the form of hydroxylation of an asparagine in C-terminal transactivation domains (C-TAD) by factor inhibiting HIF (FIH), which obstructs interaction with transcriptional coactivator p300 and thus inhibits transcriptional activation of HIF- α target genes (Lando et al., 2002). HIF-3 α is exempt from FIH regulation because this isoform does not possess a C-TAD, and instead contains a leucine zipper. As such, HIF-3 α is unable to interact with p300 and induce gene expression (Gu et al., 1998). HIF-1 α and HIF-2 α are associated with driving transcription of target genes, whereas HIF-3 α is a negative regulator of HIF-transcription, possibly by sequestering HIF-1 β in a transcriptionally inactive heterodimer (Hara et al., 2001). Hydroxylation activity of PHD enzymes is O₂-dependent. In hypoxia, PHD enzymes are inactivated and unable to catalyse hydroxylation of HIF- α ODDD prolyl residues. PHD enzymes are also inhibited by Dimethylxalylglycine (DMOG), resulting in normoxic accumulation of HIF- α (Liu et al., 2009a). The result of hypoxia or DMOG is mass accumulation of HIF- α protein (Bruick and McKnight, 2001). When stable, HIF- α forms a heterodimer with HIF-1 β and translocate into the nucleus. HIF-1 α /HIF-2 α – HIF-1 β associate with p300 at HRE sequences and drive transcription of target genes that have functional roles in angiogenesis such as vascular endothelial growth factor A (*VEGFA*), glucose transport, such as glucose transporter 1 (*GLUT1*) or pH regulation including Na⁺/H⁺ exchanger 1 (*NHE1*) and carbonic anhydrase IX (*CA9*) to ensure cell survival and maintain metabolism during hypoxic stress (Forsythe et al., 1996; Wykoff et al., 2000; Chen et al., 2001; Shimoda et al., 2006).

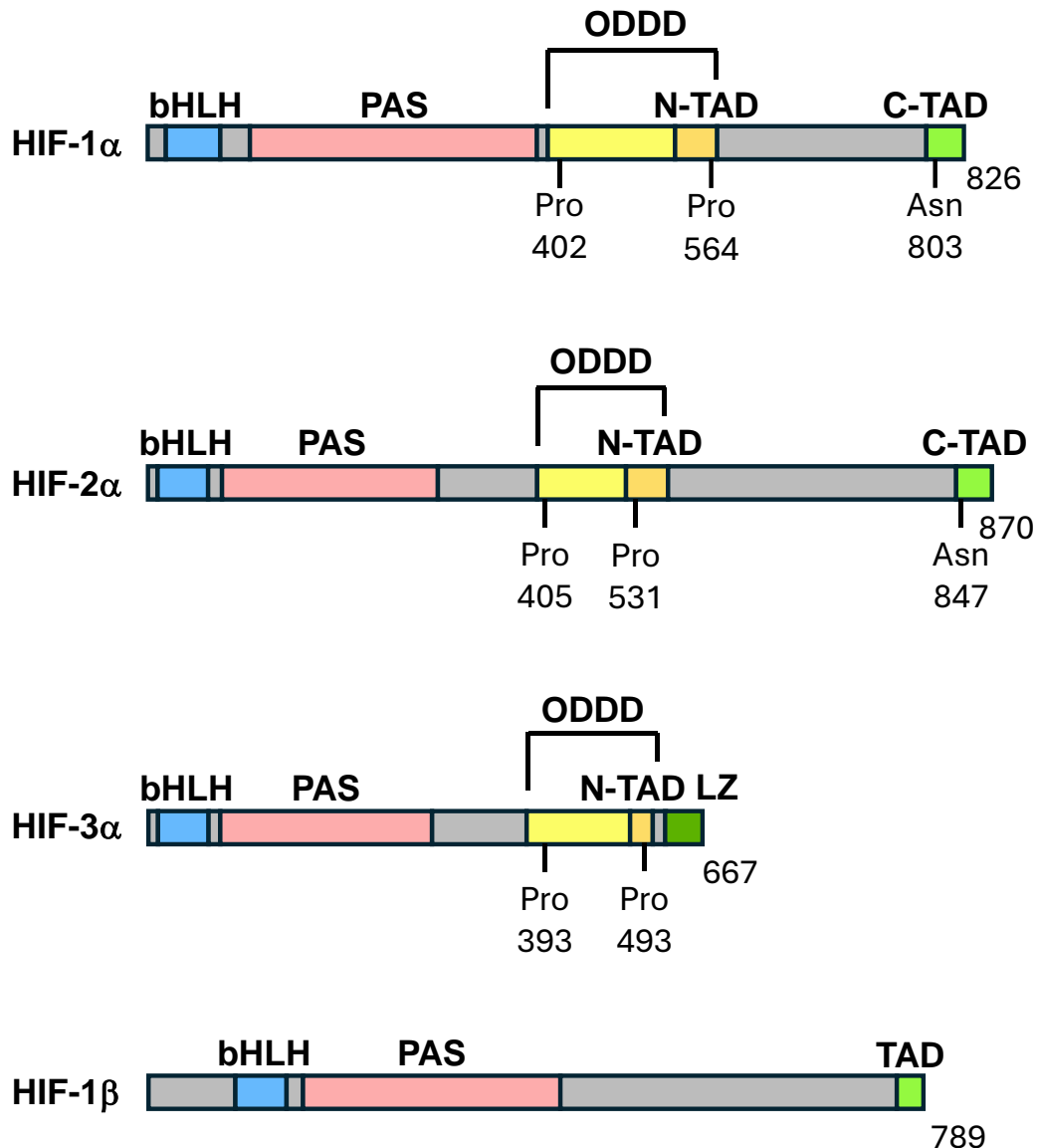


Figure 1.3 Domain Organisation of HIF Proteins. Hypoxia-inducible factors HIF-1 α (826 aa), HIF-2 α (870 aa), HIF-3 α (667 aa) and ARNT (789 aa) are segmented into distinct functional and regulatory domains. All four HIF proteins contain a basic helix-loop-helix (bHLH) domain involved in DNA binding, a PER-ARNT-SIM (PAS) domain which is required for protein interactions and dimerization and a transcriptional activation domain (TAD). HIF-1 α , HIF-2 α and HIF-3 α contain an oxygen-dependent degradation domain (ODDD) and N-terminal TADs. HIF-3 α does not have a C-terminal TAD and instead has a Leucine Zipper (LZ). HIF-1 β does not contain ODD as it exists in an oxygen-independent manner. Turnover of HIF- α in the presence of O₂ occurs through a stepwise process of involving hydroxylation of proline (Pro) residues in highly conserved ODD by proline hydroxylases, binding of von Hippel Lindau (VHL) E3 ubiquitin ligase complex and polyubiquitination, and proteasomal degradation. An additional level of HIF- α regulation occurs by factor inhibiting HIF (FIH) hydroxylating asparagine (Asn) residues in C-TAD which compromises transcriptional potential of these factors.

1.3.1 Hypoxia in cancer

Hypoxia is essential for orchestrating transcriptional programs that regulate cell differentiation and tissue development during embryogenesis, and also prevalent in adult stem cell niches necessary to maintain undifferentiated cell states (Mohyeldin et al., 2010; Pimton et al., 2015; Woods et al., 2018; López-Anguila et al., 2022). Concordant with developmental processes often being hijacked during malignant progression, hypoxia and HIFs are recognised as important contributors to cancer development (Zhong et al., 1999). Hypoxia is a common feature of many solid tumours including: non-small cell lung cancer (NSCLC), neuroblastoma, glioma, head and neck squamous cell carcinoma (HNSCC), prostate cancer and breast cancer (Zhong et al., 1999; Jögi et al., 2002; Nordmark and Overgaard, 2004; Jensen et al., 2014; Samanta et al., 2014; Yan et al., 2024). Accordingly, 53% of formalin-fixed paraffin-embedded (FFPE) malignant tumours are positively stained for HIF-1 α expression (Talks et al. 2000). In breast tumours, low O₂ tension is in part due to increased consumption of O₂ in rapidly dividing cancer cells, but also due to an overall decrease in O₂ supply as tumours out-grow local blood vessels. To try and combat dysfunctional O₂ levels, hypoxia induces *de novo* angiogenesis to promote new blood vessel formation through HIF-1 α mediated VEGFA induction (Forsythe et al., 1996). However, newly developed vessels are leaky and inefficient in O₂ delivery (Muz et al., 2015). Further to an attempt at restoring O₂ equilibrium, HIF-mediated blood vessel development provides malignant cells entry into circulatory systems, an important first step in metastasis and a hallmark of cancer (Jahroudi and Greenberger, 1995; Hanahan and Weinberg, 2000; Carmeliet, 2005). The breast TME has regions of hypoxia, with O₂ partial pressure (PO₂) ranging from 2.5 to 2.8 mm of mercury (Hg), compared to a PO₂ of 65 mm Hg in normal breast tissue (Vaupel et al., 2007). Hypoxia and HIF expression in solid tumours is strongly associated with more advanced disease and resistance to radiation and chemotherapy (Gray et al., 1953; Horsman et al., 2012; Samanta et al., 2014; Rankin et al., 2016; Ebright et al., 2020; Yong et al., 2022). In breast cancer cells, hypoxia promotes chromatin remodelling to induce epithelial-to-mesenchymal transition (EMT) in a HIF-1 α -dependent manner (Kakani et al., 2024). Thus, hypoxic signatures are significantly associated with more aggressive basal TNBC tumours compared to other breast cancer subtypes (Ye et al., 2018). Indeed, it is estimated that more than 80% of TNBC tumours overexpress HIF-1 α , and the HIF-1 α pathway is overactive in TNBC compared to other subtypes (Liu et al.,

2023). Hypoxia has been significantly implicated in TNBC immune escape by causing immune effector cell dysfunction and subsequent resistance to immunotherapy, in a HIF-1 α -dependent manner (Ma et al., 2022). Furthermore, expression of hypoxia-induced CA9 has been shown in TNBC primary samples to be an independent marker of increased tumour size, higher histological grade and significantly worse disease-free survival and overall survival (Ong et al., 2022).

Low O₂ in cancer is not the only mechanism in which HIF- α are stabilised. Loss of tumour suppressor gene pVHL causes higher levels of HIF-1 α protein, as do functional mutations in p53 and PTEN which ordinarily suppress HIF-1 α stabilisation in hypoxia (An et al., 1998; Zundel et al., 2000; Pollard et al., 2007). Tumour suppressor regulation of HIF- α labels HIF transcription factors as oncoproteins, able to drive breast cancer development through regulation of key genes involved in growth, proliferation and metastasis.

1.3.2 Implications of Hypoxia in ER α + breast cancers

In ER α + Luminal A and Luminal B breast cancers, HIF-1 α and CA9 expression is significantly associated with decreased disease-free survival, whereas HIF-2 α is not linked to disease outcome (Shamis et al., 2022). Loss of functional ER α is an important event preceding endocrine therapy resistance (Lindström et al., 2012, 2018). Hypoxic culture of ER α + MCF-7 and T-47D breast cancer cell lines significantly reduces *ESR1* transcription in a HIF-1 α -dependent manner (Ryu et al., 2011). Accordingly, prolonged culture of MCF-7 and T-47D cells in low O₂ tension induces proteasomal degradation of ER α and ER β protein (Wolff et al., 2017). Furthermore, a comprehensive investigation of 10 ER α + breast cancer cell lines revealed hypoxia induces HIF-1 α -dependent proteasomal degradation of ER α in all models, regardless of basal ER α abundance (Padró et al., 2017). Conversely, MDA-MB-231 TNBC cells increase ER α expression in response to HIF-1 α stabilisation with a chemical hypoxia mimetic (Wolff et al., 2017). Investigation of primary Luminal A tumours show ER α is negatively correlated with expression of HIF-1 α within a cycling hypoxia microenvironment (Kang and Li, 2022).

Further to hypoxia-mediated proteasomal degradation regulating ER α levels, the hormone receptor is also regulated through reactive oxygen species

(ROS)-dependent epigenetic modification. Hypoxia increases ROS by acting on complexes I, II and III of the mitochondrial ECT. In turn, ROS destabilise PHD enzymes and enhances HIF- α stabilisation (Wang et al., 2007; Kondoh et al., 2013). MCF-7 cells cultured with hydrogen peroxide (H_2O_2) as a source of ROS exhibit increased cell growth, colony formation and up-regulation of pro-metastatic genes such as *VEGF* and *WNT1* (Mahalingaiah and Singh, 2014). MCF-7 cells adapted to chronic oxidative stress are significantly less responsive to oestradiol and tamoxifen which is reversed by the demethylating agent 5-Aza-2'-deoxycytidine (5-aza-dC) (Mahalingaiah et al., 2015). Concurrent with desensitisation to oestradiol and tamoxifen is increased expression of DNA methyltransferases *DNMT1* and *MBD4*, increased methylation surrounding *ESR1* and decreased abundance of *ESR1* mRNA and ER α protein. *ESR1* is methylated in ER α null MDA-MB-231, MDA-MB-468 and Hs578t cells (Ottaviano et al., 1994). Importantly, *ESR1* is hypermethylated in primary breast tumours, which strongly correlates with reduced ER α protein expression and more advanced disease (Yoshida et al., 2000; Ramos et al., 2010; Wei et al., 2012). Additional epigenetic modifications are implicated in *ESR1* gene silencing. TWIST, a bHLH transcription factor, reduces ER α expression by (i) recruiting DNA methyltransferase 3B (DNMT3B) to the *ESR1* promoter which induces methylation and (ii) re-organising the chromatin landscape by assembling HDAC1 to the *ESR1* locus (Vesuna et al., 2012). TWIST expression is enhanced in hypoxia through HIF- α activity, and drives EMT in solid tumours (Yang et al., 2008a; Sun et al., 2009; Zhang et al., 2013a).

In endocrine-resistant breast cancer, FOXA1 is significantly amplified and enhances tumour aggressiveness by activating IL-8 signalling to further promote tumour invasion, metastasis and therapy resistance (Britschgi et al., 2012; Singh et al., 2013; Fu et al., 2016). FOXA1 transcriptional reprogramming increases active enhancer H3K27ac and H3K4me1 marks across chromatin. Genes within the vicinity of gained active enhancer deposits are associated with pro-proliferation, anti-apoptosis and developmental signalling (Fu et al., 2019). *EPAS1* (encoding HIF-2 α) shows increased FOXA1 binding and significant induction in a FOXA1-dependent, hypoxia-independent manner, and this is associated with ER α -positive metastasis to the liver, pancreas and bone (Fu et al., 2019).

1.3.3 Hypoxia, glycolysis and pathological transport of ions and solutes

Hypoxia inhibits O₂-dependent metabolism of glucose to CO₂ in the tricarboxylic acid (TCA) cycle and oxidative phosphorylation (OXPHOS). Instead, O₂ deprived cells utilise the less energy-efficient metabolism of pyruvate to lactic acid to generate ATP required for cellular needs. Of the many HIF- α target genes identified over the last two decades, enzymes of glycolysis have been shown to be strongly upregulated in response to hypoxia, including phosphoglycerate kinase-1 (*PGK1*) and lactate dehydrogenase (*LDH*), which are key enzymes in conversion of glucose into pyruvate and lactate respectively, and pyruvate dehydrogenase kinase 1 (*PDK1*) which inhibits pyruvate entry into the TCA cycle (Firth et al., 1994; Kim et al., 2006). Additionally, glucose transport into the cell is increased through HIF-1 α -mediated upregulation of hypoxia responsive *GLUT1* and *GLUT3* transporters (Chen et al., 2001; Hayashi et al., 2004; Liu et al., 2009b). Activities of these transporters provide malignant cells with a high supply of glucose to be used in glycolysis. Cancer cells often utilise glycolysis even when O₂ is not limiting, shifting metabolism to “aerobic glycolysis” in a process known as the Warburg effect, which underpins the reprogramming energy metabolism hallmark of cancer (Hanahan and Weinberg, 2011). With glycolytic conversion of glucose into lactic acid in malignant cells, a highly acidic intracellular pH (pH_i) might be expected. However, it is important for cancer cells to export acids from the cytoplasm to survive. HIF-1 α regulates several membrane transporters in response to hypoxia to maintain a favourable pH_i, such as monocarboxylate transporter (MCT)-4 which co-transport both H⁺ and lactate out of cytosol into extracellular matrix (ECM), and *NHE1* which uses the inward Na⁺ gradient to simultaneously push H⁺ out into ECM, contributing to intracellular alkalinisation and extracellular acidification (Shimoda et al., 2006; Ullah et al., 2006). As such, extracellular pH (pH_e) is decreased to pH 6.6 compared to physiological pH_e of pH 7.4 in healthy tissues (Swietach et al., 2014; Pedersen et al., 2017; Pethő et al., 2020). An acidic ECM supports activity of matrix metalloproteinases (MMPs) which degrade supporting networks allowing for invasion of cancer cells and infiltration of new blood vessels through angiogenesis (Liotta et al., 1980; Bergers et al., 2000). Stabilisation of HIF-1 α by either hypoxia or MCT-4 inhibitor bandalitinib decreases ER α + breast cancer cell line sensitivity to tamoxifen, whereas inhibition of HIF-1 α resensitises ER α + breast cancer cell lines to tamoxifen (Nadai et al., 2021).

1.4 Na⁺ homeostasis and dysregulated Na⁺ transport in cancer

Dysregulation of various ion channels and transporters is significantly implicated in solid tumours and haematological malignancies. Indeed, ion channels have been extensively studied in cancer following observations of impaired tumour development and improved responses to therapy by pharmacological attenuation of ion transport more than three decades ago (Yamashita et al., 1987; Lee et al., 1988; Pancrazio et al., 1989; Taylor and Simpson, 1992). Of great importance for breast cancer development is dysregulated sodium (Na⁺) handling, contributing to raised intracellular [Na⁺] ([Na⁺]_i) and corresponding to a more aggressive phenotype. Despite advancements in characterising Na⁺ levels in breast tumours by ²³Na MRI, and greater understanding of clinical implications of altered Na⁺ channel expression or activity, mechanisms driving elevated [Na⁺]_i are underexplored (Ouwerkerk et al., 2007; Zaric et al., 2016; Arponen et al., 2024). Several types of Na⁺ and solute transporters are responsible for maintaining Na⁺ homeostasis in cells, such as: voltage gated Na⁺ channels (VGSCs), epithelial Na⁺ channels (ENaCs), acid-sensing ion channels (ASICs), Na⁺/K⁺/Cl⁻ cotransporter (NKCC), Na⁺/glucose cotransporter (SGLT2) and Na⁺/K⁺ ATPase (NKA). Dysregulated Na⁺ handling through such channels has been implicated in various aspects of tumour progression (Leslie et al., 2019).

1.4.1 Voltage gated Na⁺ channels

VGSCs are responsible for initiating action potentials and modulating conduction in excitable cells including neurons, cardiomyocytes and muscle cells (Dutta et al., 2018). In addition, VGSCs are found in non-excitabile cells including fibroblasts, glia, immune cells, and invasive breast cancer cells (Brackenbury, 2012; Djamgoz et al., 2019). VGSCs are multimeric transmembrane complexes composed of an ion conduction pore-forming α subunit and one or more auxiliary β subunits (Brackenbury and Isom, 2011; Catterall, 2012; Dutta et al., 2018; Angus and Ruben, 2019). There are nine α subunits, Na_v1.1 – Na_v1.9 (*SCN1A* – *SCN5A* and *SCN8A* – *SCN11A*) which are expressed with tissue-specific distribution and variable sensitivity to Tetrodotoxin (TTX) (Table 1.2). Functional α subunits are 230 - 260 kDa comprised of four homologous domains, each containing six transmembrane α -helices (Figure 1.4) (Leslie et al., 2022). Five β subunits have been characterised, β 1 – β 4 (*SCN1B* – *SCN4B*) which are transmembrane proteins, and β 1B which is an

alternative splice variant of $\beta 1$ that lacks conserved β -subunit transmembrane domain, making it a soluble protein (Patino et al., 2011). β subunits contain an extracellular immunoglobulin (Ig) domain which is used for a functional role as a cell adhesion molecule (CAM).

The crystal structure of the VGSC α subunit was first resolved in 2011 in *Arcobacter butzleri* (Payandeh et al., 2011). The Na^+ -selective pore exists at the 5th and 6th segments of each domain (Guy Hr Seetharamulu, 1986). Voltage sensing is carried out by the 4th segment, which moves across the membrane with segments 1 and 3 upon depolarisation of membrane potential (V_m) and opens the channel to establish fast inward Na^+ current (I_{Na}), significantly raising $[\text{Na}^+]_i$ (Guy Hr Seetharamulu, 1986; Yarov-Yarovoy et al., 2006). Rapid inactivation occurs within 1 – 3 milliseconds of channel opening by an intracellular inactivation loop between domains III and IV allosterically blocking the channel to prevent Na^+ entry (Armstrong and Bezanilla, 1977; Bezanilla and Armstrong, 1977; Vassilev et al., 1988; Pan et al., 2018). A small number of channels fail to elicit fast inactivation following channel opening events, which allows a “persistent” Na^+ current to continue to pass through open VGSCs into the cytosol. VGSCs in breast cancer cells do not open in response to membrane depolarisation but can intermittently open at the resting V_m . Consequently, persistent Na^+ current has been recorded in breast cancer cells (Roger et al., 2007; Driffort et al., 2014). Although a functional VGSC can exist as a single α subunit, auxiliary β subunits modulate gating kinetics, amplify activation and inactivation rates of VGSCs, and enhance membrane expression of channels (Isom, 2001; Angus and Ruben, 2019).

Table 1.2 Tissue Specificity of VGSCs and TTX Sensitivity. Highlighted VGSCs (green) are “TTX-resistant”, requiring μM concentrations to block channel activity. Remaining channels are “TTX-sensitive” as nM concentrations are required for inhibition. Abbreviations: central nervous systems (CNS), peripheral nervous systems (PNS) dorsal root ganglion (DRG). (Akiba et al., 2003; Vanoye et al., 2013; Tsukamoto et al., 2017; Sanchez-Sandoval et al., 2023)

VGSC	Gene symbol	Primary tissue	TTX-sensitivity (IC_{50})
Nav1.1	<i>SCN1A</i>	CNS neurons	4.1 nM
Nav1.2	<i>SCN2A</i>	CNS neurons	14 nM
Nav1.3	<i>SCN3A</i>	CNS neurons	5.3 nM
Nav1.4	<i>SCN4A</i>	Skeletal muscle	7.6 nM
Nav1.5	<i>SCN5A</i>	Cardiomyocytes	1 μM
Nav1.6	<i>SCN8A</i>	CNS neurons	2.3 nM
Nav1.7	<i>SCN9A</i>	PNS neurons	36 nM
Nav1.8	<i>SCN10A</i>	DRG neurons	73.3 μM
Nav1.9	<i>SCN11A</i>	DRG neurons	30 μM

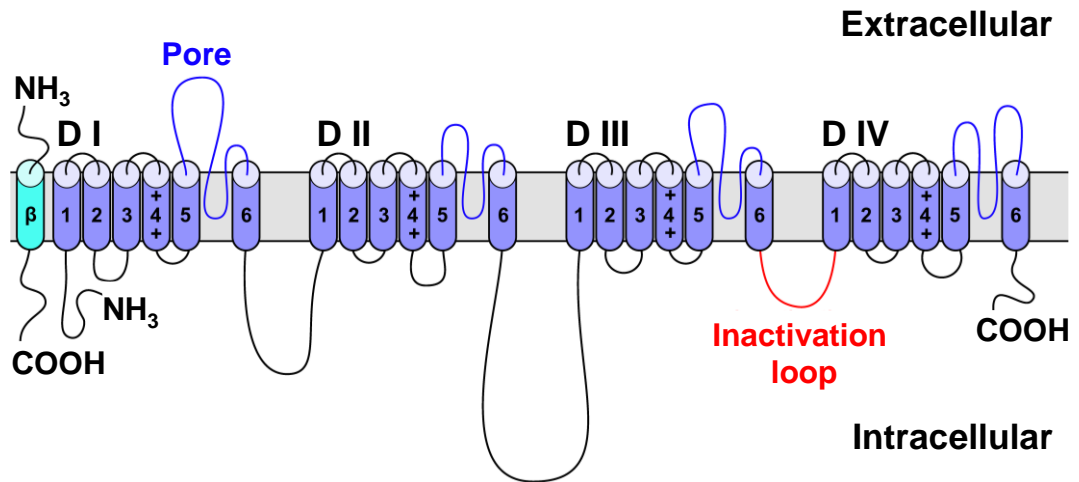


Figure 1.4 Schematic of VGSC Structure. VGSCs at plasma membrane contain a single α subunit and one or more β subunit. VGSC β subunits (cyan) have an intracellular carboxyl terminal (COOH) and external N-terminal (NH₃) Ig-like domain. VGSC α subunits contain four homologous domains (D I – D IV), each comprised of six transmembrane segments (1 – 6). Voltage sensing is carried out by segment 4. Na⁺ pore formation exists as a loop between segments 5 and 6 of each domain. Inactivation loop is formed by an intracellular loop (red) between segment 6 of D III and segment 1 of D IV. NH₃ and COOH termini are both intracellular. Adapted from (Denomme et al., 2019).

1.4.1.1 Expression of VGSC subunits in cancer

Non-invasive ^{23}Na MRI shows solid brain, breast and prostate tumours have raised $[\text{Na}^+]_i$ compared to healthy surrounding tissues (Ouwkerk et al., 2003, 2007; Barrett et al., 2018). VGSC α subunits are overexpressed in many types of solid tumours, whereas β subunits can be either upregulated or downregulated (Figure 1.5). VGSC α subunits are found in gliomas, small-cell lung cancer (SCLC), NSCLC, prostate cancer, colorectal carcinoma (CRCa), cervical cancer, ovarian cancer, mesothelioma, melanoma, neuroblastoma and breast cancer cells and tissues (Blandino et al., 1995; Allen et al., 1997; Bennett et al., 2004; Ou et al., 2005; Fulgenzi et al., 2006; Diaz et al., 2007; Roger et al., 2007; Gao et al., 2010; House et al., 2010; Brackenbury, 2012; Hernandez-Plata et al., 2012; Fraser et al., 2014a; Nelson et al., 2015b; Lopez-Charcas et al., 2021, 2022; Ai et al., 2023). β subunits are dysregulated in NSCLC, prostate cancer, cervical cancer, colorectal cancer and breast cancer (Roger et al., 2007, 2015; Diss et al., 2008; Chioni et al., 2009; Brackenbury, 2012; Hernandez-Plata et al., 2012; Djamgoz et al., 2019).

In highly metastatic MDA-MB-231 cells, a neonatal splice variant of $\text{Nav}_1.5$ ($\text{nNav}_1.5$) is overexpressed, which drives invasion of TNBC cells *in vitro* (Brackenbury et al., 2007; Dutta et al., 2018). Differential splicing of *SCN5A* is developmentally regulated, and occurs in exon 6, encoding domain I segment 3 (DI:S3) (Onkal et al., 2008). $\text{nNav}_1.5$ allows a greater quantity of Na^+ to enter cells when compared to the adult splice variant (Chioni et al., 2010; Fraser et al., 2014a). Importantly, expression of $\text{nNav}_1.5$ is observed in metastatic breast cancer biopsies, and is strongly associated with tumour progression and metastasis (Fraser et al., 2005; Yamaci et al., 2017; Leslie et al., 2024). Levels of $\text{Nav}_1.5$ are negatively correlated with $\text{ER}\alpha$, and positively correlated with HER2 in primary breast tumours (Leslie et al., 2024). Selective $\text{nNav}_1.5$ expression impacts regulation of pH_i and pH_e , enzyme activity and Na^+ and Ca^{2+} exchange. Replacing negative aspartate in $\text{Nav}_1.5$ to a positive lysine in $\text{nNav}_1.5$ at position 211 alters reactions to extracellular chemical factors as well as protein-protein interactions on the plasma membrane (Onkal et al., 2008; Fraser et al., 2014a).

Cell-based studies of CRCa identified $\text{nNav}_1.5$ as the predominant VGSC isoform at mRNA and protein level, whereas $\text{Nav}_1.6$ mRNA levels are significantly lower in CRCa tumours compared to matched healthy tissue (House et al., 2010;

Baptista-Hon et al., 2014; Djamgoz et al., 2019; Lastraioli et al., 2021). Expression of nNav1.5 in human CRCa tumours is significantly associated with decreased progression-free survival and high “Tumour-Node-Metastasis” (TNM) staging (Lastraioli et al., 2021). Pre-cancerous colorectal adenomas also have elevated nNav1.5 expression compared to healthy tissue, suggesting upregulation of VGSCs is involved in malignant development (Lastraioli et al., 2021). In prostate cancer biopsies, immunohistochemistry and RT-PCR revealed variable expression of several VGSC α subunits, namely: Nav1.2, Nav1.3, Nav1.5, Nav1.7 and Nav1.9. (Diss et al., 2005). Nav1.7 transcript levels are most prevalent, being 27-fold higher in prostate tumours compared to healthy prostate tissue (Djamgoz et al., 2019). In cervical cancer cells, Nav1.6 and Nav1.7 transcripts are elevated ~40 and ~20 fold respectively relative to normal tissue, which correspond to functional channels. In particular, Nav1.6 contributes almost one-third of Na⁺ current passing into cervical cancer cells (Hernandez-Plata et al., 2012). Nav1.7 overexpression is detected in gastric cancer biopsies and is associated with increased invasion and proliferation (Xia et al., 2016). In ovarian cancer, levels of Nav1.1, Nav1.3, Nav1.4, Nav1.5 and Nav1.7 mRNA are significantly elevated compared to benign ovarian tumours or normal ovaries. However, Nav1.5 is translated into functional VGSC, and is thought to be a contributing factor in the transition from benign to malignant ovarian cancer (Gao et al., 2010).

All isoforms of β subunits are expressed in prostate cancer cells, however β 1 is most prevalent and is correlated with expression of Nav1.7 (Diss et al., 2008). In breast cancer, β 1 is inversely correlated with Nav1.5 and metastatic potential of breast cancer cells (Brackenbury, 2012; Djamgoz et al., 2019). β 1 mRNA and protein are highly expressed in non-metastatic ER α + MCF-7 breast cancer cells compared to metastatic TNBC MDA-MB-231 cells (Luo et al., 2020). Additionally, in MCF-7 cells β 2 and β 4 mRNA are 20- and 50-fold greater relative to MDA-MB-231 cells, respectively (Chioni et al., 2009). β 2 is also expressed in several models of prostate cancer (Diss et al., 2008; Jansson et al., 2012). In C4-2B cells there is a 15% increase in β 2 protein relative to LNCaP, correlating with castration resistance and disease progression (Jansson et al., 2012). Expression of β 3 is less well characterised in malignant cells, however there is some evidence of low levels of expression in NSCLC and prostate cancer cell lines, and hepatocellular carcinoma (Roger et al., 2007; Diss et al., 2008; Li et al., 2020). Additionally, β 4 is expressed in NSCLC cell lines (Roger et al., 2007). In cervical cancer biopsies, β 4 has low

transcript levels but is still more abundant when compared to non-cervical cancer tissues (Hernandez-Plata et al., 2012). $\beta 4$ is expressed at low levels in prostate cancer cells, but favoured in weakly metastatic LNCaP cells compared to strongly metastatic PC-3 cells (Diss et al., 2008).

Several studies have explored mechanisms contributing to aberrant expression of VGSCs, including: transforming growth factor (TGF)- $\beta 1$ and epidermal growth factor (EGF) signalling, silencing of negative regulator Salt-Inducible Kinase 1 (SIK1), and inhibition of repressor element silencing transcription factor (REST) and HDACs (Kamarulzaman et al., 2017; González-González et al., 2019; Gradek et al., 2019). Concordantly, hypoxia has been linked to synergistic growth factor signalling, SIK1 inhibition and modulating REST nuclear localisation and activity, suggesting hypoxia may be important in dysregulated VGSC expression in solid tumours (Cavadas et al., 2016; Mallikarjuna et al., 2019; Mamo et al., 2020; Pu et al., 2022).

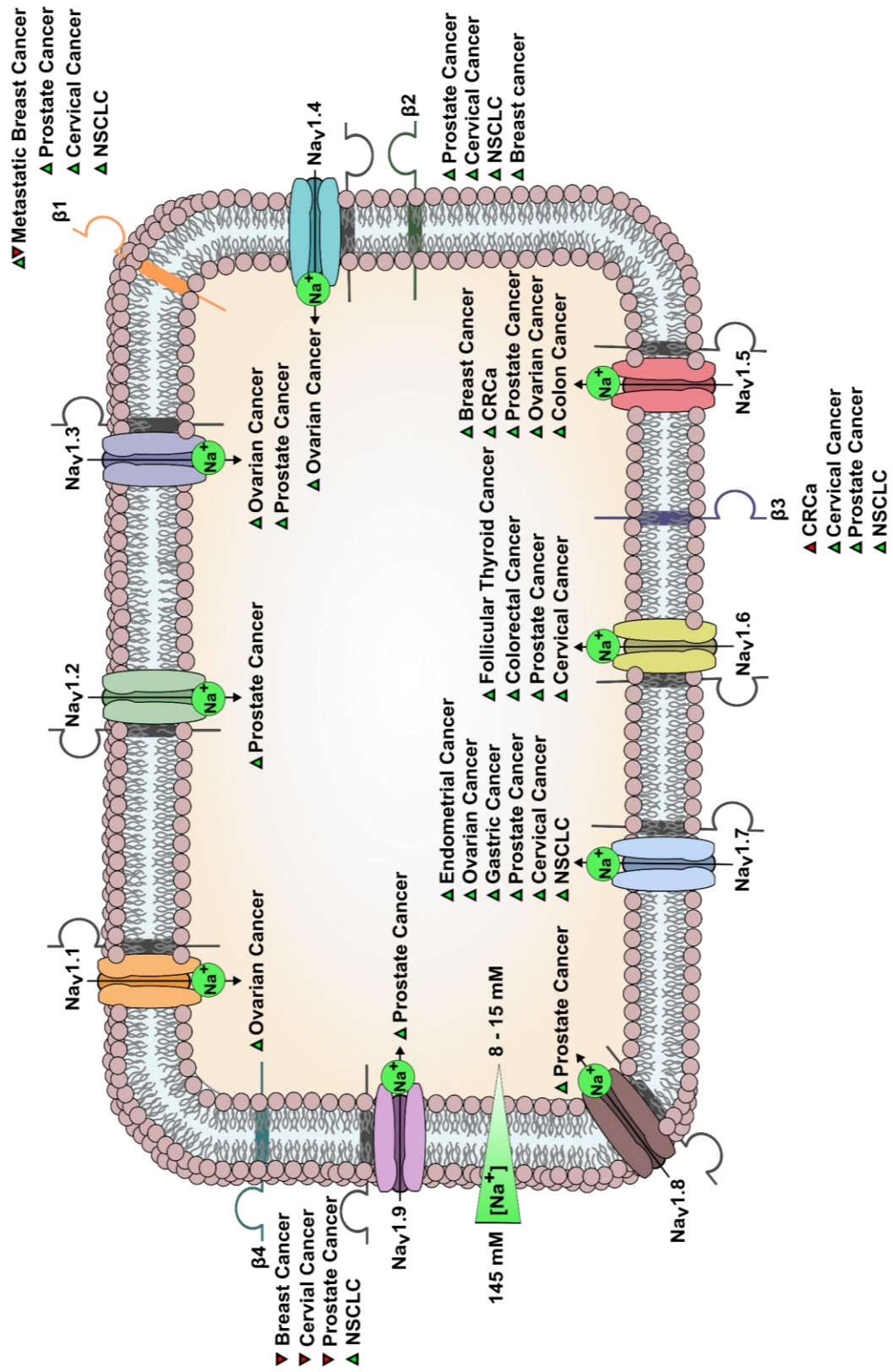


Figure 1.5 VGSCs in solid tumours. VGSC α and β subunits are dysregulated in several solid tumour types. VGSCs are made of one α subunit, and one or more auxiliary β subunits. VGSCs exhibit dysregulated expression in several malignant cancer types, contributing to altered sodium homeostasis in solid tumours. The α subunits of VGSCs are overexpressed (green triangle) in transformed cells relative to matched healthy tissue or cell line counterpart, whereas β subunits can be overexpressed, mutated or under-expressed (red triangle) in malignancies (Malcolm et al., 2023).

1.4.1.2 Tumour progression and VGSC activity

Tumour invasion is an important hallmark of cancer, requiring key changes in cell morphology to enhance mobility and invasion into surrounding stroma (Hanahan and Weinberg, 2000; Martin et al., 2013). Processes involved in this malignant progression include breakdown of surrounding ECM, upregulation of pro-metastatic genes, and dysregulation of cell surface CAMs. Aberrant expression and activity of VGSCs in malignant cells is strongly implicated in driving such processes. VGSC α subunits facilitate cell invasion and metastasis in a variety of cancer types (Diss et al., 2001; Bennett et al., 2004; Fulgenzi et al., 2006; Campbell et al., 2013; Nelson et al., 2014; House et al., 2015; Mohammed et al., 2016; Xia et al., 2016; Li et al., 2020, 2022a; Sui et al., 2021; Erdogan et al., 2023). For effective breakdown of ECM, a low pH_e is optimal for proteolytic MMPs and cathepsins. VGSCs contribute to an acidic ECM, which is particularly favourable for cysteine protease cathepsin B (Giusti et al., 2008). For example, in breast cancer cells $\text{Na}_v1.5$ drives I_{Na} which elevates NKA activity to export Na^+ , increasing ATP demand. $\text{Na}_v1.5$ fulfils additional ATP requirement by increasing the rate of glycolysis, which elevates lactate production and therefore H^+ . To overcome intracellular acidification, $\text{Na}_v1.5$ increases NHE1 activity to export H^+ , facilitating extracellular acidification and therefore sustaining optimal pH_e for MMPs and cathepsins to digest ECM (Gillet et al., 2009; Brisson et al., 2011, 2013; Leslie et al., 2024).

Fast metastasis-promoting I_{Na} is specific to TNBC MDA-MB-231 cells, sensitive to μM TTX and is not observed in weakly metastatic MCF-7 cells (Roger et al., 2003). Expression of $\text{nNa}_v1.5$ specifically confers invasive properties which are diminished upon siRNA knockdown targeting this channel (Roger et al., 2003; Brackenbury et al., 2007). EMT is induced by $\text{Na}_v1.5$ upregulation in invasive breast cancer cell lines, in a manner dependent on loss of SIK1 and concurrent increase in EMT-promoting transcription factor *SNAI1* (Gradek et al., 2019). Additionally, $\text{nNa}_v1.5$ enhances eukaryotic elongation factor-2 kinase (EF2K) expression, which promotes breast tumour growth and lung metastasis by activating tumorigenic drivers including c-Myc and cyclin D1 (Erdogan et al., 2023). In colon cancer, $\text{Na}_v1.5$ is a key transcriptional driver of several pro-migratory signalling pathways including Wnt and MAPK, the latter of which can be negatively regulated in response to VGSC inhibitor lidocaine (House et al., 2010, 2015). JAK-STAT signalling pathway in follicular thyroid carcinoma is activated by $\text{Na}_v1.6$

phosphorylation of JAK2 which enhances cell proliferation, EMT and invasion (Li et al., 2022a). In NSCLC, TTX-sensitive Na⁺ currents through VGSCs promote invasiveness and EGF signalling upregulates expression of Nav1.7, which is crucial for increased invasive potential (Roger et al., 2007; Campbell et al., 2013). Nav1.7 drives endometrial cancer progression, and pharmacological inhibition of this channel significantly impairs cancer cell invasion (Liu et al., 2019). Nav1.7 expression is correlated with NHE1 and metastasis-associated in colon cancer-1 (*MACC1*) in gastric tumours. TTX inhibition of Nav1.7 decreases NF-κB p65 nuclear translocation by p38 activation, inhibiting *MACC1* expression and further reducing NHE1 levels due to impaired c-Jun phosphorylation (Xia et al., 2016)

As members of the Ig superfamily of CAMs, β subunits regulate cell adhesion and migration. β1 forms heterophilic associations with other CAMs and ECM proteins, such as β2, contactin, neurofascin-186 and *N*-cadherin (Kazarinova-Noyes et al., 2001; Ratcliffe et al., 2001; Malhotra et al., 2004; McEwen and Isom, 2004). In MCF-7 cells, high β1 expression corresponds to a weakly invasive phenotype which is reversed by siRNA targeting β1. TNBC cell lines have low levels of β1. Stable transfection of β1 into MDA-MB-231 cells increases adhesion, and decreases migration and proliferation (Chioni et al., 2009). β2 and β4 mRNA are 20- and 50- fold higher in MCF-7 cells compared to MDA-MB-231 cells (Chioni et al., 2009). Conversely, β2 expression in prostate cancer cells, increases association with nerve axons, and enhances cell growth, migration and invasion (Jansson et al., 2012, 2014). β3 is implicated in hepatocellular carcinoma tumorigenicity, by negatively regulating p53 and promoting HepG2 cell proliferation and tumour growth *in vivo* (Li et al., 2020). Loss of β4 protein correlates to high-grade primary and metastatic breast tumours and activated RhoA activity, increased cell migration and metastasis. Overexpressing *SCN4B* in breast cancer cells reduces invasion and tumour progression (Bon et al., 2016). Hypermethylation of *SCN1B* DNA results in loss of β4 in papillary thyroid cancer (PTC) and is associated with decreased recurrence-free survival (Gong et al., 2018). Taken together, β subunits can be anti- or pro-tumorigenic and expression of these molecules could present a novel therapeutic target for some cancer patients or be used as biomarkers for predicting disease outcomes.

1.4.2 NKA and ENaC

NKA was discovered in 1957 in shore crab nerves (Skou, 1957). A functional pump is minimally composed of a catalytic α subunit and an auxiliary β subunit. Some NKAs utilise a tissue-specific γ subunit that belongs to the FXYD family of small membrane proteins (Mercer et al., 1993). There are three highly conserved isoforms of α subunit that are ~87% identical (*ATP1A1*, *ATP1A2*, and *ATP1A3*) encoding $\alpha1 - \alpha3$, and a less-well conserved sperm-specific $\alpha4$ subunit (*ATP1A4*) (McDermott et al., 2015). The β subunit has three isoforms that share ~40% identity (*ATP1B1*, *ATP1B2* and *ATP1B3*) encoding $\beta1 - \beta3$ (Blanco et al., 1994). In addition, there are seven FXYD γ subunits. NKA establishes and maintains electrochemical and osmotic gradients by utilising energy from the hydrolysis of a single ATP molecule to simultaneously export three Na^+ and import two K^+ across basolateral plasma membranes against natural concentration gradients. In kidneys, it is estimated that 50 million NKA are expressed per cell of the distal convoluted tubule, where 2,000 molecules of ATP can be hydrolysed per minute, per K^+ site, at maximum ATP turnover rate (El Mernissi and Doucet, 1984). In neurons, NKA activity is essential as the pump maintains high extracellular $[\text{Na}^+]$ ($[\text{Na}^+]_e$) for efficient firing of action potentials, and reverses postsynaptic Na^+ flux. NKA can use up to 75% of available ATP in a cell (Attwell and Laughlin, 2001; Clausen et al., 2017).

Structurally, the α subunits contain 10 transmembrane helices with extracellular binding sites for K^+ and cardiac glycosides such as ouabain, and intracellular binding sites for ATP and Na^+ on an intracellular catalytic loop (Figure 1.6). The β subunits are type II membrane proteins with a short intracellular N terminus and a larger extracellular C terminus that is glycosylated to release β proteins from endoplasmic reticulum (Tokhtaeva et al., 2010). The β subunits regulate localisation and stabilisation of the α complex in plasma membranes, fine-tune affinity of NKA for Na^+ , K^+ and cardiac glycosides, and establish adhesion contacts with *E*-cadherin and β -catenin (Geering, 2001; de Souza et al., 2014). The γ subunit is not essential for NKA activity and can be delivered to plasma membranes independent of α and β subunits. The function of the γ subunit appears to centre around modifying voltage dependence of K^+ and Na^+ of $\alpha\beta$ complex (Minor et al., 1998; Geering, 2005).

Activity of NKA is coupled with passive Na⁺ influx through ENaCs that are expressed at apical membranes in kidney tubules, lung, reproductive organs and colon (Canessa et al., 1994a; Duc et al., 1994; Hanukoglu and Hanukoglu, 2016). Na⁺ is a major electrolyte in extracellular fluid. Transport of Na⁺ is accompanied by flow of water, which means ENaCs are essential in regulating extracellular fluid volume and blood pressure (Bourque, 2008; Rossier et al., 2015). Na⁺ entry into epithelial cells through ENaC dampens the Na⁺ gradient. As a result, NKAs at basolateral membranes export Na⁺ into the interstitial fluid to reestablish a Na⁺ and osmotic gradient (Feraille and Dizin, 2016). Four homologous ENaC genes are in the human genome: *SCNN1A*, *SCNN1B*, *SCNN1D* and *SCNN1G*, encoding α -, β -, δ -, and γ -ENaC proteins, respectively (Canessa et al., 1994b; Waldmann et al., 1995). Each of the four ENaC subunits share ~28% sequence identity with each other, and ~20% identity with ASIC subunits (Hanukoglu and Hanukoglu, 2016). Expression of ENaC subunits is regulated by epigenetic modifications, where DNA methylation is inversely correlated to ENaC mRNA (Pierandrei et al., 2021). Channel activity is affected by hormones such as aldosterone, which enhances passive Na⁺ current through ENaC by promoting open conformation, without affecting mRNA or protein levels of the channel (Chen et al., 1999). Typical ENaC is comprised of α -, β - and γ -ENaC subunits (Figure 1.6). Each subunit comprises two transmembrane domains which form the ENaC pore. Both N and C termini are located intracellularly, and a large extracellular domain links the two transmembrane domains together (Kashlan and Kleyman, 2011). A novel δ -, β - and γ -ENaC increases Na⁺ current two-fold compared to α -containing channels (Waldmann et al., 1995). However, γ -ENaC is less-well understood owing to mice and rats which are used as animal models to study channel kinetics not expressing this subunit (Paudel et al., 2021).

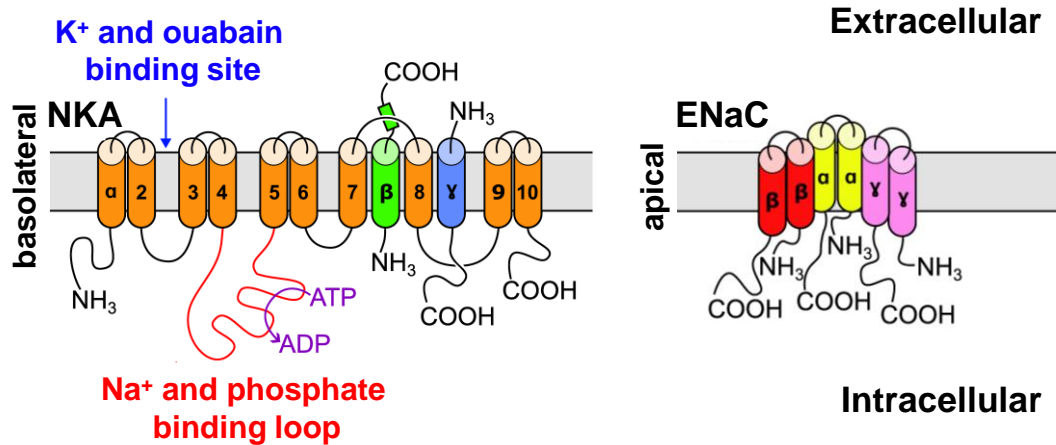


Figure 1.6 Schematic of NKA and ENaC Structures. NKA (left) is comprised of a single catalytic α subunit (orange), a regulatory glycosylated β subunit (green) and a FXYD γ subunit (blue). The α subunit comprises 10 transmembrane segments with NH_3 and COOH termini both on intracellular side of the membrane. Catalytic hydrolysis of ATP to ADP occurs in intracellular Na^+ and phosphate binding loop (red). K^+ (or ouabain) bind to extracellular compartments of α subunit. ENaC (right) comprises α (yellow), β (red) and γ (pink) subunits existing as a heterotrimer. Each subunit consists of two transmembrane helices with internal NH_3 and COOH termini, and an extracellular loop. Adapted from (Gonçalves-de-Albuquerque et al., 2017; Ahmad et al., 2023).

1.4.2.1 Evidence of NKA and ENaC in cancer

Several malignancies have altered expression of NKA and ENaC subunits, with significant clinical implications (Liu et al., 2016; Silva et al., 2021). In CRCa, NKA α 1 expression is decreased compared to normal accompanying mucosa, and α 3 β 1 is the predominant isozyme (Sakai et al., 2004; Baker Bechmann et al., 2016). In CRCa liver metastases, only α 3 β 1 is present, and this combination is not found in healthy liver tissue, implicating this isozyme as a novel biomarker of CRCa progression (Baker Bechmann et al., 2016). Similarly, ENaCs are expressed in CRCa HCT116 and HT29 cells, which are downregulated by resveratrol in an AMPK-dependent manner, significantly increasing apoptosis of cancer cells. The ENaC inhibitor amiloride also significantly decreases CRCa cell viability *in vitro* (Gündođdu and Özyurt, 2023). In aggressive melanoma cell lines and primary cells, α 3 of NKA is abundant. UNBS1450, a cardiac glycoside that specifically blocks NKA activity, significantly blocks pro-tumorigenic activity *in vitro* and *in vivo* (Mathieu et al., 2009). All ENaC isoforms are expressed in human melanoma G-361 cells, with δ -ENaC being most prevalent. However, ENaC's role in neoplastic progression of melanoma has of yet, not been characterised (Yamamura et al., 2008). In clear-cell renal cell carcinoma (RCC), diffuse intracellular NKA α 1 expression was identified by immunofluorescence *in vivo*, relative to basolateral plasma membrane localisation of α and β subunits in normal kidney cells. Additionally, RCC cells have a 95% reduction in β 1 expression, and a corresponding decrease in NKA activity in membranes implicating loss of NKA function as a malignant determinant in clear-cell RCC (Rajasekaran et al., 1999). Decreased expression of NKA β 1 has also been reported in poorly differentiated CRCa, breast and pancreatic cancer lines, and this corresponds to decreased levels of *E*-cadherin and increased Snail expression, linking NKA β 1 to EMT (Espineda et al., 2004). In contrast, *ATP1A1* mRNA expression is elevated and *ATP1A2* is decreased in Luminal A, Luminal B, HER2 and TNBC tumours compared to normal breast tissue (Bogdanov et al., 2017). In *de novo* and acquired endocrine resistant breast cancer cell lines, ouabain treatment significantly inhibits cell proliferation, invasion and motility, suggesting pharmacological attenuation of NKA activity may prolong survival for a population of women with advanced Luminal breast cancers (Khajah et al., 2018). Conversely, high α -ENaC expression in breast cancer is associated with a less aggressive and less proliferative phenotype, whereas decreased α -ENaC levels correspond to a more aggressive mesenchymal subtype (Ware et al., 2021).

1.4.3. Tumour microenvironment and dysregulated Na⁺ homeostasis

Altered Na⁺ homeostasis in the TME is implicated in several hallmarks of cancer, such as sustaining proliferative signalling, activating invasion and metastasis and evading immune response (Prevarskaya et al., 2010; Hanahan and Weinberg, 2011; Leslie et al., 2019). Innate immune system signalling molecules including selectins, chemokines and chemokine receptors are expressed by malignant cells in order to evade detection by infiltrating immune cells and provide additional survival advantages (Coussens and Werb, 2002). Cytokines and chemokines hone leukocytes to the TME, which increase levels of tumour-promoting factors including ROS, tumour necrosis factor (TNF)- α , MMPs, serine and cysteine proteases, interleukins and interferons (Wahl and Kleinman, 1998; Kuper et al., 2000; Coussens and Werb, 2002). High concentration of monocyte chemoattractant protein (MCP) localises tumour-associated macrophages (TAMs) to the TME, with significant clinical implications for patients with CRCa, NSCLC and breast cancer (Schoppmann et al., 2002; Watanabe et al., 2008; Zhang et al., 2013c; Yoshimura et al., 2023). As such, cancer cells direct a variety of immune cells to tumours to support cell survival, promote angiogenesis and drive cancer progression and metastasis (Rossi and Zlotnik, 2000; Schoppmann et al., 2002). One of the most abundant cell types in tumours is cancer-associated fibroblasts (CAFs), which secrete chemokines to enhance recruitment and activation of immune cells and remodel ECM to support growth and metastasis of transformed cells (Servais and Erez, 2013; Tao et al., 2017; Mishra and Banerjee, 2023; Wright et al., 2023).

A link between inflammation, cytokine and chemokine secretion, and Na⁺ transport has been explored (Viviani et al., 2007). Microglia express VGSCs Na_v1.1, Na_v1.5 and Na_v1.6, and NHE1 (Black et al., 2009; Shi et al., 2011). Phenytoin or TTX inhibition of VGSCs, or cariporide targeting of NHE1 decreases phagocytic and migratory capacity of activated microglia (Black et al., 2009; Hossain et al., 2013). Inhibition of NHE1 in lipopolysaccharide (LPS)-stimulated microglia reduces [Na⁺]_i, and decreases proinflammatory and pro-tumorigenic cytokine activities, production of TNF- α , ROS and H₂O₂ (Hossain et al., 2013). DRG neuron cells incubated with pro-tumorigenic chemokine CXCL1 increase TTX-resistant and TTX-sensitive Na⁺ currents, which corresponds to elevated Na_v1.1, Na_v1.7 and Na_v1.8 transcription,

further establishing a connection between immune signalling and Na⁺ transport (Wang et al., 2008).

Cancer cells use growth factors and chemokines secreted by CAFs for protection against immune attack within the TME (Loeck and Schwab, 2023). CAFs enhance solid tumour progression by activating *VEGF*, *CXCL12*, *FGF*, and *PDGF* for angiogenesis, or secreting MMPs to degrade ECM and remove physical barriers impeding cancer cell invasion (Tang et al., 2016; Sahai et al., 2020; Loeck and Schwab, 2023). CAFs express Na⁺/Ca²⁺ exchanger (NCX)-1, which moves Ca²⁺ out of a cell (forward mode) in exchange for Na⁺ into the cell, or vice versa (reverse mode). NCX1 activity is regulated by pH_i, whereby acidic pH_i inhibits forward mode action and affects Na⁺ transport with significant implications for cell growth, proliferation and migration of glioblastoma, pancreatic and gastric cancer cells (Philipson et al., 1982; Hu et al., 2019; Wan et al., 2022; Loeck et al., 2023).

1.4.4 Hypoxia and Na⁺ transport in solid tumours

Hypoxia significantly increases persistent Na⁺ current through VGSCs in cardiac cells, and such an increase in Na⁺ influx is linked to increased invasive capacity of cancer cells (Ju et al., 1996; Hammarström and Gage, 2002; Roger et al., 2003; Fraser et al., 2005; Nelson et al., 2015b; Plant et al., 2020). Na_v1.7 mRNA is elevated in hypoxic rat prostate cancer cells, and is inhibited by the non-selective VGSC inhibitor riluzole (Rizaner et al., 2020). HIF-1 α enhances Na_v1.5 expression in TNBC cells subject to the hypoxia-mimetic agent cobalt chloride (CoCl₂), and siRNA targeting HIF-1 α reduced Na_v1.5 mRNA, cell viability and migration of MDA-MB-231 cells (Dewadas et al., 2019). Hypoxia- and normoxia-mediated invasiveness of CRCa SW620 cells is dependent on persistent Na⁺ currents mediated by nNa_v1.5, and is inhibited by the VGSC blocker ranolazine (Guzel et al., 2019). In primary prostate cancer samples, it is thought that [Na⁺]_i is elevated by hypoxia-induced persistent Na⁺ current through VGSCs occurring in solid tumours (Djamgoz and Onkal, 2013; Djamgoz et al., 2019). Thus, VGSCs upregulated by low O₂ tension could represent novel diagnostic biomarkers, or therapeutic targets that would be responsive to repurposing of VGSC inhibitors ranolazine or riluzole (Diss et al., 2005; Djamgoz et al., 2019).

Hypoxia further disrupts Na⁺ homeostasis via NHE1 and Na⁺ driven bicarbonate transporters (NDBTs) (Shimoda et al., 2006; Carroll et al., 2022). Hypoxia and tumour acidosis are closely linked (Corbet and Feron, 2017). NHE1 is upregulated in hypoxia and drives alkalinisation of pH_i, cell migration and invasion of human tongue squamous cell carcinoma by enhancing MMP-9 activity (Shimoda et al., 2006; Lv et al., 2012; Persi et al., 2018). Besides transcriptional regulation, hypoxia enhances NHE1 activity by phosphorylation of p90 Ribosomal S6 Kinase (p90RSK), causing formation of invadopodia and invasion of fibrosarcoma BT-1080 cells (Lucien et al., 2011). Hypoxia also upregulates SLC4A4 and SLC4A5 NDBTs in breast and colon cancers in a HIF-1 α -dependent manner, which elevates pH_i and promotes EMT and metastasis *in vivo* (Carroll et al., 2022). NDBTs work together with CA9 in regulating pH_i and driving migration of HeLa cells and this is impaired by the CA9 inhibitor acetazolamide (Svastova et al., 2012). NCX1 forms a complex with CA9 and NHE1 in hypoxic tumours which causes extracellular acidosis and cancer cell migration (Liskova et al., 2019). Hypoxia disrupts V_m by decreasing the number of active NKAs at the plasma membrane in a ROS-dependent mechanism, causing endocytosis and proteasomal degradation of the pump (Dada et al., 2003; Gusarova et al., 2009). In contrast, hypobaric hypoxia increases NKA α 2 electrogenic activity and membrane abundance in rat diaphragm and soleus muscles, without affecting total protein content (Kravtsova et al., 2022). Expression of α -, β - and γ -ENaC mRNA is decreased in primary rat alveolar epithelial cells cultured in 1.5% O₂, with a corresponding reduction in Na⁺ transport and active ENaC subunits at apical membranes (Baloglu et al., 2020). Conversely, ENaC is endogenously expressed in rat neuronal cells and is activated during acute hypoxia (Bae et al., 2013). Taken together, hypoxia is implicated in modulating Na⁺ transport in a variety of cell types, but responses are nuanced and context dependent.

1.4.5 The future of targeting dysregulated Na⁺ transport in cancer

VGSCs overexpressed in many solid tumours present novel therapeutic targets for treatment of aggressive malignancies and provide an exciting opportunity to repurpose FDA approved VGSC inhibitors (Roger et al., 2006; Brackenbury and Isom, 2008; Brackenbury, 2012; Fraser et al., 2014b). VGSCs share highly conserved sequences and domain organisation making development of isoform-specific inhibitors challenging, further highlighting a necessity to repurpose existing drugs over investing significant funds, and especially time, in developing new VGSC

inhibitors (Corry, 2018). However, VGSC isoform-specific compounds do exist, with unexplored potential in cancer therapy (Bian et al., 2023). Altered VGSC activity contributes to cardiac arrhythmias, epilepsy, depression and neuropathy (Clare et al., 2000; Fairhurst et al., 2016). Consequently, a wide variety of VGSC inhibitors exist to block aberrant conductance of VGSCs, including ranolazine, phenytoin, lamotrigine and valproate (Mantegazza et al., 2010). Potential of using VGSC inhibitors to halt tumour progression has been explored in models of prostate cancer, breast cancer and colon cancer (Abdul and Hoosein, 2002; Anderson et al., 2003; Angelucci et al., 2006; Fortunati et al., 2008; Li et al., 2012; Papi et al., 2012; Jafary et al., 2014; Fairhurst et al., 2015). Ranolazine or phenytoin inhibition of Nav1.5 reduces breast tumour growth, local invasion and metastasis *in vivo* (Driffort et al., 2014; Nelson et al., 2015b, 2015a). Culture of prostate cancer cells with eicosapentaenoic acid decreases *SCN9A* and *SCN8A* mRNA and reduces proliferation and invasion by inhibiting I_{Na} (Nakajima et al., 2009). Valproic acid in combination with a retinoid ligand of retinoic X receptor significantly reduces HT-29 and LoVo colon cancer cell viability, and further decreases HT-29 invasion by inhibiting MMP expression (Papi et al., 2012). A recent retrospective study of an association between VGSC inhibitor use and survival of patients with colon, breast and prostate cancer found significantly improved cancer-specific survival in patients exposed to class 1c (encainide, flecainide or propafenone) and 1d (ranolazine) antiarrhythmics prior to cancer diagnoses, which are fast and late Na^+ current blockers, respectively (Fairhurst et al., 2023; King et al., 2024). However, patients exposed to VGSC inhibitors used as local anaesthetics, tricyclic antidepressants or anticonvulsants had increased risk of cancer-specific mortality (Fairhurst et al., 2023).

Attenuation of NKA is also being explored as a promising therapeutic avenue. In acute myeloid leukaemia, NKA β subunit *ATP1B1* is poorly expressed in malignant cells of haematopoietic lineage. To maintain V_m cells instead express paralogous *ATP1B3* which is not ubiquitously expressed in other tissues, making inhibition of this subunit an attractive candidate for patients with haematological malignancies (Schneider et al., 2024). Cardiac glycosides are naturally-derived selective inhibitors of NKA used in clinic for treatment of some types of cardiac arrhythmias (Calderón-Montaña et al., 2014). Bufalin suppresses proliferation in melanoma and NSCLC (Yang et al., 2006; Jiang et al., 2010). HIF-1 α is also inhibited by bufalin through activation of mTOR signalling in hepatocellular

carcinoma (Wang et al., 2016). In BT20 breast cancer and DU145 prostate cancer cells, ouabain significantly inhibits cell proliferation by inducing NKA endocytosis and degradation (Tian et al., 2009). LNCaP cells are sensitive to cardiac glycoside digitalis treatment compared to other prostate cancer cell lines, significantly increasing intracellular Ca^{2+} influx, causing cell toxicity and apoptosis (Yeh et al., 2001). Therefore, repurposing cardiac glycosides as novel cancer therapeutics may further attenuate malignant progression when used in combination with current standard of care chemotherapeutics, or alongside surgery and radiotherapy.

1.5 Project rationale, hypotheses and aims

Work carried out in this thesis focused on understanding contributions of $\text{ER}\alpha$ and hypoxia in dysregulating important cellular processes that propel breast cancer progression. Studies were set out to expand understanding of $\text{ER}\alpha$ regulation of Pol III transcription of tRNA and other class III genes in breast cancer cells. In addition, hypoxia, and to a lesser extent $\text{ER}\alpha$, were explored to delineate mechanisms of aberrant Na^+ transport which stimulates breast cancer progression. Thus, the two main hypotheses tested in this thesis were: i. $\text{ER}\alpha$ is recruited to many tRNA genes in breast cancer cells by a protein tethering mechanism, where it can coordinate rapid changes in expression in response to oestradiol (Hah et al., 2011), and ii. Hypoxia and $\text{ER}\alpha$ significantly contribute to dysregulated Na^+ homeostasis in breast cancer by affecting expression of Na^+ channels, including VGSCs, NKA and ENaC.

The main aims of this thesis were:

1. To quantify $\text{ER}\alpha$ enrichment at tRNA genes and delineate the mechanism in which $\text{ER}\alpha$ is recruited to Pol III-transcribed loci (Chapter 3).
2. To identify robust reference genes (RGs) that can be used for sensitive RT-qPCR investigations of hypoxia-mediated gene expression alterations in a panel of breast cancer cell lines (Chapter 4).
3. To determine to what extent hypoxia and $\text{ER}\alpha$ alter Na^+ transport in TNBC and Luminal A breast cancers (Chapter 5).

2. Materials and Methods

2.1 Cell culture

2.1.1 Cell lines

MCF-7 breast cancer cells used in Chapter 3 were purchased from the European Collection of Authenticated Cell Cultures (ECACC). For Chapter 4 and Chapter 5, T-47D cells were provided by Dr. Andrew Holding (University of York), originally from ATCC, and MDA-MB-231 cells were a gift from Prof. Mustafa Djamgoz (Imperial College London). Both T-47D and MDA-MB-231 cell lines were authenticated once by Eurofins commercial STR profiling (Masters et al., 2001). The MCF-7 and MDA-MB-468 cell lines were newly purchased at the time of experiments from the American Type Tissue Collection (ATCC), which confirms STR profiling of cell lines at time of purchase.

2.1.2 Maintenance of cells

Culture medium for MCF-7 cells used in chapter 3 was Dulbecco's Modified Eagle Medium (DMEM; Gibco; 41966-029), supplemented with 10% (v/v) Foetal Bovine Serum (FBS; Gibco; 10270-098) and 1% (v/v) Penicillin Streptomycin (PenStrep; Gibco; 15070-063). Hormone-free medium was phenol red-free DMEM (Gibco; 31053-028), supplemented with 10% (v/v) hormone-depleted FBS (see 2.1.2.3) and 1% (v/v) PenStrep. Cells were maintained in a humidified CO₂ Galaxy B 150-400 incubator at 37°C and 5% CO₂. Culture medium for all cell lines used in Chapter 4 and Chapter 5 was DMEM supplemented with 5% (v/v) FBS (Gibco; 10270-106) and no antibiotic. Cell lines were maintained in a humidified Binder C150 CO₂ incubator at 37°C and 5% CO₂. All breast cancer cell lines throughout this thesis were grown in 75 cm² treated canted neck culture flasks with vented caps (Corning) for standard culturing needs.

To passage cells, medium was removed, and cells were washed with phosphate buffered saline (PBS; Gibco; 14200-067) before incubating at 37°C in 0.05% Trypsin-EDTA (Gibco; 15400-054) in PBS. Once cells had detached, Trypsin-EDTA was inactivated by the addition of culture medium and cell suspension was transferred to 15 ml falcon tubes before centrifugation (5 minutes, 1,200 Revolutions

Per Minute (RPM)). The supernatant was then aspirated, and remaining cell pellets were resuspended in culture media and split 1:5 into new 75 cm² flasks. A maximum of 10 passages following thawing from long-term liquid nitrogen (LN₂) storage were performed before cells were discarded and fresh cell stocks from LN₂ were established.

2.1.2.1 Cell counts and viability check

Cells were detached from the surface of the flask with 0.05% trypsin-EDTA in PBS, as described in Section 2.1.2. Following centrifugation, cell pellets were resuspended in 10 ml culture medium. An aliquot of cell suspension was diluted 1:5 in Trypan Blue (Sigma-Aldrich; T8154) and viable and non-viable cells were counted using a Neubauer Haemocytometer and a Motic AE2000 inverted microscope. The number of cells/ml and cell viability was calculated by:

$$\text{Cells/ml} = \frac{\text{\# of cells counted}}{\text{\# of squares counted}} \times 10^4 \times \text{dilution factor}$$

$$\% \text{ Viability} = \frac{\text{\# of viable cells counted}}{\text{\# total number of cells counted}} \times 100$$

2.1.2.2 Hypoxic culture of breast cancer cell lines

For studies investigating hypoxic effects, breast cancer cell lines were incubated in a humidified Baker Ruskin InvivO₂ oxygen workstation (37°C, 1% O₂, 5% CO₂ and 96% N₂) for the duration of the experiment.

2.1.2.3 Charcoal stripping Hormone-depletion of FBS

Activated charcoal (Sigma-Aldrich; C9157) and Dextran (mW 60-76 kDa; Sigma-Aldrich; D8821) were incubated in FBS at a concentration of 1% (w/v) and 0.1% (w/v) respectively, for one hour at room temperature with agitation. The charcoal was pelleted by centrifugation (15 minutes, 12,000 g). The supernatant was vacuum filtered, and filter sterilised using a 0.2 µm stericup. This process was repeated twice to allow for sufficient depletion of endogenous steroids present in FBS. FBS stripping protocol was provided by Dr. Andrew Holding (Department of

Biology, University of York) who adapted the Dembinski method of hormone-depletion (Dembinski et al., 1985).

2.1.3 Freezing and thawing of breast cancer cells

Stocks of breast cancer cell lines were routinely kept in LN₂ for long-term storage. To generate a cell line stock, early passage cells were grown to confluency in 75 cm² flasks before trypsinisation and pelleting as described in 2.1.2. Cell pellets were resuspended in 1 ml freezing medium comprised of 70% (v/v) DMEM, 20% (v/v) FBS and 10% (v/v) dimethylsulfoxide (DMSO; PanReac AppliChem A3672,0100). Cells in freezing medium were divided into 200 µl aliquots in Greiner cryovials and placed at -80°C for one week before being transferred to a LN₂ dewar.

To thaw cells, cryovials were removed from LN₂ and 1 ml of warmed culture medium (37.5°C) was used to gently wash over the frozen suspension. Thawed cells were transferred to a 75 cm² flask containing culture medium and left overnight to adhere to the flask surface. Culture medium containing DMSO was removed the following day and replaced with fresh culture medium.

2.1.4 *Mycoplasma* testing of cells

Breast cancer cells used in Chapter 3 were tested for the presence of *Mycoplasma* by sending MCF-7 culture media to Eurofins Genomics *Mycoplasma* Service. Here, cells were cultured for one week without antibiotic. Following trypsinisation, cell culture supernatant was boiled at 95°C for 10 minutes. Supernatant was briefly centrifuged to pellet cellular debris, and a sample of medium was collected and sent off to Eurofins for PCR analysis to test for the presence of *Mycoplasma* species: *M. arginini*, *M. fermentans*, *M. orale*, *M. hyorhinis*, *M. hominis*, *M. genitalium*, *M. salivarium*, *M. synoviae*, *M. pirum*, *M. gallisepticum*, *M. pneumoniae*, *M. yeatsii*, *Spiroplasma citri* and *Acholeplasma laidlawii*.

Routine *Mycoplasma* testing of breast cancer cell lines used in Chapter 4 and Chapter 5 was conducted in-house monthly. For this, cancer cell lines were seeded onto sterile 13 mm coverslips (Scientific Laboratory Supplies (SLS)) in 4-well plates for 24 - 48 hours, until they had reached 50-80% confluency. Cells were fixed to coverslips with 100% methanol and allowed to air dry. Coverslips were

mounted onto microscopy slides with ~20 μ l ProLong Gold DAPI slide fix (Invitrogen; P36935). The slide was left to air dry and sealed by clear nail varnish. The presence of DAPI-stained contaminating *Mycoplasma* DNA was investigated using fluorescence microscopy (Russell et al., 1975).

2.1.5 Pharmacology

Breast cancer cell lines were treated with various pharmacological agents during the work carried out in Chapter 3 and Chapter 5 (Table 2.1). Here, drugs were prepared in breast cancer culture medium and applied to cells. Cell lines were incubated at 37°C, 5% CO₂ and 20% or 1% O₂ for the duration of experiments. As a negative control, vehicle-only experiments were conducted in parallel to the drug treatment experiments.

Table 2.1 Pharmacological agents and their properties

Drug	Source	Final Drug Concentration	Final Vehicle Concentration	Molecular Target
17 β -Oestradiol	Sigma-Aldrich E2758	100 nM	0.1% EtOH	ER α
4-hydroxytamoxifen	Sigma-Aldrich H6278	12.5 μ M	0.1% EtOH	ER α
Fulvestrant	Thermo 16627042	100 nM	0.1% EtOH	ER α
Ouabain octahydrate	Calbiochem 4995	100 nM	0.001% DMSO	NKA

2.2 Chromatin immunoprecipitation

Per ChIP sample, 1×10^7 MCF-7 cells were used. For chromatin extraction, cells were crosslinked with 1% formaldehyde in culture medium (v/v) for eight minutes at room temperature. Crosslinking was inhibited by adding equal volume (v/v) of ice-cold quenching buffer to the formaldehyde-culture medium solution (250 mM Glycine/ 2mM EDTA / TBS). Cells were scraped off the flask surface, and cell suspension was collected into 50 ml falcon tubes followed by centrifugation (5 minutes, 1,100 g, 4°C). Cells were washed twice more in ice cold quenching buffer with centrifugation (5 minutes, 1,100 g, 4°C). To lyse cell membranes, cells were washed in Buffer 1 (50 mM HEPES-KOH [pH 7.5], 140 mM NaCl, 1mM EDTA, 10% glycerol, 0.5% NP-40, 0.25% Triton X-100) for 10 minutes at 4°C. Cell lysate was collected by centrifugation (5 minutes, 1,100 g, 4°C), supernatant was discarded and pellet was resuspended and washed in Buffer 2 for 10 minutes at 4°C, in order to remove detergents (10 mM Tris-HCl [pH8.0], 200 mM EDTA, 1 mM EGTA). Nuclei were harvested by centrifugation (5 minutes, 1,100 g, 4°C), supernatant was discarded, and pellet was resuspended in Buffer 3 to disrupt nuclei (10 mM Tris-HCl [pH 8.0], 100 mM NaCl, 1 mM EDTA, 0.5 mM EGTA, 0.1% sodium deoxycholate, 0.5% N-lauroylsarcosine). Nuclei were then sonicated (Bioruptor; 30 seconds per sonication cycle for a total of 12 sonication cycles). Finally, 0.1% of Triton X-100 was added to nuclear extract and debris was pelleted by centrifugation (5 minutes, 5,000 g, 4°C).

For immunoprecipitation, Protein A Dynabeads™ were briefly washed in blocking solution (0.5% BSA in PBS (w/v)) and collected on a magnetic stand. Next, Dynabeads were incubated in blocking solution containing either pre-immune, anti-RNA Polymerase III serum or anti-GTF3C5, anti-ER α or anti-FOXA1 antibodies for 2 hours at 4°C. Full details of antibodies and their dilutions are provided in Table 2.2. Protein A: antibody-containing beads were added to nuclear lysate and mixed overnight at 4°C. Next, Dynabeads were collected on a magnetic rack and washed in RIPA buffer (50 mM HEPES-KOH [pH 7.6], 500 mM LiCl, 1 mM EDTA, 1% NP-40, 0.7% Na-Deoxycholate) for six washes (5 minutes per wash, 4°C). Beads containing sample were washed with wash buffer (50 mM NaCl Tri- EDTA) twice (5 minutes per wash, 4°C) before incubating with elution buffer (100 mM NaHCO₃ + 1% SDS (w/v)) at 50°C for 10 minutes. Crosslinking was reversed by heating at 55°C overnight. Chromatin was collected by adding 1.8x (v/v) SPRY beads and placing samples on

a magnetic stand after 10 minutes incubation with gentle agitation. Beads were washed twice with 80% ethanol. Finally, DNA was eluted from SPRY beads by resuspending in dH₂O and heating for 5 minutes at 65°C for a total of two elution steps. Eluates were pooled together.

Table 2.2 Antibody Information and Experimental Applications. Abbreviations: Chromatin immunoprecipitation (ChIP), co-immunoprecipitation (Co-IP), western blot (WB), immunocytochemistry (ICC).

Molecular Target	Source	Molecular Weight (kDa)	Application	Dilution
1901 pre-immune (no target)	Prof. R. J. White, University of York	N/A	ChIP	1.5:100
1901 RNA Polymerase III	Prof. R. J. White, University of York	156	ChIP	1.5:100
Ab2 GTF3C1	Prof. R. J. White, University of York	220	Co-IP	1:1,000
3208 GTF3C2	Prof. R. J. White, University of York	110	Co-IP	2.5:100
GTF3C5	Bethyl; A301-242A	63	ChIP Co-IP	1.5:100 2.5:100
ER α	Abcam; Ab32063	67	ChIP WB ICC	3:1,000 1:1,000 1:500
FOXA1	GeneTex; GTX100308	49	ChIP	4:1,000
Ki67	Abcam; Ab15580	319	ICC	1:300
AlexaFluor488 2 $^{\circ}$ goat anti-rabbit	Invitrogen; 10236882	N/A	ICC	1:500
HIF-1 α	Cell Signalling; 36169	96	WB	1:1,000
HIF-2 α	ProteinTech; 26422-1-AP	96	WB	1:1,000
α -Tubulin	Merck; T6199	50	WB	1:5,000
β -actin	Santa Cruz; sc-47778	43	WB	1:1,000
Anti-rabbit IgG HRP-linked 2 $^{\circ}$	Cell Signalling; 7074S	N/A	WB	1:10,000
Anti-mouse IgG HRP-linked 2 $^{\circ}$	Cell Signalling; 7076	N/A	WB	1:10,000

Table 2.3 Sequence Information of Primers Used in ChIP-qPCR and RT-qPCR Studies.

All primers were made into 10 mM stocks before final dilution in qPCR reaction mixture.

Gene	Primer Sequences 5' – 3'	Method	Source
<i>Pro-TGG-1-1</i>	FWD: TTCTGGCTCGTTGGTCTAG REV: AGGGGCTCGTCCGG	ChIP-qPCR	(Malcolm et al., 2022)
<i>Arg-CCF-2-1</i>	FWD: GTGGCCTAATGGATAAGGCATCA REV: CTAATCTCACGCGACCCAGATG	ChIP-qPCR	(Malcolm et al., 2022)
<i>Met-CAT-1-1</i>	FWD: ACTAGGTGCCTCGTTAGCGCAG REV: ACAAATTATTGTGCCCCGTGTGAGG	ChIP-qPCR	(Malcolm et al., 2022)
<i>Leu-AAG-2-4</i>	FWD: CATATTGCAGCTGGGTAGCG REV: CCGAAGAGACTGGAGCCTTA	ChIP-qPCR	(Malcolm et al., 2022)
<i>RMRP</i>	FWD: AAGAAGCGTATCCCGCTGAG REV: GCACTGCCTGCGTAACTAGA	ChIP-qPCR	(Malcolm et al., 2022)
<i>RN7SL1</i>	FWD: TATCCGACCGCCGGGC REV: AGTGGCTATTACAGGCGCG	ChIP-qPCR	(Malcolm et al., 2022)
<i>GREB1 ERE</i>	FWD: GTGGCAACTGGGTCATTCTGA REV: CGACCCACAGAAATGAAAAGG	ChIP-qPCR	(Sun et al., 2007)
Gene Desert	FWD: CATCCCTGGACTGATTGTCA REV: GGTTGGCCAGGTACATGTTT	ChIP-qPCR	(Petrie et al., 2019)
<i>nSCN5A</i>	FWD: CATCCTCACCAACTGCGTGT REV: AAAGTTCGAAGAGCCGACAA	RT-qPCR	(Brackenbury et al., 2007)
<i>SCN8A</i>	FWD: AGACCATCCGCACCATCCTG REV: TGTCAAAGTTGATCTTCACG	RT-qPCR	This Thesis
<i>SCN9A</i>	FWD: TATGACCATGAATAACCCAC REV: TCAGGTTTCCCATGAACAGC	RT-qPCR	This Thesis
<i>CA9</i>	FWD: GTGCCTATGAGCAGTTGCTGTC REV: AAGTAGCGGCTGAAGTCAGAGG	RT-qPCR	(Hou et al., 2014)
<i>OAZ1</i>	FWD: ATAAACCCAGCGCCACCATC REV: AGGGAGACCCTGGA ACTCTCA	RT-qPCR	(Malcolm et al., 2024)
<i>ACTB</i>	FWD: CCTCGCCTTTGCCGATCC REV: GGATCTTCATGAGGTAGTCAGTC	RT-qPCR	(Zhang et al., 2005)

<i>TBP</i>	FWD: GTGAGGTCGGGCAGGTTC REV: AAGAAACAGTGATGCTGGGTCA	RT-qPCR	(Malcolm et al., 2024)
<i>RPL27</i>	FWD: ATCGCCAAGAGATCAAAGATAA REV: TCTGAAGACATCCTTATTGACG	RT-qPCR	(de Jonge et al., 2007)
<i>RPL30</i>	FWD: ACTGCCCAGCTTTGAGGAAAT REV: GCCACTGTAGTGATGGACACC	RT-qPCR	(Malcolm et al., 2024)
<i>RPLP1</i>	FWD: AGGAAGCTAAGGCTGCGTTG REV: GCATTGATCTTATCCTCCGTGACT	RT-qPCR	(Malcolm et al., 2024)
<i>CCSER2</i>	FWD: GACAGGAGCATTACCACCTCAG REV: CTTCTGAGCCTGGAAAAGGGC	RT-qPCR	(Hauck et al., 2022)
<i>GUSB</i>	FWD: CTGTACACGACCCCACCAC REV: ATTCGCCACGACTTTGTT	RT-qPCR	(Caradec et al., 2010)
<i>TFRC</i>	FWD: GGACGCGCTAGTGTTCTTCT REV: CATCTACTTGCCGAGCCAGG	RT-qPCR	(Kaneko et al., 2020; Zheng et al., 2022)
<i>PGK1</i>	FWD: GGAGCTCCTGGAAGGTAAAGTC REV: TCCTGGCACTGCATCTCTTG	RT-qPCR	(Malcolm et al., 2024)
<i>EPAS1</i>	FWD: CACCTCGGACCTTCACCACC REV: TCCTCTCCGAGCTACTCCTTTTC	RT-qPCR	(Malcolm et al., 2024)
<i>ATP1A1</i>	FWD: CTAGCTCCCTCCACTTGGCT REV: ATCACGTCCAACCCCTTC	RT-qPCR	This Thesis
<i>NHERF1</i>	FWD: CACCAGCGAGGAGCTGAAT REV: AGTCTAGGATGGGGTCGGAG	RT-qPCR	This Thesis
<i>SCN1B</i>	FWD: CACAGGAGAATGCCTCGGAA REV: TTACGGCTGGCTCTTCCTTG	RT-qPCR	This Thesis
<i>SFXN2</i>	FWD: GGGAATCTGCGTGAAGGACA REV: CTGGCAGCAAGATCATCCCA	RT-qPCR	This Thesis
<i>SFXN3</i>	FWD: CAAATCCCTCACCAAGCACC REV: GAGTAGCCAAGCCTCTGACC	RT-qPCR	This Thesis
<i>SLC16A3</i>	FWD: CTTTGGCATCTCCTACGGCA REV: CATCCAGGAGTTGCCTCCC	RT-qPCR	This Thesis

2.3 Immunocytochemistry and confocal microscopy

MCF-7 cells were seeded onto sterile 16 mm coverslips to a density of 1×10^5 cells/well of a 12-well plate in hormone-free DMEM. Cells were incubated for four days, with daily PBS washes and replenishment of hormone-free media. Experiments were started on the fifth day. At experimental end point, culture medium was aspirated, and cells were fixed to coverslips by incubation with 4% paraformaldehyde (Thermo Fisher; 043368-9M) in PBS (v/v) for 10 minutes at room temperature. Coverslips were washed twice with PBS and cells were permeabilized with 0.1% Triton X100 for 15 minutes. Coverslips were washed twice with PBS and blocked with 1% BSA in PBS (BSA-PBS w/v) for 30 minutes. The cells were washed twice with PBS and incubated with anti-ER α or anti-Ki67 antibody in BSA-PBS for one hour (Table 2.2). Coverslips were washed three times with PBS and incubated with AlexaFluor488 goat anti-rabbit antibody in BSA-PBS for 1 hour. Coverslips were washed three times with PBS and left to air-dry for 15 minutes before mounting onto glass slides using EverBrite Hardset Mounting Medium with DAPI (Biotium; 23004). Cells were visualized on a Zeiss LSM 710 confocal microscope with an AxioImager.M2 upright platform using 405 and 488 nm laser lines, for DAPI and ER α or Ki67, respectively.

2.4 Wound healing assay

MCF-7 and T-47D cells were seeded to a density of 5×10^6 cells/well of a 6-well plate. Three biological replicates were carried out. Cells were left for 72 hours to attach and grow to complete confluency. A single wound was created down the centre of each well using a P1000 pipette tip before culture medium was aspirated and wells were washed for a total of three times with PBS to ensure detached cells from the wound were removed. Next, cells were treated with 100 nM Fulvestrant or corresponding vehicle, or 100 nM Ouabain or corresponding vehicle made up in culture medium (Table 2.1). Initial wound size was measured at 15 intersections (Figure 2.1) on a Motic AE2000 inverted microscope with an eyepiece graticule. Plates were then either returned to the incubator at 20% O₂ or placed into the InvivoO₂ hypoxic workstation at 1% O₂ for 24 hours. Finally, wound closure was measured at each of the 15 intersections, and Motility Index (MI) was calculated by:

$$MI = 1 - \left(\frac{\text{wound size after 24 hours}}{\text{initial wound size}} \right)$$

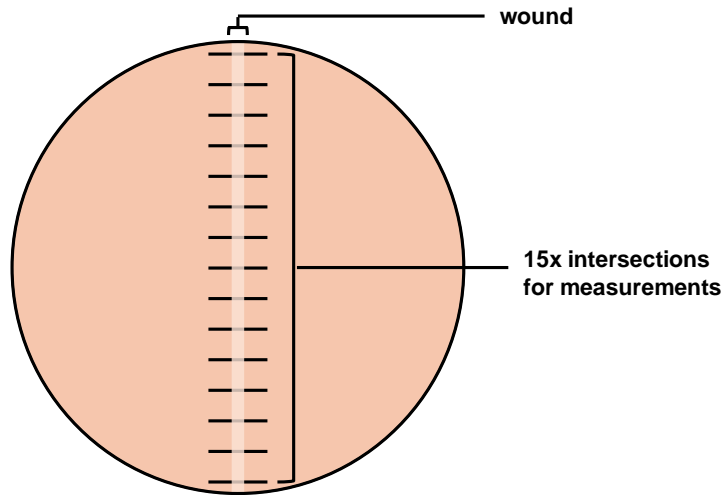


Figure 2.1 Example Figure to Demonstrate how Measurements were Taken in Each Well to Calculate MI.

2.4 RNA Extraction, cDNA synthesis and quantitative PCR

2.4.1 RNA extraction

MCF-7, T-47D, MDA-MB-231 and MDA-MB-468 cell lines were seeded to a density of 2×10^5 per well of a 6-well plate and were left for a minimum of 24 hours before starting experiments. Each experiment comprised three biological replicates, consisting of three technical replicates. At the end of the experimental time point, all samples from each biological replicate were collected on the same day. To collect samples, cold QIAzol lysis reagent (QIAGEN; 79306) was used as per manufacturer's guidelines. To isolate nucleic acids, phenol/chloroform with isopropanol precipitation was carried out as previously described (Toni et al., 2018). To enhance nucleic acid yield, GlycoBlue Coprecipitant (Invitrogen; AM9515) was included in the isolation step. Nucleic acid was re-suspended in 0.2 μm -filtered RNase-free water (Ambion; AM9937). To remove contaminating DNA, samples were treated with DNase I (New England BioLabs; M0303S) and incubated at 37°C for 10 minutes. DNase I reaction was inhibited by the addition of 5 mM EDTA and heat inactivation at 75°C for 10 minutes. Final RNA concentration and purity were measured using a NanoDrop™ One/OneC Microvolume UV-Vis Spectrophotometer (Thermo Fisher Scientific). RNA with an A260/280 of ≥ 2.0 was used.

2.4.2 Luminal A cell line sample preparation for RNA-sequencing

MCF-7 and T-47D cells were seeded to a density of 6,500 cells/cm² in 10 cm culture dishes and left for 24 hours before starting experiments. MCF-7 and T-47D experiments were comprised of triplicate and quadruplicate biological replicates, respectively. At the end of the experiment, culture medium was aspirated, and cells were washed with PBS before trypsinisation for 5 minutes to detach cells. Trypsin was inactivated by culture media and cells were pelleted by centrifugation (300 g, 5 minutes). The supernatant was discarded, and the cell pellet was washed with 1 ml of PBS and centrifuged (500 g, 5 minutes). The supernatant was discarded, and the cell pellet was resuspended in PBS-RNA later (Sigma; R0901) and stored at -80°C prior to RNA extraction. Samples were thawed and PBS was added prior to RNA isolation with Monarch Total RNA mini kit (New England Biolabs; T2010S), as per manufacturer guidelines.

2.4.2 cDNA synthesis

RNA was reverse transcribed using SuperScript IV cDNA Synthesis Kit as per manufacturer's instructions (Invitrogen; 18091050). The final reaction volume was 20 μl , consisting of 1 μl 0.1M DTT, 4 μl SSIV buffer, 1 μl RNaseOUT, 1 μl SSIV Enzyme, 1 μg of RNA in 11 μl of dH_2O , 1 μl of random hexamer and 1 μl of 10 mM dNTP. Reactions were carried out on a Bioer LifePro thermocycler, comprising an initial step at 65°C for 05:00 (mm:ss), followed by 23°C for 10:00 (mm:ss), 55°C for 10:00 (mm:ss), 80°C for 10:00 (mm:ss) and then 4°C for 10:00 (mm:ss). cDNA was diluted to 5 ng / μl in 0.2 μm -filtered RNase-free water (Ambion; AM9937). A standard curve was prepared from pooled RNA from each biological replicate, and diluted to 20 ng / μl , 4 ng / μl , 0.8 ng / μl , 0.16 ng / μl and 0.032 ng / μl . Samples were stored at -30°C until further downstream analysis.

2.4.3 qPCR for ChIP experiments

Quantitative PCR (qPCR) was performed on a QuantStudio™ 3 qPCR system (Thermo Fisher). Duplicate reactions were performed using LUNA Universal qPCR Master Mix (NEB; M3003L). Final reaction volume was 20 μl and consisted of 10 μl LUNA, 1 μl primer stock, 8 μl dH_2O and 1 μl of ChIP sample. For input, 2 ng of DNA (2 ng / μl) was used. All details of primer sequences are provided in Table 2.3. RT-qPCR cycling parameters comprised an initial denaturation step at 95°C for 03:00 (mm:ss), followed by 42 cycles of 00:20 (mm:ss) at 95°C, 00:15 (mm:ss) at 62°C and 00:15 (mm:ss) at 72°C. Melt curve analysis was carried out in the final cycle of the RT-qPCR by increasing the temperature from 60°C to 95°C at 0.1°C per second.

2.4.4 qPCR

RT-qPCR was performed using the QuantStudio™ 7 qPCR system (Thermo Fisher) in MicroAmp optical 384-well reaction plates (Applied Biosystems; 4309849) sealed with Expell™ optical sealing membranes (CAPP; 510400C). Technical reactions were performed in duplicate using 2X SYBR Green SuperMix (Applied Biosystems; 4385612). Each reaction mixture had a final working volume of 12 μl , containing 6 μl SuperMix, 1 μl 10 μM primer stock (Table 2.3) and 4 μl of 5 ng / μl cDNA. For primer design, National Centre for Biotechnology Information (NCBI)

Primer BLAST was used to generate primer pair sequences that span the exon-exon junction with an amplicon size of between 70 and 200 bp and an optimal melting temperature of $60^{\circ}\text{C} \pm 3^{\circ}\text{C}$. All primer sequences were run through NCBI Primer BLAST to ensure no unintended gene targets could be amplified, but predicted transcript variants of the same gene were allowed. Primers were purchased from Integrated DNA Technologies.

For the standard curve, 80 ng, 16 ng, 3.2 ng, 0.64 ng and 0.128 ng of pooled cDNA was used. No-template reactions were included as a negative control. RT-qPCR cycling parameters comprised an initial denaturation step at 95°C for 01:35 (mm:ss), followed by 40 cycles of 00:03 (mm:ss) at 95°C and 00:30 (mm:ss) at 60°C . Melt curve analysis was carried out in the final cycle of the RT-qPCR by increasing the temperature from 60°C to 95°C at 0.1°C per second.

2.4.5 qPCR analysis

Following qPCR, reaction summaries were exported from Thermo Fisher Design and Analysis Data Gallery and analysed in Microsoft Excel. A standard curve was used to calculate primer efficiency (PE) using the equation:

$$\text{PE}\% = (10^{(-1/m)} - 1) * 100$$

where m denotes the slope of the standard curve. Then,

$$\text{PE} = \text{SUM}(\text{PE}\%/100) + 1.$$

Efficiency-corrected Ct values (CtE) were calculated using the equation

$$\text{CtE} = \text{SUM}(\text{Ct} * (\text{Log}(\text{PE})/\text{Log}(2)))$$

mRNA expression (mE) of normoxic reference genes was determined by

$$\text{mE} = 10^{((\text{CtE} - a)/m)}$$

Where a refers to the Y intercept.

2.5 Protein extraction and western blotting

2.5.1 Protein extraction

In Chapter 3, cells were washed with ice-cold PBS and collected in lysis buffer (150 mM NaCl, 20 mM Tris pH 8, 1 mM EDTA, 0.5 % NP-40 and protease inhibitor cocktail). In Chapter 4, cells were washed with ice-cold PBS and collected in RIPA buffer (Merck; R0278) with cOmplete™ EDTA-free protease inhibitor cocktail (Sigma-Aldrich; 05892791001) and PhosSTOP™ phosphatase inhibitor (Roche; 04906845001). Samples were left to sit on ice for 10 minutes and then centrifuged to pellet cellular debris (16,000 g, 10 minutes, 4°C). Supernatant was collected for western blot analysis and pellet was discarded.

2.5.2 Co-immunoprecipitation

Protein lysate was pre-cleared by incubating with Protein A magnetic beads (Pierce: 88846) for 2 hours with rotation at room temperature. Magnetic beads were collected on a magnetic stand and lysates were transferred to fresh Eppendorf tubes. Samples were incubated overnight at 4°C with anti-ER α antibody, anti-GTF3C5 antibody or anti-GTF3C2 antisera (Table 2.2). A “mock” was prepared by incubating magnetic beads overnight without antibody. Protein A magnetic beads were washed three times with PBST and added to samples. Antibody-protein complexes were isolated and purified by incubation with protein A magnetic beads for 2 hours with rotation at room temperature. Magnetic beads were collected and washed three times in lysis buffer. Antibody-protein complexes were eluted from magnetic beads by incubating in Laemmli Buffer + β -Mercaptoethanol at 95°C for 5 minutes and quenching on ice.

2.5.3 Western blot

Cell lysate was prepared 1:4 (v/v) in Laemmli sample Buffer (Bio-Rad; 1610747) with β -mercaptoethanol (1:9 v/v) and boiled at 100°C for 5 or 15 minutes. Samples were quenched on ice, briefly centrifuged and loaded onto a 10% or 12% polyacrylamide gel (Table. 2.4). Samples were brought through the stacking gel by applying 70 V for 15 minutes. Samples were then resolved at 120 V until sample dye was at the bottom of the gel.

For Chapter 3, gels were equilibrated in 20% EtOH (v/v) for 10 minutes with gentle rocking, rinsed in dH₂O loaded onto an iBlot™ 2 nitrocellulose transfer stack (Invitrogen; IB23001), and transferred in an iBlot™ 2 Gel Transfer Device (Invitrogen; 15217995) using a default program of 25 V for 7 minutes. Nitrocellulose membranes were blocked overnight at 4°C in blocking solution comprised of 5% (w/v) non-fat dairy milk (Marvel) and 1% (w/v) polyvinylpyrrolidone (PVP) in PBS with 0.1% (v/v) Tween 20 (PBST). Membranes were washed three times in PBST (5 minutes per wash) before incubating at room temperature for one hour in anti-ER α or anti- β -actin antibodies (Table 2.2) prepared in 5% (w/v) BSA, 1% (w/v) PVP and 0.05% (w/v) sodium azide in PBST. Membranes were washed three times in PBST (5 minutes per wash) and incubated at room temperature for two hours in anti-rabbit (ER α) or anti-mouse (β -actin) IgG HRP-linked antibody (Table 2.2) in 5% (w/v) BSA and 1% (w/v) PVP in PBST. Membranes were washed three times in PBST (5 minutes per wash). Finally, membranes were incubated for 5 minutes in SuperSignal™ West Pico PLUS Chemiluminescent Substrate (Thermo Fisher; 34580) and imaged on the iBright FL500 imager.

For Chapter 4, gels were loaded onto Trans-Blot Turbo Mini polyvinylidene difluoride (PVDF) membranes (Bio-Rad; 1704156EDU) and transferred in a Trans-Blot Turbo Transfer Device (Bio-Rad; 1704150) using a default 1.5 mm gel program of 25 V for 10 minutes. Nitrocellulose membranes were blocked at room temperature for 1 hour in a blocking solution comprised of 4% (w/v) non-fat dairy milk (Marvel) in Tris-buffered saline (TBS) with 0.1% (v/v) Tween 20 (TBST). Membranes were washed three times in TBST (5 minutes per wash) before incubating overnight at 4°C in anti-HIF-1 α , HIF-2 α or α -Tubulin antibodies (Table 2.2) prepared in blocking solution. Membranes were washed three times in TBST (5 minutes per wash) and incubated at room temperature for one hour in anti-rabbit (HIF-1 α and HIF-2 α) or anti-mouse (α -Tubulin) IgG HRP-linked antibody (1:4,000 v/v (Table 2.2)) in blocking solution. Membranes were washed three times in TBST (5 minutes per wash). Membranes were incubated for 5 minutes in western blotting luminol reagent (Santa Cruz; sc-2048) and imaged on the iBright FL500 imager.

2.5.2.1 Densitometry Analysis of HIF α and α -Tubulin bands

ImageJ was used to carry out densitometry analysis of protein bands following image development. The “rectangle” tool was used mark out individual lanes containing HIF- α and α -Tubulin bands. The *Analyze > Gels* functions were used to plot each lane, and the “wand” tool was used to measure the area under the curve (AUC) for each band in each lane. AUC values were used to normalise HIF-1 α or HIF-2 α band density to corresponding α -Tubulin band density

$$\text{Normalised density} = \frac{\text{AUC of HIF-}\alpha}{\text{AUC of }\alpha\text{-Tubulin}}$$

Fold change of normalised HIF-2 α after 8 or 48 hours in hypoxia was compared to normoxic (0 hour) normalised HIF-2 α band density

$$\text{Fold Change} = \frac{\text{Normalised hypoxic HIF-2}\alpha}{\text{Normalised normoxic HIF-2}\alpha}$$

Table 2.4 Western blot polyacrylamide gel recipes.

Reagent	Stacking	12% Resolving	10% Resolving
30% Acrylamide / 0.8% bisacrylamide	0.98 ml	9 ml	7.5 ml
4x Tris-Cl/SDS, pH 6.8	1.9 ml	-	-
4x Tris-Cl/SDS, pH 8.8	-	5.6 ml	5.6 ml
dH ₂ O	4.6	7.9 ml	9.4 ml
10% Ammonium Persulfate (w/v)	37.5 μ l	75 μ l	75 μ l
TEMED	7.5 μ l	15 μ l	15 μ l

2.6 Bioinformatic approaches to investigate ER α association with tRNA genes in breast cancer cell lines and patient specimens

2.6.1 Acquiring MCF-7, MDA-MB-231 and clinical breast cancer ER α and FOXA1 ChIP-seq datasets

Publicly available ChIP-seq datasets are available from the Encyclopaedia of DNA Elements (ENCODE) or the National Institutes of Health Sequence Read Archive (NIH SRA). Specific information regarding the datasets used in this thesis is in Table 2.5.

To access datasets from the NCBI SRA, usegalaxy.org (version 21.05.rc1) was used to acquire files in *Fastq* format with “download and extract reads in FASTA/Q format from NCBI SRA”. Next, *Fastq* files were converted to Binary Alignment and Map (BAM) format. For this, Bowtie2 was implemented to map sequencing reads against a reference genome (Table 2.5).

Table 2.5 Details of Public ChIP-Seq Datasets.

Repository and Experiment ID	File ID	Target	Tissue Type	Source
ENCODE ENCSR463GOT	ENCFF365BIT	ER α	MCF-7 (CRISPR insertion: stable C-terminal LAP-tag containing eGFP, fused to <i>ESR1</i>)	(ENCODE Project Consortium, 2012)
	ENCFF063JMY			
SRA PRJNA147213	SRR1021787	ER α	MCF-7	(Ross-Innes et al., 2012; Caizzi et al., 2014)
	SRR1021788			
	SRR1021789			
	SRR1021801	FOXA1		
	SRR1021803			
	SRR1021749	ER α	Invasive Ductal Carcinoma	
	SRR1021750			
	SRR1021756			
	SRR1021758			
	SRR1021790	ER α	ZR-75-1	
	SRR1021765	ER α	Metastasis	
	SRR1021766			
SRR1021767				
SRA PRJNA129093	GSM560853	ER α	MDA-MB-231 (stable expression of a wildtype ER α construct)	(Stender et al., 2010)

2.6.2 EaSeq for the quantification of transcription factor enrichment

ChIP-Seq datasets were uploaded into EaSeq “Datasets”. Complete tables of tracked GRCh38 (hg38), GRCh37 (hg19) and NCBI36 (hg18) tRNA genes, or hg38 snoRNA and miRNA genes were downloaded from the UCSC Table Browser, (available at <https://genome.ucsc.edu>) and imported as EaSeq “Region Set”. Complete RefSeq mRNA genome assemblies were downloaded directly into “Region Sets” from EaSeq. To quantify transcription factor peaks at tRNA or protein coding genes, EaSeq “quantify” tool was used. This tool counts the number of reads from the “Dataset” that overlaps with the specified regions of interest in the “Region set”. For this process, default setting of “normalize signal to a size of 1000 bp” was unchecked. Quantification analyses were performed at ± 500 bp from the start of tRNA genes. A wider window was used for protein coding genes if necessary. Quantification values are referred to as “Q-values” in this thesis. Data visualisation was performed using EaSeq “heatmap”, “average signal intensity plot” and “filltrack” tools. EaSeq is available at <http://easeq.net> (Lerdrup et al., 2016).

2.6.3 Characterisation of ER α -bound tRNA genes based on their role in cellular processes

Classification of tRNA gene function was previously conducted in order to characterise their primary role in cellular processes of proliferation, differentiation or other processes by Gingold *et al.* (Gingold et al., 2014). To determine if tRNA genes enriched with ER α signals were more involved in differentiation or proliferation, the top 50 ER α -bound tRNA genes from the ENCODE MCF-7 ChIP-seq dataset were independently compared against the Gingold classifier list using Excel conditional formatting.

2.6.4 tRNA gene coordinate remapping

To determine overlap between ER α -associated tDNA in MCF-7 cells aligned to hg38 and hg18 invasive ductal carcinoma samples, NCBI genome remapping service was implemented to remap hg38 tDNA coordinates to NCBI36 hg18 tDNA coordinates (available at <https://www.ncbi.nlm.nih.gov/genome/tools/remap>). Of the 631 hg38 tDNA coordinates provided, 80% were successfully remapped (Malcolm et al., 2022).

2.7 Motif analysis

Motif investigations were conducted in high confidence tRNA genes with the largest ER α Q-values following analysis of ENCODE and Ross-Innes MCF-7 ER α CHIP-seq datasets (n = 19). The tRNA sequences \pm 20 kbp were obtained using the NCBI Gene database and supplied to the Multiple Expectation Maximization for Motif Elicitation (MEME) Suite CentriMo (v 5.3.0) to search for known sequences, using default settings. Sequence motifs of the TFIIIC-recognised conserved A box (TRGYNNARNNG) and B box (RGTTCRANTCC), and of the ERE (GGTCAnnnTGACC) or half EREs (GGTCA; TGACC) were supplied.

2.8 Analysing public qPLEX-RIME data

Multiplexed (qPLEX) Rapid Immunoprecipitation Mass spectrometry of Endogenous proteins (RIME) was performed in MCF-7 cells and five independent ER α + human breast cancer tumours and compared to IgG controls. Data were acquired from Papachristou *et al.* supplementary data sets 2, 8 and 11 (Papachristou *et al.*, 2018).

2.9 Reference gene candidate selection and validation

2.9.1 Analysis of public RNA-seq data to identify reference genes

High throughput RNA-seq datasets of 32 breast cancer cell lines cultured in 20% or 1% O₂ for 24 hours are available from the NCBI Gene Expression Omnibus (GEO; Series Accession: GSE111653) (Ye *et al.*, 2018; Godet *et al.*, 2019). Using the University of York's Viking 2 cluster, we recovered paired-end fastq files for hypoxic and normoxic MCF-7, T-47D, MDA-MB-231 and MDA-MB-468 breast cancer cells with *fastq-dump* (Table 2.6). Low-quality reads were trimmed with *trimmomatic* (ILLUMINACLIP: TruSeq3-PE.fa:2:30:20 LEADING:3 TRAILING:3 SLIDINGWINDOW:4:15 MINLEN:36) and fastQC reports were generated with *fastQC*. Reads were pseudoaligned to the GRCh38.p14 annotation (release 111) and quantified using *kallisto*. Hierarchical Data Format (h5) files containing quantified reads for each experiment were input into RStudio (version 4.3.3). Here, quantified reads were aggregated on the gene level using *sleuth_prep* (*gene_mode* = TRUE) for differential analysis.

Table 2.6 SRA Accession Numbers. Hypoxic (1% O₂, 24 hours) and Normoxic Breast Cancer Cell Lines from BioProject PRJNA437670, Series GSE111653 (Ye et al., 2018; Godet et al., 2019)

SRA Run Accession number	Breast Cancer Cell Line	Breast Cancer Subtype	Environmental Oxygen Status
SRR6822831	MCF-7	Luminal A	Hypoxic
SRR6822832			Normoxic
SRR6822837	MDA-MB-231-PSOC	Basal B	Hypoxic
SRR6822838			Normoxic
SRR6822841	MDA-MB-468	Basal A	Hypoxic
SRR6822842			Normoxic
SRR6822857	T-47D	Luminal A	Hypoxic
SRR6822858			Normoxic

2.9.2 Stability score determination

To determine relative stability across a selection of common reference genes (RGs), and generate a shortlist of RG candidates, normalised reads in transcript per million (TPM) at common RGs in hypoxia and normoxia were assessed independently for each cell line. A shortlist of RG candidates was selected based on (i) the appearance of the RG in literature searches and/or (ii) had a calculated similarity (s) score of ≤ 0.3 between the 20% and 1% O₂ conditions in at least two of the breast cancer cell lines. s was calculated by $s = 1 - \text{MIN}(A,B) / \text{MAX}(A,B)$ (Microsoft Excel), where A is the read count value for a gene in 1% O₂, B is the read count value for a gene in 20% O₂, MIN refers to the smallest value between A and B and MAX determines the maximum value between A and B. Additionally, s scores were calculated across remaining RNA-seq datasets of 28 breast cancer cell lines previously described (GSE111653), by accessing author-generated TPM data available in “GSE111653_GilkesSalmonCounts.csv.gz” from NCBI GEO (Ye et al., 2018; Godet et al., 2019).

2.9.3 RefFinder for RG selection

Following RT-qPCR (Section 2.4), CtE values were supplied to RefFinder, (<https://www.ciidirsinaloa.com.mx/RefFinder-master>) for determination of most stable reference genes to be used in normoxic vs. hypoxic breast cancer cell lines (Xie et al., 2012). RefFinder is a comprehensive program which employs computational RG analysis tools GeNorm (Vandesompele et al., 2002), NormFinder (Andersen et al., 2004), BestKeeper (Pfaffl et al., 2004) and the comparative ΔCt method (Silver et al., 2006) to rank candidate RGs based on the ranking from each RG analysis tools.

2.10 RNA-seq analysis of ER α + breast cancer cell lines

Experimental design, execution and sample preparation was carried out by Dr. Susanna Rose from Dr. Andrew Holding’s lab (University of York). I carried out bioinformatic analysis of RNA-seq data generated by these experiments described in 2.10.1 – 2.10.3. After RNA extraction samples were sent for Illumina next generation sequencing (NGS), at the University of York Bioscience Technology Facility, Genomics Laboratory. cDNA libraries were prepared (by the Genomics lab in the Bioscience Technology Facility at the University of York) from 1 ug total RNA

from each sample using the NEBNext Ultra II Directional Library prep kit for Illumina in conjunction with the NEBNext® Poly(A) mRNA Magnetic Isolation Module (New England Biolabs), according to the manufacturer's instructions. A 13-minute fragmentation time was used when eluting mRNA from polyA magnetic beads. Amplification of the final libraries involved 8 cycles of PCR using the NEBNext multiplex Oligos from Illumina (New England Biolabs). The samples were pooled at equimolar ratios, then run for paired-end 150 base sequencing on an Illumina NovaSeq 6000 instrument.

2.10.1 Preparation of RNA-seq datasets

RNA-seq files were stored on the University of York's Viking 2 HPC. Datasets were handled as described in 2.9.1, including *trimmomatic* to remove low-quality reads, psuedoalignment to GRCh38.p14 annotation with *kallisto* and quality checks of RNA-seq data with *fastQC*.

2.10.2 Differential expression and gene set enrichment analysis

To conduct differential gene expression analysis (DGEA), h5 files containing kallisto-quantified reads for each experiment were input into RStudio (version 4.3.3). Here, *biomaRt* was used to generate a data frame containing human transcript and gene ID's from Ensembl (release 111). Next, *DESeq2* was implemented to investigate differential gene expression analysis in each cell line. Due to the experimental setup (Figure 2.2), the following comparisons could be made:

- **vehicle_normoxia** vs. fulvestrant_normoxia
- **vehicle_normoxia** vs. vehicle_hypoxia
- **vehicle_normoxia** vs. fulvestrant_hypoxia
- **vehicle_hypoxia** vs. fulvestrant_hypoxia
- **vehicle_hypoxia** vs. fulvestrant_normoxia
- **fulvestrant_normoxia** vs. fulvestrant_hypoxia

Where the object is written in **bold**, this signifies the control condition in which comparisons were made against. For DGEA, *DESeq2* undertakes the Wald test to determine significant differential gene expression. Here the null hypothesis is that there is no differential expression between two sample groups (log fold change = 0).

A significant result is reported where $p < 0.05$. To control for false discovery rate (FDR) the Benjamini-Hochberg (BH) method is implemented, generating *Padj* scores (Benjamini and Hochberg, 1995).

To carry out GSEA, *clusterProfiler* was used. This allows identification of coordinated differential regulation of sets of genes which collectively may be involved in a specific molecular function (MF) or biological process (BP) (Subramanian et al., 2005; Yu, 2022, 04 / 24 / 2022). Following DGEA, ranked gene lists were created using significantly differentially expressed genes (*DESeq2*; $padj < 0.05$) ordered by Log_2FC , and GSEA was implemented to investigate which MFs, or BPs are significantly enriched in each experimental comparison. Additionally, MFs or BPs associated with Na^+ transport and homeostasis were specifically looked for during using *grep* command to search for “sodium” in GSEA outputs. To report significantly enriched gene sets, *clusterProfiler* incorporates three main elements:

1. Calculation of an enrichment score which represents the degree to which an a priori defined set of genes in a gene set are over-represented at the top or bottom of a ranked *DESeq2* list (ranked in order of $\text{Log}_2\text{FoldChange}$)
2. Estimation of enrichment score significance to generate a p -value using a permutational approach. Specifically, a Kolmogorov-Smirnov-like test is implemented (Subramanian et al., 2005)
3. Adjustment for multiple hypothesis testing and false discovery rate control with the BH method.

2.11 Statistical analysis

Statistical analysis was performed on raw (non-normalised, unless stated otherwise) data using GraphPad Prism 8.0.2. RNA-seq statistics were determined using *DESeq2* and *clusterProfiler* as described in 2.10.3. Multiple comparisons of normally distributed data were made using ANOVA with Dunnett’s, Tukey’s or Sidak’s post hoc tests. Pairwise statistical significance was determined with Student’s unpaired t-tests. Statistical testing of contingency tables was carried out with Fisher’s exact test. Results were considered statistically significant where $p < 0.05$, or $padj < 0.05$ for DGEA (Benjamini and Hochberg, 1995; Mistry et al., 2017; Love et al., 2024). Levels of significance used: * $p < 0.05$, ** $p < 0.01$ and *** $p < 0.001$.

3. Investigating ER α localisation at tRNA genes in ER α + Breast Cancer Cell Lines and Patient Breast Tumours

3.1 Introduction

RNA polymerase III (Pol III) is the largest of the three RNA polymerase enzymes that transcribe the human genome and is essential for the transcription of small non-coding (nc)RNAs, including 5S rRNA, tRNA and U6 spliceosome nuclear RNA (Cramer, 2002; Dieci et al., 2007; Vannini and Cramer, 2012). Due to the fundamental role ncRNAs play in regulating transcription, RNA processing and translation, mechanisms controlling their transcription are tightly regulated during the cell cycle and coupled to growth and differentiation (Dumay-Odelot et al., 2010). The recruitment of Pol III to its target genes is directed by promoter architecture, of which there are three main types (Type I, II and III). For Type II ncRNA, including tRNA, internal A and B box elements are bound by the hexameric complex TFIIIC, which in turn recruits TFIIIB upstream of the TSS, followed by Pol III at its target genes (Schramm and Hernandez, 2002; Ramsay and Vannini, 2018). Several tumour suppressors have been identified to negatively control Pol III transcription, including RB, p54, PTEN and BRCA1 (White et al., 1996; Cairns and White, 1998; Woiwode et al., 2008; Veras et al., 2009). Inactivation of such tumour suppressors, or activation of oncogenes Ras and Myc has been strongly implicated in many malignancies, including breast and ovarian tumours (White et al., 1996; Cairns and White, 1998; Johnson et al., 2000; Gomez-Roman et al., 2003; White, 2005; Woiwode et al., 2008; Veras et al., 2009; Grewal, 2015).

Where tRNA are concerned, the observation that breast tumours exhibit significantly increased tRNA levels relative to healthy tissues has been reported, though the mechanism of aberrant induction is not yet fully understood (Pavon-Eternod et al., 2009). Additionally, dysregulated tRNA expression has been identified in several other types of cancer, including but not limited to oesophageal, bladder, lung and prostate cancers (Zhang et al., 2018). In 2011, some insight into the potential driving force behind tRNA overexpression in breast cancer was first described. Here, global run on (GRO)-sequencing demonstrated significant oestradiol-mediated induction of 32% of tRNA genes within a 10 - 160 minute treatment window in MCF-7 cells (Hah et al., 2011). The rapid nature of this increased tRNA expression in response to oestradiol suggests a primary and direct mechanism of induction. To the best of our knowledge, this study by Hah *et al.* is the

only significant large-scale investigation implicating ER α in regulating the tRNA^{ome}. However, the ER α has been shown to occupy tRNA^{Leu} and 5S rRNA promoters in MCF-7 cells, enhancing their alcohol-mediated expression, an effect that can be repressed by modulating ER α activity with tamoxifen (Zhang et al., 2013b; Zhong et al., 2014; Fang et al., 2017). Together, these findings implicate the ER α in regulating tRNA gene expression in breast cancer cells. Additionally, some evidence suggests that the ER α may interact directly with Pol III transcriptional machinery, as well as recruit essential co-regulators such as p300 to tRNA promoters to enhance transcription efficiency (Mertens and Roeder, 2008; Zhang et al., 2013b; Zhong et al., 2014; Fang et al., 2017). Notably, a previous study by Finlay-Shultz *et al.* identified PgR but not ER α to be significantly associated with tRNA genes in patient-derived xenograft tumours, mediated by a physical interaction between PgR and Pol III (Finlay-Schultz et al., 2017).

3.1.1 Aims and hypotheses

The first hypothesis of this Chapter was that the ER α is directly associated with many tRNA promoters in breast cancer cells, where it can elicit rapid induction of tRNA expression in response to oestradiol (Hah et al., 2011). Secondly, the ER α is directed to target tDNA loci either through a canonical DNA binding mechanism, or a protein tethering mechanism, as seen for protein-coding gene targets of the hormone receptor. These hypotheses were tested by:

- Analysing public ER α ChIP-seq datasets from breast cancer cell lines, primary breast tumours and metastatic patient samples to quantify ER α recruitment to tRNA genes,
 - Confirming major findings with ChIP-qPCR.
- *In silico* analysis of tRNA sequences to search for proximal and distal canonical ERE motifs to test a DNA-binding mechanism of ER α recruitment
- Comparing Pol III, TFIIIC and FOXA1 enrichment at tDNA loci with or without ER α by ChIP-qPCR in MCF-7 cells to investigate the role of ER α in PIC assembly.
- Analysing qPLEX-RIME datasets from MCF-7 cells and primary breast tumours to identify proteins strongly interacting with ER α , to explore protein-protein interactions that direct ER α to target tRNA promoters.
 - Validating results with co-immunoprecipitation.

3.2 Results

3.2.1 Cellular localisation of ER α in MCF-7 breast cancer cells is responsive to hormone stimulation

First, the effect of hormone stimulation on the cellular localisation of ER α was assessed *in vitro* in MCF-7 breast cancer cells. This was an important consideration, as MCF-7 cells were to be used as the primary cell line for investigating mechanisms of ER α -dependent altered tRNA gene expression in ER α + breast cancer. Prior to hormone stimulation, MCF-7 cells were serum starved for four days with daily PBS washes to ensure complete removal of exogenous hormone present in culture medium. MCF-7 cells were stimulated with either 100 nM oestradiol or corresponding vehicle for 24 hours, and ER α expression and localisation were determined by immunocytochemistry (ICC). Here, ICC revealed a diffuse localisation of ER α in cytosol and nuclei of MCF-7 cells that were treated with the vehicle control for 24 hours (Figure 3.1). In contrast, strong induction of ER α localisation to nuclei is observed in MCF-7 cells stimulated with oestradiol, with moderate cytosolic distribution detected (Figure 3.1).

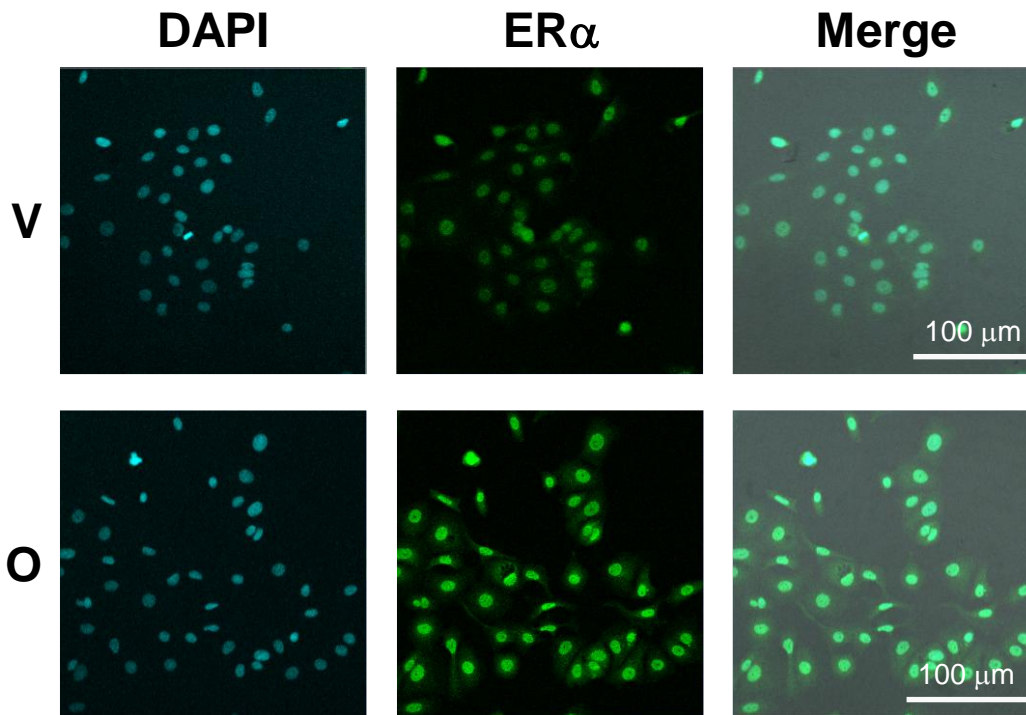


Figure 3.1 The ER α is Localised in Cytosol and Nuclei of MCF-7 Cells. MCF-7 cells were stimulated with 100 nM oestradiol (O) or corresponding vehicle (V) for 24 hours. Immunocytochemistry was carried out to determine cellular localisation of ER α in MCF-7 cells with or without hormone. Images are split into nuclei staining with DAPI (blue), ER α (green) and merge of DAPI and ER α .

To further demonstrate MCF-7 cell line suitability for downstream investigations of ER α and tRNA transcription mechanisms, changes in proliferation due to oestradiol stimulation or negative regulation of ER α by tamoxifen in MCF-7 cells was studied. ICC of nuclear protein Ki67 was used as a positive marker of MCF-7 cells actively undergoing cell division (Gerdes et al., 1983, 1991). Here, ICC analysis of Ki67-stained nuclei demonstrated that most serum-starved vehicle-treated MCF-7 cells were exhibiting cell cycle arrest, as shown by the low proportion of cell nuclei positive for Ki67 expression (Figure 3.2a). Conversely, stimulation of MCF-7 cells with oestradiol for 24 hours resulted in great enrichment of nuclei positively stained for Ki67, suggesting cells are re-entering the cell cycle and are proliferating in response to hormone. Quantification of the proportion of cells positive for Ki67 shows significant increase in the number of actively proliferating MCF-7 cells in response to oestradiol, when compared to vehicle treated cells (Figure 3.2b). Finally, 12.5 μ M of ER α antagonist tamoxifen was added alone or in conjunction with 100 nM oestradiol. The specified concentration of tamoxifen was selected as it has previously been shown to compromise ethanol-induced mRNA and protein expression of Brf1, a key regulator of Pol III activity and tRNA expression, and of great importance to the aims being tested further in Chapter 3 (Fang et al., 2017). In this Chapter, addition of tamoxifen alone or with oestradiol significantly inhibited MCF-7 cell re-entry into the cell cycle (Figure 3.2a – Figure 3.2b).

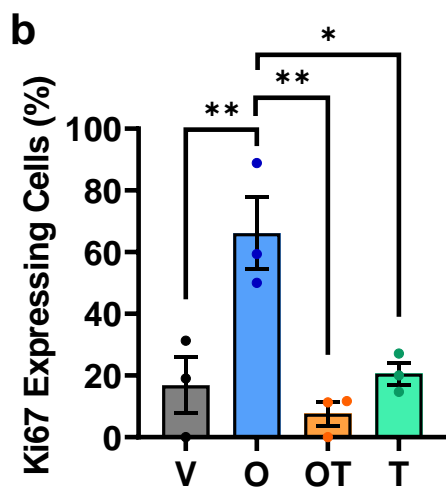
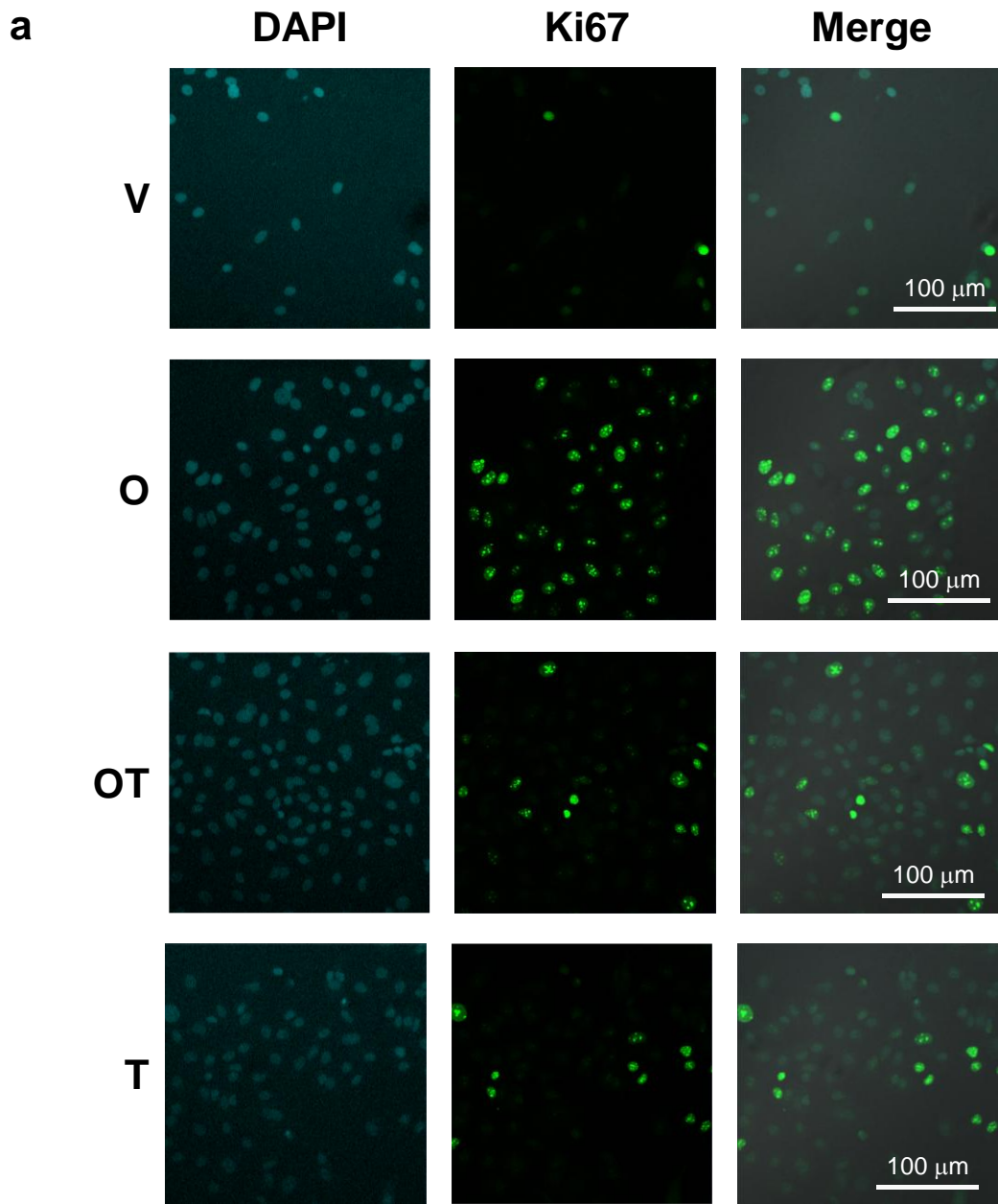


Figure 3.2 MCF-7 Breast Cancer Cells Proliferate in Response to Oestradiol. MCF-7 cells were stimulated with 100 nM oestradiol (O), 100 nM oestradiol and 12.5 μ M Tamoxifen (OT), 12.5 μ M Tamoxifen alone (T), or the corresponding vehicle (V) for 24 hours. **(a)** Immunocytochemistry of Ki67 in MCF-7 breast cancer cell lines. Images are split into nuclei staining with DAPI (blue), Ki67 (green) and merge of DAPI and Ki67. **(b)** Quantification of Ki67 stained MCF-7 breast cancer cells (%) following 24-hour treatment with 100 nM oestradiol (O), 100 nM oestradiol and 12.5 μ M Tamoxifen (OT), 12.5 μ M Tamoxifen alone (T), or vehicle (V). One-way ANOVA with Tukey's multiple comparisons was performed. * $p < 0.05$, ** $p = < 0.01$. Error bars are \pm SEM. $n = 3$.

In summary, MCF-7 cells to be used in this Thesis for the basis of investigating ER α -mediated dysregulated tRNA synthesis in breast cancer showed (i) expected expression of ER α , which was appropriately translocated to the nucleus upon hormone stimulation and (ii) demonstrated conventional proliferation responses to oestrogen and tamoxifen, in line with previous observations (Xu et al., 2013; Tian et al., 2018). Therefore, MCF-7 cells were suitable for experiments investigating the relationship between the ER α , Pol III and tRNA gene expression.

3.2.2 The localisation of ER α at tRNA genes in ER α + cell lines is widespread

To investigate the extent to which tRNA genes are under the positive regulation of oestradiol signalling previously suggested by Hah *et al.* in 2011, replicate ER α ChIP-seq datasets carried out in MCF-7 cells were obtained from ENCODE (ENCSR463GOT) and interrogated for identification of potential tRNA targets of the steroid receptor (ENCODE Project Consortium, 2012). UCSC table browser was used to generate complete tracks of 631 annotated tRNA genes (Lee et al., 2022; Raney et al., 2024). Analysis revealed that of the 631 annotated tRNA genes in the human genome, a robust association of ER α with approximately 300 tRNA genes in MCF-7 cells is found. Specifically, a heatmap of ER α binding revealed a specific concentration of ER α at about half of all tDNA, within 10 kb upstream and downstream flanking region from the centre of tRNA genes (Figure 3.3a). Investigating an additional independent ER α ChIP-seq dataset from MCF-7 cells confirmed this finding (Figure 3.3b). Biological reproducibility was validated with ZR-75-1 cells, another ER α + breast cancer cell line which also demonstrated strong ER α enrichment across many tRNA genes (Figure 3.3c) (Dai et al., 2017). To understand the selectivity of the ER α when it comes to binding non-coding RNAs, two other classes of short non-coding RNA were investigated for ER α enrichment in MCF-7 cells. Here, a very small proportion of snoRNAs and miRNAs were found to be bound by the ER α in comparison to tRNA genes (Figure 3.3d). This result suggested that the ER α is targeting tRNA genes, and that the enrichment identified at this class of small non-coding RNAs was not an artefact of the sequencing process. Additionally, an average signal intensity plot confirmed peaks of ER α binding overlap with tRNA genes, whereas no representative signal was observed in a 10 kb upstream and downstream surrounding sequence (Figure 3.3e).

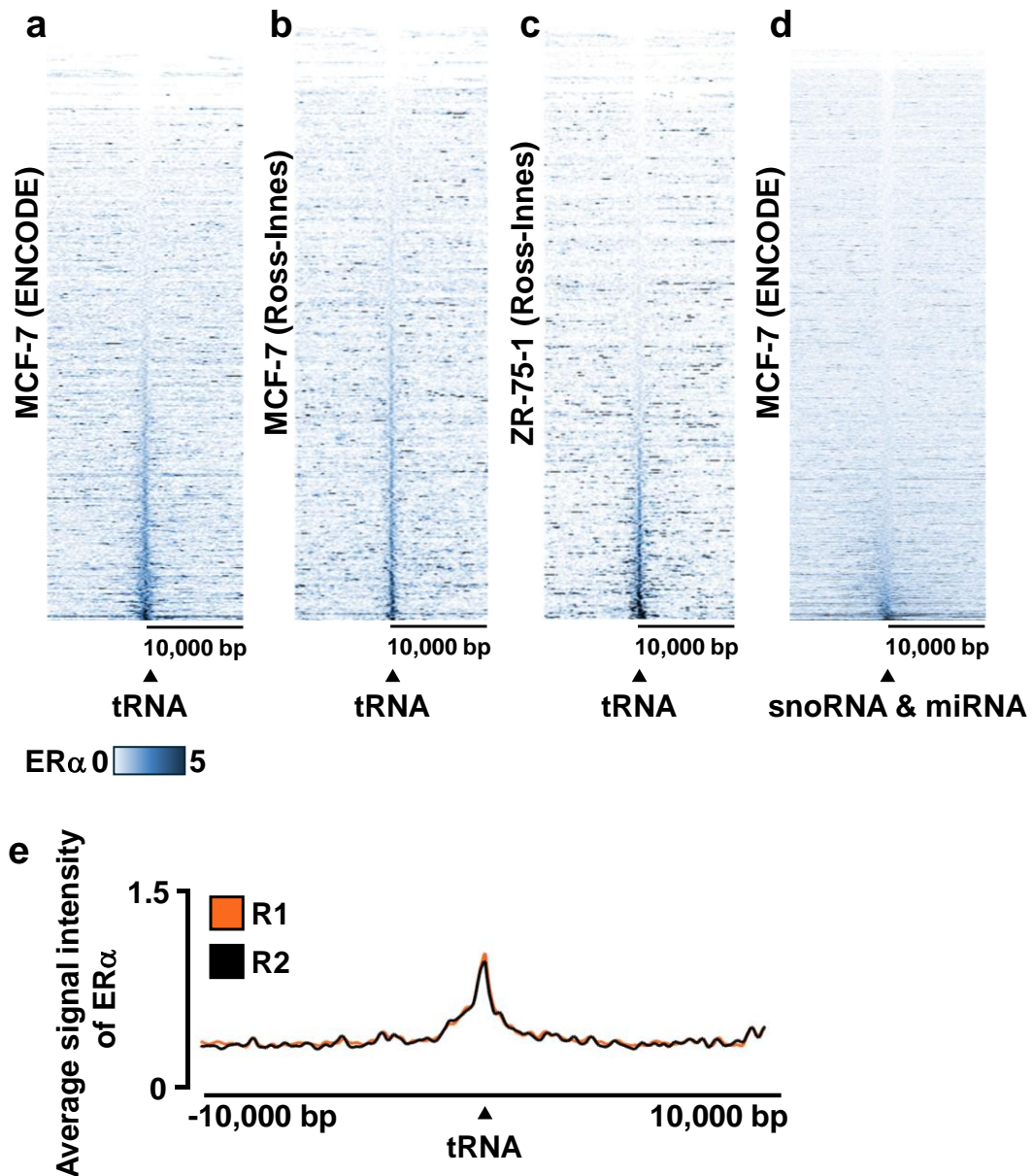


Figure 3.3 ER α is Enriched at tRNA Genes in ER α + Cell Lines. Heatmap of ER α binding events across tRNA genes in ER α + MCF-7 cells from (a) ENCODE or (b) Ross-Innes *et al.*, or (c) ER α + ZR-75-1 breast cancer cells. Window represents the \pm 10 kb region from the centre of tRNA genes. (d) Heatmap of ER α binding events across snoRNA and miRNA genes in the MCF-7 (ENCODE) cell line. Window represents the \pm 10 kb region from the centre of snoRNA and miRNA genes. (e) Average signal intensity overlay of ER α ChIP-seq replicates (R1 and R2) from the ENCODE dataset, across all tRNA genes in the MCF-7 cell line. Window represents the \pm 10 kb region from the centre of tRNA genes.

Next, ER α signal intensity across tRNA genes was quantified using EaSeq “quantify” tool, generating quantification (Q)-values (Lerdrup et al., 2016). The top ER α -bound tRNA gene was tRNA-Pro-TGG-1-1 with an average Q-value of 6.1, followed by tRNA-Arg-CCG-2-1 with a Q-value of 4.6. In comparison, known ER α -regulated genes *CTSD*, *GREB1*, *TFF1* and *CCND1* had Q-values in the range of 0.5 - 4.1. This indicates that a Q-value of 0.5 is a suitable minimum threshold of *bone fide* targets of the ER α . With that in mind, quantification of ER α binding across the tRNAome in MCF-7 cells revealed 47.4 % of tRNA genes with a Q-value exceeding the minimum threshold of Q > 0.5, including three initiator methionine (iMet) tRNA genes, which had Q-values in the range of 1.68 - 1.97 and were ranked in the top 40 - 65 genes associated with predicted genuine ER α interactions.

Enriched binding of the ER α was seen when reads at individual tDNAs were plotted. Here, clear overlap of ER α with tDNA loci is evident, such as at tRNA-Pro-TGG-1-1, tRNA-Arg-CCG-2-1 and tRNA-Met-CAT-1-1 (Figure 3.4a). Examples were also found of binding nearby rather than at a particular tRNA genomic locus, e.g. tRNA-Leu-AAG-2-4. To validate the ChIP-seq findings, ER α and Pol III ChIP-qPCR was carried out in MCF-7 cells. As expected, there was a strong enrichment of Pol III at tRNA-Pro-TGG-1-1, tRNA-Arg-CCG-2-1, tRNA-Met-CAT-1-1 and tRNA-Leu-AAG-2-4 (Figure 3.4b). Additionally, ER α binding was enriched at these tDNAs, relative to the 1901 pre-immune control (e.g., the sera taken from a rabbit before it was immunized with the RNA Pol III antigen) (Figure 3.4b). The enrichment of ER α at tRNA genes by ChIP-qPCR independently supports the ChIP-seq evidence that ER α binds to tRNA genes in MCF-7 cells.

Next, overlap in ER α binding between the MCF-7 and ZR-75-1 cell lines was tested, using the Ross-Innes and ENCODE ER α ChIP-seq datasets. Of the 631 hg18 tRNA genes downloaded from UCSC Table Browser, 180 of the same tRNA had an ER α binding event exceeding the 0.5 Q-value threshold in both MCF-7 and ZR-75-1 cells from the Ross-Innes dataset, and the MCF-7 cells from the ENCODE dataset (Figure 3.4c). For ZR-75-1 cells, only 14 out of 219 tRNA genes with enriched ER α binding (Q > 0.5) was unique to this cell line. Additionally, 241 ER α binding events were shared between both MCF-7 ER α -ChIP-seq datasets. However, more than 100 ER α binding events were also found to be unique to either the ENCODE or Ross-Innes MCF-7 ChIP-seq datasets.

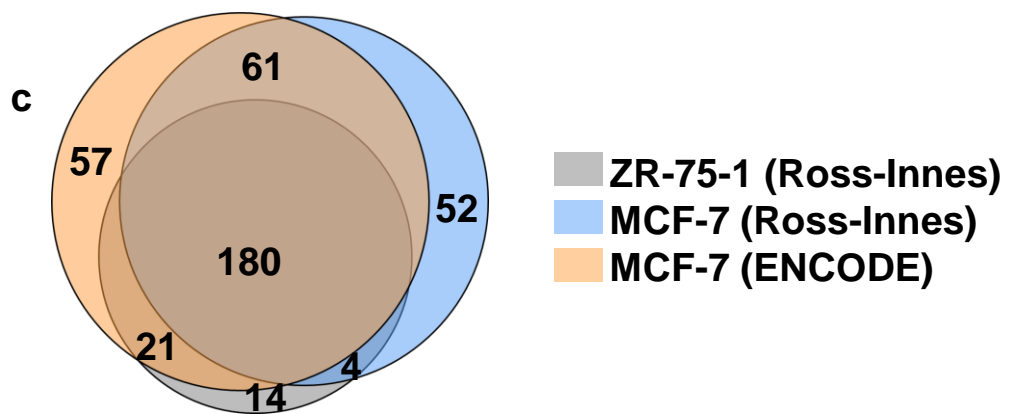
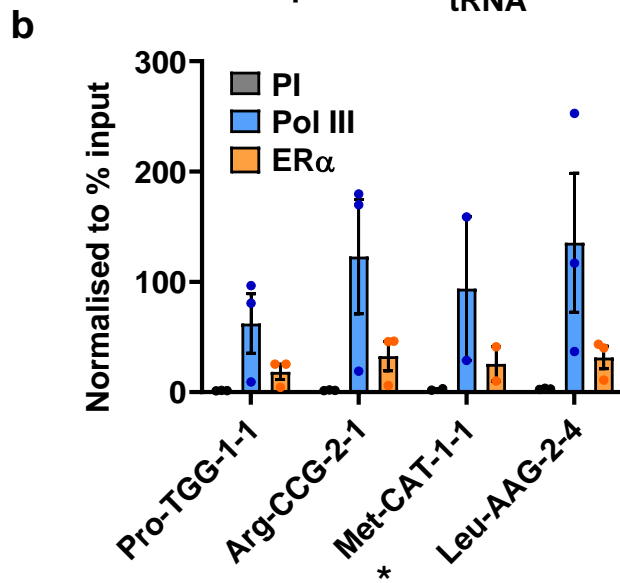
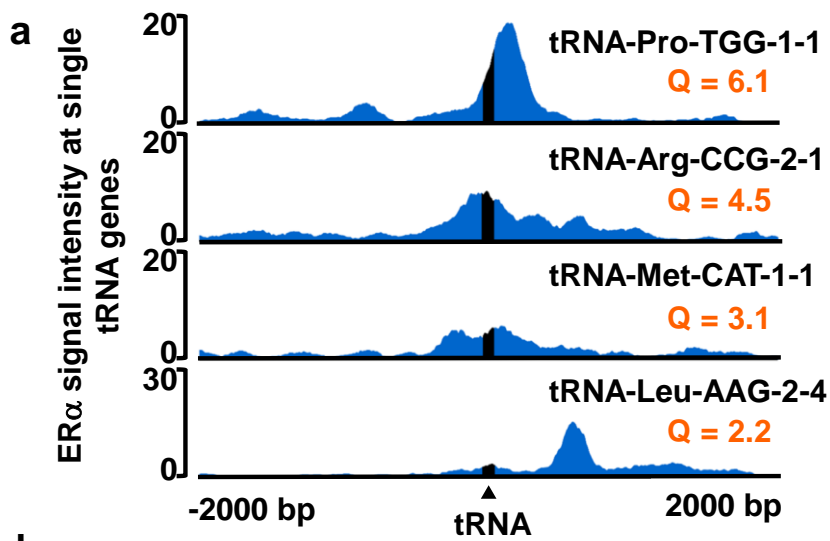


Figure 3.4 Identification of ER α at Individual tRNA Loci. **(a)** Representative fill tracks of ER α binding at individual tRNA genes (tRNA-Pro-TGG-1–1, tRNA-Arg-CCG-2–1, tRNA-Met-CAT-1–1, and tRNA-Leu-AAG-2–4). Q-values (Q) are shown in orange. **(b)** ChIP-qPCR assays carried out at individual tRNA genes (tRNA-Pro-TGG-1–1, tRNA-Arg-CCG-2–1, tRNA-Met-CAT-1–1*, and tRNA-Leu-AAG-2–4) to confirm pol III and ER α enrichment. N = 3, *N = 2. PI refers to pre-immune serum, used as a negative control. Error bars are \pm SEM. qPCR values have been normalised to % input. **(c)** Overlap in tRNA genes that have an ER α binding event with a Q-value > 0.5 in MCF-7 and ZR-75-1 cells from the Ross-Innes dataset, and the MCF-7 cells from the ENCODE dataset.

In conclusion, ER α was found to preferentially bind almost half of the tRNA genes in the human genome by analysis of multiple public ChIP-seq datasets carried out in ER α + MCF-7 and ZR-75-1 breast cancer cell lines. The enrichment of ER α to tRNA loci was preferential relative to other small non-coding RNA, which did not see the same level of steroid receptor recruitment. The finding of ER α association with tRNA genes was confirmed by ChIP-qPCR, and suggests previous findings of oestradiol-dependent increase in tRNA gene expression could be due to ER α recruitment to tDNA promoters (Hah et al., 2011).

3.2.3 ER α -targeted tRNA genes are not preferentially implicated in proliferation or differentiation

To build on the findings that the ER α was associated with many tRNA genes in breast cancer cell lines, analysis into the functional role of ER α -bound tDNAs was implemented to ascertain the biological significance of these associations. A previous investigation aimed to stratify tRNA gene expression into those preferentially induced during cell differentiation or cell proliferation, based on the observation that protein-coding genes exhibit distinct codon patterns according to their roles in different biological processes (Gingold et al., 2012, 2014). The stratification of tRNAs based on their prevalence in differentiated or proliferating cells was carried out in a variety of cell types, including human embryonic stem cells (hESCs), as well as bladder, colon and prostate cancer cells (Gingold et al., 2014). Gene Ontology terms of “pattern specification” and “M phase of mitotic cell cycle” were used to identify genes involved in differentiation or proliferation respectively. Differential codon usage within the two disparate GO gene identifiers was studied to distinguish preferential tRNA codon selection. Although breast cancers were not included, analysis of the dataset was used to elucidate whether tRNA targets of ER α identified by ChIP-seq in MCF-7 cells are enriched in either the differentiation or proliferation categories. Interrogation of the dataset revealed the top 75 ER α -bound tRNA genes were moderately depleted in the differentiation category relative to the proliferation group (Figure 3.5a). The majority of the top 75 ER α -enriched tDNAs were involved in “other” biological process, such as cell adhesion, receptor signalling and formation of the ECM (Figure 3.5a). Next, Q-values of the top 75 ER α binding events at tRNA loci was investigated in the proliferation and differentiation categories. Here, Q-values were found to not be significantly different, suggesting

that ER α recruitment does not discriminate between the previously suggested functional tRNA categories in MCF-7 cells (Figure 3.5b).

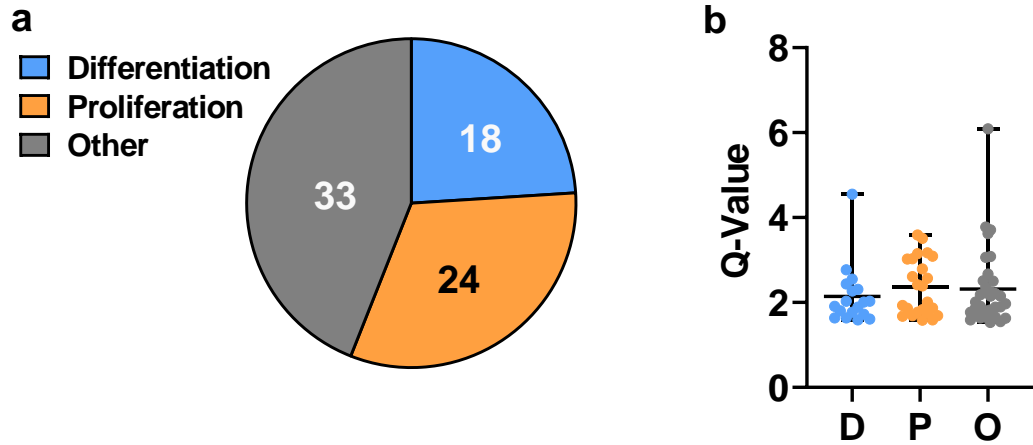


Figure 3.5 Functional Stratification of tRNA Genes Targeted by ER α . (a) Proportion of top 75 ER α -bound tRNA genes in MCF-7 cells in accordance with their involvement in differentiation (n = 18; blue), proliferation (n = 24; orange) or other cellular processes (n = 33; grey). (b) Quantified (Q) ER α binding at top 75 ER α -bound tRNA genes based on their preferential association with differentiation (D), proliferation (P) or other cellular processes (O).

3.2.4 The ER α does not utilise consensus ERE and half ERE motifs for recruitment to target tRNA genes

Two distinct mechanisms exist by which the ER α is positioned at proximal promoters or distal enhancers of target genes to modulate their transcription: i) direct binding to a cognate DNA sequence motif (ERE) via the ER α DNA-binding domain or ii) protein tethering interactions with other DNA-binding transcription factors, such that the ER α is not directly bound to DNA (Heldring et al., 2011; Ikeda et al., 2015). To advance knowledge on the mechanism behind ER α recruitment to target tRNAs, motif analysis was conducted to investigate if full or half ERE consensus sequences are involved in priming ER α around tRNA genes with the strongest ER α enrichment in MCF-7 cells. The search included tRNA sequences expanded by 20 kb up- and downstream, as ERE sequences can be found in distal regulatory elements, demonstrating long-range activation of target genes by the ER α , and *in situ* Hi-C has previously revealed coordinated long-range regulation of tRNA expression, particularly where tDNA are connected by DNA loops proximal to CTCF binding sites (Sun et al., 2007; Van Bortle et al., 2017). Targeted motif analysis conducted in MEME-Suit CentriMo did not identify either full or half ERE sequences in these regions. Lack of ERE identification was not a result of technical failure, as conserved A and B box promoter sequences that are essential for Pol III loading were strongly enriched in all tRNA genes studied, as expected (Figure 3.6). Therefore, at least for the tRNA genes investigated, recognition of consensus ERE sequences seemed not to be involved in ER α recruitment. It is possible that non-canonical ERE sequences may establish ER α association at tRNA loci, or a preferential protein tethering mechanism may be involved in positioning the hormone receptor at target tRNA gene promoters.

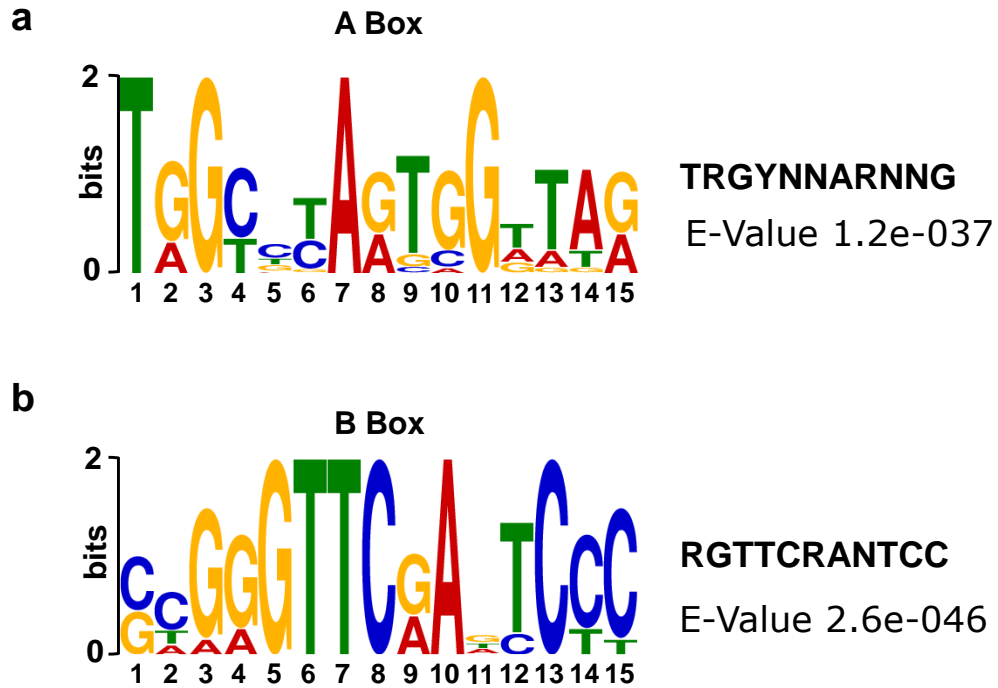


Figure 3.6. ER α Localisation at tRNA Genes Does Not Require Consensus ERE

Motifs. Position Weight Matrices (PWMs) of **(a)** A box and **(b)** B box promoter sequences identified within top 19 ER α -bound tRNA genes, and the correct consensus sequence of each promoter element. E-Value denotes the significance of the motif according to CentriMo motif discovery. Nucleotide symbols are: (A) Adenine, (C) Cytosine, (G) Guanine, (T) Thymine, (R) Purine – Guanine or Adenine, (Y) Pyrimidine – Cytosine or Thymine, and (N) any nucleotide. Canonical ERE or half-ERE sequences were not identified.

3.2.5 Exogenous ER α is not associated with tRNA genes in MDA-MB-231 cells

Considering the observation that tRNA genes enriched for ER α binding lack canonical full or half ERE sequence motifs, an exploration of a protein tethering mechanism for priming ER α at tRNA promoters was conducted. If the ER α is recruited to tRNA genes through interactions with other proteins, then accessibility of the ER α to tRNA promoters might vary between cell types according to availability of the necessary factor(s) and/or chromatin accessibility. To begin to explore this possibility, tRNA promoter binding by a wild type exogenous ER α stably transfected into MDA-MB-231 breast cancer cells negative for endogenous ER α was investigated in a public ChIP-seq dataset (Stender et al., 2010). To demonstrate functionality of the exogenous ER α in the MDA-MB-231 cell line, enrichment of ER α at a *GREB1* ERE was studied in relation to ER α binding at the same site in MCF-7 cells. Here, ER α was found to strongly bind to the *GREB1* ERE in transfected MDA-MB-231 cells, to a greater extent than endogenous ER α in MCF-7 cells (Figure 3.7a). Global heatmap analysis of exogenous ER α ChIP-seq across 77,814 annotated gene entries in the MDA-MB-231 genome reveals very moderate intensity of hormone receptor binding. However, further analysis of ER α enrichment across 631 tRNA genes revealed minimal interaction of the hormone receptor at tRNA loci (Figure 3.7b). Furthermore, plotting the average signal intensity of exogenous ER α binding showed no discernible peak of hormone receptor enrichment in a 20 kb window spanning tRNA genes (Figure 3.7c). The observation that exogenous ER α was not recruited to tRNA promoters in MDA-MB-231 cells despite robust enrichment at a well characterised ERE has several plausible explanations but alludes to the possibility that association of ER α with tRNA genes requires additional post-translational modifications and/or transcription factors which influence ER α access to, or retention at, tRNA promoters and are absent from MDA-MB-231 cells.

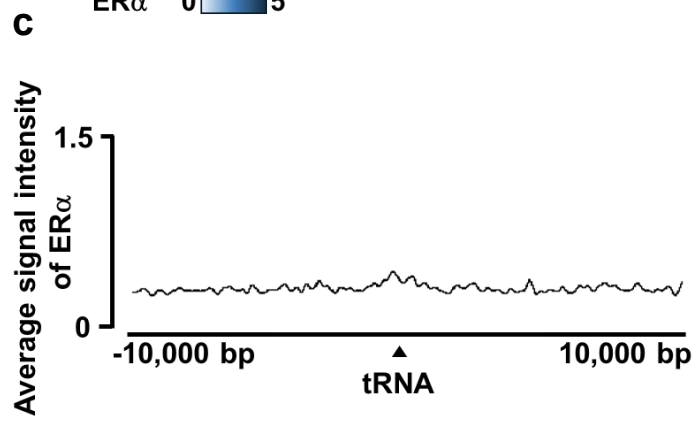
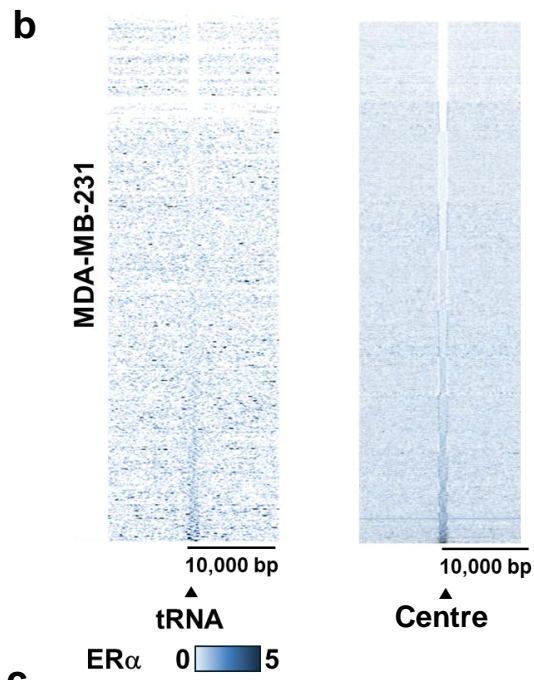
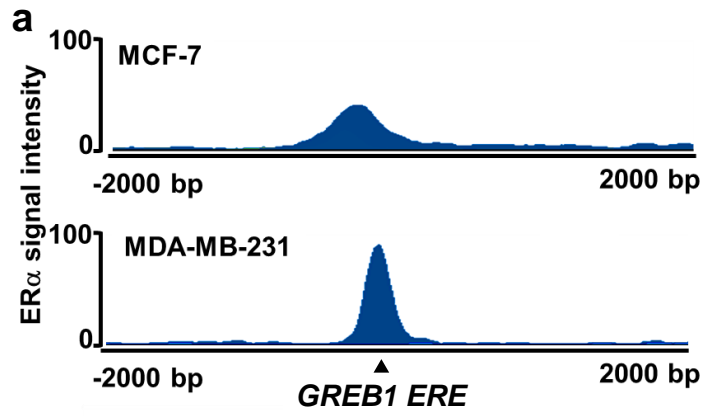


Figure 3.7. Exogenous ER α Does Not Associate at tRNA Genes in TNBC Cells.

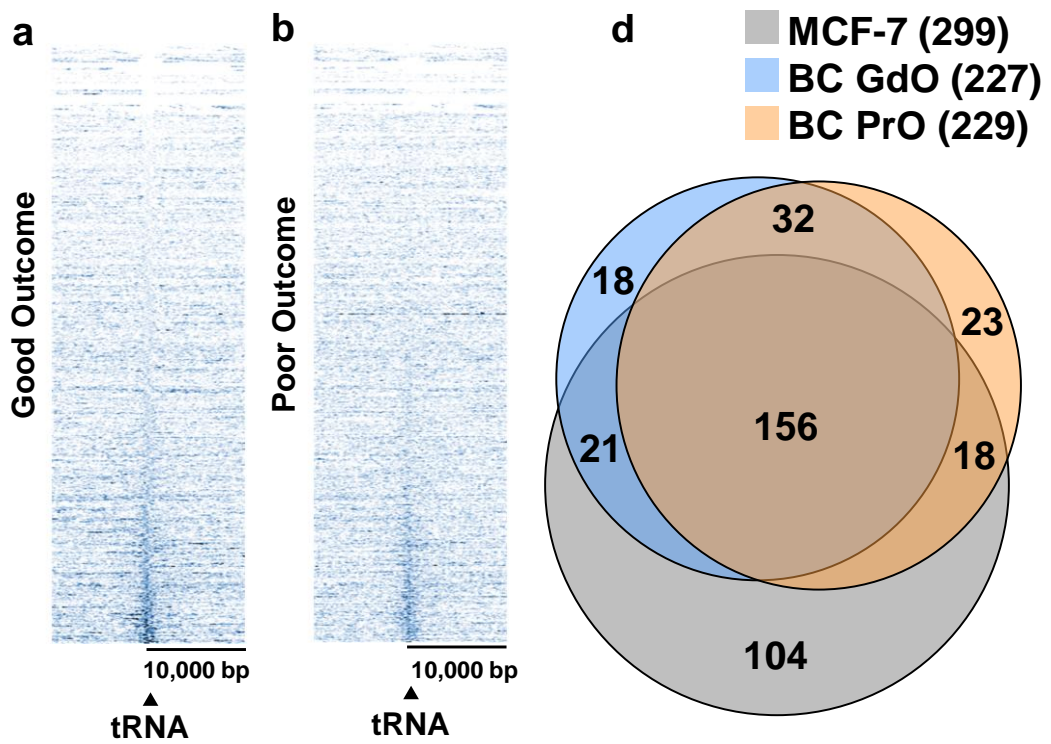
ER α enrichment at a known ERE 1.7 kb upstream of the *GREB1* promoter in **(a)** MCF-7 or MDA-MB-231 TNBC cells stably transfected with an active ER α construct. Window represents ± 2 kb region surrounding *GREB1* ERE. *GREB1* is located at Chr2:11591693-11700363. **(b)** Heatmap to show ER α binding events across tRNA genes (n = 637) or from the centre of all hg18 genes (n = 77,814) in MDA-MB-231 cells. Window represents the ± 10 kb from the centre of tRNA genes. **(c)** Average signal intensity of ER α ChIP-seq signal across all tRNA genes in the MDA-MB-231 cell line. Window represents the ± 10 kb from the centre of tRNA genes.

To summarise, investigations into the mechanism of ER α recruitment to tRNA promoters showed that ER α does not require canonical ERE sequences to bind to tRNA regulatory elements. Additionally, ChIP-seq analysis of ER α -null MDA-MB-231 cells indicated that ER α expression alone was not sufficient for its access or retention at tRNA genes. The same is not true where a known DNA binding mechanism is involved, as seen by strong ER α enrichment at the *GREB1* ERE in the same cell line. These findings collectively suggest a protein tethering mechanism, where unknown factors are essential for efficient loading of ER α at tRNA promoters.

3.2.6 The ER α is localised at tDNA in primary and metastatic breast tumours

To understand the clinical relevance of ER α association with tRNA genes observed in MCF-7 and ZR-75-1 cell lines, additional ChIP-seq datasets that analysed genome-wide binding of ER α in primary breast tumour samples from patients with invasive ductal carcinomas (IDC) was analysed (Ross-Innes et al., 2012). The ER α ChIP-seq was performed in tumours of patients who had a good outcome (GdO) or who had died because of breast cancer (poor outcome; PrO), as determined by long-term clinical follow-up. As seen in ER α + cell lines, heatmaps showed ER α association with many tRNA genes in breast tumours, confirming the observations in cell lines reflect the situation in clinical specimens (Figure 3.8a, Figure 3.8b). Plots of average ER α signal intensity revealed peaks of ER α binding at the tRNA genes, within a 20 kb of upstream and downstream surrounding genomic regions. However, no apparent differences in ER α binding were detected between the GdO and PrO tumours in terms of numbers of tDNAs bound or average signal intensity (Figure 3.8a - Figure 3.8c). Next, the degree to which tRNA genes bound by ER α in MCF-7 cells represent tRNA genes bound by ER α in patient samples was investigated, with the minimum threshold of Q > 0.5 representing an ER α binding event. Considerable overlap was observed between the identities of tDNAs bound by ER α in GdO and PrO clinical samples, while MCF-7 cells exhibited greater number of ER α associations with tRNA genes (Figure 3.8d). Despite the variation in the number of ER α -bound tRNA genes in MCF-7 cells and primary tumours, the ChIP-seq data demonstrated large numbers of tRNA genes were targeted by endogenous ER α in primary breast cancer biopsies.

Next, the MCF-7, GdO and PrO tRNA genes which shared ER α enrichment was further studied to determine if tRNA preferentially upregulated in differentiating or proliferating cell types were selected for across the three sample types. Of the 156 shared tRNA, 147 genes were able to be compared against Gingold's tRNA classifier list (Gingold et al., 2012, 2014). Here, almost equal proportion of tRNA genes bound by ER α in MCF-7, GdO and PrO samples were associated with either proliferation (n = 38) or differentiation (n = 33) (Figure 3.8e). The remaining 72 tRNA genes were associated with "other" cellular processes.



ER α 0 5

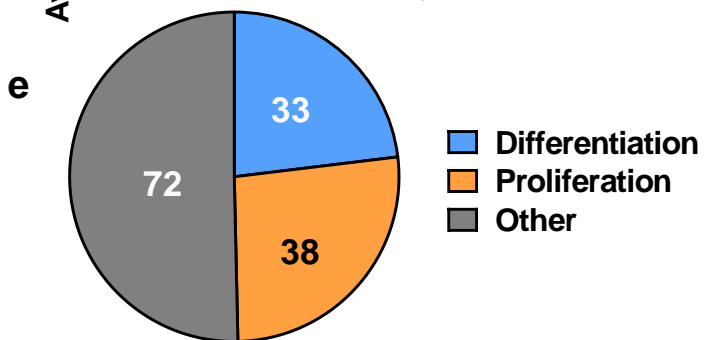
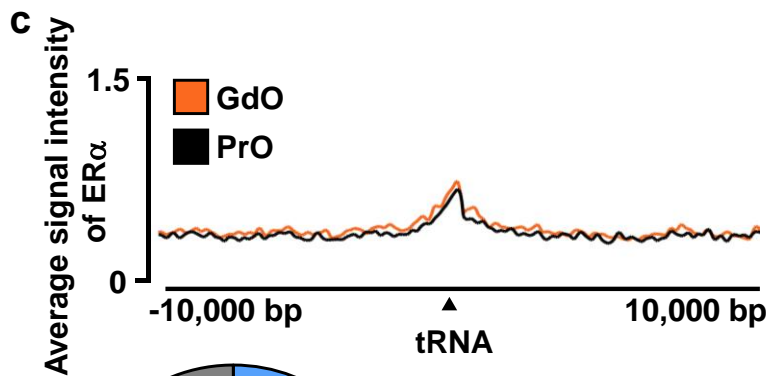


Figure 3.8. ER α is Enriched at tRNA Genes in Primary Breast Tumours. Heatmap of ER α enrichment across tRNA genes in breast cancer patient samples stratified into either a **(a)** good outcome or **(b)** poor outcome. Window represents the \pm 10 kb from the centre of tRNA genes. **(c)** Average signal intensity of ER α enrichment across all tRNA genes in good outcome (GdO) and poor outcome (PrO) ChIP-seq datasets. Window represents the \pm 10 kb from the centre of tRNA genes. **(d)** Venn diagram demonstrating ER α enrichment overlap between MCF-7 cells and good outcome (GdO) or poor outcome (PrO) breast cancer (BC) datasets. A positive enrichment of ER α was determined where a Q-value of $>$ 0.5 was obtained at a tRNA gene. **(e)** Proportion of overlapping ER α -bound tRNA genes in MCF-7 cells and GO and PO primary tumours, in accordance with their involvement in differentiation (n = 33; blue), proliferation (n = 38; orange) or other cellular processes (n = 72; grey).

In addition to exploring primary breast tumours, ChIP-seq of distant ER α + metastases from three patients were analysed, to understand if enriched association of the ER α with tRNA genes is implicated in breast cancer progression (141). First, ChIP-seq tracks of ER α binding at *GREB1* ERE showed individual patient metastases had strong and comparable ER α signal at this genomic locus (Figure 3.9a). In contrast, plotting heatmaps of ER α signals across the tRNAome in individual metastatic samples showed clear yet variable accumulation of ER α at many tRNA genes, within the 10 kb upstream and downstream flanking regions (Figure 3.9b). In particular, the metastatic sample from one patient (Met 2) displayed substantial ER α binding at tDNA, whereas the enrichment of ER α at tRNA genes in Met 1 and Met 3 was much more discrete in comparison. The variability in ER α enrichment at tRNA genes was further demonstrated in an average signal intensity plot which showed Met 2 has greater average ER α binding intensity, compared to Met 1 and Met 3 (Figure 3.9c). Additionally, smaller peaks of ER α enrichment were observed in 10 kb upstream and downstream flanking regions of tRNA in Met 2 but not in the other metastases. The observation of additional ER α binding events near tRNA genes in Met 2, but not in Met 1 or Met 3, may indicate uncontrolled recruitment of ER α to unspecified genomic loci. Alternatively, elevated ER α enrichment seen in the Met 2 patient sample could be further explained by overall higher ER α expression compared to Met 1 and Met 3, or additional unknown differences in the tumour content. Nevertheless, the enhanced ER α binding seen in Met 3 may have significant clinical implications, which warrant further exploration.

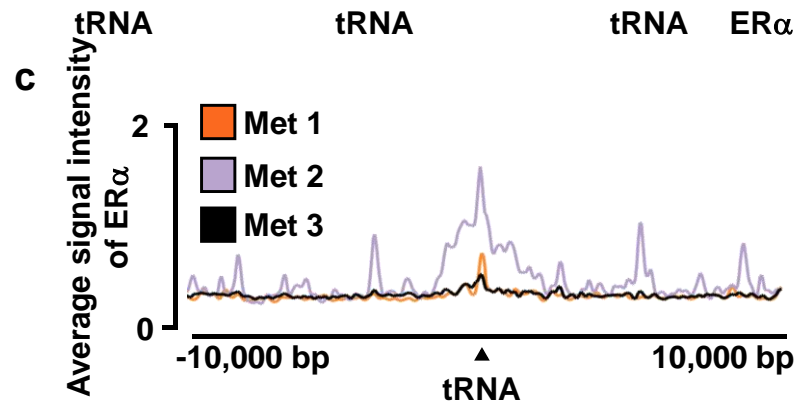
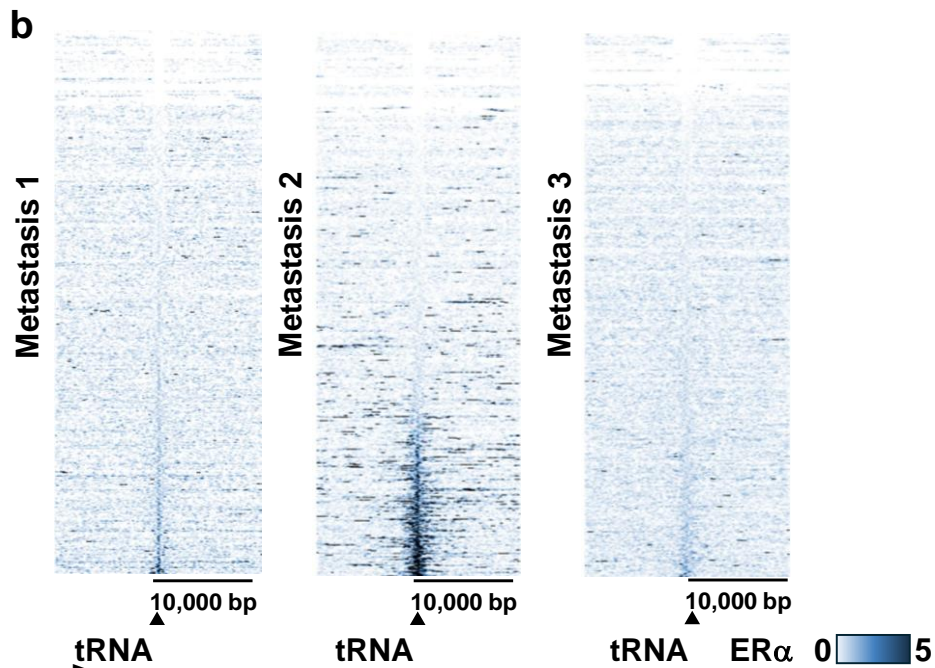
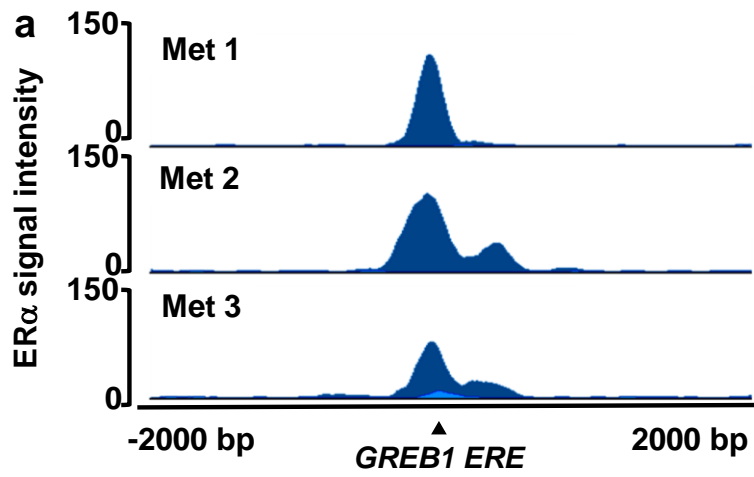


Figure 3.9. Breast Cancer Metastasis are Positive for ER α Enrichment at tRNA

Genes. (a) Fill tracks of ER α binding at a known ERE 1.7 kb upstream of the *GREB1* promoter in three metastatic (Met) patient samples. Window represents a ± 2 kb region from the centre of the ERE loci. *GREB1* is located at Chr2:11591693-11700363. **(b)** Heatmap of ER α binding events in three metastatic patient samples. Window represents the ± 10 kb from the centre of tRNA genes. **(c)** Average signal intensity of ER α enrichment across all tRNA genes in three metastatic (Met 1, 2 and 3) patient samples. Window represents the ± 10 kb from the centre of tRNA genes.

To compare differences in the intensity of ER α enrichment at tRNA genes in MCF-7 cell lines, primary breast tumours and metastatic biopsies, the Q-value of ER α at 631 tRNA genes in each of the samples was investigated (Figure 3.10). The strength of ER α enrichment at tRNAs was significantly higher in the MCF-7 cell line (mean 0.74 ± 0.77 sd, range 0 - 6.09) compared to the GdO (mean 0.57 ± 0.56 sd, range 0 - 5.26) and PrO (mean 0.52 ± 0.44 sd, range 0 - 4.93) primary tumours, as well as Met 1 (mean 0.43 ± 0.50 sd, range 0 - 5.86) and Met 3 (mean 0.40 ± 0.38 sd, range 0 - 6.56) metastatic samples. No significant difference was seen in ER α associations with tDNAs between GdO and PrO patient samples. However, the increase in association of ER α with tRNA loci seen in Met 2 was highly significant relative to all other samples (mean 1.02 ± 1.84 sd, range 0 - 13.18).

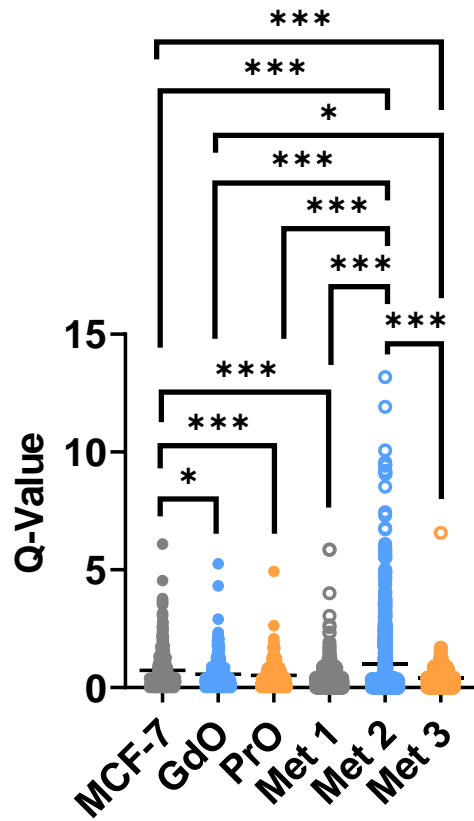


Figure 3.10. Quantification of ER α Enrichment in the MCF-7 Cell Line, Primary Breast Tumours and Metastatic Patient Samples. Scatter plot showing Q-values of ER α binding at tRNA genes in MCF-7 cells (grey, closed), GdO (blue, closed) and PrO (orange, closed) primary tumours and three distant metastatic patient samples: Met 1 (grey, open), Met 2 (blue, open) and Met 3 (orange, open). One-way ANOVA with Tukey's multiple comparisons was performed. * $p < 0.05$, *** $p < 0.001$.

In conclusion, comprehensive investigations of ER α + cell lines, but especially clinical primary and metastatic ER α + breast tumours have revealed widespread association of the ER α with ~30 to ~50 % of all tRNA genes annotated in the human genome. This was a significant finding that may have clinical implications in the progression of breast cancer. Despite there being no discernible differences in the number of tRNA genes enriched for ER α binding between primary IDC tumours, a more varied and significant interaction of ER α at tDNA loci was evident in advanced and aggressive metastatic samples.

3.2.7. FOXA1 and ER α enhance Pol III loading at tRNA genes

Expanding on earlier findings that expression of the ER α alone was not sufficient for its localisation at tRNA promoters, the involvement of additional regulatory factors for efficient ER α loading at tDNA loci was explored in greater detail. FOXA1 is a pioneer factor with an essential role in remodelling chromatin to allow the ER α access to cognate *cis*-regulatory elements (Hurtado et al., 2011). Additionally, FOXA1 is suggested to be a critical determinant of ER α associations with target genes, even at sites that do not contain an ERE for direct DNA binding (Carroll et al., 2005; Hurtado et al., 2011). Indeed, independent analysis of ER α and FOXA1 ChIP-seq in MCF-7 cells identified a significant overlap in 230 tRNA genes bound by both ER α and FOXA1 transcription factors, with Q-values > 0.5 (Figure 3.11a).

To ascertain the importance of the ER α for efficient positioning of Pol III transcriptional machinery at tRNA promoters, ER α protein was knocked down in MCF-7 cells with a six-hour treatment of 100 nM fulvestrant, a potent SERD used in clinic to treat advanced ER α + breast cancer (Vergote and Abram, 2006). Western blot revealed substantial reduction in ER α protein in fulvestrant treated MCF-7 cells, relative to the vehicle control, and in line with a previous study which similarly observed reduction of ER α protein in MCF-7 cells following a 6-hour treatment with 100 nM Fulvestrant (Figure 3.11b) (Yeh et al., 2013). However, the ER α was not completely degraded, and a more prolonged treatment of 100 nM Fulvestrant may be required to fully eradicate the hormone receptor. Additionally, evidence of possible ER α proteasomal degradation is apparent in vehicle-treated cells, but not in untreated whole cell lysate from the same cell line. This observation is likely due

to sample handling at the time of lysis, and the inclusion of protease inhibitor cocktail may prevent unexpected proteolysis of the hormone receptor in future experiments.

Proteasomal degradation of ER α in fulvestrant treated MCF-7 cells, a showed a corresponding significant reduction in ER α occupancy at the *GREB1* ERE, as observed by CHIP-qPCR (Figure 3.11c). Pol III enrichment at tRNA-Arg-CCG-2-1, tRNA-Leu-AAG-2-4 and tRNA-Met-CAT-1-1 was slightly reduced following fulvestrant treatment, although this finding was not significant. However, where Pol III was most strongly enriched at the tRNA-Pro-TGG-1-1 promoter, significant loss of Pol III assembly at this tRNA gene occurred following ER α depletion (Figure 3.11d). Reduced positioning of Pol III at tDNA loci was not due to decreased occupancy of GTF3C5, which forms part of the TFIIIC complex essential for facilitating recruitment of Pol III to tRNA promoters, as only a moderate reduction in GTF3C5 recruitment to tRNA genes was seen upon fulvestrant treatment of MCF-7 cells (Figure 3.11e). Additionally, knockdown of the ER α only partially reduced ER α recruitment to tRNA genes (Figure 3.11f), which could be explained by incomplete fulvestrant-mediated ER α degradation (Figure 3.11b). Similar to the reduction in Pol III enrichment at tRNA-Arg-CCG-2-1, tRNA-Leu-AAG-2-4 and tRNA-Met-CAT-1-1, FOXA1 observed a notable but non-significant decrease in occupancy at these genes post fulvestrant treatment. However, ER α knockdown significantly impeded the ability of FOXA1 to bind to tRNA-Pro-TGG-1-1 in MCF-7 cells (Figure 3.11g).

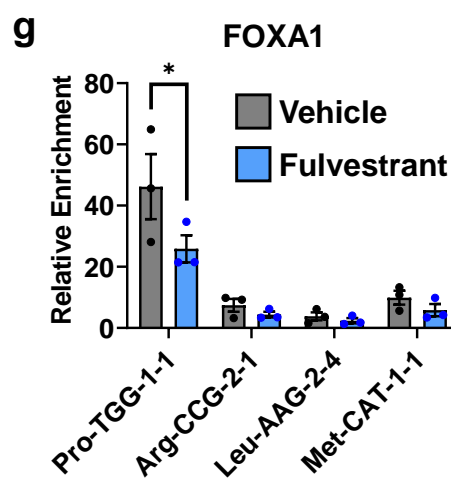
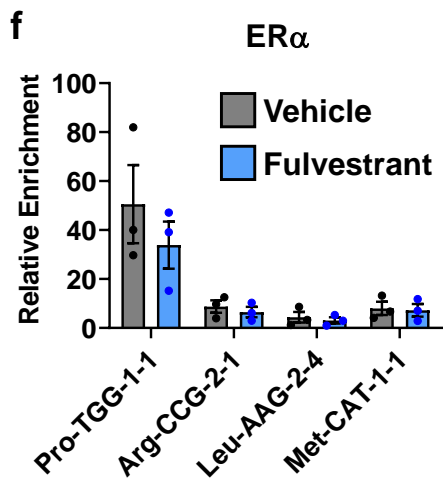
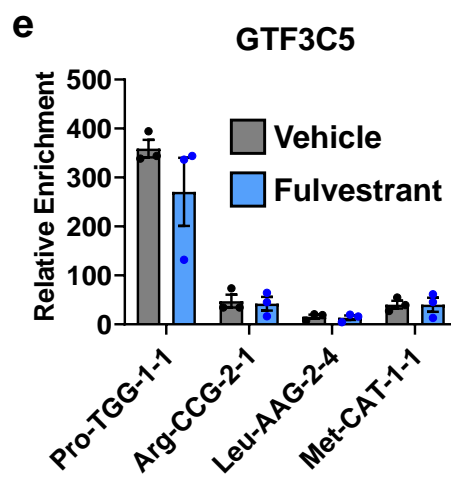
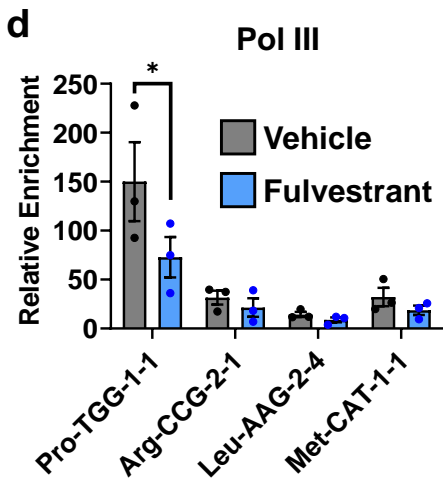
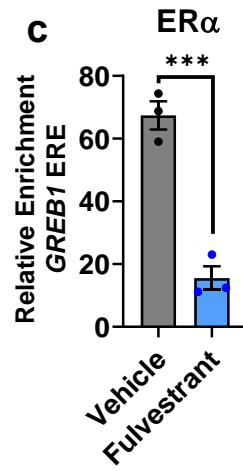
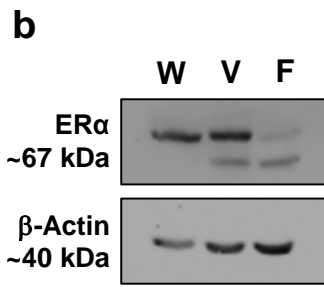
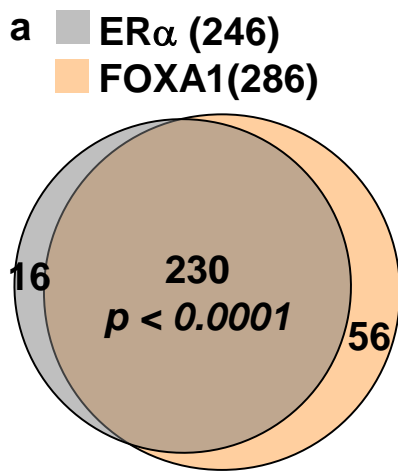


Figure 3.11. FOXA1 is Recruited to tRNA Genes by the ER α and is Required for RNA Polymerase III Loading at tDNA Promoters. (a) Overlap in tRNA genes that have an ER α and FOXA1 binding event with a Q-value > 0.5 from two publicly accessible ChIP-seq datasets in MCF-7 cells. Fisher's exact test was performed to determine significant overlap between tRNA genes bound by both transcription factors. $p < 0.0001$. (b) Western blot to show ER α (top window) and β -actin (bottom window) in MCF-7 cells treated with vehicle (V) or fulvestrant (F) for 6 hours, or untreated whole cell lysate (W). (c) ChIP-qPCR of ER α at *GREB1* ERE in MCF-7 cells treated with vehicle (grey) or fulvestrant (blue) for 6 hours. qPCR Ct values normalised to gene desert. Student's t-test performed against vehicle. *** $p = < 0.001$. Error bars are mean \pm SEM. N = 3. ChIP-qPCR of (d) Pol III, (e) GTF3C5, (f) ER α and (g) FOXA1 at tRNA genes (tRNA-Pro-TGG-1-1, tRNA-Arg-CCG-2-1, tRNA-Leu-AAG-2-4 and tRNA-Met-CAT-1-1) in MCF-7 cells treated with vehicle (grey) or fulvestrant (blue) for 6 hours. qPCR Ct values normalised to gene desert. One-way ANOVA with Tukey's multiple comparisons was performed against vehicle. * $p < 0.05$. Error bars are \pm SEM. N = 3.

In summary, ChIP-seq analysis demonstrated significant overlap in ER α - and FOXA1-bound tRNA genes in MCF-7 cells. Fulvestrant knockdown of ER α reduced occupancy of Pol III at tDNA genes, as seen by ChIP-qPCR. Where Pol III was the most enriched at tRNA-Pro-TGG-1-1, perhaps suggesting active transcription, ER α knockdown had a significant effect on the ability of Pol III to be efficiently loaded at the promoter, which was not due to reduced GTF3C5 occupancy at this tDNA locus. However, FOXA1 recruitment was also significantly reduced at this tRNA gene following fulvestrant-mediated ER α knockdown. This striking finding provides valuable insight into the necessary regulatory factors required for ER α loading at tRNA genes and suggests a co-operative relationship between the ER α and FOXA1 is involved in recruiting Pol III to tDNA promoters.

3.2.8 The ER α associates with other Pol III transcribed genes

To assess if ER α is implicated in expression of other Pol III-transcribed non-coding RNA that are significant in breast cancer progression, ER α ChIP-seq datasets were analysed to ascertain ER α recruitment to ncRNA genes, *BC200*, *RN7SL1* and *RMRP*. Like tRNA genes, *BC200* has a Type II promoter characterised by an ICR, and A and B boxes (Dieci et al., 2007; Orioli et al., 2012). Additionally, analysis of the proximal region surrounding *BC200* promoter revealed an ERE-like sequence located -585 bp upstream of the TSS, previously reported to have enriched ER α binding in MCF-7 cells (Singh et al., 2016). *BC200* is typically expressed in the brain, and is a regulator of protein synthesis (Samson et al., 2018). However, expression of *BC200* is elevated in several malignancies, including breast cancer, where a high level of this transcript is associated with advanced disease (Chen et al., 1997; Iacoangeli et al., 2004; Singh et al., 2016; Samson et al., 2018). Specifically, increased expression of *BC200* in the MCF-7 cell line inhibits apoptosis through modulation of the alternative splicing of Bcl-x (Singh et al., 2016). However, analysis of ER α ChIP-seq datasets from MCF-7 cells, MDA-MB-231 cells stably transfected with exogenous ER α , as well as GdO and PrO primary tumours and three distant metastatic samples provided minimal evidence of ER α targeting at the *BC200* promoter, in contrast to previous studies (Figure 3.12).

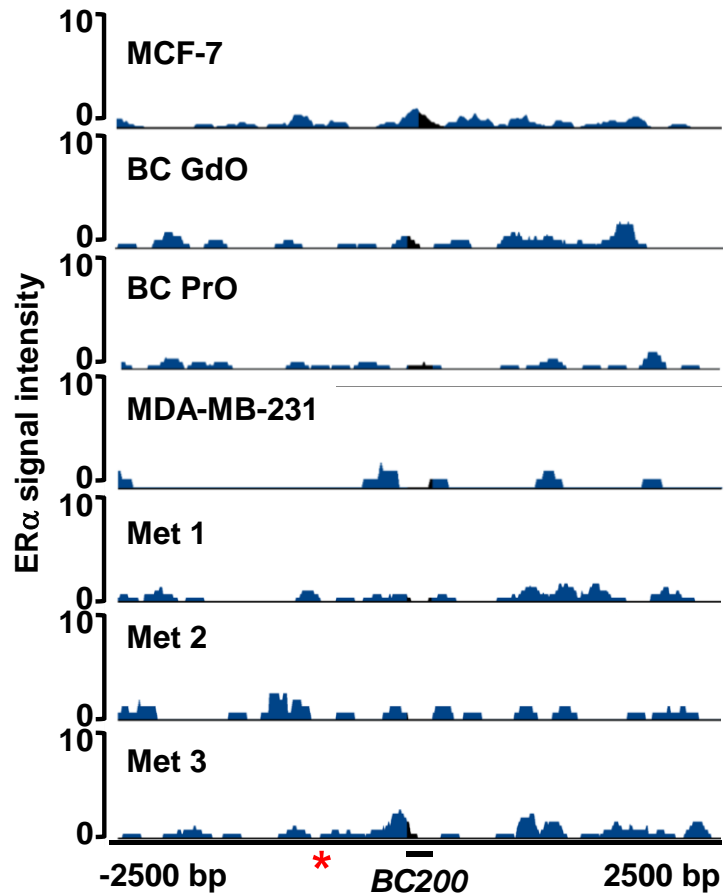


Figure 3.12. ER α is not Found at an ERE in Proximity of the *BC200* Promoter. ER α ChIP-seq fill tracks of *BC200* genomic loci in MCF-7 cells, BC GdO and PrO patient samples, MDA-MB-231 cells stably expressing an ER α construct and three distant metastatic (Met 1, 2 and 3) patient samples. Red asterisk (*) represents the approximate location of an ERE -585 bp upstream of the *BC200* TSS (Singh et al., 2016). Window represents the ± 2.5 kb region from the centre of the *BC200* gene.

RN7SL1 is essential for protein secretion and intracellular trafficking, as the RNA constituent of the signal recognition particle (SRP) (Walter and Blobel, 1982; Ullu and Tschudi, 1984). In contrast to tRNA genes and *BC200*, *RN7SL1* has a Type III promoter formed of a PSE and a TATA box, and atypical for Type III promoters, A and B box motifs (Dieci et al., 2007; Orioli et al., 2012). Aberrant expression of *RN7SL1* has been implicated in promoting inflammatory responses in breast cancers, influencing tumour growth, metastasis and therapy resistance (Nabet et al., 2017). Furthermore, *RN7SL1* has been shown to sequester translation of tumour-suppressor p53 by hybridising with *TP53* mRNA (Abdelmohsen et al., 2014).

To investigate if ER α potentiates aberrant *RN7SL1* expression, ChIP-seq in ER α + breast cancer cell lines and patient samples were studied. Here, strong enrichment of ER α at *RN7SL1* gene locus in MCF-7 cells and metastatic sample Met 3 was identified (Figure 3.13a). Moderate ER α enrichment was also observed in proximity to the *RN7SL1* promoter in primary breast tumours (Figure 3.13a). In contrast, *RN7SL1* promoter occupancy by ER α was not observed in the MDA-MB-231 cell line expressing exogenous ER α or Met 1 and Met 3 tumour samples, suggesting heterogeneity in ER α association with *RN7SL1* in breast cancer cells (Figure 3.13a).

Next, ChIP-qPCR was performed to confirm the findings of ER α binding at the *RN7SL1* locus and investigate the involvement of the ER α and FOXA1 in assembling Pol III at *RN7SL1* promoter. As expected, *RN7SL1* was highly enriched for RNA Pol III binding, which was markedly reduced upon fulvestrant-mediated knockdown of the ER α (Figure 3.13b). In support of the ChIP-seq findings, ER α was also found to occupy the *RN7SL1* gene locus, with a moderate decrease in recruitment following fulvestrant treatment (Figure 3.13c). Next, FOXA1 association with *RN7SL1* was studied by ChIP-qPCR, which revealed pioneer factor occupancy at this gene. Like the ChIP-qPCR findings of tRNA genes, FOXA1 was also reduced when ER α was knocked down (Figure 3.13d). Although reduction in the enrichment of Pol III, ER α and FOXA1 was not significant following fulvestrant treatment, a clear downward trend in polymerase and transcription factor loading at *RN7SL1* locus was observed, which suggests ER α and FOXA1 may have auxiliary roles in Pol III positioning and transcription of this gene.

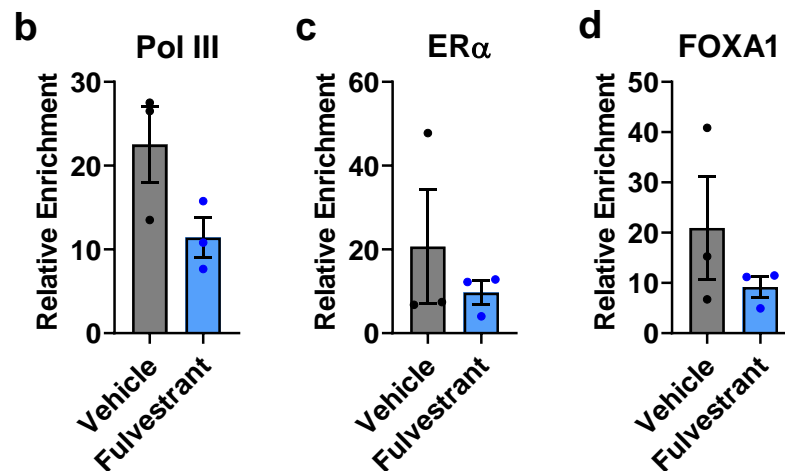
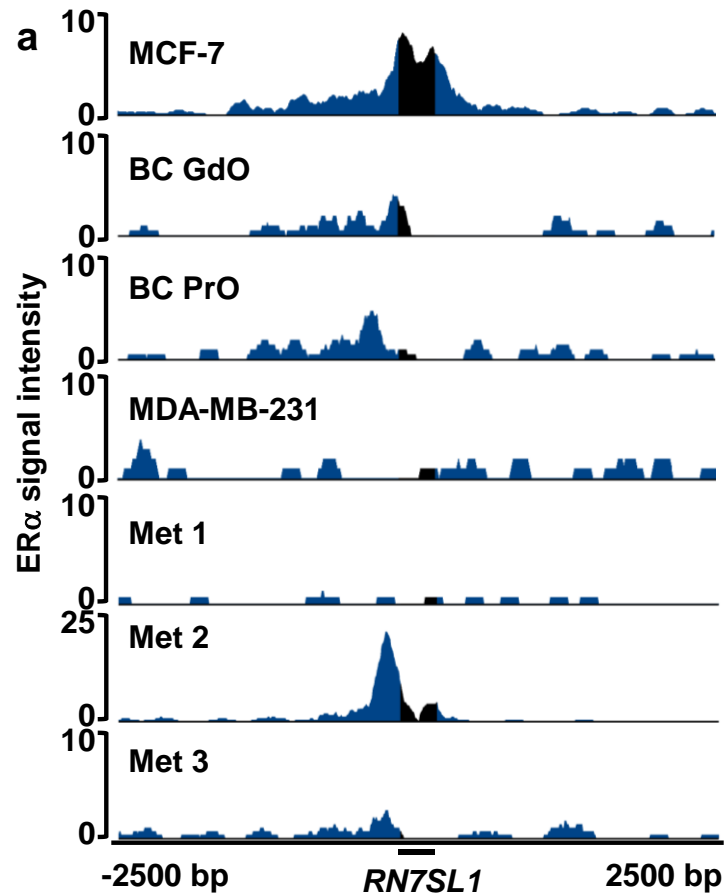


Figure 3.13. ERα is Localised at *RN7SL1* in MCF-7 Cells and Patient Metastasis.

ERα ChIP-seq fill tracks of *RN7SL1* genomic loci in MCF-7 cells, BC GdO and PrO patient samples, MDA-MB-231 cells stably expressing an ERα construct and three distant metastatic (Met 1, 2 and 3) patient samples. Window represents the ± 2.5 kb region from the centre of the *BC200* gene. ChIP-qPCR of (b) Pol III, (c) ERα and (d) FOXA1 at *RN7SL1* in MCF-7 cells treated with vehicle (grey) or fulvestrant (blue) for 6 hours. qPCR Ct values normalised to gene desert. Student's t-test performed against vehicle. Error bars are ± SEM. N = 3.

RMRP is involved in mitochondrial DNA replication, rRNA processing, and cell cycle control (Thiel et al., 2005; Martin and Li, 2007; Goldfarb and Cech, 2017; Vakkilainen et al., 2019). Germline mutations in *RMRP* cause the inherited syndrome cartilage-hair hypoplasia, whereas somatic mutations in the Type III promoter of *RMRP* elevates expression and is significantly implicated in breast cancer development (Ridanpää et al., 2001; Rheinbay et al., 2017, 2020). When ChIP-seq data were investigated to explore ER α association with *RMRP*, strong enrichment of the hormone receptor was observed in all metastatic samples, and to a lesser extent in MCF-7 cells and MDA-MB-231 cells expressing exogenous ER α . In contrast, no ER α enrichment was seen in primary breast cancer samples (Figure 3.14a). Next, ChIP-qPCR was implemented to validate ChIP-seq findings. Here, Pol III ER α and FOXA1 were enriched at *RN7SL1* promoters, but only to a modest extent (Figure 3.14b – Figure 3.14d). However, despite limited occupancy at the *RN7SL1* locus, Pol III recruitment to the promoter was still decreased following fulvestrant-mediated knockdown of the ER α , as was FOXA1, albeit not significantly.

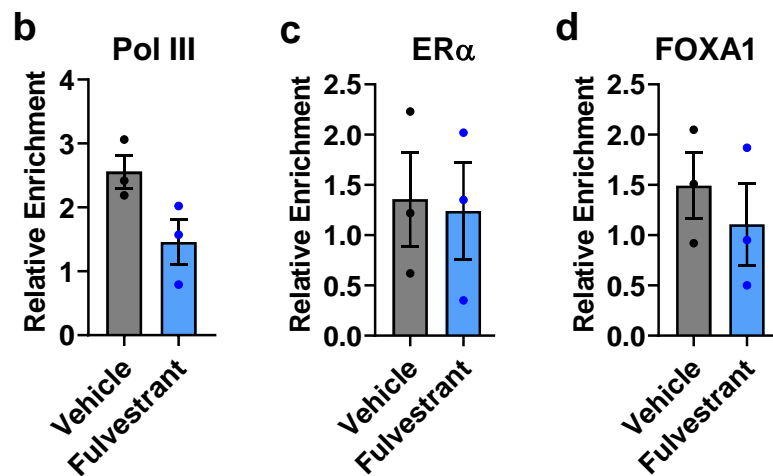
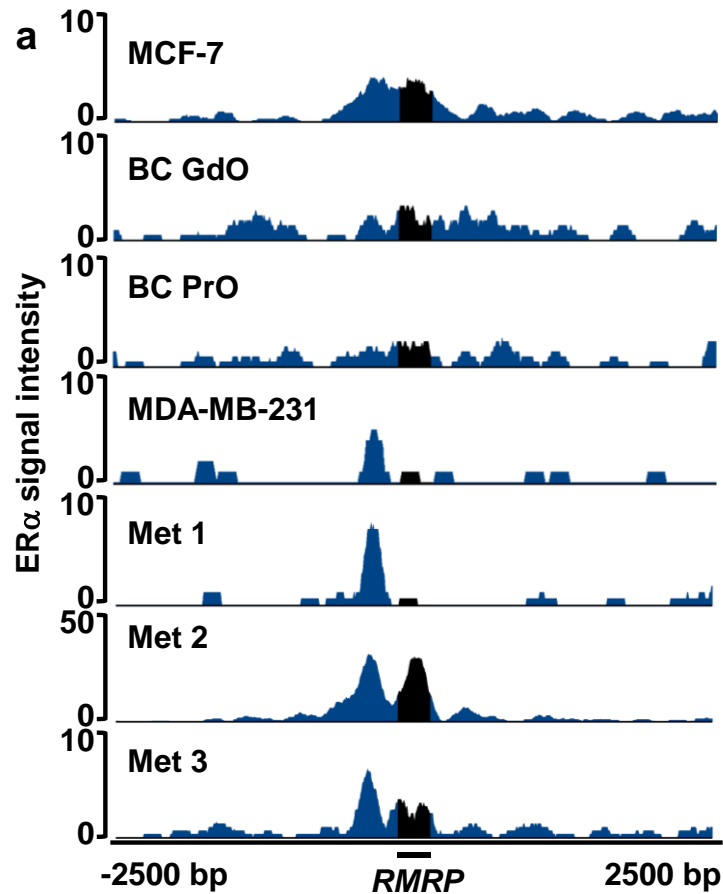


Figure 3.14. ERα is Localised at RMRP in MCF-7 Cells and Patient Metastasis.

ERα ChIP-seq fill tracks of RMRP genomic loci in MCF-7 cells, BC GdO and PrO patient samples, MDA-MB-231 cells stably expressing an ERα construct and three distant metastatic (Met 1, 2 and 3) patient samples. Window represents the ± 2.5 kb region from the centre of the BC200 gene. ChIP-qPCR of (b) Pol III, (c) ERα and (d) FOXA1 at RMRP in MCF-7 cells treated with vehicle (grey) or fulvestrant (blue) for 6 hours. qPCR Ct values normalised to gene desert. Student's t-test performed against vehicle. Error bars are mean ± SEM. N = 3.

To summarise, the association of the ER α with other classes of Pol III-transcribed non-coding RNAs was investigated in ER α + cell lines, primary breast cancer tumours and metastatic samples. *BC200* did not display any ER α enrichment in the promoter, or proximal up and downstream regions, despite having an ERE-like sequence motif, and the same promoter architecture as tRNA genes which are able to recruit the hormone receptor. In contrast, *RN7SL* had enriched ER α binding in the MCF-7 cell line, primary breast tumours and one metastatic sample. Additionally, *RMRP* had ER α promoter occupancy in MCF-7 cells, three metastatic breast tumour samples and in MDA-MB-231 cells expressing exogenous ER α . For both *RMRP* and *RN7SL1*, ER α association at promoters was confirmed by ChIP-qPCR. Further investigating the significance of ER α recruitment to the non-coding promoters with ER α knockdown found reduced Pol III positioning at the genomic loci when MCF-7 cells were treated with fulvestrant. The decreased Pol III occupancy could be explained by concurrent reduction in FOXA1 recruitment to the same ncRNA genes which was also seen following ER α knockdown in MCF-7 cells.

3.2.9 The ER α interacts with Pol III subunits in MCF-7 cells and human breast tumours

Following on the earlier results that i) the ER α was recruited to tRNA genes in the absence of canonical full or half ERE motifs, ii) GTF3C5 occupancy at tRNA genes was unaffected by ER α knockdown and iii) Pol III occupancy was reduced at tRNA promoters in the absence of the ER α , the relationship between the ER α , TFIIC and Pol III was further explored. Here, qPLEX-RIME datasets were analysed to assess if members of the Pol III transcription machinery were interacting with the ER α , in support of a protein tethering mechanism of ER α association at tRNA genes (Papachristou et al., 2018). In MCF-7 cells, immunoprecipitation of ER α followed by mass-spectrometry revealed strong molecular interactions between the hormone receptor and four out of six TFIIC subunits, including GTF3C5 (Figure 3.15a). The intensity of the ER α -TFIIC interactions were comparable to the intensity of ER α with nuclear receptor coregulator proteins, NCOA2, NCOR2 and FOXA1 (Figure 3.15a). In contrast, Pol III subunits were not found to have significant associations with the ER α . Interaction of GTF3C1 with ER α , GTF3C2 and GTF3C5 was confirmed by co-immunoprecipitation in MCF-7 cells. Here the band corresponding to GTF3C1 in the ER α IP was more intense than the GTF3C1 band from the

GTF3C2 and GTF3C5 IPs, suggesting a strong interaction of the hormone receptor with the largest subunit of the TFIIC complex (Figure 3.15b). The increased intensity of the ER α IP band was not due to non-specific binding to Protein A magnetic beads used in the IP procedure, as no GTF3C1 band is observed in a mock control IP.

Next, analysis of qPLEX-RIME data of MCF-7 cells treated with 100 nM tamoxifen for 6 hours were analysed. Tamoxifen is a SERM, that induces systemic reprogramming of ER α activity towards a transcriptional repressor instead of a prolific activator of gene expression in breast cancer cells (Wickerham, 2002; Keeton and Brown, 2005). Here, tamoxifen treatment of MCF-7 cells significantly increased association of the ER α with GTF3C1, GTF3C3 and GTF3C4, as well as nuclear corepressors NCOR1 and NCOR2 (Figure 3.15c). To contextualise the MCF-7 cell line findings of ER α interactions with TFIIC within a clinical framework, qPLEX-RIME of primary breast cancer tumours was analysed (Papachristou et al., 2018). As in the MCF-7 cells, the ER α exhibited significant interactions with GTF3C1, GTF3C3 and GTF3C5 (Figure 3.15d). Additionally, the intensity of ER α interactions with coactivators NCOA2 and NCOA5, as well as FOXA1, was greater than the intensity of ER α interactions with corepressors NCOR1 and NCOR2 (Figure 3.15d). The enhanced association of ER α with coactivators and FOXA1 in primary breast tumours suggests that the hormone receptor may exhibit activating activity at target genes. Additionally, the strong association of ER α with TFIIC, along with earlier evidence that ER α specifically targets tRNA genes in MCF-7 cells and breast tumours, provides insight into the mechanisms enhancing tRNA gene expression in oestradiol-stimulated MCF-7 cells (Hah et al., 2011).

In summary, investigating a protein tethering mechanism involved in recruiting ER α to target tRNA genes identified a strong and significant association of the hormone receptor with several subunits of the TFIIC complex, which binds to A and B box sequences in tRNA promoters and serves as the foundation for Pol III complex assembly. The evidence that ER α strongly interacts with TFIIC could explain how ER α is located to tRNA loci in the absence of a canonical DNA binding mechanism.

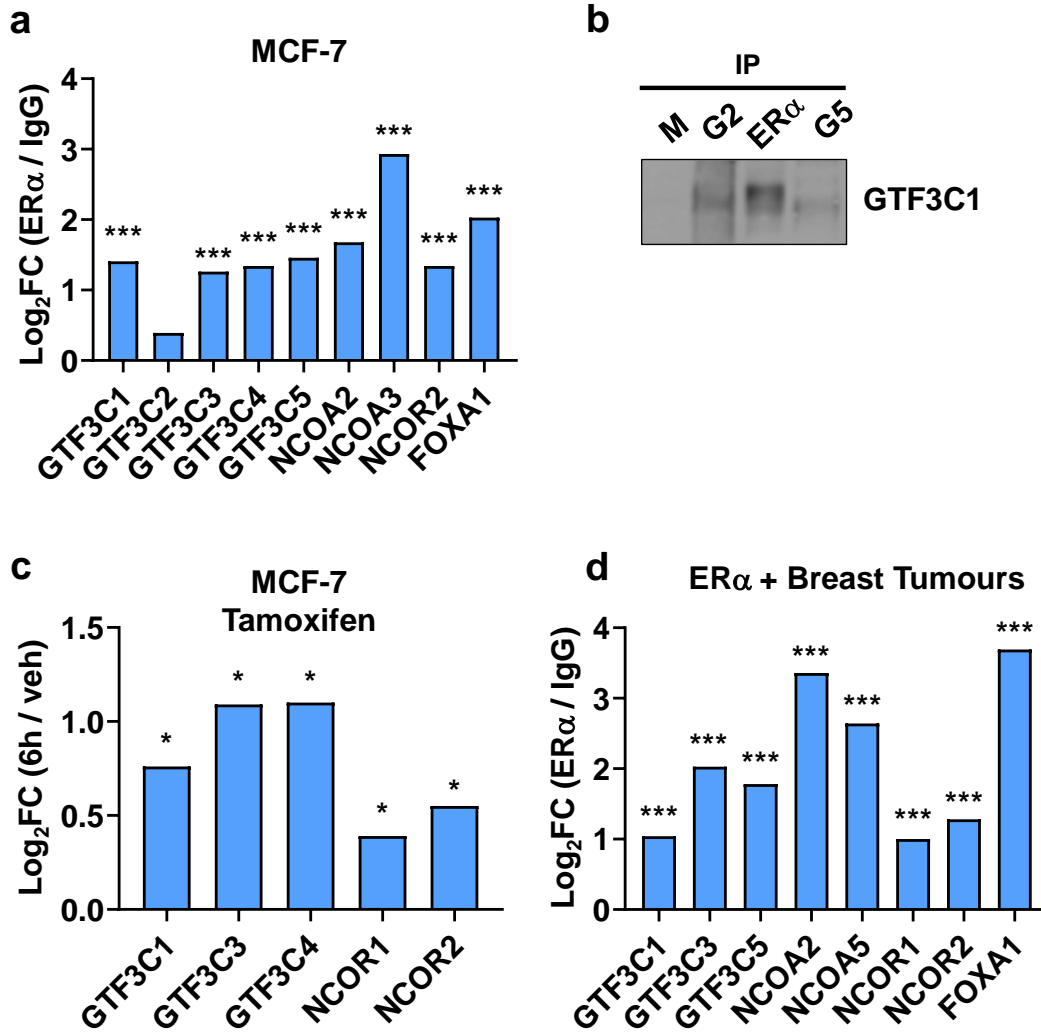


Figure 3.15. Pol III Subunits Physically Interact with ER α in MCF-7 Cells and ER α + Breast Tumours. (a) Log₂FC (ER α /IgGs) of ER α interactions with subunits of Pol III (GTF3C1 – GTF3C5), nuclear receptor coactivator 2 (NCOA2) and 3 (NCOA3), nuclear receptor corepressor 2 (NCOR2) and FOXA1 in MCF-7 cells as determined by analysing qPLEX-RIME dataset (Papachristou et al., 2018). ****padj* < 0.001. (b) Western blot of GTF3C1 following immunoprecipitation of GTF3C2 (G2), ER α and GTF3C5 (G5). A mock (M) IP was included to detect any non-specific binding of proteins to the Protein A beads. (c) Log₂ fold change in ER α association with Pol III subunits (GTF3C1, GTF3C3 and GTF3C4), NCOR1 and NCOR2 following 6-hour treatment with 100 nM tamoxifen. * *p* < 0.05. (d) ER α interaction intensity with GTF3C1, GTF3C3, GTF3C5 NCOA2, NCOR2 and NCOR1 in five independent ER α + breast cancer patient (ER α +, PR+, HER2- and Grade2/Grade3) samples, as determined by qPLEX-RIME. ****padj* < 0.001.

3.3 Discussion

The research carried out in this Chapter aimed to advance understanding of ER α -mediated dysregulated tRNA gene expression in breast cancers by uncovering the extent to which tRNA genes are under the regulatory influence of the hormone receptor, and to identify the mechanism of ER α recruitment to its target tDNAs. The main hypothesis being tested was that the ER α is directly associated with many tRNA genes where it can coordinate rapid changes in response to oestradiol (Hah et al., 2011). The investigations incorporated a combination of bioinformatic approaches utilising public ChIP-seq and qPLEX-RIME datasets, as well as molecular biology experiments to validate *in silico* findings and further enhance insight into the ER α -Pol III regulatory axis.

3.3.1 Summary of main findings

- The ER α was robustly associated with ~50 % of tRNA genes in the human genome in MCF-7 cells. Importantly, this observation was recapitulated in the clinical context, where primary and metastatic breast tumours also observed widespread association of the ER α with tRNA genes.
- No difference in the association of ER α with tRNA genes was seen in primary tumours of patients with a good or poor outcome, whereas metastatic tumours were more heterogeneous in the numbers of tDNAs bound by the ER α , and the strength of these associations.
- The specific identity of codons associated with the tRNA genes most targeted by ER α were not preferentially involved in conferring a differentiated or proliferative phenotype in MCF-7 cells.
- Recruitment of the ER α to target tRNA genes was not through recognition of a canonical ERE sequence in proximal or distal regions surrounding tDNA loci.
- Knock down of the ER α reduced occupancy of Pol III and FOXA1 at tRNA promoters, whereas GTF3C5 was still able to retain tight interactions with target A and B boxes in the absence of the hormone receptor.
- The ER α was found to have significant interactions with several subunits of the TFIIIC complex, both in MCF-7 cells and primary breast tumours. ER α -TFIIIC tethering was responsive to modulation of the ER α with tamoxifen.

3.3.2 Localisation of the ER α with tRNA and ncRNA genes *in vitro* and *in vivo*

Association of the ER α with tRNA loci in breast cancer cell lines was found to be extensive, whereby nearly 50% of tRNA genes in the human genome were identified as *bone fide* ER α targets in MCF-7 cells, as determined by setting a minimum Q-value threshold of $Q > 0.5$, based on quantified ER α read peaks at known ER α protein-coding target genes. To validate *in silico* observations of ER α binding to tRNA genes, CHIP-qPCR of Pol III and ER α in MCF-7 cells was carried out which confirmed ER α occupancy at specific tDNA loci, relative to a pre-immune control. While such comprehensive investigations into ER α interactions with Pol III promoters have not been reported, the finding of ER α recruitment to tRNA genes is in line with the previous observation that ER α occupies the promoter of tRNA^{Leu} in MCF-7 cells (Fang et al., 2017). Enriched ER α binding was also observed at *RMRP* and *RN7SL1* loci in MCF-7 cells by CHIP-seq and CHIP-qPCR, which has not previously been identified. Thus, ER α targeting of Pol III-transcribed genes is not limited to those containing Type II promoter architecture, and greatly expands the repertoire of ER α targets to include some of the most highly abundant transcripts in cells (Boivin et al., 2018). However, occupancy of ER α at the *BC200* promoter was not identified in any of the CHIP-seq datasets analysed, despite previous identification of ER α binding to an ERE-like sequence upstream of the *BC200* TSS in MCF-7 cells (Singh et al., 2016). The reason for the discrepancy between the lack of ER α association with *BC200* in MCF-7 cells described in this Chapter, and the ER α interaction with an ERE-like sequence proximal to *BC200* TSS identified by Singh *et al.* is unclear but could be attributed to previously described heterogeneity of the MCF-7 cell line (Ben-David et al., 2018).

To demonstrate clinical relevance of the CHIP-seq findings in ER α + cell lines, the association of ER α with tRNA genes in primary and metastatic breast tumours was explored. Again, robust and widespread association of the ER α at tRNA loci was found, confirming interactions of ER α with tRNA genes seen in MCF-7 and ZR-75-1 cell lines are applicable to a clinical setting. It is worth noting that in MCF-7 cells, ER α occupied ~ 20% more tRNA genes than in the primary tumour specimens. The difference in ER α associations at tDNA loci could be explained by the homogeneity of cell lines versus tumour heterogeneity (Choi et al., 2014). No detectable difference in tRNA targets of the ER α were identified between primary

tumours that came from patients with a better prognosis (alive at a ten year follow up) or those that had died due to having breast cancer. However, metastatic tumours displayed significant variation in ER α association at tDNAs, both in terms of numbers of ER α -occupied tRNA loci and strength of these associations.

In the context of breast cancer progression, tRNA expression has been found to be elevated 10-fold in breast tumours compared to healthy breast tissue (Pavon-Eternod et al., 2009). Overexpression of tRNA in transformed cells support dysregulated growth and proliferation by facilitating translation, ensuring effective and unimpeded transportation of tRNA isoforms to the ribosome, and rapid decoding of mRNA codons (Dana and Tuller, 2014). In particular, elevated tRNA expression is significantly associated with poor prognosis in breast cancer (Pavon-Eternod et al., 2009; Goodarzi et al., 2016; Krishnan et al., 2016; Zhang et al., 2018). Exploring ER α ChIP-seq datasets for associations of the hormone receptor with tDNAs in MCF-7 cells found tRNA-Arg-CCG-2-1 to be among the most strongly enriched for ER α binding, an important finding considering specific overexpression of this gene has been shown to promote breast cancer invasion and metastasis *in vitro* and *in vivo* through codon-dependent effects on stability and translation of pro-metastatic proteins (Goodarzi et al., 2016). Additionally, upregulation of tRNA^{Met} has been implicated in cancer progression where elevation of this special isoform bypasses the initiation bottleneck of protein synthesis, and has been implicated in driving cell proliferation, tumour growth and modulating ECM to enhance invasion (Pavon-Eternod et al., 2013; Gingold et al., 2014; Birch et al., 2016; Clarke et al., 2016). Thus, the observation that 30 % of genes encoding tRNA^{Met} were preferentially targeted by the ER α could also have significant implications for patients with ER α + disease.

3.3.3 Exploring ER α recruitment to target tRNA genes

Targeted motif analysis of top ER α -bound tRNA genes was unable to identify full or half ERE sequences within a 40 kb window centred around tDNAs, suggesting ER α recruitment to these 19 tRNA loci does not involve a DNA recognition mechanism. However, there are some important considerations to the finding that EREs may not be involved in ER α recruitment to target tDNAs. Firstly, the possibility of a non-canonical ERE that is recognised by the ER α remains.

Indeed, the ER α has been found to recognise diverse ERE-like sequence elements, demonstrating flexibility of the hormone receptor in sequence identity requirements for DNA binding (Mason et al., 2010; Stender et al., 2010). Secondly, the vast majority (~95%) of ER α binding sites occur in distal enhancer regions which can be up to ~ 150 kb away from the TSS in ER α protein-coding gene targets (Carroll et al., 2006), a distance that was not covered in the directed motif analysis conducted in this Chapter. Lastly, a significant proportion of ER α -bound tRNA genes were not included in the investigation into hormone receptor recruitment to target tDNA loci (top 6% of ER α enriched tRNA genes were studied for an ERE). As such, it is possible that remaining tRNA genes targeted by the ER α but not included in the motif analysis do contain canonical ERE sequences. Nevertheless, a DNA-binding mechanism was not further explored in this thesis and remains an interesting question to be addressed.

Instead, investigations into ER α positioning at tRNA genes was directed towards testing recruitment of ER α to tDNA loci through associations with other regulatory factors and a protein tethering mechanism, which is thought to account for 10 - 35 % of ER α binding events in the human genome (O'Lone et al., 2004; Stender et al., 2010). Analysis of a ChIP-seq dataset in MDA-MB-231 breast cancer cells expressing exogenous ER α revealed strong enrichment of the hormone receptor to a well characterised ERE, approximately 20 kb upstream of the *GREB1* TSS (Sun et al., 2007). However, the extensive recruitment of ER α to tDNA loci observed in MCF-7 cells expressing endogenous ER α failed to be recapitulated in the TNBC cell line following stable transfection of the hormone receptor. The lack of ER α binding to previously identified tDNA targets suggest that expression of the ER α alone is not sufficient to direct and maintain ER α interactions with tRNA genes, and additional regulatory factors that are not present in the MDA-MB-231 cells are essential for effective loading of ER α at tDNA promoters. FOXA1 is preferentially expressed in epithelial breast cancers, and is a key regulator of the ER α transcriptome (Hurtado et al., 2011; Glont et al., 2019; Seachrist et al., 2021). Additionally, FOXA1 is lost when cells become mesenchymal, and is not expressed in TNBC tumours or MDA-MB-231 cells (Anzai et al., 2017; Kumar et al., 2021). Analysis of FOXA1 and ER α ChIP-seq datasets in MCF-7 cells found significant overlap in the tRNA genes targeted by both the pioneer factor and the

hormone receptor, as expected on the basis of literature where FOXA1 is found to occupy 50 - 60% of ER α binding sites (Hurtado et al., 2011).

When ER α was knocked down by a short time course of fulvestrant, a reduction in promoter occupancy by both Pol III and FOXA1 was seen at all tRNA genes studied, which was significantly decreased at the tRNA-Pro-TGG-1-1 locus, where Pol III was found to be the most enriched in vehicle treated MCF-7 cells. In contrast, ER α knockdown did not affect the ability of TFIIIC subunit GTF3C5 to maintain contact with tDNA loci, nor was ER α association at the selected tDNA affected by fulvestrant treatment, in contrast to the significant reduction in ER α occupancy at the GREB1 ERE that was observed. The mechanism by which ER α is associated with target genes could provide an explanation as to why tRNA genes are not as susceptible to fulvestrant as other *bona fide* ER α targets, such as *GREB1*. If a protein tethering mechanism is sequestering the hormone receptor in tight complexes at the DNA, it may render ER α at these promoters resistant to fulvestrant-induced proteasomal degradation, whereas ER α that is directly associated with EREs may be more open to pharmacological attenuation. Such a speculation requires further exploration.

While FOXA1 is essential for ER α accessibility to many of its *cis* regulatory elements in proximal and distal regions surrounding target genes, dynamic interactions between the ER α and FOXA1 exist such that ER α can also dictate FOXA1 localisation and enhance FOXA1 binding (Swinstead et al., 2016). The observation that ER α knockdown reduced FOXA1 and Pol III occupancy at tRNA loci in MCF-7 cells suggests a mechanism where ER α recruits FOXA1 to target tDNA, which in turn facilitates Pol III positioning at tRNA gene TSS. The link between FOXA1 and Pol III has not been further investigated in this thesis. However, one potential explanation for how FOXA1 could influence Pol III loading at tDNA involves the pioneer factor enhancing chromatin accessibility around tDNAs to improve accessibility at these loci by Pol III. The increased open conformation of chromatin could then facilitate TFIIIB binding near the TSS, which in turn recruits Pol III to its templates, a process that occurs downstream of TFIIIC localisation to tRNA A and B boxes (Kassavetis et al., 1990). When occupancy of tRNA genomic loci by FOXA1 is reduced, the chromatin surrounding target genes remains tightly wrapped around histones and impedes the ability of TFIIIB and/or additional auxiliary factors to navigate tDNA and recruit Pol III.

ER α knockdown also decreased occupancy of Pol III and FOXA1 at *RMRP* and *RN7SL1*. While *RMRP* has true Type III promoter architecture and thus no A and B box or requirement for TFIIC, *RN7SL1* does not strictly conform to this definition of a Type III, as A and B box elements which recruit TFIIC are found in this gene (Canella et al., 2010; de Llobet Cucalon et al., 2022). However, a similar auxiliary role for FOXA1 could still be applied to the efficient loading of Pol III to both *RMRP* and *RN7SL1*. A commonality between Type II and Type III promoters is the recruitment of TFIIB to Pol III-transcribed genes. However, In Type III promoters, TFIIB is comprised of a Brf2 subunit as opposed to Brf1. In addition, Type III TFIIB recognises an upstream TATA box by the TBP member of the complex, whereas no TATA binding is involved in Type II TFIIB recruitment (Alla and Cairns, 2014). Here, FOXA1 may be brought to proximal regions surrounding promoter structures by ER α where it can enhance chromatin accessibility, allowing TBP of TFIIB to recognise and bind to the TATA box with less difficulty. TFIIB association with the TATA box would deliver Pol III to the TSS. Recruitment of FOXA1 to *RMRP* and *RN7SL1* may further facilitate localisation of SNAPc to the PSE to initiate assembly of the Pol III machinery (Figure 3.16)

The observation that GTF3C5 was unaffected by the absence of ER α in MCF-7 cells suggests that the recruitment of the hormone receptor to tDNA loci is secondary to the recruitment of TFIIC to its cognate A and B box elements. The association of TFIIC with tDNA is stable and does not require auxiliary support by ER α or associated coregulators to maintain strong interactions with *cis* regulatory elements. Despite the resilient interaction of TFIIC at tDNA in the absence of hormone receptor, the ER α was found to be strongly associated with several members of the TFIIC subunit, including GTF3C5, both by qPLEX-RIME, and by co-immunoprecipitation and western blot. The strong interactions between ER α and TFIIC could suggest that the ER α is directed to target tRNA and maintains occupancy at these loci by robust protein tethering with TFIIC. In addition to evidence of an ER α - TFIIC complex existing at tRNA genes, the ER α also co-immunoprecipitates with TFIIB in MCF-7 cells (Fang et al., 2017). Thus, there is a possibility that in ER α + cell lines, the ER α is in complex with several members of Pol III transcriptional machinery to facilitate rapid upregulation of tRNA gene expression in response to oestradiol (Hah et al., 2011). In addition to tight associations with TFIIC, the ER α was also found to be strongly interacting with coregulatory proteins, including co-activators (NCOA), co-repressors (NCOR) and

FOXA1, as expected (Hall and McDonnell, 2005; Hurtado et al., 2011). Importantly, the findings of ER α in complex with TFIIIC subunits and coregulatory factors in MCF-7 cells was also identified in qPLEX-RIME of primary breast tumours. Thus, the proposed ER α -TFIIIC-TFIIIB complex identified in MCF-7 cells could be implicated in clinical development and progression of breast cancer. Indeed, following a 6-hour treatment of tamoxifen in MCF-7 cells, a significant increase in ER α -TFIIIC contact was induced, as was the association of ER α with co-repressors NCOR1 and NCOR2, suggesting that pharmacological modulation of ER α not only exerts a repressive function to the hormone receptor but also impairs Pol III translation of tRNA genes, potentially by the activities of repressive co-regulators associated with the ER α at tDNA loci. The recruitment of coregulators to the promoters of tDNA, and corresponding changes in tRNA expression in response to ER α agonism or antagonism needs to be further investigated. If it is true that coregulators are recruited to tDNA through interactions with ER α , a ChIP-seq experiment designed to identify changes in chromatin acetylation or methylation deposits surrounding tRNA loci would further assist in delineating the mechanism by which ER α may regulate tRNA expression in breast tumours. Similarly, inclusion of oestradiol stimulation or tamoxifen or fulvestrant attenuation could provide additional insight into the molecular changes that happen at the chromatin level, specifically surrounding tDNA, in response to alterations of ER α activity or availability.

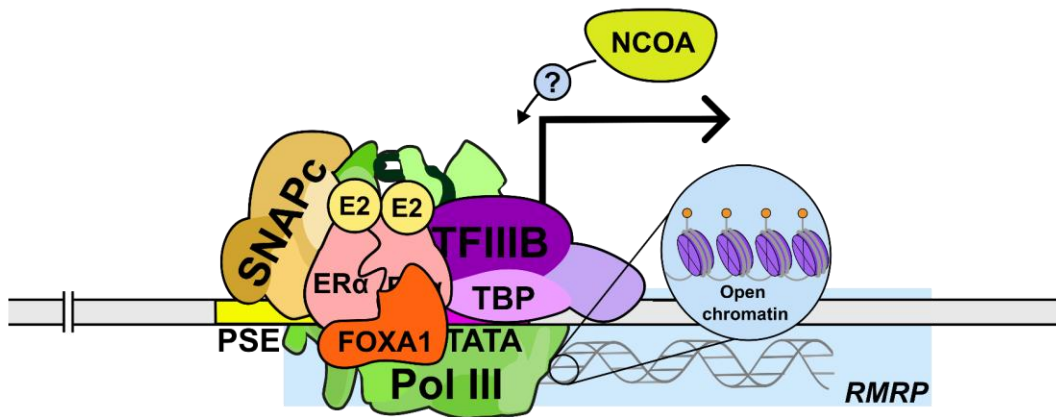


Figure 3.16. Proposed mechanism of ER α recruitment to Type III promoters.

At Type III promoters, such as in *RMRP*, FOXA1 may be directed to the TATA box by ER α where it can enhance chromatin accessibility, allowing TBP of TFIIB to bind to the TATA box and efficiently deliver Pol III to the TSS. FOXA1 may also open chromatin around the PSE, which would facilitate localisation of SNAPc to the PSE and the initiation of Pol III assembly.

3.3.4 Differential codon usage for tRNA isotypes and the implications in cellular processes and disease

The ER α was not found to significantly or preferentially associate with tRNA genes encoding anticodons involved in cell differentiation or proliferation, as proposed by Gingold *et al.* in 2014. Instead, of the top 75 ER α -bound tDNA, almost equal proportions of genes were found between the “differentiation”, “proliferation” and “other” gene classifier groups, and no significant difference in the strength of ER α associations with tRNA in each group was observed. This result is unexpected, as one might assume ER α targeted tRNA genes in breast cancer cell lines would be specifically geared towards driving pathogenicity and associated with proliferation. Indeed, tRNA isoacceptor expression has been linked to favouring the translation of cancer-related genes (Pavon-Eternod *et al.*, 2009). Furthermore, synonymous codon usage changes have been identified in malignant cells relative normal tissue. For example, decrease in tRNA-Gly-GGC is observed in breast cancers, in favour of increased usage of tRNA-Gly-GGT, exemplifying changes to codon usage patterns in malignancies (Meyer *et al.*, 2021). Additionally, tRNA-Glu-UUC and tRNA-Arg-CCG are found to be promoters of metastatic breast cancer by enhancing translation efficiency and increasing expression of EXOSC2 and GRIPAP1 (Goodarzi *et al.*, 2016). Of course, classification of ER α -bound tDNA loci into functional groups only provides information on the *potential* functionality of these genes. As expression of tRNA genes bound by ER α has not been investigated in this Chapter, it is not possible to state whether an ER α binding event at tDNA loci signifies an actively transcribed gene, or if these genes associated with ER α are repressed. Therefore, to be able to further characterise the significance of ER α targeted tRNA genes in breast cancer using Gingold’s classifier list, transcriptional studies need to be carried out to see the functional consequence of an ER α binding event at tRNA loci.

3.3.5 Future work

As highlighted in Section 3.3.3, a DNA binding mechanism behind ER α recruitment to tRNA loci has not been fully explored. While there is strong evidence in support of a protein tethering mechanism, only a small proportion of tRNA targets of the ER α were investigated. To assess a DNA binding mechanism further, expanding the motif search to include all tRNA genes identified as ER α targets, and

utilising a more high-powered computational program, such as the *TFBSTools* package in R could inform in greater detail the requirement of canonical and non-canonical ERE motifs in proximal and distal enhancer regions of tDNA loci (Tan and Lenhard, 2016). Additionally, a key principle of ER α binding to the DNA is the presence of a functional DBD (Björnström and Sjöberg, 2002; Stender et al., 2010; Huang et al., 2018). Three mutations in the human ER α DBD, namely E203G, G204S and A207V, have been shown to disrupt ER α binding to EREs by up to 95% (Mader et al., 1989; Stender et al., 2010). Thus, generating ER α DBD mutants and conducting ChIP-seq would allow the discrimination of tRNA genes targeted by the ER α through protein tethering mechanisms - which would be unaffected by DBD mutations, and tDNAs that are targeted by the ER α through a direct interaction with DNA at tRNA loci - which would see a reduction in ER α occupancy with DBD mutant relative to wild type ER α .

It would also be useful to further explore the co-regulator axis of ER α with tRNA genes and Pol III transcriptional machinery. Findings discussed in Section 3.2.7 and Section 3.2.8 implicate FOXA1 in Pol III recruitment to some Type II and Type III promoters, although the exact mechanism underlying this remains unclear. FOXA1 recruitment appears to fall between the positioning of TFIIC, whereby the GTF3C5 subunit is unaffected by reduced ER α and FOXA1 occupancy at tDNA loci, and the subsequent loading of Pol III at the TSS. TFIIB is directed to TFIIC and is responsible for the efficient recruitment of Pol III to target promoters by an interaction with Brf1 (or Brf2 in Type III promoters) and at least three distinct Pol III sites (Kassavetis et al., 2001; Gouge et al., 2015). How FOXA1 affects the complete assembly of the Pol III apparatus prior to ncRNA transcription could be explored more comprehensively. Specifically, ChIP-qPCR of fulvestrant treated, or FOXA1-depleted (siRNA) MCF-7 cells could be undertaken to assess Brf1 and Brf2 occupancy at tDNA and *RMRP/RN7SL1*, respectively. If the TFIIB subunits are also reduced at their target promoters, it would support the hypothesis that FOXA1 promotes open chromatin around these loci to facilitate cognate TFIIB binding. Many other co-regulatory proteins associated with the ER α are essential for the ability of the hormone receptor to carry out transcriptional activation or repression of target genes. Such accessory factors include P300, CBP, AP-1, SP-1 as well as nuclear receptor coactivators (NCOA) and corepressors (NCOR) (Hanstein et al., 1996; Kraus and Kadonaga, 1998; deGraffenried et al., 2002; Altwegg and Vadlamudi, 2021; Waddell et al., 2021). The intricate and dynamic co-regulatory

network of the ER α - Pol III axis could therefore be further explored in the context of specific recruitment of such transcription factors, and their involvement in securing robust protein-tethering interactions or facilitating rapid upregulation of ncRNA in response to hormone stimulation. Further ChIP-seq or ChIP-qPCR experiments could help unravel the complexes that form with the ER α at Pol III promoters and ascertain the biological significance of such recruitment in terms of gene expression. To understand codon usage bias and the biological properties of tRNAs targeted by the ER α in breast cancer cells, studies that investigate the transcriptional response to i) ER α knockdown, ii) oestradiol stimulation and iii) ER α antagonism could be carried out. Specifically, single-read tRNA-seq could discriminate preferential codon usage in breast cancer cells vs. normal breast tissue, as well as elucidate specific direction of tRNA gene transcription in response to hormone stimulation or ER α repression (Hernandez-Alias et al., 2023). Additionally, analysis of such datasets would further help to stratify *active* targets of the ER α into Gingold's functional classifier groups, to ascertain if tDNA loci with robust ER α associations are providing an anticodon pool that serves to enhance efficient translation of proliferative genes in breast cancer (Gingold et al., 2014).

Finally, an interesting feature of tDNA biology is their propensity to be linearly organized into genomic clusters with other tDNAs. In particular, almost one-third (158) of annotated human tRNA genes are closely spaced within 2.67 million base pairs of the class I major histocompatibility complex genes on the short arm of chromosome 6, and are similarly proximal to many genes which encode histone proteins and zinc-finger transcription factors (Mungall et al., 2003; Pan, 2018). Other smaller tRNA cluster hotspots are located on chromosomes 1, 5, 14, 16 and 17. Additionally, a cluster of tRNA genes are present on chromosome 7, which is 90% comprised of tRNA^{Cys} genes (Mungall et al., 2003). The genomic organisation of tDNA therefore have been studied in some depth, and suggest that tDNA clusters are functional in preserving hetero-euchromatic borders by acting as barriers or insulators (Sizer et al., 2022). By acting in this way, tDNA insulators maintain distinct genomic boundaries but also perpetuate high-level Pol III transcription due to tDNAs being close to other tDNAs on the same chromosome. Further, the compact nature of chromosomes means tDNAs that may be spaced kilo bases away from another tDNA in linear organisation are in fact in proximity in 3D space, due to chromatin folding. As such, domain-level and loop-based organisation of tDNA are of significant importance when considering how these tRNA genes are regulated (Van

Bortle et al., 2017). Therefore, it would be of great interest to further explore the relationship between ER α bound tDNA in breast cancer cells using methods that can capture topological chromatin interactions of transcription factors, such as Hi-C, an improved Chromatin Conformation Capture method that would allow unbiased probing of all chromosomal interactions occurring around ER α binding sites (Belton et al., 2012). Such experiments would permit inference regarding the full extent to which ER α may regulate tDNA expression. For instance, if Hi-C captured ER α associated with two distinct tRNA genes present on the same chromosome, one could assume that these tDNA are preferentially targeted for regulation by the hormone receptor. However, if Hi-C instead captured a tRNA gene and a known ER α regulated gene (e.g., *GREB1*), it could be possible that ER α is only associated with the tRNA gene in 3D space, rather than being a genuine ER α target gene, with subsequent alterations in tRNA expression being a byproduct of ER α and coregulator association at Pol II, not Pol III promoters.

3.4 Conclusion

The aim of this Chapter was to quantify ER α enrichment at tRNA genes and delineate the mechanism in which ER α is recruited to Pol III-transcribed loci. Between 30 and 50% of tRNA genes are specifically targeted by the ER α in ER α + cell lines and breast tumours. The recruitment of the hormone receptor to the tDNAs with the strongest association was not via canonical ERE sequence motifs as originally hypothesised, but instead appears to be a consequence of robust interactions of ER α with TFIIIC subunits bound to A and B boxes of target tRNA genes. ER α facilitates Pol III positioning at tRNA promoters, possibly by reinforcing assembly of necessary Pol III transcriptional machinery through enhanced protein tethering mechanisms, or by enhancing chromatin accessibility for TFIIIB and Pol III with the recruitment of pioneer factor FOXA1 to tDNA loci.

4. Identification of Robust RT-qPCR Reference Genes for Studying Changes in Gene Expression in Response to Hypoxia in Breast Cancer Cell Lines

4.1 Introduction

Hypoxia is a key driver of breast cancer progression. In particular, breast tumours positive for HIF-1 α or hypoxic signatures are associated with increased 10-year breast cancer recurrence, therapy resistance and breast cancer-related death (Li et al., 2022b; Tutzauer et al., 2022). As HIF-1 α and HIF-2 α are the predominant transcription factors mediating the hypoxic response, important changes occurring at the transcriptional level because of HIF activity need to be investigated. Identifying novel targets of HIF-1 α and/or HIF-2 α could have significant therapeutic benefit for women with hypoxic breast tumours.

To assess complex transcriptional changes occurring during hypoxia-mediated breast cancer progression and therapy resistance, reverse transcription - quantitative real-time polymerase chain reaction (RT-qPCR) is gold standard for accurately quantifying gene transcription and capturing dynamic changes in gene expression that may be serving as molecular drivers of advanced disease (Ginzinger, 2002). A fundamental component of RT-qPCR is inclusion of reference genes (RGs) which act as internal controls for endogenous normalisation of measured target gene expression. RGs are selected on the basis of constitutive expression, and relative abundance not being altered by experimental conditions (Suzuki et al., 2000). The substantial adjustment to the epigenome and transcriptome of cells that occurs under hypoxic conditions renders traditional RGs such as glycolytic enzymes *GAPDH* or *PGK1* unsatisfactory for this use; despite this, comprehensive, systemic determination of RGs for hypoxia studies in breast cancer cell lines has yet to be performed (Yang et al., 2008b; Higashimura et al., 2011; Zhang et al., 2020; Wang et al., 2021).

An additional consideration for investigating hypoxia-driven changes in gene transcription is ascertaining which HIF isoform is responsible for such aberrations in expression. The “HIF switch” refers to the transition from HIF-1 α to HIF-2 α -dependent transcription and is recognised by rapid accumulation of HIF-1 α in response to acute O₂ deprivation, followed by loss of HIF-1 α during periods of chronic hypoxia and accumulation of HIF-2 α protein as this secondary isoform

becomes the predominant driving force of a long-term hypoxic response (Zhong et al., 1999; Holmquist-Mengelbier et al., 2006; Franovic et al., 2009; Koh and Powis, 2012). Identification of the molecular transitions between HIF isoforms will inform which transcription factor may be responsible for observed expression changes of genes of interest. Therefore, it is important to conduct studies in hypoxic breast cancer cells with the HIF switch in mind.

4.1.1 Aims and objectives

As determination of robust RGs for studying the effects of hypoxia on breast cancer cell lines has not been carried out, an important knowledge gap exists, whereby RGs suitable for this purpose need to be identified. To address this need, four widely used breast cancer cell lines representing both ER α + Luminal A (MCF-7 and T-47D) and TNBC (MDA-MB-231 and MDA-MB-468) subtypes were used. To estimate the timing of the HIF switch, breast cancer cell lines were cultured in normoxia (20% O₂), or hypoxia (1% O₂) under an acute (8 hours) or chronic (48 hours) time course and western blot was used to monitor HIF isoform abundance. To identify RG candidates, a publicly available RNA-seq dataset of hypoxic breast cancer cell lines was analysed (Ye et al., 2018; Godet et al., 2019). With 10 RG candidates, a comprehensive investigation to identify RGs with the least variability in expression after being cultured in normoxia, acute hypoxia or chronic hypoxia was implemented. RG candidates not abundantly expressed or associated with poor primer efficiencies were filtered out of the selection process. RGs were chosen by employing web-based RG tool RefFinder (Xie et al., 2012, 2023). The finding of robust RT-qPCR RGs in the context of hypoxic breast cancer cell lines will provide a valuable resource for future studies investigating important transcriptional changes occurring during breast cancer progression.

4.2 Results

4.2.1 The HIF Switch in Hypoxic Breast Cancer Cell Lines Occurs between 8 and 48 Hours of O₂ Deprivation

The overall aim of this study was to identify optimal RGs for investigations of normoxic vs. hypoxic ER α + Luminal A (MCF-7 and T-47D) and TNBC (MDA-MB-231 and MDA-MB-469) cell lines. Cell lines were selected based on widespread use in breast cancer research: MCF-7, T-47D and MDA-MB-231 represent more than two-thirds of cell lines used within such studies (Dai et al., 2017).

To select optimal timepoints for investigating hypoxia-mediated changes in transcription, it was important to identify the HIF switch in chosen breast cancer cell lines. To estimate HIF switch timepoints, MCF-7, T-47D, MDA-MB-231 and MDA-MB-468 breast cancer cell lines were cultured in normoxia, or in hypoxia for 8 or 48 hours to observe changes in HIF protein accumulation. In normoxic cell lysate from all cell lines, no HIF-1 α protein was observed (Figure 4.1a). For a loading control, α -Tubulin was immunoblotted for on the same membrane which confirmed equal loading of cell lysate in all lanes. Densitometry analysis of HIF-1 α and α -Tubulin showed a maximum induction of HIF-1 α protein after 8 hours culture in hypoxia, which was markedly reduced after 48 hours, in all cell lines. MDA-MB-231 cells saw the greatest induction of HIF-1 α during acute hypoxia and saw the greatest loss of HIF-1 α after chronic exposure to a hypoxic environment. When HIF-2 α was investigated, normoxic cell lysate demonstrated moderate levels of this transcription factor in all cell lines (Figure 4.1b). Densitometry analysis revealed positive fold change increase in HIF-2 α protein levels following acute and chronic hypoxic culture. For MCF-7s, this induction was small after 48 hours, whereas for T-47D cells, HIF-2 α protein levels reached a nearly 2-fold increase by the end of the experiment. MDA-MB-231 cells saw a 1.5-fold induction in HIF-2 α protein after 8 hours of hypoxic culture, however the levels of this isoform returned to normoxic levels by 48 hours. The greatest induction of HIF-2 α was seen in the second TNBC cell line. Here, MDA-MB-468 cells increased HIF-2 α protein levels more than 2-fold after acute hypoxic culture, which was sustained up to the 48 hours' time point. Despite cell line variability, HIF-1 α was strongly induced in all cell lines at 8 hours of hypoxic culture, demonstrating rapid stabilisation in response to O₂ deprivation. HIF-2 α was already present in all cell lines, even in normoxic conditions, but as HIF-1 α

protein was nearly absent after 48 hours while HIF-2 α persists, it was reasonable to assume that HIF-2 α mediates the prolonged hypoxic response at this time point. Therefore, hypoxic culture of 8 hours was used to determine HIF-1 α transcriptional targets, whereas 48 hours would recapitulate chronic hypoxia and was used to ascertain HIF-2 α targets. For the purposes of identifying non-variable RGs for RT-qPCR studies, a hypoxic time course of 8 or 48 hours was used.

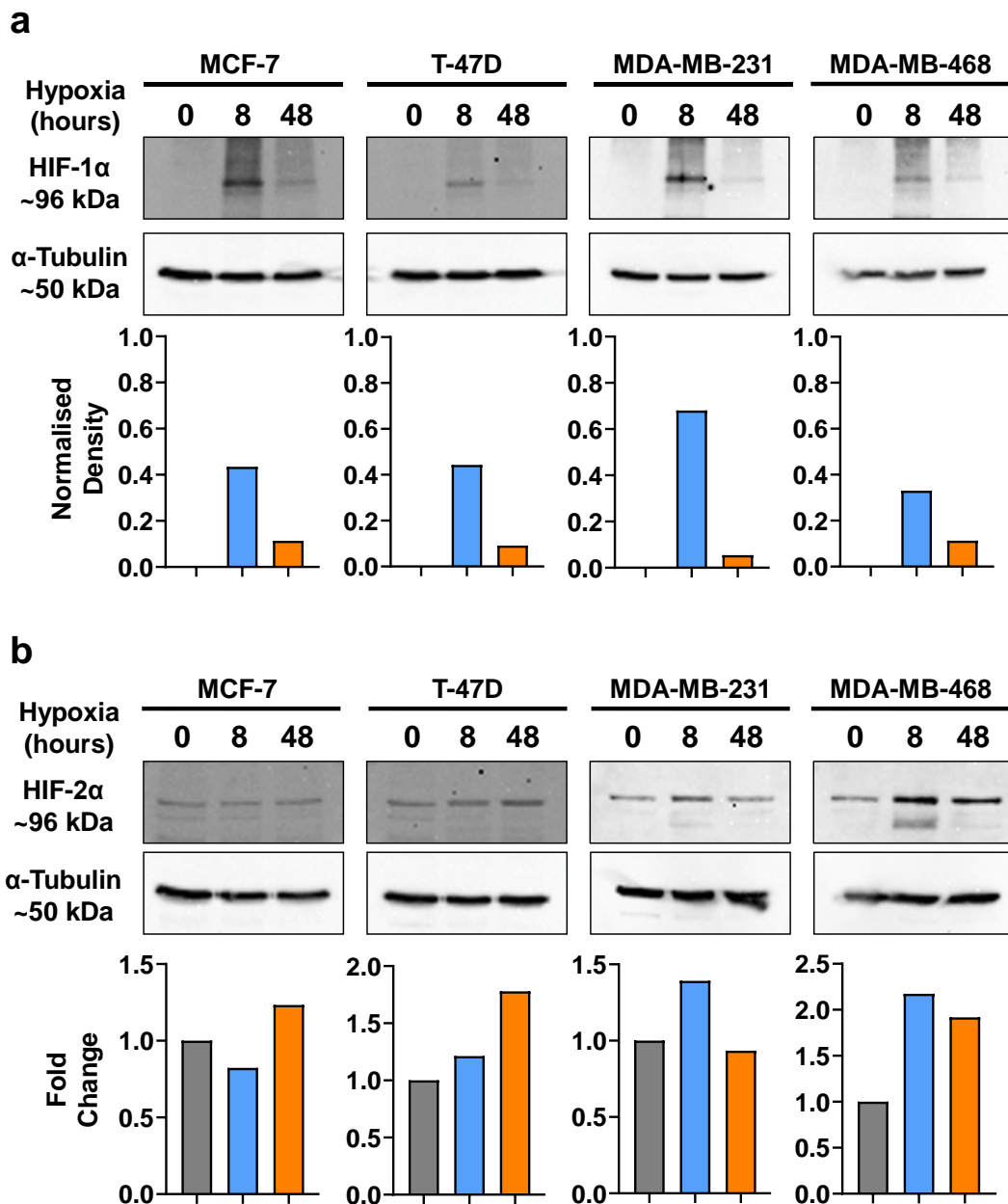


Figure 4.1 Identifying the “HIF Switch” in Breast Cancer Cell Lines (a) Western blot analysis of HIF-1 α (top western blot windows) and α -Tubulin (bottom western blot windows) in MCF-7, T-47D, MDA-MB-231 and MDA-MB-468 breast cancer cell lines. Plots under western blots demonstrate normalised densitometry analysis where density of HIF-1 α bands from 8 and 48 hours of hypoxic culture were normalised to density of α -Tubulin bands of the same time point, in each cell line. N = 1. **(b)** Western blot analysis of HIF-2 α (top western blot windows) and α -Tubulin (bottom western blot windows) in MCF-7, T-47D, MDA-MB-231 and MDA-MB-468 breast cancer cell lines. Plots under western blots represent fold change in normalised density values of HIF-2 α following 8 or 48 hours of hypoxic culture relative to normalised normoxic (0 hour) HIF-2 α band density. N = 1.

4.2.2 Analysis of public RNA-seq dataset identifies 10 RG candidates

To address the need for robust RGs for studying hypoxia in breast cancer cell lines, a publicly available RNA-seq dataset was utilised to generate a shortlist of RG candidates. The original study investigated genome-wide transcriptional changes taking place in 32 breast cancer cell lines as a consequence of O₂ deprivation, and RNA-seq datasets were deposited to the NCBI SRA (Table 2.6) (Ye et al., 2018; Godet et al., 2019). In order to benefit from the public sequencing files for the purpose of exploring potential RG candidates, *fastq* files for normoxic and hypoxic MCF-7, T-47D, MDA-MB-231 and MDA-MB-468 breast cancer cells were obtained and reads quantified using *kallisto* (Bray et al., 2016). From the 30,187 genes evaluated in selected ER α + and TNBC cell lines, sample to sample distances were measured in a Euclidean Distance Matrix (EDM) plot which showed samples from the same cell lines were clustered closer together than samples from different cell lines, as expected (Figure 4.2A). Additionally, TNBC cell lines were grouped together, as are Luminal A cell lines, whereas greater divergence was seen between cell lines representing different subtypes of breast cancer. Therefore, the result from the EDM analysis confirmed no sample outliers.

To further validate the use of the public RNA-seq dataset, responsiveness of hypoxia-regulated genes was assessed to ensure cell lines behaved as expected when cultured in the absence of O₂. Analysis demonstrated increased expression of *CA9*, *PGK1* and *VEGFA* in all cell lines, in response to hypoxic culture and in line with previous findings (Figure 4.2B – Figure 4.2D) (Forsythe et al., 1996; Wykoff et al., 2000; Turner et al., 2002; Zhang et al., 2020). Therefore, the public dataset had undergone thorough validation and quality control and was suitable for identifying RG candidates.

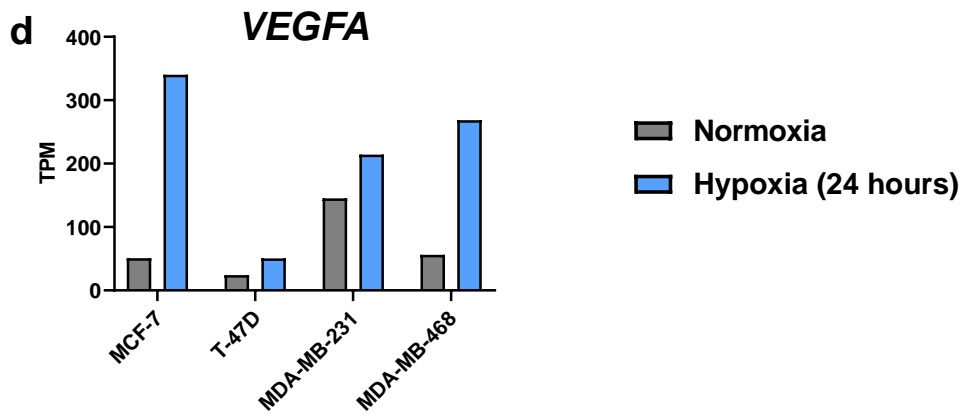
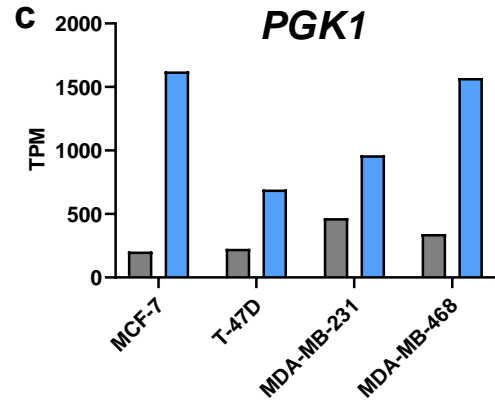
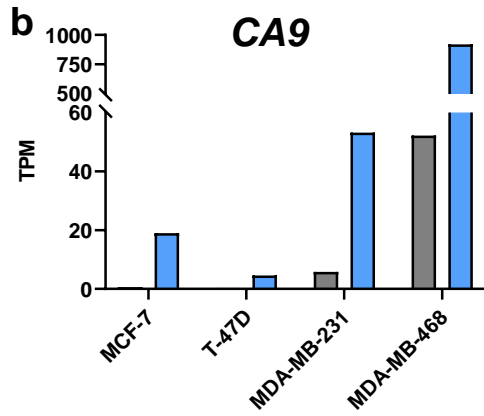
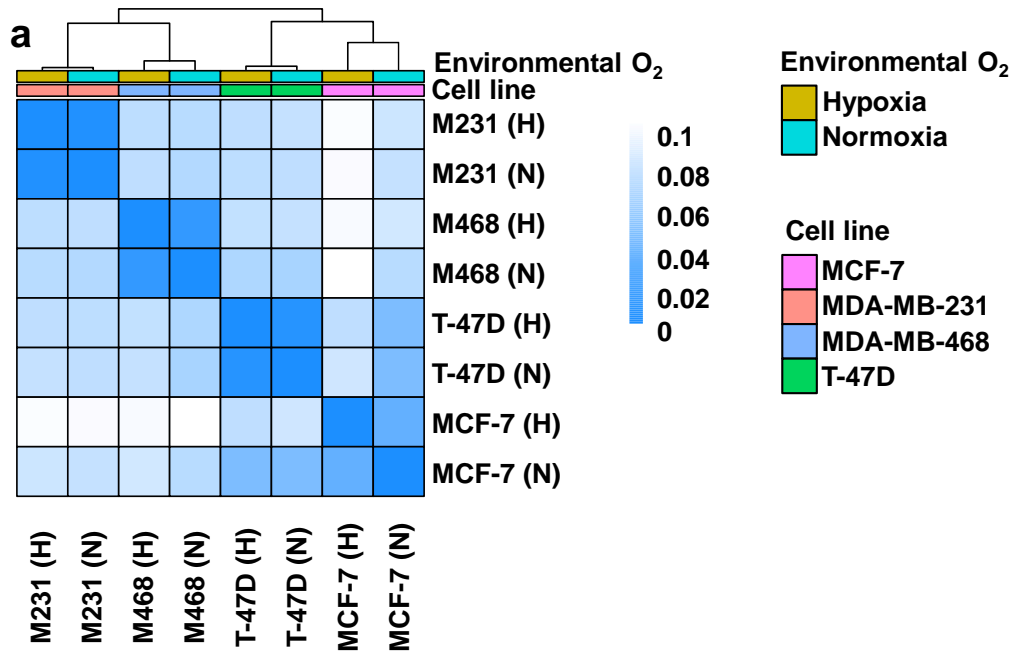


Figure 4.2 Responsiveness of Breast Cancer Cell Lines to Hypoxia in a Publicly Available RNA-seq Dataset (GSE111653) (a) EDM of squared distances between MCF-7, (pink) MDA-MB-231 (M231; salmon), MDA-MB-468 (M468; blue) and T-47D (green) breast cancer cell lines cultured in normoxia (N; teal) or hypoxia (H; gold). Transcripts per million (TPM) of hypoxic-responders (b) *CA9*, (c) *PGK1* and (d) *VEGFA* in breast cancer cell lines cultured in normoxia (20% O₂; grey) or hypoxia (1% O₂; blue) for 24 hours. N = 1.

As HIFs are constitutively transcribed, translated and turned over, the expression of HIF genes *ARNT* (HIF-1 β), *ARNT2* (HIF-2 β), *EPAS1*, *HIF1A* and *HIF3A* was analysed to see if any of the hypoxic responders could serve as suitable RGs in the study of hypoxic breast cancer cell lines (Figure 4.3). Interestingly, *EPAS1*, the gene encoding HIF-2 α , appeared to be relatively stable in expression in TNBC but not ER α + cell lines (Figure 4.3c; Table 4.1). Specifically, *EPAS1* was not expressed in MCF-7s, but was expressed in T-47D and MDA-MB-231 cells, and more so in the MDA-MB-468 cell line. As this study aims to identify RGs that can be used when comparing all breast cancer cell lines together, as well as RGs optimised for cell lines stratified into breast cancer subtype, or individual cell lines, *EPAS1* was included as a promising candidate for an RG when studying transcriptional changes occurring in hypoxic MDA-MB-231 and MDA-MB-468 cells.

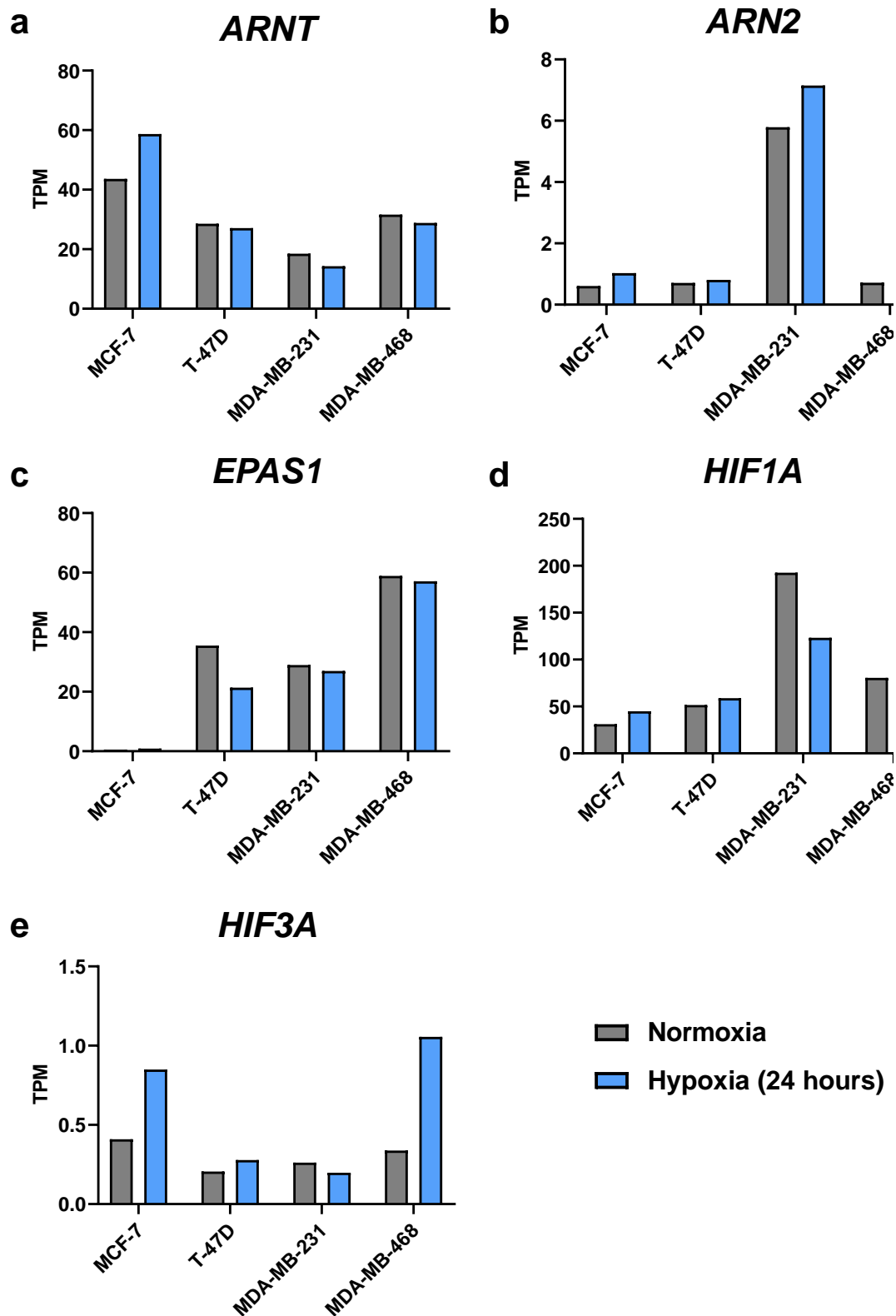


Figure 4.3 Members of the HIF Complex are Variable in their Expression in Normoxia and Hypoxia RNA-seq analysis (GSE111653) of HIF genes (a) *ARNT* (b) *ANT2* (c) *EPAS1* (d) *HIF1A* and (e) *HIF3A* in breast cancer cell lines cultured in normoxia (20% O₂; grey) or hypoxia (1% O₂; blue) for 24 hours. N = 1.

Next, read count stability of common RGs was determined when ER α + and TNBC cells were cultured in hypoxia or normoxia, to identify RG candidates that may be stable in expression in each cell line, regardless of O₂ availability. From this, a shortlist of 10 RG candidates was generated (Table 4.1). Candidates were initially selected based on common use as RGs in breast cancer cell lines (e.g. *CCSER2* in MCF-7, T-47D, MDA-MB-231 and MDA-MB-468 cell lines), or as stable RGs in other models of hypoxia (e.g. *RPLP1* in hypoxic pre-conditioned human neural stem cells) (Tilli et al., 2016; Kang et al., 2019; Jain et al., 2020), and further stratified based on a calculated similarity score (s) which was used to determine how similar read counts are in genes from breast cancer cell lines cultured in 20% or 1% O₂. Where $s = 0$, transcripts per million (TPM) are the same between the two conditions. A minimum threshold was established where $s \leq 0.30$ in at least two of the cell lines, to be carried forward as an RG candidate.

Of the 10 RG candidates, ER α + MCF-7 cells had the greatest variability in RG expression compared to T-47D and TNBC cell lines, with *CCSER2*, *EPAS1*, *OAZ1* and *TFRC* exceeding the maximum threshold for RG candidate selection, achieving s scores of 0.39, 0.33, 0.34 and 0.39, respectively (Table 4.1). *EPAS1* also responded positively to hypoxic culture in T-47D cells with an s score of 0.40, whereas no induction was observed in TNBC cells. However, *EPAS1* was the only RG candidate that exceeded the maximum threshold in T-47Ds. Furthermore, for MDA-MB-231 and MDA-MB-468 cell lines, only *TFRC* or *TBP* had altered expression following O₂ deprivation, with s scores of 0.32 and 0.34, respectively. Remaining RG candidates *ACTB*, *GUSB*, *RPL27*, *RPL30* and *RPLP1* were stable in expression between the two conditions, in all cell lines (Table 4.1). When looking at the s score across all RG candidates, MCF-7 cells demonstrated the highest degree of RG variability (mean 0.26 ± 0.10 SD). MDA-MB-231 (mean 0.10 ± 0.08 SD) and MDA-MB-468 (mean 0.11 ± 0.12 SD) had the lowest degree of RG variability, suggesting TNBC cell lines may be more adapted to hypoxic environments.

Table 4.1 Similarity (*s*) Score between Hypoxic and Normoxic RNA-Sequencing Reads of RG Candidates

RG candidate	MCF-7	T-47D	MDA-MB-231	MDA-MB-468
<i>ACTB</i>	0.23	0.08	0.11	0.30
<i>CCSER2</i>	0.39	0.04	0.15	0.00
<i>EPAS1</i>	0.33	0.40	0.07	0.03
<i>GUSB</i>	0.11	0.20	0.08	0.21
<i>OAZ1</i>	0.34	0.11	0.05	0.03
<i>RPL27</i>	0.24	0.12	0.06	0.10
<i>RPL30</i>	0.29	0.07	0.04	0.01
<i>RPLP1</i>	0.15	0.22	0.01	0.03
<i>TBP</i>	0.14	0.19	0.09	0.34
<i>TFRC</i>	0.39	0.27	0.32	0.03
Mean	0.26	0.17	0.10	0.11
SD	0.10	0.10	0.08	0.12

4.2.3 Assessment of RG candidate mRNA expression confirms eight highly expressed genes

To demonstrate suitability of RG candidates, RG expression in TNBC and ER α + breast cancer cell lines cultured in normal O₂ conditions was determined against a standard curve of pooled cDNA from independent biological replicates. *ACTB* was expressed most highly among the breast cancer cell lines but also showed greatest variation between biological replicates ranging from 8 - 202 arbitrary units (A.U.) in MCF-7 cells, and 30 - 179 A.U. in T-47D cells (Figure 4.4a). *EPAS1* was only amplified in one biological replicate in MDA-MB-231 and MDA-MB-468 cells, expression levels of A.U. and 6 A.U., respectively (Figure 4.4c). Additionally, *TBP* did not have detectable levels of expression in any cell lines (Figure 4.4j). *TBP* and *EPAS1* were therefore removed from further investigation. The next lowest expressed RG was *CCSER2* which was expressed at 0.21, 0.31, 1.15 and 2.36 A.U. in MCF-7, T-47D, MDA-MB-468 and MDA-MB-231 cell lysates, respectively (Figure 4.4b). The remaining RG candidates (*GUSB*, *OAZ1*, *RPL27*, *RPL30*, *RPLP1* and *TFRC*) and *PGK1* were more highly expressed in all cell lines (Figure 4.4d – Figure 4.4i, Figure 4.4k).

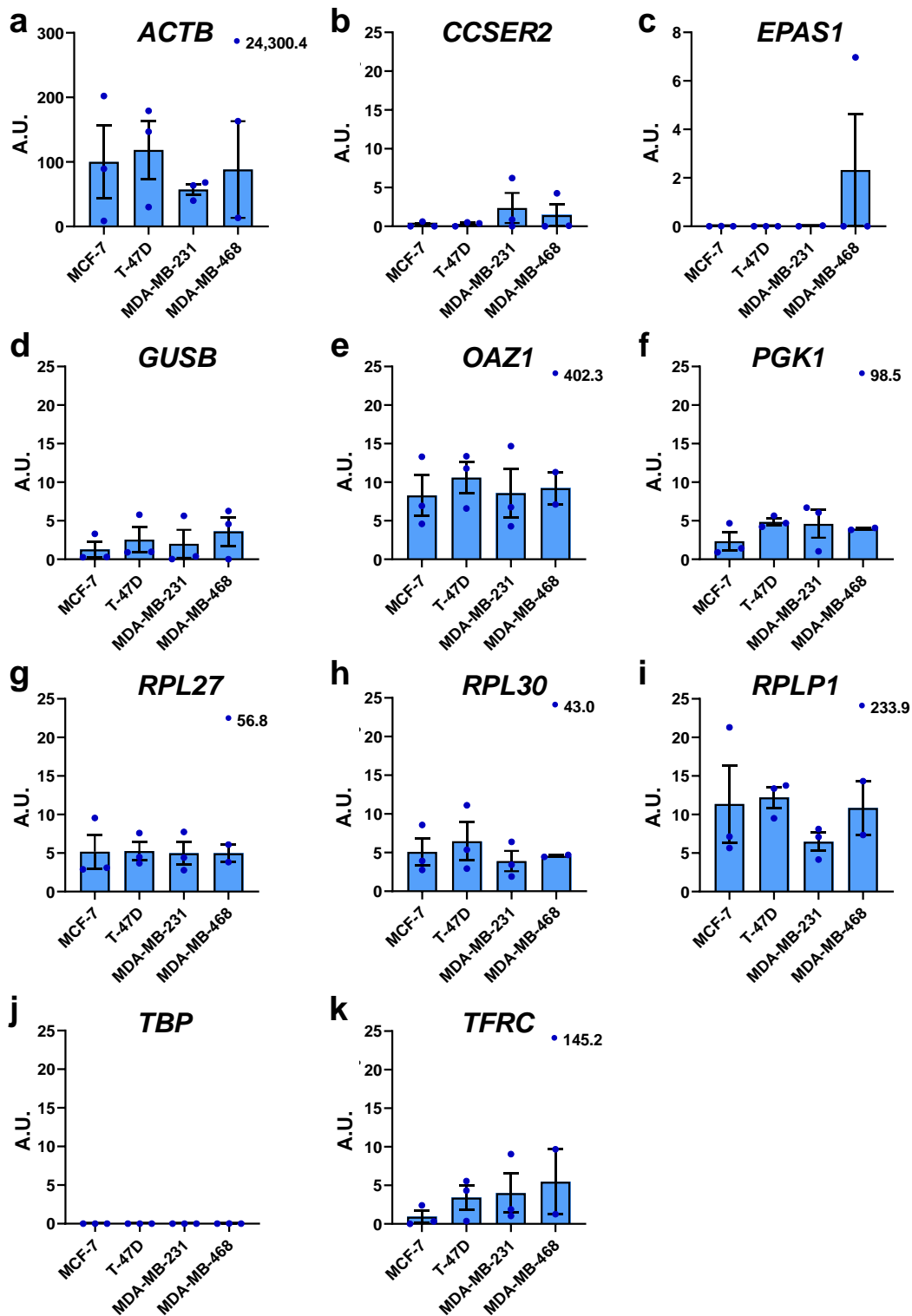


Figure 4.4 Expression of RG Candidates in MCF-7, T-47D, MDA-MB-231 and MDA-MB-468 Breast Cancer Cell Lines Cultured in 20% O₂. RG candidates (a) *ACTB* (b) *CCSER2* (c) *EPAS1* (d) *GUSB* (e) *OAZ1* (f) *PGK1* (g) *RPL27* (h) *RPL30* (i) *RPLP1* (j) *TBP* and (k) *TFRC* were evaluated for expression in breast cancer cell lines cultured in normal conditions for 72 hours post seeding. Arbitrary Units (A.U.) were determined from a standard curve of pooled cDNA sample from each cell line. Error bars are \pm SEM. N = 3. Where there is an outlier, the data point is displayed above the relevant box plot with mRNA expression value included.

4.2.4 Evaluating RG expression in normoxic vs. hypoxic breast cancer cell lines filters out poor RG candidates and identifies robust RGs with the least variability in expression

Next, expression stability of RG candidates was investigated following breast cancer cell line culture in normoxia, or in hypoxia for 8 or 48 hours (Figure 4.5). Primer efficiencies (PEs) from standard curves were also included in RT-qPCR experiments (Table 4.2). *ACTB*, *CCSER2* and *GUSB* displayed poor PE (Table 4.2; *ACTB* mean 1.70 ± 0.17 SD; *CCSER2* mean 2.43 ± 0.35 SD; *GUSB* mean 2.22 ± 0.15 SD). These RG candidates were therefore removed from downstream analysis. *OAZ1*, *RPL27*, *RPL30* and *RPLP1* were expressed at comparatively similar levels across all cell lines, and in each condition (Figure 4.5a - Figure 4.5d). *TFRC* showed inter-cell line stability when cultured in normoxia, or acute or chronic hypoxia. However, intra-cell line CtE was more varied. In particular, *TFRC* had higher CtE values in MCF-7 cells, which suggests this gene was not as highly expressed in MCF-7s compared to other breast cancer cell lines (Figure 4.5e). As predicted based on evidence in the literature, *PGK1* CtE values decreased in all cell lines following hypoxic culture for 8 or 48 hours, which conferred increased expression of *PGK1* in response to limited O₂ availability (Figure 4.5f). This result is in line with previous observations of hypoxic induction of *PGK1* (Hu et al., 2003; Jain et al., 2020; Zhang et al., 2020; Ong et al., 2023).

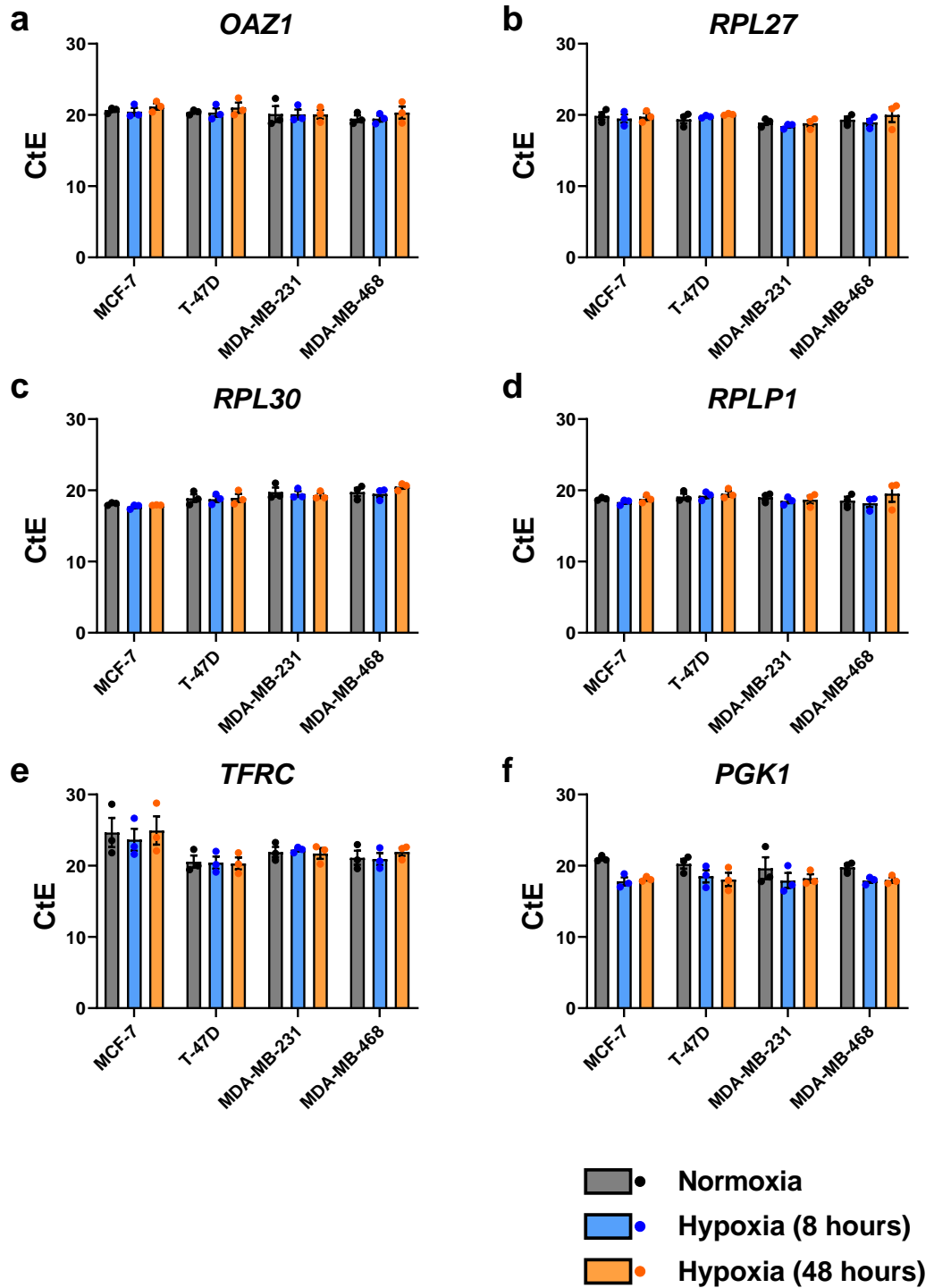


Figure 4.5 RG Stability in Breast Cancer Cell Lines Cultured in Normoxia or Hypoxia. RT-qPCR was used to determine the variance in gene expression of selected RG candidates: (a) *OAZ1*, (b) *RPL27*, (c) *RPL30*, (d) *RPLP1*, (e) *TFRC* and (f) *PGK1* following culture of MDA-MB-231, MDA-MB-468, MCF-7 or T-47D breast cancer cell lines in normoxia (grey) or hypoxia for 8 hours (blue) or 48 hours (orange). Error bars are mean \pm SEM. N = 3

Table 4.2 Primer Efficiencies of RG Candidates. *ACTB*, *CCSER2* and *GUSB* have PE's above or below an acceptable PE range and were therefore excluded.

	<i>ACTB</i>	<i>CCSER2</i>	<i>GUSB</i>	<i>OAZ1</i>	<i>PGK1</i>	<i>RPL27</i>	<i>RPL30</i>	<i>RPLP1</i>	<i>TFRC</i>
MDA-MB-231	1.88	2.05	2.07	2.01	1.99	2.01	2.01	2.01	2.04
	1.64	2.19	2.23	1.99	1.94	1.97	2.05	1.96	2.18
	1.74	2.49	2.29	2.05	2.07	2.04	2.09	1.99	2.12
MDA-MB-468	1.96	2.08	2.03	2.02	1.98	2.02	2.06	1.98	2.01
	1.73	3.26	2.44	2.01	1.99	2.04	2.02	1.96	2.06
	1.51	2.39	2.50	1.99	1.96	1.99	2.04	1.90	2.21
MCF-7	1.95	2.16	2.05	2.03	2.02	2.01	2.03	1.98	2.07
	1.59	2.50	2.27	2.02	2.02	2.08	2.06	1.99	2.29
	1.48	2.99	2.33	2.03	1.97	2.01	2.04	1.93	2.63
T-47D	1.87	2.23	2.04	2.04	1.99	2.05	2.04	1.98	2.06
	1.49	2.52	2.24	2.00	1.95	2.09	2.00	1.96	2.42
	1.55	2.30	2.19	1.97	1.98	2.04	2.04	1.99	2.09
Mean	1.70	2.43	2.22	2.01	1.99	2.03	2.04	1.97	2.18
SE	0.03	0.06	0.02	0.00	0.01	0.01	0.00	0.00	0.03
SD	0.17	0.35	0.15	0.02	0.03	0.03	0.02	0.03	0.18
CV	0.10	0.14	0.07	0.01	0.02	0.02	0.01	0.01	0.08

CtE values of the five remaining RG candidates that met all our criteria, *OAZ1*, *RPL27*, *RPL30*, *RPLP1* and *TFRC*, as well as hypoxia-responder *PGK1*, were then submitted to RefFinder, with intent to rank RG candidates in order of expression stability across all cell lines in normoxia or acute or chronic hypoxia. RefFinder first employs GeNorm, NormFinder, BestKeeper and the comparative ΔCt method to independently rank RGs. Next, RefFinder assigns a weight to an individual gene based on RG performance in the prerequisite programs, and calculates the geometric mean of candidate weights to provide a final ranking of the most stable RGs (Xie et al., 2012, 2023). In all iterations of RG stability analysis across all cell lines, *PGK1* and *TFRC* were ranked 5th and 6th, respectively (Table 4.3). According to BestKeeper and the comparative ΔCt method, *RPLP1* had the least variable inter- and intra-cell line expression in normoxic and hypoxic environments. *RPLP1* was also the highest ranked RG candidate by RefFinder (Table 4.3; Figure 4.6a). Conversely, NormFinder ranked *OAZ1* as the best RG candidate, and placed *RPL27* and *RPLP1* as the second and third best RG candidates (Table 4.3). A benefit of GeNorm over the other programs is the additional assessment of the optimal number of RGs to use for accurate normalisation (Vandesompele et al., 2002). For the study of hypoxia-mediated alterations in gene expression between MCF-7, T-47D, MDA-MB-231 and MDA-MB-468 breast cancer cell lines, GeNorm recommended the combined use of *RPL27* and *RPLP1*.

Next, optimal RGs to be used for RT-qPCR of hypoxic breast cancer cell lines following stratification into breast cancer subtypes was investigated. When CtE values from ER α + MCF-7 and T-47D breast cancer cell lines were supplied, *RPLP1* was again ranked top RG candidate with the least variability in expression, according to RefFinder, BestKeeper and the comparative ΔCt method (Table 4.3, Figure 4.6b). As in all cell lines, NormFinder suggested *OAZ1* to be the optimal RG to use when investigating hypoxic induction of genes of interest in the ER α + Luminal A breast cancer group. GeNorm recommended the combined use of *RPLP1* and *RPL30*, instead of *RPL27* as previously put forward for all cell lines. *PGK1* and *TFRC* were ranked as the least stable RGs in all outputs as before. For the TNBC MDA-MB-231 and MDA-MB-468 cell lines, *RPL30* was placed first by all programs (Table 4.3, Figure 4.6c), apart from GeNorm which recommended *RPL27* and *RPLP1*, the same as for all breast cancer cell lines. Computational analysis of individual cell lines cultured in normoxia, and acute or chronic hypoxia was also

performed. Here, *RPLP1* and *RPL30* were the least variable and most suitable RGs for the MCF-7 (Table 4.3; Figure 4.6d) or T-47D (Table 4.3; Figure 4.6e) cell lines. Additionally, GeNorm identified *RPLP1* and *RPL27* as the least variable and most suitable RGs for MDA-MB-231 (Table 4.3; Figure 4.6f) or MDA-MB-468 cell lines (Table 4.3; Figure 4.7g), but *RPL30* was ranked as the least variable single RG by RefFinder in both TNBC models.

Table 4.3 Summaries of Ranked RG Stability According to RefFinder and Prerequisite programs Ranked in order from least variable / best (1) to most variable / worst (6).

Cell lines	Method	1	2	3	4	5	6
All Cell Lines MCF-7 T-47D MDA-MB-231 MDA-MB-468	Δ Ct	RPLP1	RPL27	OAZ1	RPL30	PGK1	TFRC
	BestKeeper	RPLP1	RPL27	OAZ1	RPL30	PGK1	TFRC
	NormFinder	OAZ1	RPL27	RPLP1	RPL30	PGK1	TFRC
	GeNorm	RPL27 RPLP1		RPL30	OAZ1	PGK1	TFRC
	RefFinder	RPLP1	RPL27	OAZ1	RPL30	PGK1	TFRC
Luminal A MCF-7 T-47D	Δ Ct	RPLP1	RPL30	OAZ1	RPL27	PGK1	TFRC
	BestKeeper	RPLP1	RPL27	RPL30	OAZ1	PGK1	TFRC
	NormFinder	OAZ1	RPL27	RPLP1	RPL30	PGK1	TFRC
	GeNorm	RPL30 RPLP1		OAZ1	RPL27	PGK1	TFRC
	RefFinder	RPLP1	RPL30	OAZ1	RPL27	PGK1	TFRC
TNBC MDA-MB-231 MDA-MB-468	Δ Ct	RPL30	OAZ1	RPL27	RPLP1	TFRC	PGK1
	BestKeeper	RPL30	RPL27	RPLP1	OAZ1	TFRC	PGK1
	NormFinder	RPL30	OAZ1	RPL27	TFRC	RPLP1	PGK1
	GeNorm	RPL27 RPLP1		RPL30	OAZ1	TFRC	PGK1
	RefFinder	RPL30	RPL27	RPLP1	OAZ1	TFRC	PGK1
MCF-7	Δ Ct	RPL30	RPLP1	OAZ1	RPL27	PGK1	TFRC
	BestKeeper	RPL30	RPLP1	OAZ1	RPL27	PGK1	TFRC
	NormFinder	RPL30	RPLP1	RPL27	OAZ1	PGK1	TFRC
	GeNorm	RPL30 RPLP1		OAZ1	RPL27	PGK1	TFRC
	RefFinder	RPL30	RPLP1	OAZ1	RPL27	PGK1	TFRC
T-47D	Δ Ct	RPLP1	RPL30	RPL27	OAZ1	PGK1	TFRC
	BestKeeper	RPL27	RPLP1	RPL30	OAZ1	TFRC	PGK1
	NormFinder	RPLP1	RPL30	OAZ1	RPL27	PGK1	TFRC
	GeNorm	RPL30 RPLP1		RPL27	OAZ1	PGK1	TFRC
	RefFinder	RPLP1	RPL30	RPL27	OAZ1	PGK1	TFRC
MDA-MB-231	Δ Ct	RPL30	OAZ1	TFRC	RPL27	RPLP1	PGK1
	BestKeeper	RPL27	RPLP1	RPL30	TFRC	OAZ1	PGK1
	NormFinder	RPL30	OAZ1	TFRC	RPL27	RPLP1	PGK1
	GeNorm	RPL27 RPLP1		RPL30	TFRC	OAZ1	PGK1
	RefFinder	RPL30	RPL27	RPLP1	OAZ1	TFRC	PGK1
MDA-MB-468	Δ Ct	RPL30	RPL27	OAZ1	RPLP1	PGK1	TFRC
	BestKeeper	RPL30	OAZ1	PGK1	RPL27	RPLP1	TFRC
	NormFinder	RPL30	OAZ1	RPL27	PGK1	RPLP1	TFRC
	GeNorm	RPL27 RPLP1		RPL30	OAZ1	PGK1	TFRC
	RefFinder	RPL20	RPL27	OAZ1	RPLP1	PGK1	TFRC

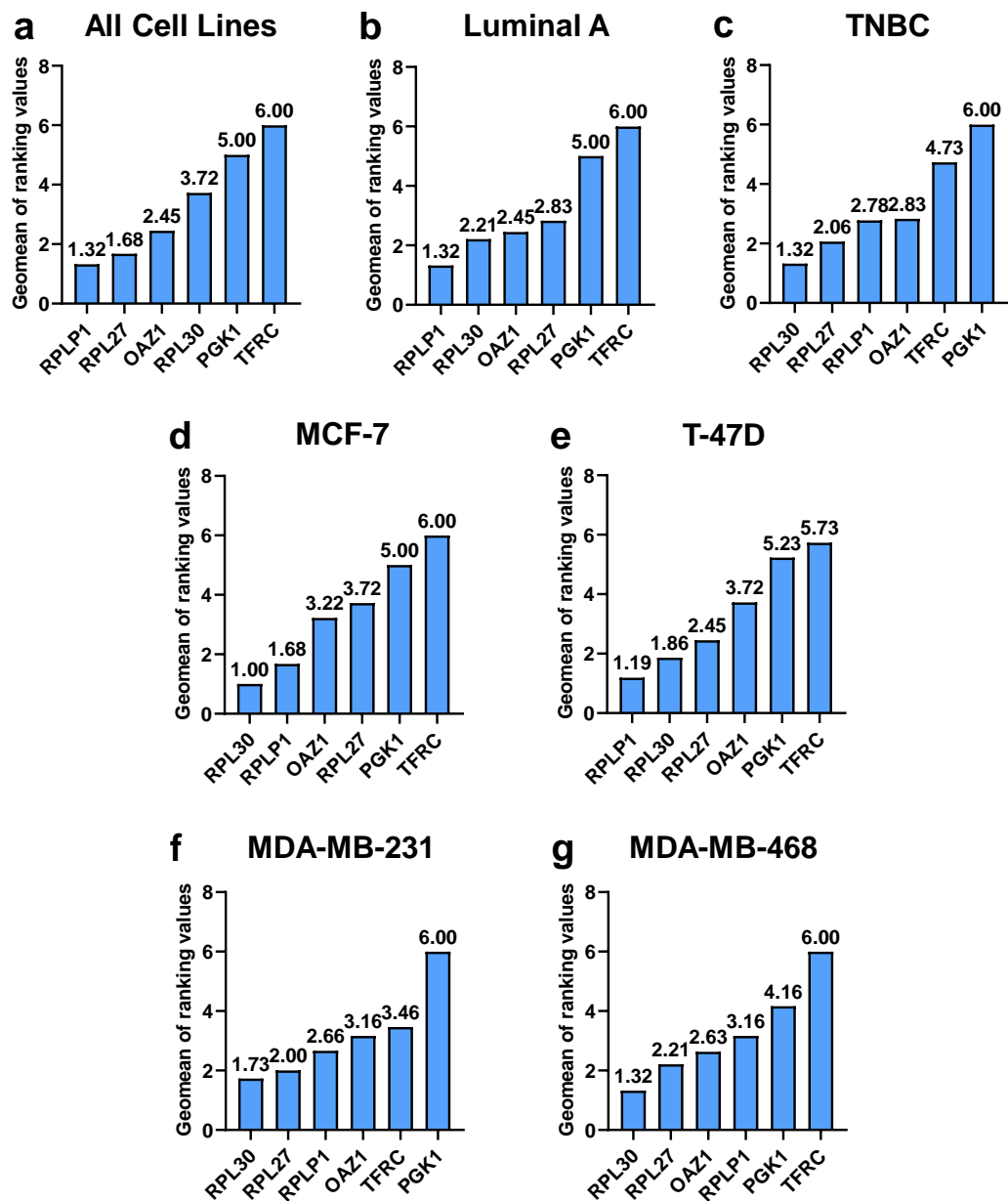


Figure 4.6 Geomean of Ranking Values for RG Candidates The final overall ranking of RG candidates was determined by RefFinder based on the geometric mean of the weights of each RG from GeNorm, NormFinder, BestKeeper and the comparative ΔCt method for (a) all breast cancer cell lines, (b) ER α + breast cancer cell lines MCF-7 and T-47D, (c) TNBC cell lines MDA-MB-231 and MDA-MB-468, or (d) MCF-7, (e) T-47D, (f) MDA-MB-231 and (g) MDA-MB-468 cell lines individually.

4.2.5 *RPLP1* and *RPL27* are suitable RGs for normalising gene expression in normoxic vs. hypoxic ER α + and TNBC cell lines

Following identification of optimal RGs, the combined use of *RPLP1* and *RPL27* for normalisation of *CA9* expression in breast cancer cell lines cultured in normoxia or hypoxia for 8 or 48 hours was assessed. The geometric mean of *RPLP1* and *RPL27* was used to normalise *CA9* CtE values, before fold change induction ($2^{-\Delta\Delta Ct}$) of *CA9* was calculated (Livak and Schmittgen, 2001). Expression (CtE) of *RPLP1* and *RPL27* in MCF-7 (19.4 ± 0.4 SD), T-47D (19.7 ± 0.5 SD), MDA-MB-231 (18.8 ± 0.5 SD) and MDA-MB-468 (19.6 ± 0.9 SD) cells were consistent, regardless of environmental O₂ (Figure 4.7a). Conversely, all cell lines demonstrated significant induction of *CA9* following hypoxic culture (Figure 4.7b). In MCF-7 cells, *CA9* was increased 470-fold after chronic exposure to a hypoxic environment. For T-47Ds, acute and chronic hypoxia induced a 42- and 109-fold increase in *CA9* expression, respectively. After 8 hours of hypoxic culture, MDA-MB-231s had a moderate but significant 9-fold induction, and for MDA-MB-468s a 17-fold increase in *CA9* expression was seen following 48 hours of hypoxic culture. Importantly, *RPLP1* and *RPL27* were similarly expressed in each cell line, in each condition. Thus, combination of *RPLP1* and *RPL27* as RGs was suitable for normalising gene expression in normoxic and hypoxic breast cancer cell lines.

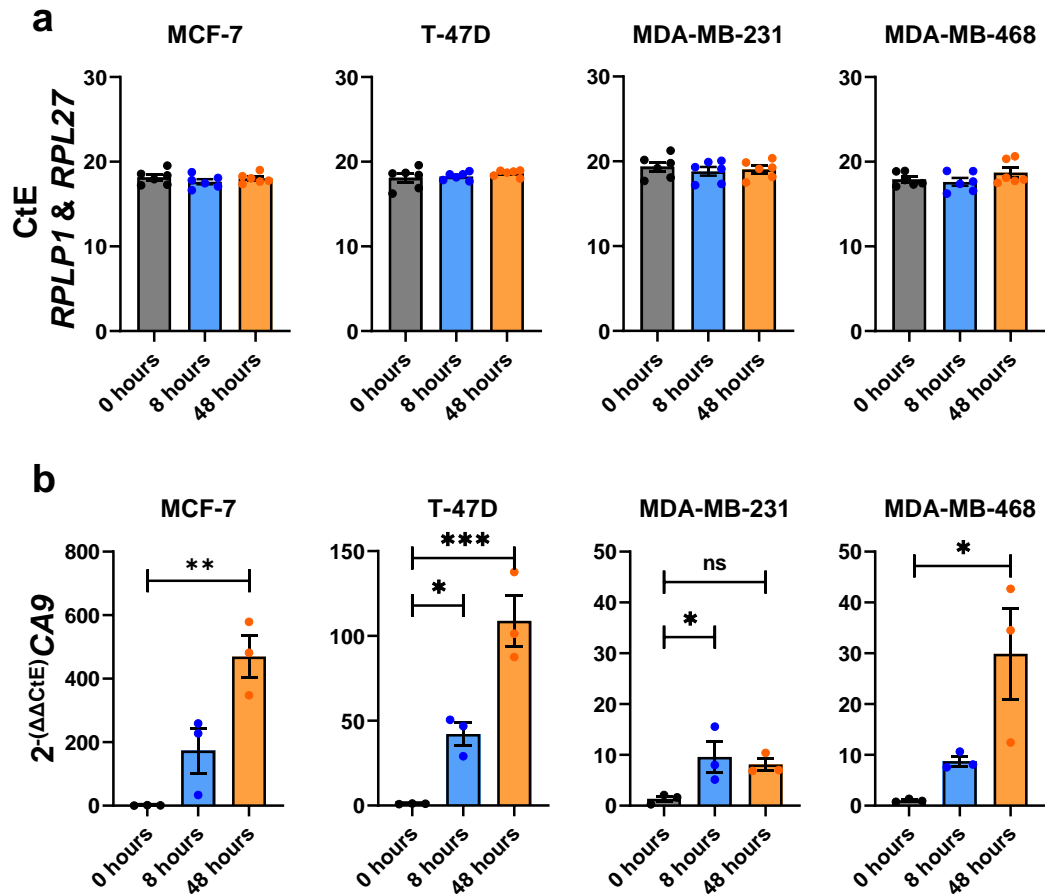


Figure 4.7 RG Expression Level Stability and Hypoxic Induction of CA9.

(a) *RPL27* (N = 3) and *RPLP1* (N = 3) expression was determined by RT-qPCR. Raw CtE values for triplicate biological replicates of the two RGs in MCF-7, T-47D, MDA-MB-231 and MDA-MB-468 breast cancer cell lines are shown. Error bars are geometric mean \pm geometric SD. (b) Expression of *CA9* was assessed in MCF-7, T-47D, MDA-MB-231 and MDA-MB-468 breast cancer cell lines following culture in normoxia (20% O₂, “0 hours”) or hypoxia (1% O₂) for 8 or 48 hours. Changes in *CA9* expression were determined by the 2^{- $\Delta\Delta$ Ct} method, using the geometric mean of RGs *RPLP1* and *RPL27* for normalisation (a). One-way ANOVA with Dunnett’s multiple comparisons was employed to investigate significant fold change in gene expression relative to normoxic control. * p = < 0.05, ** p = < 0.01, *** p = < 0.001. Error bars are \pm SEM. N = 3

4.2.6 Evaluation of RG shortlist in additional 28 breast epithelial or cancer cell lines

Finally, the initial RNA-seq dataset conducted across 32 hypoxic or normoxic breast cancer cell lines was studied to determine the s score of *OAZ1*, *RPLP27*, *RPLP30*, *RPLP1* and *TFRC* across a broad range of breast cancer models. As previously shown in MCF-7 cells (Table 4.1), Luminal breast cancer cell lines tend to experience greater variability in the expression of the RG candidates, with ZR-75-1 being the most stable cell line in all five RG candidate expression when cultured in normoxia or in hypoxia, and achieving a mean s score of 0.29 ± 0.09 SD (Table 4.4). In contrast, 38% of TNBC cell lines analysed had an average s score of ≤ 0.30 . For the two HER2 cell lines included in this study, none of the RGs demonstrated an s score below the maximum cutoff. For the Luminal B cell line, BT474, *TFRC* showed very minimal variation in expression between normoxic and hypoxic conditions suggesting that this transferrin receptor may be a suitable RG for RT-qPCR experiments in this cell line. Non-tumorigenic mammary epithelial (NTME) cell lines were also included in the analysis. NTME cell lines from the MCF series were greatly affected by hypoxic culture, whereas HME cells maintained relatively stable expression of *OAZ1*, *RPL30* and *RPLP1*. From our panel of RG candidates that made it to RefSeq analysis in MCF-7, T-47D, MDA-MB-231 and MDA-MB-468 cells, we have demonstrated potential application of these RGs to a broader range of cell lines that expand beyond the four that have been intensively studied throughout this Chapter. Further work will be required to validate the use of *OAZ1*, *RPL27*, *RPL30*, *RPLP1* and *TFRC* in additional breast cancer cell lines.

Table 4.4 s scores of top five RG candidates in 28 breast cancer or normal mammary epithelial cell lines. Data available from NCBI GEO – GSE111653. Cell lines have been arranged in accordance with the subtype of breast cancer they represent. Abbreviations: Non-Tumorigenic Mammary Epithelial (NTME)

Cell Line	Subtype	<i>OAZ1</i>	<i>RPL27</i>	<i>RPL30</i>	<i>RPLP1</i>	<i>TFRC</i>	Mean	SD
HME	NTME	0.26	0.31	0.28	0.20	0.57	0.32	0.13
MCF10A	NTME	0.55	0.57	0.67	0.66	0.42	0.57	0.09
MCF12A	NTME	0.37	0.51	0.48	0.46	0.95	0.55	0.20
CAMA1	Luminal A	0.39	0.50	0.49	0.55	0.55	0.49	0.06
HCC1428	Luminal A	0.59	0.54	0.52	0.59	0.69	0.58	0.06
MDA-MB-175	Luminal A	0.58	0.57	0.54	0.54	0.69	0.58	0.06
SUM185	Luminal A	0.61	0.63	0.60	0.62	0.59	0.61	0.01
ZR-75-1	Luminal A	0.34	0.32	0.29	0.37	0.11	0.29	0.09
BT474	Luminal B	0.46	0.46	0.47	0.44	0.05	0.38	0.16
HCC1569	HER2	0.60	0.68	0.69	0.70	0.44	0.62	0.10
SKBR3	HER2	0.62	0.59	0.58	0.56	0.47	0.56	0.05
BT20	TNBC	0.52	0.49	0.48	0.54	0.67	0.54	0.07
BT549	TNBC	0.40	0.36	0.41	0.42	0.13	0.35	0.11
DU4475	TNBC	0.03	0.01	0.10	0.05	0.38	0.11	0.14
HCC1806	TNBC	0.55	0.46	0.37	0.39	0.78	0.51	0.15
HCC1937	TNBC	0.51	0.54	0.55	0.54	0.77	0.58	0.09
HCC38	TNBC	0.55	0.57	0.59	0.54	0.46	0.54	0.04
HS578T	TNBC	0.37	0.38	0.37	0.31	0.05	0.30	0.12
MDA-MB-157	TNBC	0.61	0.64	0.62	0.64	0.49	0.60	0.06
MDA-MB-436	TNBC	0.19	0.15	0.13	0.19	0.15	0.16	0.02
SUM1315	TNBC	0.21	0.28	0.32	0.27	0.10	0.23	0.08
SUM149	TNBC	0.21	0.09	0.02	0.06	0.79	0.23	0.28
SUM159	TNBC	0.49	0.45	0.42	0.39	0.92	0.53	0.20
SUM229	TNBC	0.41	0.38	0.33	0.37	0.18	0.33	0.08
HBL100	Distinct	0.05	0.02	0.05	0.11	0.31	0.11	0.11
htert-HME	Distinct	0.69	0.63	0.64	0.64	0.28	0.58	0.15
Sum225CWN	Distinct	0.47	0.51	0.54	0.55	0.36	0.49	0.07

4.3 Discussion

RT-qPCR has been the gold standard for quantifying mRNA expression since its inception in 1993, but interpretation of results is dependent on appropriate use of internal controls as a means of normalisation (Higuchi et al., 1993; Rebouças et al., 2013). Common RGs previously deemed stable in expression include *GAPDH*, *ACTB*, *PGK1* and *18S rRNA*, which have subsequently been shown to have variation in abundance across different experimental conditions, emphasising the notion that there is no such thing as an RG that works for all investigations (Dheda et al., 2004). Indeed, in the context of cellular hypoxia, *ACTB* is under the influence of insufficient O₂ supply, as are *GAPDH* and *PGK1* which are specifically regulated by the activity of HIF-1 α (Higashimura et al., 2011; Zhang et al., 2020; Wang et al., 2021; Ong et al., 2023). Thus, when looking to identify novel therapeutic targets to combat hypoxia-induced therapy resistance for breast cancer patients, suitable RGs need to be selected prior to RT-qPCR investigation of genes of interest, so hypoxia-induced alterations in RG expression do not obscure novel and important biological findings.

4.3.1 Summary of main findings

- The HIF switch occurred within a 48-hour time course of low O₂ tension in MCF-7, T-47D, MDA-MB-231 and MDA-MB-468 cells. HIF-1 α had maximum protein accumulation at approximately 8 hours which was almost completely dissipated at 48 hours. HIF-2 α remained constitutively present at the protein level, even in normoxic lysate.
- For comparing transcriptional changes occurring in MCF-7, T-47D, MDA-MB-231 and MDA-MB-468 cells cultured in normoxia, or acute or chronic hypoxia, *RPLP1* and *RPL27* were the most stably expressed RGs that would allow accurate normalisation of gene expression measured by RT-qPCR.

4.3.2 The “HIF switch” in Luminal A and TNBC cell lines

The hypoxic response is complex and multifaceted, with changes in gene transcription due to hypoxia being regulated by temporal changes in HIF-1 α or HIF-2 α protein expression, signifying acute or chronic hypoxic stress, respectively (Holmquist-Mengelbier et al., 2006). To meet the demand for robust RGs for

investigations of hypoxic ER α + and TNBC cell lines, western blot of HIF- α isoforms was first carried out to estimate the timing of the HIF switch. Densitometry analysis predicted the molecular transition from HIF-1 α to HIF-2 α to occur between 8 and 48 hours of hypoxic culture, and these timepoints were used as markers of acute and chronic hypoxia. It is interesting that HIF-2 α appeared in normoxic lysates, as the accepted model of HIF- α regulation involves constitutive translation and degradation under normoxic conditions (Mole et al., 2001). However, aberrant HIF- α accumulation has been purported in normoxic cancer cell lines, and within well-vascularised solid tumours (Holmquist-Mengelbier et al., 2006; Mills et al., 2009). In 90% of high-risk renal cell carcinoma tumours, inactivating germline pVHL mutations correspond to constitutive HIF- α expression in physiological levels of O₂ and increased tumorigenesis (Kaelin, 2008). Thus, in the breast cancer cells studied in this Chapter, it is possible that alternative activating pathways have been established to selectively enable the accumulation of HIF-2 α in the presence of O₂.

4.3.3 Ribosomal constituents as stably expressed RGs for hypoxic breast cancer studies

A comprehensive investigation combining bioinformatic analysis of publicly available RNA-seq datasets to select 10 RG candidates, RT-qPCR of candidates to assess expression levels and variability, and utilisation of the online RG tool RefFinder was implemented. The 10 RG candidates identified included genes that are generally considered RGs (*ACTB*, *RPL30*, *RPLP1*, *GUSB*, *TBP* and *TFRC*), and novel RGs (*OAZ1*, *RPL27*, *CCSER2*, and *EPAS1*) (de Jonge et al., 2007; Gubern et al., 2009; Valente et al., 2009; Tilli et al., 2016; Kang et al., 2019; Jain et al., 2020). When CtEs of candidates were supplied to RG selection tools, it is perhaps unsurprising that constituents of the ribosome (*RPLP1*, *RPL27* and *RPL30*) which are abundantly and consistently expressed in human tissues were selected as the optimal RGs with the least variability in expression in breast cancer cell lines cultured in normoxia, or acute or chronic hypoxia (Hsiao et al., 2001; Zhou et al., 2010; Nakayama et al., 2018). This result is supported by the observation that breast cancer cells can bypass hypoxia-mediated inhibition of protein synthesis through gene silencing of 4E-BP1, eEF2 kinase or tuberous sclerosis complex 2 (TSC2), maintaining a continuous requirement of translational machinery (Connolly et al., 2006).

To highlight the importance of selecting RGs for individual cell types and experimental conditions, an initial s score was calculated to demonstrate RG expression stability in MCF-7, T-47D, MDA-MB-231 and MDA-MB-468 cells using a public RNA-seq dataset. Among the 10 RG candidates, four candidates exceeded the maximum s score threshold in MCF-7 cells, whereas only one RG candidate in the other cell lines had an s score > 0.3 . Additionally, MCF-7s had the highest average s score compared to T-47D and TNBC cells. The higher s score observed in MCF-7 cells suggests that this cell line undergoes dramatic transcriptional changes in response to hypoxia, altering the expression of more genes to survive hypoxic environments. Conversely, TNBC MDA-MB-231 and MDA-MB-468 cells had a much lower s score compared to both Luminal A cell lines. This observation suggests TNBC cell lines undergo fewer dramatic transcriptional changes in response to hypoxia, which is supported by the evidence that TNBC tumours are inherently more aggressive and more hypoxic than other subtypes of breast cancer (Cancer Genome Atlas Network, 2012; Tutzauer et al., 2022).

Throughout this study, the process of RG candidate deselection based on assessment of gene expression and primer efficiencies was included, as it is important to understand peripheral results which impact the quality of data interpretation. Thus, for full transparency of the RG selection process, negative filtration of poor candidates as well as positive selection of stable candidates was shown. To ensure precision in normalising expression of genes of interest, it is recommended that two RGs are included in RT-qPCR studies, as use of a single RG for normalising gene expression may result in erroneous interpretation, whereas inclusion of two RGs should ensure accurate normalisation of target gene abundance (Tricarico et al., 2002; Bustin et al., 2009).

4.3.4 Limitations and considerations of this study

With respect to selection of the 10 RG candidates, the RNA-seq dataset used to curate the shortlist was limited by a single replicate for each cell line in each condition being available for analysis (Ye et al., 2018; Godet et al., 2019). The original study is an impressive investigation into the molecular portrait of hypoxia spanning 32 breast cancer cell lines and for the purpose of RG candidate selection, provided a meaningful starting point for determining approximate RG stability in hypoxic breast cancer cell lines. Further, the RNA-seq dataset was used to

determine if any of the five RG candidates that were tested with RefFinder in MCF-7, T-47D, MDA-MB-231 or MDA-MB-468 cell lines could also be used for any of the remaining 28 breast epithelial or cancer cell lines available in the GSE111653 dataset. Comparison of s scores across *OAZ1*, *RPL27*, *RPL30*, *RPLP1* and *TFRC* in a wide selection of NTME, Luminal, HER and TNBC cell lines demonstrated potential use of some of the RGs in hypoxic studies. However, the RNA-seq dataset alone would not be sufficient to draw robust conclusions about the optimal RGs to use in hypoxic breast cancer studies involving RT-qPCR, and additional work is required to validate RG use in the extended panel of breast cells. As such, identification of ribosomal proteins as suitable RGs may only be applicable to those wishing to capture hypoxia-induced changes in gene expression in MCF-7, T-47D, MDA-MB-231 and/or MDA-MB-468 breast cancer cell lines, where this result has been appropriately tested. How these results translate to other cancer cell lines, or patient samples, remains unclear. Cell lines representing the same disease model often display variation in response to environmental or experimental conditions and have unique gene expression signatures and molecular portraits (Dai et al., 2017). This is exemplified in MCF-7 and T-47D cell lines, where oestradiol has been shown to confer disparate changes in gene expression between the two models of Luminal A breast cancer, despite both cell lines being driven by ER α activity (Rangel et al., 2017). For patient derived samples, the answer to identifying suitable RGs for RT-qPCR is more unclear, due to the complexity of individuality between patients, heterogeneity of cell types within the TME uneven distribution of hypoxia observed throughout tumours (Gay et al., 2016; Oda et al., 2016). Cancer grade at diagnosis, and samples coming from secondary metastatic sites will also require further optimisation of RGs. Indeed, patterns of dysregulated ribosomal protein expression have been observed in human tissues, primary cell lines and tumours (Guimaraes and Zavolan, 2016). Thus, careful identification of suitable RGs for such studies needs to be implemented prior to carrying out the experiment, and perhaps consideration of including a greater number of RGs (3 – 5 for more complex tissue samples) would narrow variability and allow more accurate normalisation in such instances (Vandesompele et al., 2002). Nonetheless, a robust strategy for selection of suitable RGs that can be implemented to a broad range of studies wishing to identify important transcriptional aberrations acting as drivers of breast cancer progression has been outlined in this Chapter.

4.4 Conclusion

A comprehensive investigation to identify the most suitable RGs with the least variability in expression has been carried out, which can be used in RT-qPCR studies of breast cancer cell lines cultured in normoxia or hypoxia. Identification of the HIF switch in breast cancer cell lines guided hypoxic timepoints for this investigation, to ensure HIF-dependent gene transcription can be captured. Use of robust computational RG selection programs following stringent criteria of RG candidates resulted in the recommendation of *RPLP1* and *RPL27* as internal controls in RT-qPCR studies for accurate interpretation of gene expression results. This important finding provides the means to assess the impact of hypoxia within breast cancer development and progression.

4.5 Data Availability

Code and supporting data available at zenodo.org/doi/10.5281/zenodo.13166160

5. Effect of Hypoxia and the ER α on Na⁺ Transport in Breast Cancer Cells

5.1 Introduction

Maintenance of Na⁺ homeostasis is essential for many biological processes including: regulating extracellular fluid and cell volume, perpetuating nutrient and substrate transport, and conducting action potentials in electrically excitable nerve and muscle cells (Hille, 1984; Kato and Romero, 2011; Strazzullo and Leclercq, 2014; Dutta et al., 2018). The delicate balance of intra- and extracellular Na⁺ transport is predominantly mediated by an electrochemical gradient set up by the NKA exporting three Na⁺ out of the cell and importing two K⁺ into the cell, in an ATP-dependent manner (Skou and Esmann, 1992). The activities of NKA work against the natural Na⁺ and K⁺ gradients, maintaining high [Na⁺]_e and thus ensuring a substantial driving force of Na⁺ back into the cell through a myriad of Na⁺ transporters present on the plasma membrane, such as: ENaCs, ASICs, NKCC, NHE and VGSCs.

Despite tight regulation of Na⁺ transport, elevated [Na⁺]_i has been observed in several solid malignancies, including in brain, breast and prostate tumours (Ouwkerk *et al.*, 2003, 2007; Barrett *et al.*, 2018). Heightened Na⁺ influx has been implicated in driving aberrant proliferation and migration of high grade glioma cells (Kapoor *et al.*, 2009; Rooj *et al.*, 2012). Furthermore, elevated [Na⁺]_i is a critical determinant of breast cancer progression, linked to several hallmarks of cancer including increased invasive and metastatic potential (Fraser *et al.*, 2005; Brackenbury *et al.*, 2007). In fact, there is great overlap in ion channel dysfunction and many hallmarks of cancer (Prevarskaya *et al.*, 2018). Thus, dysregulated Na⁺ handling through Na⁺ channels has been strongly implicated in tumour progression (Leslie *et al.*, 2019). The aberrant expression and/or activity of Na⁺ channels could therefore be used as clinical biomarkers and therapeutic targets in many types of malignancy, including in breast cancer.

MDA-MB-231 cells were shown to carry TTX-sensitive I_{Na} associated with metastatic potential by Roger *et al.* in 2003 (Roger *et al.*, 2003). While pathological Na⁺ influx was identified in aggressive TNBC cells, weakly metastatic MCF-7 cells do not possess such a phenotype. Further investigations into the driver of aberrant Na⁺ transport in MDA-MB-231 cells identified nNav1.5 encoded by *SCN5A* as the primary contributor to elevated Na⁺ influx (Fraser *et al.*, 2005; Brackenbury *et al.*,

2007). Importantly, expression of nNav1.5 is found in human metastatic TNBC tumours (Fraser *et al.*, 2005; Yamaci *et al.*, 2017). Expression of nNav1.5 over the adult isoform allows greater Na⁺ influx, owing to alternative splicing of the S3-S4 linker in domain 1 (D1), which replaces a negative aspartate in the adult variant with a positive lysine residue in the neonatal variant, further increasing [Na⁺]_i with significant implications for breast cancer progression (Onkal *et al.*, 2008). The link between hormone receptor status of breast tumours and Nav1.5 expression has been explored. Nav1.5 is found to be negatively associated with ER α and PgR expression, but positively associated with HER2 (Leslie *et al.*, 2024). These findings suggest a negative selective pressure acting on Nav1.5 expression in ER α + breast tumours which could be enacted by ER α activity.

TNBC tumours have a more pronounced hypoxic signature than other subtypes of breast cancers, including Luminal A / ER α + tumours (Cancer Genome Atlas Network, 2012; Tutzauer *et al.*, 2022). Hypoxia and the transcriptional regulators of the hypoxic response HIF-1 α and HIF-2 α , have been implicated in modulating ion channel expression and function. For example, voltage-gated K⁺ channel expression is upregulated in response to acute (18 hour) hypoxic challenge in a HIF-1 α -dependent manner (Dong *et al.*, 2012). Additionally, expression of NHE1 is induced by hypoxia-mediated cellular acidosis and promotes cell proliferation, EMT and metastasis in breast cancer cells (Gatenby *et al.*, 2007; Takatani-Nakase *et al.*, 2022). Furthermore, activation kinetics of the large-conductance Ca²⁺-activated K⁺ channel is significantly increased in glioblastoma (GBM) U87-MG cells following exposure to chronic hypoxic treatment, enhancing GBM aggressiveness and chemoresistance (Rosa *et al.*, 2018). Thus, hypoxia and HIF-1 α have significant roles in modulating the ionic tumour microenvironment. Hypoxia and the transcriptional activity of HIF-1 α and/or HIF-2 α could therefore provide a potential mechanism for positive upregulation of nNav1.5 in hypoxic TNBC tumours. Furthermore, emerging roles of other members of the Na⁺ channel family in breast cancer development and progression have been reported (Khajah *et al.*, 2018; Chen *et al.*, 2019; Ware *et al.*, 2021). The underlying mechanism behind dysregulated Na⁺ transport through nNav1.5 channels in breast cancer has been underexplored.

Nav1.6 and Nav1.7 encoded by *SCN8A* and *SCN9A*, respectively, are two additional VGSCs that are well-documented in many solid malignancies (Figure 1.5) (Malcolm et al., 2023). In particular, hormone-driven prostate cancer cells have elevated Nav1.6 and Nav1.7 transcript levels, and TTX or siRNA targeting these VGSCs significantly inhibits metastatic progression *in vitro* (Diss et al., 2001; Nakajima et al., 2009). In prostate tumours, Nav1.7 mRNA levels are approximately 27-fold higher compared to matched healthy tissue (Shan et al., 2014). Cervical tumours have significantly elevated levels of both Nav1.6 and Nav1.7 relative to healthy adjacent tissue (Hernandez-Plata et al., 2012). Similarly, ovarian tumours observe elevated Nav1.7 mRNA (Gao et al., 2010). As with aberrant expression of Nav1.5 in breast tumours, the mechanism behind selective upregulation of Nav1.6 and Nav1.7 is largely unknown despite being important in tumour progression for many types of malignancy. Hypoxia is a key determinant of prostate cancer treatment resistance and metastasis (Bharti et al., 2019). Additionally, ovarian cancers are highly hypoxia-dependent which dampens ovarian cancer cells responsiveness to chemotherapy and immunotherapy (Klemba et al., 2020). Hypoxia is also essential for paclitaxel resistance in cervical cancers (Nishi et al., 2023).

5.1.1 Aims and hypotheses

The work in this Chapter was set to investigate hypoxia and ER α contributions to a dysregulated Na⁺ network in breast cancer cells. An RNA-seq experiment was established by Dr. Susanna Rose (University of York) in MCF-7 and T-47D breast cancer cell lines that were first treated with either vehicle or fulvestrant for 48 hours, and then subjected to either normoxic or hypoxic culture for a further 48 hours. Based on previous research implicating hypoxia in the positive modulation of ion channels in several malignancies, hypoxia was hypothesised to positively influence Na⁺ transport in the breast cancer cell lines by upregulating Na⁺ channel genes, such as VGSCs, ENaCs or NHE1, which would lead to a more invasive phenotype. In contrast, due to the observation of a negative correlation between the ER α and Nav1.5 in breast tumours (Leslie *et al.*, 2024), ER α was expected to negatively regulate expression of Na⁺ channel genes including VGSCs, and ER α knockdown would therefore increase expression of genes involved in Na⁺ transport. These hypotheses were tested by:

- Analysing RNA-seq data of Luminal A breast cancer cells cultured in normoxia or hypoxia to investigate alterations in Na⁺ transport at both the gene and gene set level.
- Analysing RNA-seq data of Luminal A breast cancer cells cultured with vehicle or fulvestrant to knockdown ER α and explore changes in Na⁺ channel gene expression.
- Validating *in silico* findings by RT-qPCR using RGs identified in Chapter 4 to normalise fold change in Na⁺ channel gene expression.
- Exploring the effects of inhibiting Na⁺ channel activity on the migratory capacity of breast cancer cells.

5.2 Results

5.2.1 mRNA expression of VGSCs is not regulated by hypoxia in TNBC or Luminal A breast cancer cell lines

Because hypoxia has been significantly implicated in the progression of breast, prostate, cervical and ovarian tumours, and aberrant VGSC expression has similarly been implicated in the advancement of such malignancies, mRNA expression of VGSC subunits in response to hypoxic challenge was explored. MDA-MB-231, MDA-MB-468, MCF-7 and T-47D breast cancer cell lines were cultured in normoxia (20% O₂), or in acute (8 hours) or chronic (48 hours) hypoxia (1% O₂), and total RNA was extracted. RT-qPCR was performed to measure transcriptional changes in *nSCN5A*, *SCN8A* and *SCN9A*, which encode nNa_v1.5, Na_v1.6 and Na_v1.7, respectively. Normoxic MDA-MB-231 cells highly expressed nNa_v1.5 (Figure 5.1a), in line with previous studies (Fraser *et al.*, 2005; Brackenbury *et al.*, 2007). However, despite a downward trend in mRNA levels, expression of nNa_v1.5 was not significantly altered by acute or chronic hypoxia in the MDA-MB-231 cell line. In contrast, no detectable transcript of nNa_v1.5 was found in normoxic or hypoxic MDA-MB-468 or MCF-7 cells (Figure 5.1a), or in T-47D cells (Appendix Figure I). There was no detectable Na_v1.6 transcript in both TNBC and Luminal A cell lines cultured in normoxia, and hypoxia had no effect on mRNA expression of this isoform (Figure 5.1b; Appendix Figure I). Normoxic MDA-MB-231 cells expressed Na_v1.7, which was unaffected by O₂ deprivation (Figure 5.1c). Conversely, MDA-MB-468, MCF-7 and T-47D cells had no detectable transcript levels of Na_v1.7 in normoxic or hypoxic cell lysates (Figure 5.1c; Appendix Figure I).

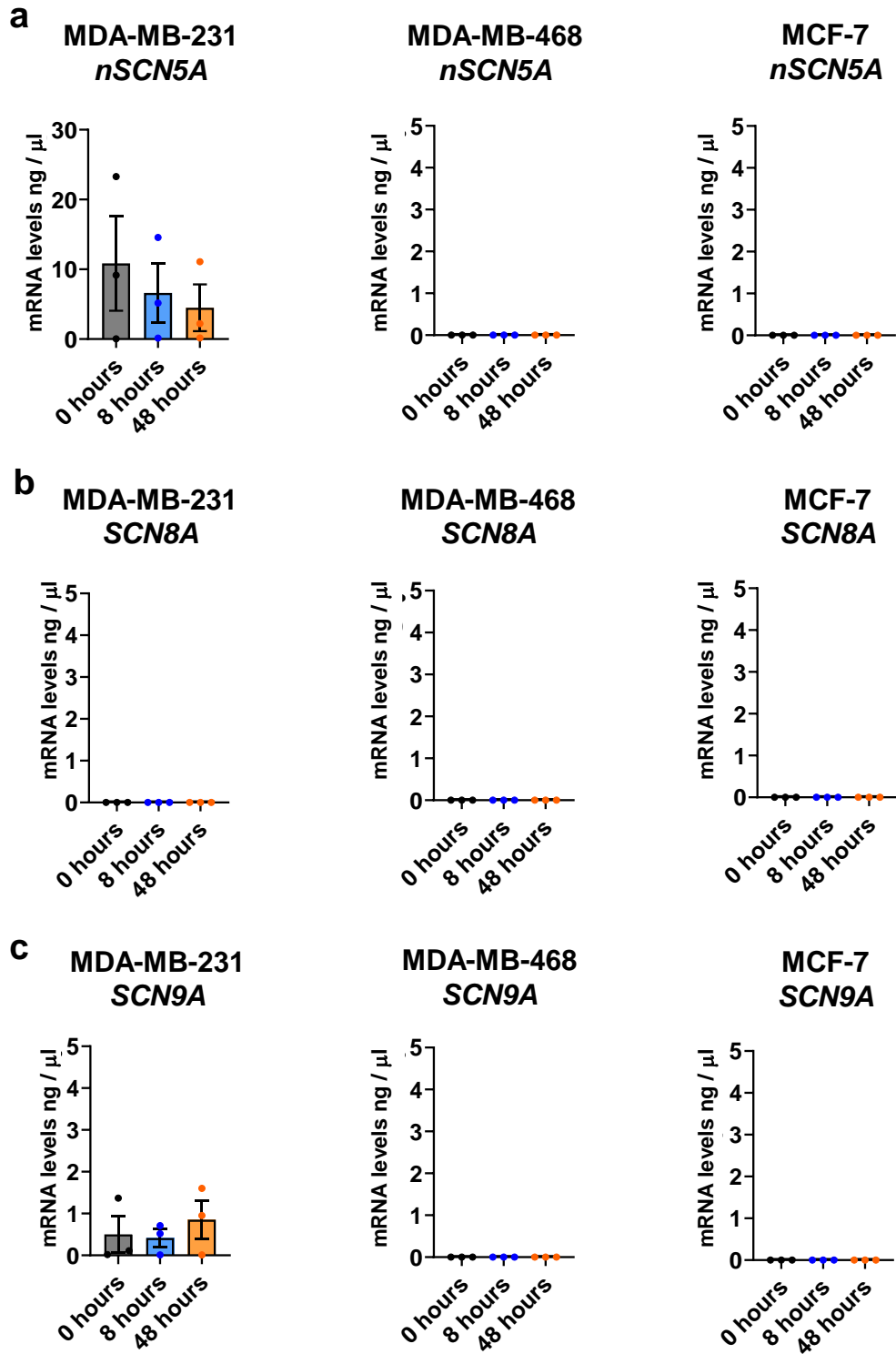


Figure 5.1 Effect of Acute or Chronic Hypoxia on VGSC Subunit mRNA Expression in TNBC and Luminal A Cell Lines. RT-qPCR of VGSC subunits **(a) *nSCN5A*** (nNav1.5), **(b) *SCN8A*** (Nav1.6) and **(c) *SCN9A*** (Nav1.7) in MDA-MB-231 (left), MDA-MB-468 (middle) and MCF-7 (right) breast cancer cells. Cell lines were cultured in normoxia (~20% O₂, "0 hours"), acute hypoxia (1% O₂, 8 hours) or chronic hypoxia (1% O₂, 48 hours). One-way ANOVA with Dunnett's multiple comparisons revealed no significant changes in expression where mRNA was detectable. No detectable mRNA was seen for each VGSC gene in MDA-MB-468 or MCF-7 cells, or for *SCN8A* in MDA-MB-468 cells. Error bars are ± SEM. N = 3.

TNBC MDA-MB-231 cells highly expressed nNav1.5 and Nav1.6, but not Nav1.7, in normoxic culture conditions which was unperturbed by acute or chronic hypoxia. However, transcript of the investigated VGSC subunits was not detected in normoxic MDA-MB-468 or Luminal A cell lines, and expression was not induced following O₂ deprivation. Therefore, hypoxia does not affect the expression of nNav1.5, Nav1.6 or Nav1.7 in the cell lines studied, and unknown mechanisms are driving VGSC expression in breast cancers, which require more investigation.

5.2.2 RNA-seq datasets are of good quality and suitable to use for the exploration of ER α and hypoxia-mediated regulation of Na⁺ transport in Luminal A cell lines

To explore the contribution of hypoxia and ER α in regulating Na⁺ transport beyond VGSC expression in breast cancer, Luminal A MCF-7 and T-47D breast cancer cell lines were cultured with fulvestrant or corresponding vehicle for 48 hours, and then cultured in normoxia or in hypoxia for a further 48 hours. Thus, breast cancer cells were subjected to one of four conditions, prior to total RNA extraction (Table 5.1). Samples were sent to Azenta for Next Generation Sequencing (NGS) using a polyadenylation (polyA) library preparation to enrich for mRNA and lncRNA (Yu *et al.*, 2020). Reads were pseudoaligned to the human transcriptome using *kallisto* (Bray *et al.*, 2016). Samples from MCF-7 (Figure 5.2a) and T-47D cells (Appendix Figure II a) were plotted as a heatmap with hierarchical clustering which showed biological replicates of samples from the same conditions were clustered together as expected. Interestingly, the effect of fulvestrant vs. vehicle appeared to be more influential on sample-sample distancing over normoxia vs. hypoxia. Principal component analysis (PCA) based on variance in gene expression also showed good separation of NV, NF, HV and HF samples in MCF-7 (Figure 5.2b) and T-47D cells (Appendix Figure II b). To identify potential influential outliers in each set of samples that could skew DGEA interpretation, Cook's distance was measured across all reads per gene, per sample. Cook's distance was similar for all 12 MCF-7 (Figure 5.2c) and all 16 T-47D samples (Appendix Figure II c) (Love *et al.*, 2014). Together, quality control checks implemented demonstrated no outliers that could significantly impact downstream gene expression analysis pipeline.

Table 5.1 Details of Experimental Conditions

Annotation	Description
NV	Normoxia and vehicle
NF	Normoxia and fulvestrant
HV	Hypoxia and vehicle
HF	Hypoxia and fulvestrat

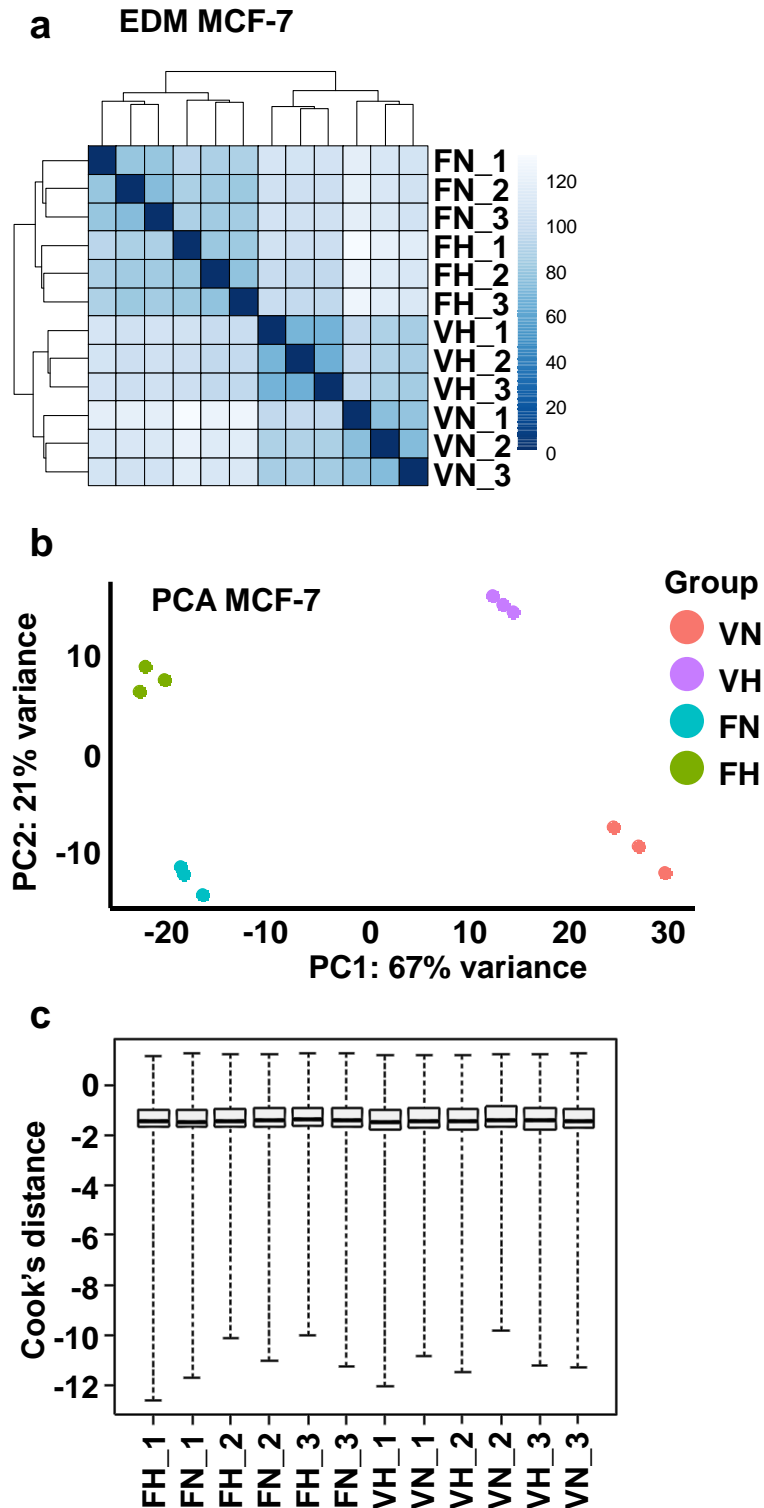


Figure 5.2 Data Quality of RNA-seq from MCF-7 Breast Cancer Cells. (a) EDM of squared distances between each sample from the MCF-7 RNA-seq. Experimental conditions for samples are vehicle and normoxia” (VN), vehicle and hypoxia (VH), fulvestrant and normoxia (FN) and fulvestrant and hypoxia (FH). N = 3. (b) Principal component analysis (PCA) plot with a PC1 variance of 67% and a PC2 variance of 21% for the 12 MCF-7 samples. (c) Boxplot of Cook’s distances for outlier detection, calculated for each gene within each MCF-7 sample.

5.2.3 Breast cancer cell lines had expected transcriptional responses to hypoxic culture and ER α knockdown

To continue investigating quality of RNA-seq datasets prior to exploring alterations in Na⁺ transport, it was necessary to ensure cell lines had the appropriate and expected transcriptional response to hypoxic and fulvestrant perturbations. *DESeq2* was implemented for DGEA in MCF-7 and T-47D cells. For DGEA, *DESeq2* ensures accurate comparisons of gene expression between samples by normalising raw read counts generated by e.g. *kallisto* to sample-specific size factors calculated from the median of ratios of observed counts per gene (Anders and Huber, 2010). Comparing vehicle treated normoxic vs. hypoxic samples demonstrated significant upregulation of *CA9*, *VEGFA* and *GAPDH* in MCF-7 (Figure 5.3a) and T-47D cells (Figure 5.3b) in response to hypoxia and in agreement with previous observations demonstrating hypoxic induction of these genes (Forsythe *et al.*, 1996; Wykoff *et al.*, 2000; Turner *et al.*, 2002; Higashimura *et al.*, 2011). Additionally, MCF-7 cells (Log₂FC - 0.4, *padj* < 0.001) but not T-47D cells (Log₂FC -0.04, *padj* 0.8) saw a significant reduction in *ESR1* transcript as a consequence of hypoxia and in accordance with previous observations of *ESR1* gene silencing during hypoxic perturbation (Ryu *et al.*, 2011; Wolff *et al.*, 2017).

Next, the effect of degradation of ER α by fulvestrant on expression of ER α -regulated genes *GREB1*, *CCND1* and *TFF1* was studied. In normoxic MCF-7 cells, a significant reduction in *GREB1* and *TFF1*, but not *CCND1* in response to fulvestrant was observed (Figure 5.4a). Additionally, significant reduction in all three ER α -regulated genes was observed in normoxic T-47D cells following ER α knockdown, as expected on the basis of literature (Ghosh *et al.*, 2000; Cicatiello *et al.*, 2004; Pancholi *et al.*, 2019, 2022).

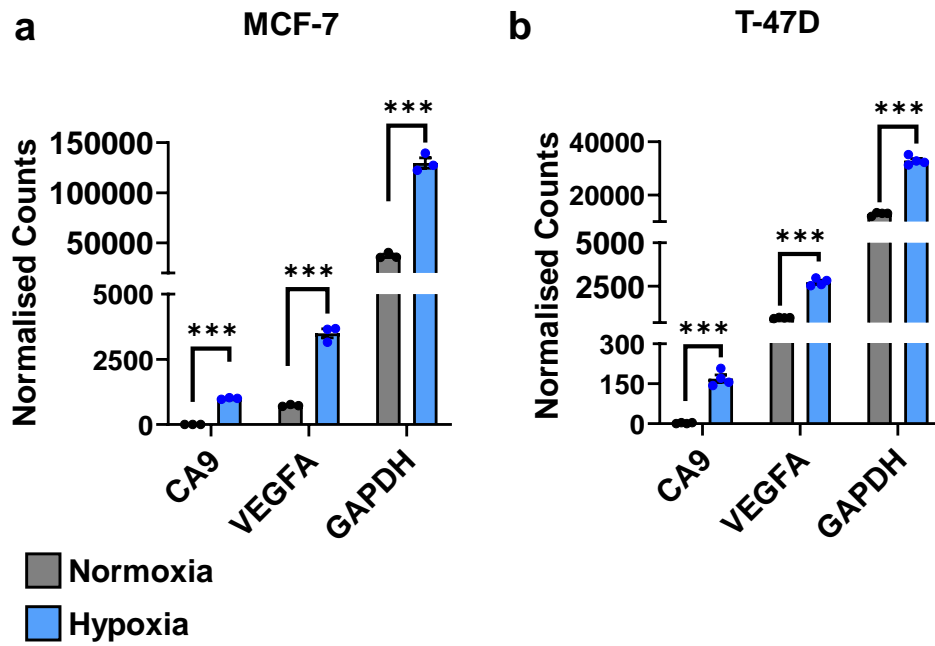


Figure 5.3 Demonstrating Cell Line Response to Hypoxia. Box plots showing normalised counts of hypoxia-responders *CA9*, *VEGFA* and *GAPDH* as determined by DGEA with *DESeq2*.in (a) MCF-7 and (b) T-47D cell lines following normoxia (grey) vs. hypoxia (blue) culture. *DESeq2* *** *padj* < 0.001. Error bars are \pm SEM. MCF-7 N = 3. T-47D N = 4.

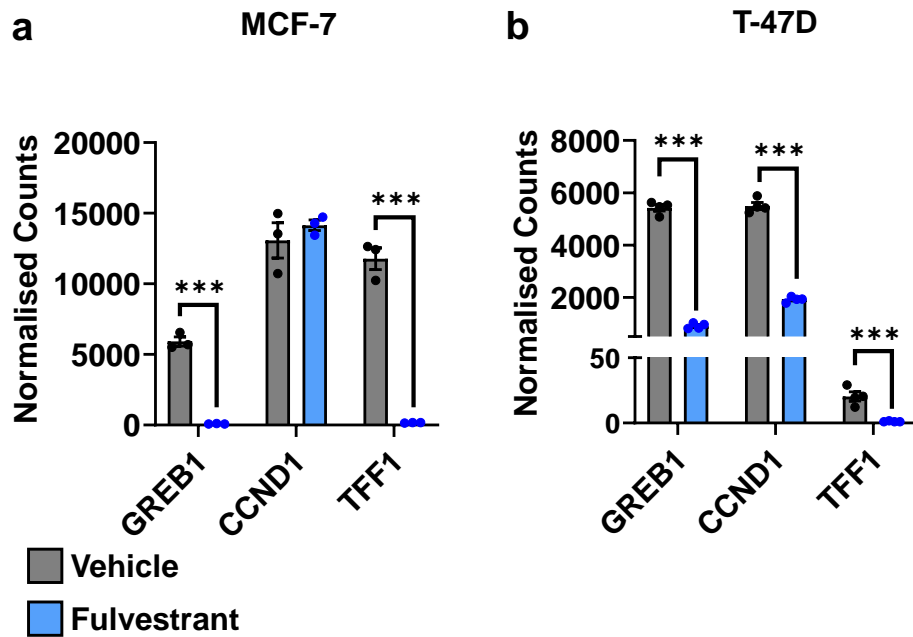


Figure 5.4 Luminal A Cell Line Response to ER α Knockdown. Box plots showing normalised counts of ER α -regulated genes *GREB1*, *CCND1* and *TFF1* as determined by DGEA with *DESeq2*.in (a) MCF-7 and (b) T-47D cell lines following treatment with vehicle (grey) vs. fulvestrant (blue) *** *padj* < 0.001. Error bars are \pm SEM. MCF-7 N = 3. T-47D N = 4.

In summary, quality control analysis described in Section 5.2.2 and Section 5.2.3 have demonstrated high quality RNA-seq data of MCF-7 and T-47D cell lines exposed to four different experimental conditions. Furthermore, cell lines exerted the appropriate transcriptional response to singular experimental challenge, namely O₂ deprivation in ER α + cell lines, or ER α knockdown in normoxic environments. Therefore, the RNA-seq datasets were suitable for exploring the effects of hypoxia and ER α in modulating Na⁺ transport in Luminal A breast cancer cells.

5.2.4 Genome-wide expression alterations because of cell line perturbations include Na⁺ transporter genes

To begin to understand the functional role hypoxia and ER α play in modulating Na⁺ transport in breast cancer, DGEA was carried out across the entire transcriptome of Luminal A cell lines, comparing expression changes in all available RNA-seq permutations:

1. NV vs. HV
2. NV vs. NF
3. NV vs. HF
4. NF vs. HV
5. NF vs. HF
6. HV vs. HF

Exploring differentially expressed genes in ER α + hypoxic vs. normoxic (NV vs. HV) MCF-7 (Figure 5.5a) and T-47D (Figure 5.5b) cell lines identified significant alterations in genome-wide expression levels with a slight preference for positive induction of gene expression over downregulation. Tables briefly detailing most up- and downregulated genes in response to hypoxic culture in MCF-7 and T-47D cells are available in the appendix (Appendix Table I – Appendix Table IV). Genes among the most upregulated in response to hypoxia according to Log₂FC included *PTPRN*, *AQP2*, *CASP1*, and *SLC28A1* which are involved in vesicle-mediated secretory processes, maintaining cell permeability, regulating inflammatory responses, and acting as a Na⁺/pyrimidine symporter, respectively.

Significant up- and downregulation of Na⁺ channel genes was evident in both Luminal A cell lines cultured under hypoxia, shown by Na⁺ channel gene annotations on volcano plots (Figure 5.5) and heatmaps (Appendix Figure V). In MCF-7 cells, low O₂ tension induced positive expression of NKA *ATP1A1* (Log₂FC 0.37, *padj* < 0.0001) and *ATP1B1* (Log₂FC 1.94, *padj* < 0.001), which encode α-NKA and β-NKA, respectively. In T-47D cells, α-NKA (Log₂FC 0.50, *padj* < 0.0001) and β-NKA (Log₂FC 1.79, *padj* < 0.001) were similarly induced by hypoxic challenge.

Additionally, positive induction of major ENaC subunits *SCNN1A* (α-ENaC) (Log₂FC 1.55; *padj* < 0.001), *SCNN1B* (β-ENaC) (Log₂FC 2.43; *padj* < 0.001) and *SCNN1G* (γ-ENaC) (Log₂FC 1.28; *padj* < 0.01) was seen in MCF-7 cells. In T-47D cells, α-ENaC (Log₂FC 0.5; *padj* < 0.001), β-ENaC (Log₂FC 1.64; *padj* < 0.001) and γ-ENaC (Log₂FC 3.78; *padj* < 0.001) were also induced in response to O₂ deprivation, providing evidence that hypoxia may potentiate dysregulated Na⁺ transport in breast cancer cell lines through NKA and ENaC. However, chronic hypoxia, here defined as a 48-hour time period, did not affect expression of any α or β VGSC subunits in Luminal A breast cancer cell lines.

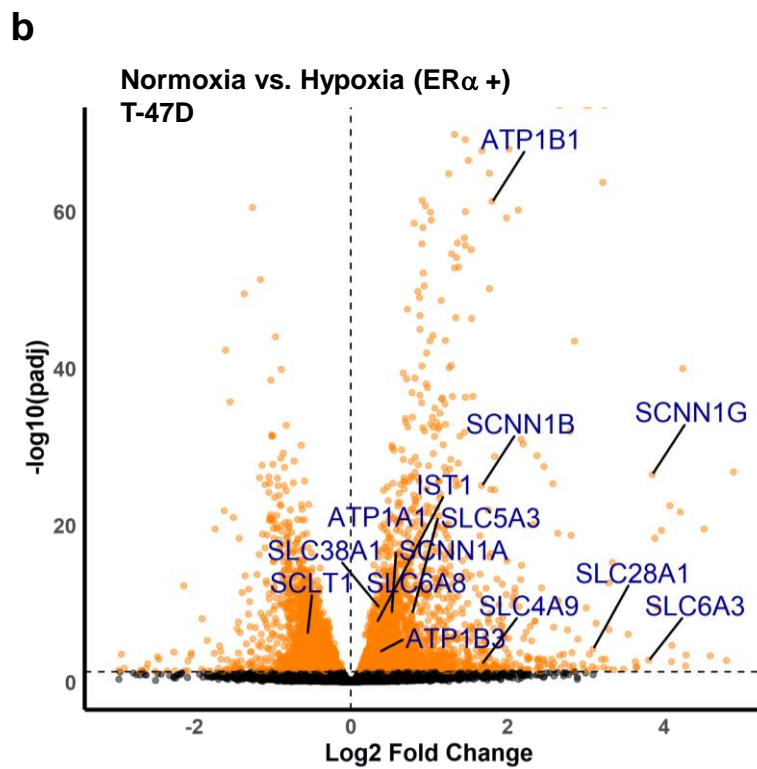
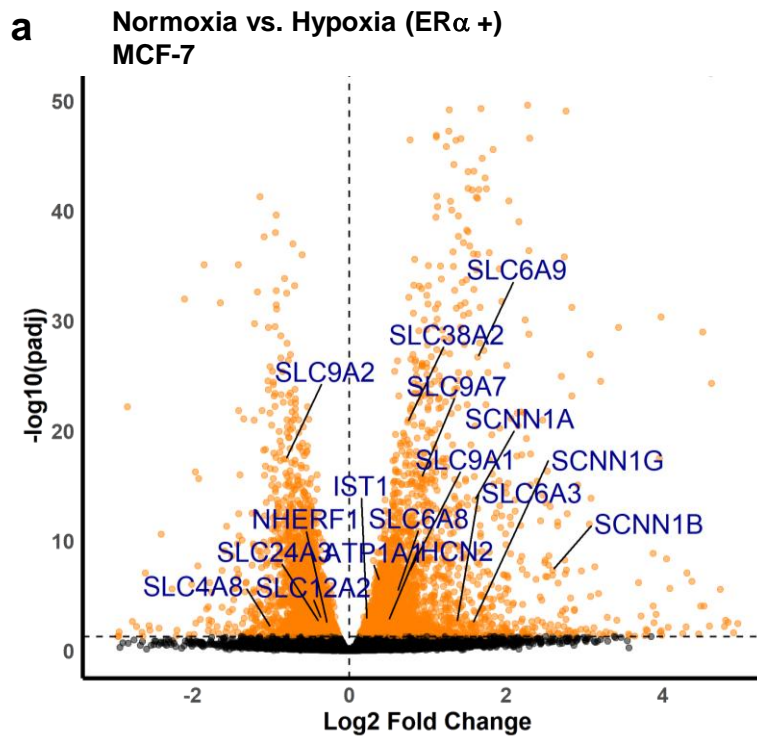


Figure 5.5 Transcriptome-Wide Expression Changes in Hypoxic Luminal A Cells.

Volcano plots of differentially expressed genes in **(a)** MCF-7 or **(b)** T-47D cells cultured in normoxia vs. hypoxia (ER α +). Orange symbols above horizontal dashed line show significant differentially expressed genes ($p_{adj} < 0.05$). Orange symbols on the left of the vertical dashed line are significantly downregulated (negative Log₂FoldChange). Orange symbols on the right of the vertical dashed line are significantly upregulated (positive Log₂FoldChange). Black symbols are genes which were not significantly differentially expressed ($p_{adj} > 0.05$). Gene annotations are significant differentially expressed Na⁺ channel genes with the smallest p_{adj} .

Next, investigations into the effect of fulvestrant on normoxic Luminal A gene expression (NV vs. NF) revealed strong genome-wide transcriptional changes with no bias towards up- or downregulation in either MCF-7 (Figure 5.6a) or T-47D (Figure 5.6b) cells. Tables exploring most up- and downregulated genes in response to ER α knockdown in MCF-7 and T-47D cells are available in the appendix (Appendix Table VI – Appendix Table VIII). Genes positively induced post-fulvestrant treatment included *AQP10* which encodes a water channel involved in water transport through the osmotic gradient across cell membranes, and *NDP* which activates the Wnt signalling pathway. Genes significantly downregulated in response to treatment with fulvestrant included *AGR3* which is required for regulating intracellular Ca²⁺ stores in the endoplasmic reticulum, and scaffold protein *PDZK1* which is thought to be involved in coordinating ion transport and second messenger cascades.

Studying specific alterations in Na⁺ channel expression demonstrated ER α -dependent regulation of many Na⁺ transporters, shown by gene annotations on volcano plots (Figure 5.6) and heatmaps (Appendix Figure VI). Of the NKA, alternative α isoform α 2-NKA (Log₂FC 4.09; *padj* < 0.01) was preferentially upregulated in MCF-7 cells treated with fulvestrant. In T-47D cells, α 4-NKA (Log₂FC 1.20; *padj* < 0.05) and β 1-NKA (Log₂FC 1.72; *padj* < 0.001) were positively upregulated following ER α -knockdown, whereas α 3-NKA (Log₂FC -1.60; *padj* < 0.001) was downregulated.

Two members of the NDBTs family *SLC4A4* (Log₂FC 7.90; *padj* < 0.001) and *SLC4A9* (Log₂FC 1.11; *padj* < 0.05) were significantly upregulated in MCF-7 but not in T-47D cells. Selectivity of Na⁺ transporter gene expression suggests that the ER α may preferentially drive expression of some Na⁺ channels but inhibit expression of others. Furthermore, the differential response between the MCF-7 and T-47D cells demonstrated cell line variability in Na⁺ channel targets of the ER α and implicates other unknown factors in ER α -mediated Na⁺ channel gene expression.

Cell line heterogeneity was further exemplified when studying fulvestrant-dependent effects on VGSC subunit expression. In MCF-7 cells, none of the α subunits were differentially expressed when ER α was knocked down, whereas in T-47D cells, transcript of Na_v1.1 encoded by *SCN1A* (Log₂FC 1.80; *padj* < 0.001) was upregulated and Na_v1.6 encoded by *SCN8A* (Log₂FC -1.05; *padj* < 0.01) was downregulated following fulvestrant treatment, suggesting ER α is important in

mediating expression of these two VGSC α subunits in T-47D cells. Additionally, $\beta 1$ encoded by *SCN1AB* saw a significant positive fold change induction of mRNA levels in MCF-7 cells post-fulvestrant (Log_2FC 1.16; $p_{\text{adj}} < 0.001$), whereas a significant downregulation in expression was seen in T-47D cells (Log_2FC -1.67; $p_{\text{adj}} < 0.001$). Interestingly, normalised counts of $\beta 1$ in normoxic and vehicle treated MCF-7 cells (719.44 ± 16.88 SD) were > 9-fold greater than in T-47D cells (77.92 ± 5.24 SD) of the same conditions, further demonstrating cell-type specific differences in VGSC expression between the two cell lines.

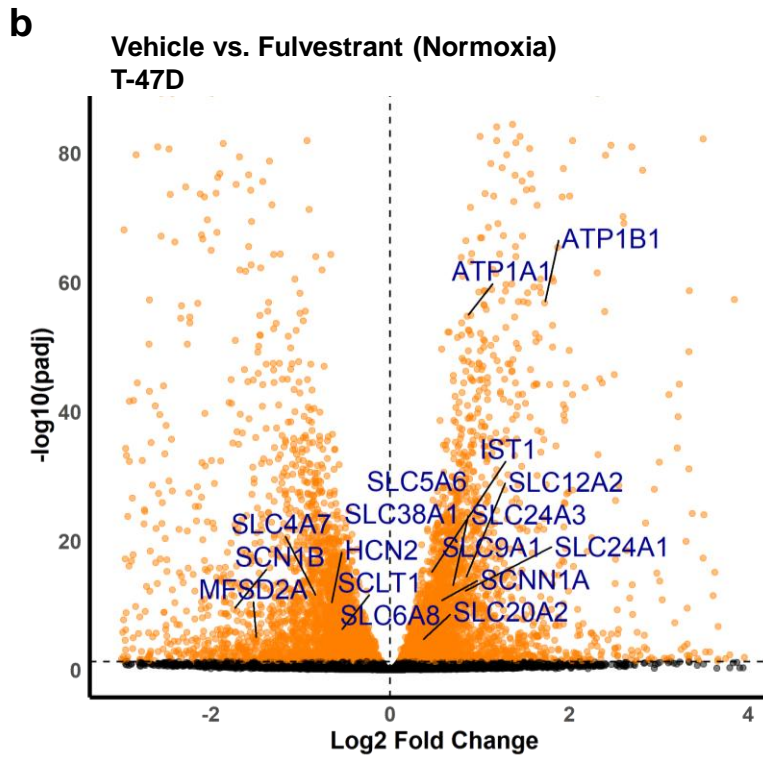
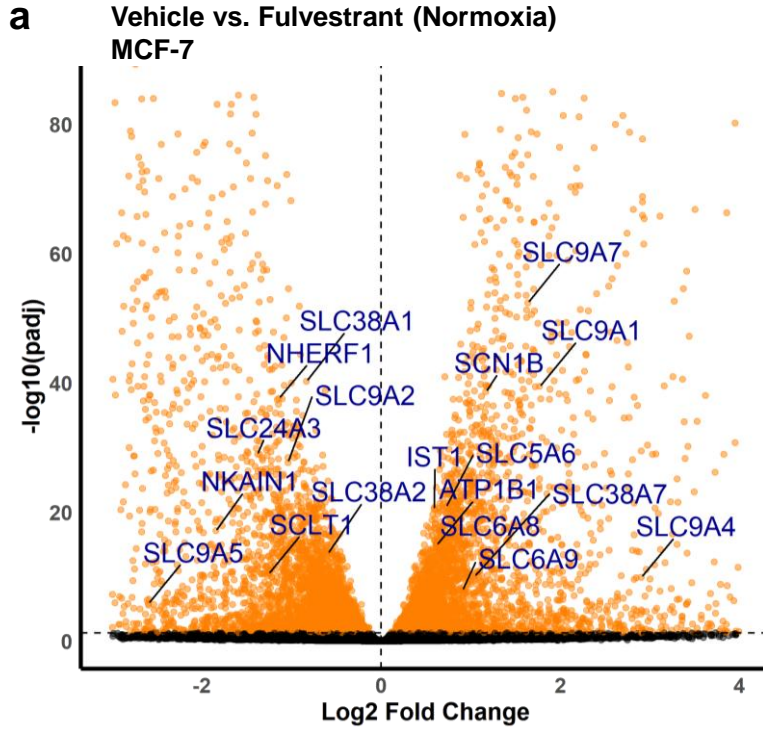


Figure 5.6 Fulvestrant-Induced Transcriptome-Wide Expression Changes in MCF-7 and T-47D Cells. Volcano plots of differentially expressed genes in **(a)** MCF-7 or **(b)** T-47D cells treated with vehicle vs. fulvestrant (normoxia). Orange symbols above horizontal dashed line show significant differentially expressed genes ($p_{adj} < 0.05$). Orange symbols on the left of the vertical dashed line are significantly downregulated (negative $\text{Log}_2\text{FoldChange}$). Orange symbols on the right of the vertical dashed line are significantly upregulated (positive $\text{Log}_2\text{FoldChange}$). Black symbols are genes which were not significantly differentially expressed ($p_{adj} > 0.05$). Gene annotations are significant differentially expressed Na^+ channel genes with the smallest p_{adj} .

Volcano plots that explore the remaining RNA-seq permutations (3 – 6) in MCF-7 and T-47D cells can be found in the appendix (Appendix Figure III, Appendix Figure IV). In brief, combinations of experimental challenge further demonstrated significant alteration in Na⁺ transporter gene expression, particularly in subunits of the NKA complex, ENaC family members, and NHE regulatory factors, and further implicated hypoxia and the ER α in modulating the Na⁺ network in breast cancer cell lines.

To summarise, DGEA has demonstrated widespread transcriptional responses in MCF-7 and T-47D cell lines in response to both hypoxic challenge and ER α knockdown. Of particular interest was the differential regulation of many Na⁺ transporter genes, including positive induction of NKA and ENaC subunits in response to hypoxia, as well as following ER α perturbation. Furthermore, VGSC subunits Na_v1.6 and β 1 appeared to be positively regulated by the hormone receptor in T-47D cells, in contrast to the original hypothesis, whereas β 1 in MCF-7 cells and Na_v1.1 in T-47D cells seemed to be repressed by ER α . Taken together, the findings discussed in Section 5.2.4 strongly implicate hypoxia in positive regulation of Na⁺ transport, whereas the response to ER α modulation was more varied amongst genes in the Na⁺ network, and between the two Luminal A cell lines used.

5.2.5 ER α knockdown or hypoxia switches off biosynthetic and cell division processes in MCF-7 and T-47D breast cancer cell lines

To investigate the extent to which ER α and hypoxia are involved in modulating Na⁺ transport in the MCF-7 and T-47D breast cancer cell lines, GSEA was performed using gene lists generated from each RNA-seq permutation of significantly differentially expressed genes (*p*_{adj} < 0.05) arranged in order from most positive to most negative Log₂FC. The R package *ClusterProfiler* was implemented to first identify gene ontology (GO) terms most enriched in Luminal A cell lines in each available RNA-seq comparison (Yu *et al.*, 2012). An unbiased GSEA approach was used to provide valuable information into major biological processes (BP) or molecular functions (MF) that are most affected because of hypoxia or fulvestrant-mediated ER α knockdown, either singularly or in combination, before investigating if BPs or MFs involved in Na⁺ transport are perturbed.

In normoxic MCF-7 cells that were treated with fulvestrant, ER α knockdown resulted in 97 significantly enriched BP GO terms that were downregulated, and 248 BP GO terms that were positively enriched. BP GO terms that had the smallest *p*_{adj} in response to fulvestrant treatment all had a negative normalised enrichment scores (NES) and included “chromosome segregation” (Figure 5.7a) and other BP terms specifically involved in cell division processes (Table 5.2). Negative NES for cell division processes suggests that MCF-7 cells are shutting down replication in response to ER α knockdown. Conversely, positively enriched BP terms included “positive regulation of epithelial cell migration” (NES:1.87; *p*_{adj} < 0.0001), “actin filament bundle assembly” (NES: 1.85; *p*_{adj} < 0.0001) and “tissue migration” (NES: 1.79; *p*_{adj} < 0.0001) indicating that fulvestrant treatment bestows upon MCF-7 cells a more motile phenotype.

MF GO term analysis demonstrated 10 significant MF GO terms that were negatively enriched, and 13 that were positively enriched. The MF GO term with the smallest *p*_{adj} was “catalytic activity, acting on DNA”, and along with negative enrichment of helicase activity, suggests gene transcription in response to fulvestrant treatment is being dampened (Figure 5.7b; Table 5.3). In contrast, positively enriched MF terms in fulvestrant treated MCF-7 cells were “heparin binding” (NES: 2.05; *p*_{adj} < 0.0001) which includes genes involved in regulating cell contacts with ECM, “cadherin binding” (NES: 1.63; *p*_{adj} < 0.0001) which includes genes involved in regulating cell-cell contacts and also “peptidase regulator activity” (NES; 1.73; *p*_{adj} < 0.001) which includes genes essential for modulating the activity of any enzyme involved in catalysing hydrolysis of peptide bonds.

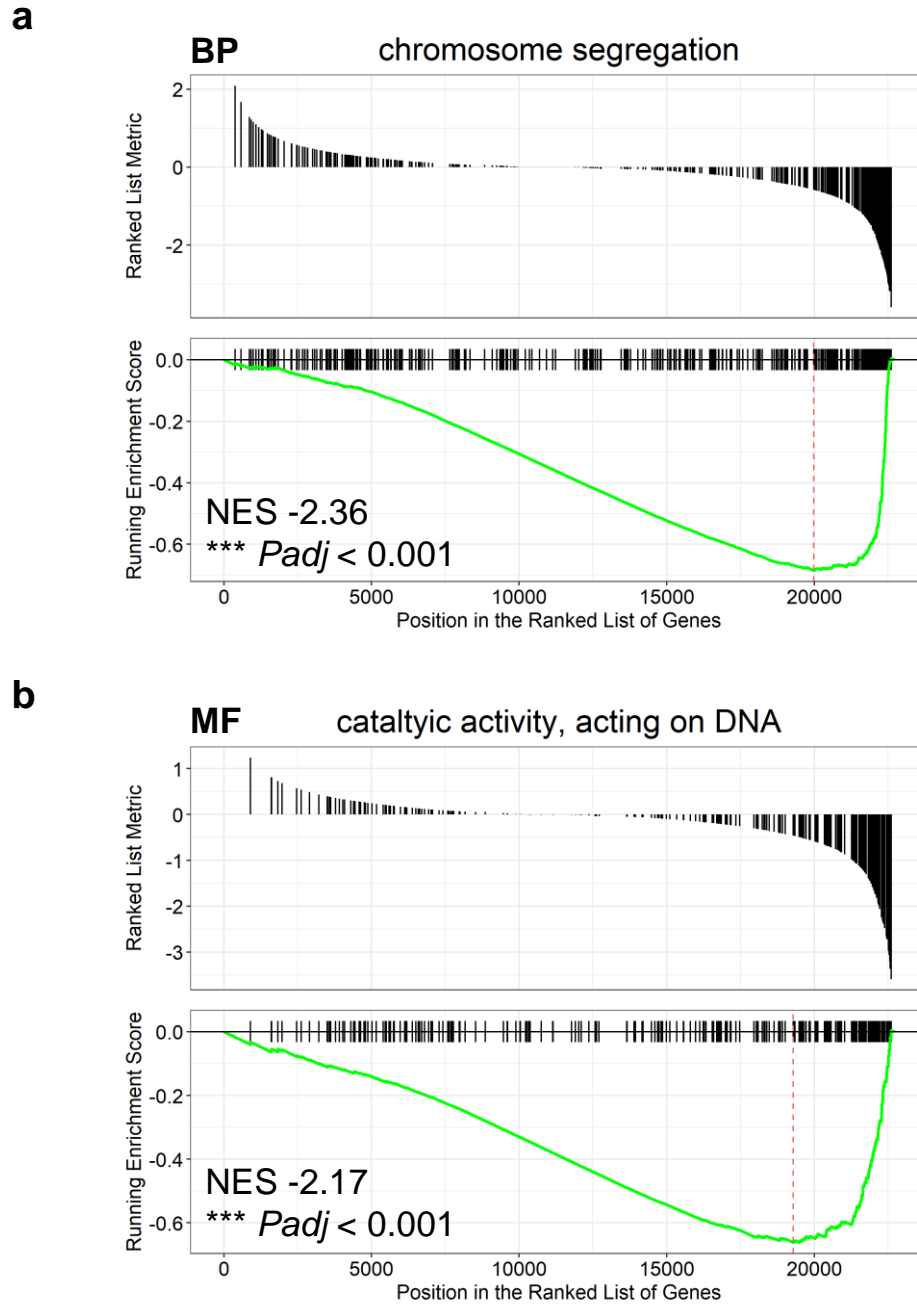


Figure 5.7 Most Enriched GO Terms in MCF-7 Cells Following ER α Knockdown.

GSEA revealing most enriched (a) BP and (b) MF GO gene sets in normoxic MCF-7 cells treated with fulvestrant compared to vehicle control. Significantly differentially expressed genes were ranked from most positive Log₂FC to most negative Log₂FC for GSEA. Top box of GSEA plots demonstrates the degree of correlation of genes with an ER α -ve phenotype (> 0 for positive correlation, < 0 for negative correlation). The y-axis of the bottom box in GSEA plots represents the running enrichment score (ES) which is shown by the green line connecting the ES to genes of the gene set (black vertical bars at 0.0). NES is normalised ES. Red dashed line shows maximum ES. *** *p*adj < 0.001.

Table 5.2 Most Enriched BP Terms in MCF-7 Cells Treated with Fulvestrant Compared to Vehicle. GO terms (Description) ranked according to FDR. ES is normalised to account for differences in gene set sizes. Set Size relates to how many genes make up the gene set. Leading Edge Tags (%) refers to the percentage of genes contributing to ES.

Description	NES	Set Size	Leading Edge Tags (%)
Nuclear division	-2.23	434	32
Nuclear chromosome segregation	-2.33	308	35
Organelle fission	-2.15	480	30
DNA replication	-2.30	275	49
DNA-templated DNA replication	-2.40	161	60
Mitotic sister chromatid segregation	-2.38	184	38
Sister chromatid segregation	-2.30	224	41
DNA recombination	-2.14	331	38
Mitotic nuclear division	-2.22	273	32
Cell cycle checkpoint signalling	-2.36	417	38

Table 5.3 Most Enriched MF Terms in MCF-7 Cells Treated with Fulvestrant Compared to Vehicle. GO terms (Description) ranked according to FDR.

Description	NES	Set Size	Leading Edge Tags (%)
ATP-dependent activity, acting on DNA	-2.17	122	39
Heparin binding	2.05	157	31
Helicase activity	-1.98	154	40
Single-stranded DNA binding	-2.02	117	41
Cadherin binding	1.62	334	34
Peptidase regulator activity	1.73	205	21
Sulphur compound binding	1.65	252	20
ATP hydrolysis activity	-1.56	409	33
Endopeptidase regulator activity	1.75	164	22
Peptidase inhibitor activity	1.71	154	23

Investigating BPs that are most enriched in T-47D cells following fulvestrant treatment demonstrated significant negative enrichment of 39 BP GO terms, and 13 positively enriched GO terms. The BP with the smallest *p*_{adj} was “ribosome biogenesis” (Figure 5.8a). Many other BPs involved in regulation of protein synthesis were also turned off as a consequence of ER α knockdown, including “cytoplasmic translation” (NES: -2.03; *p*_{adj} < 0.0001) and “ribosomal small unit biogenesis” (NES: -1.99; *p*_{adj} < 0.0001) indicating inhibition of translational processes. Similar to MCF-7 cells, T-47D cells also downregulated genes involved in cell division, as shown by negative enrichment of “DNA-templated DNA replication” (NES: -1.96; *p*_{adj} < 0.0001) and “DNA replication” (NES: -1.78; *p*_{adj} < 0.0001) (Table 5.4). In contrast, positively enriched BP GO terms included “vacuolar transport” (NES: 1.80; *p*_{adj} < 0.001) and “lysosomal transport” (NES: 1.73; *p*_{adj} < 0.01).

When ER α -dependent MFs were explored, 19 MF GO terms were negatively enriched, and three MF GO terms were positively enriched following fulvestrant-mediated knock down of the steroid receptor. The MF term with the smallest *p*_{adj} was “structural constituent of the ribosome” (Figure 5.8b), followed by negative enrichment of several MFs involved in receptor signalling and hormone activity, such as “receptor ligand activity” (NES: -1.63; *p*_{adj} < 0.0001) “signalling receptor activator activity” (NES: -1.63; *p*_{adj} < 0.001) “growth factor activity” (NES: -1.76; *p*_{adj} < 0.01) and “hormone activity” (NES: -1.79; *p*_{adj} < 0.01) (Table 5.5) which was an expected result given fulvestrant-mediated ER α knockdown. Interestingly, the MF GO terms that exhibited positive enrichment in ER α knock down in T-47D cells were centred around increased transcription factor activity: “protein heterodimerization activity” (NES: 1.46; *p*_{adj} < 0.01) “DNA-binding transcription activator activity, RNA polymerase II-specific” (NES: 1.29; *p*_{adj} < 0.05) and “DNA-binding transcription activator activity” (NES: 1.28; *p*_{adj} < 0.05), which could suggest T-47D cells are beginning to bypass ER α regulation of gene transcription by increasing expression of alternative signalling pathways, such as the EGFR2/HER2 signalling pathway observed in endocrine resistant breast cancer (Asghari *et al.*, 2022). Indeed, core enrichment of *ERBB2* (HER2), *ERBB3* (HER3) and *EPAS1* (HIF-2 α) was significant in MF GO terms associated with ER α -depleted T-47D cells.

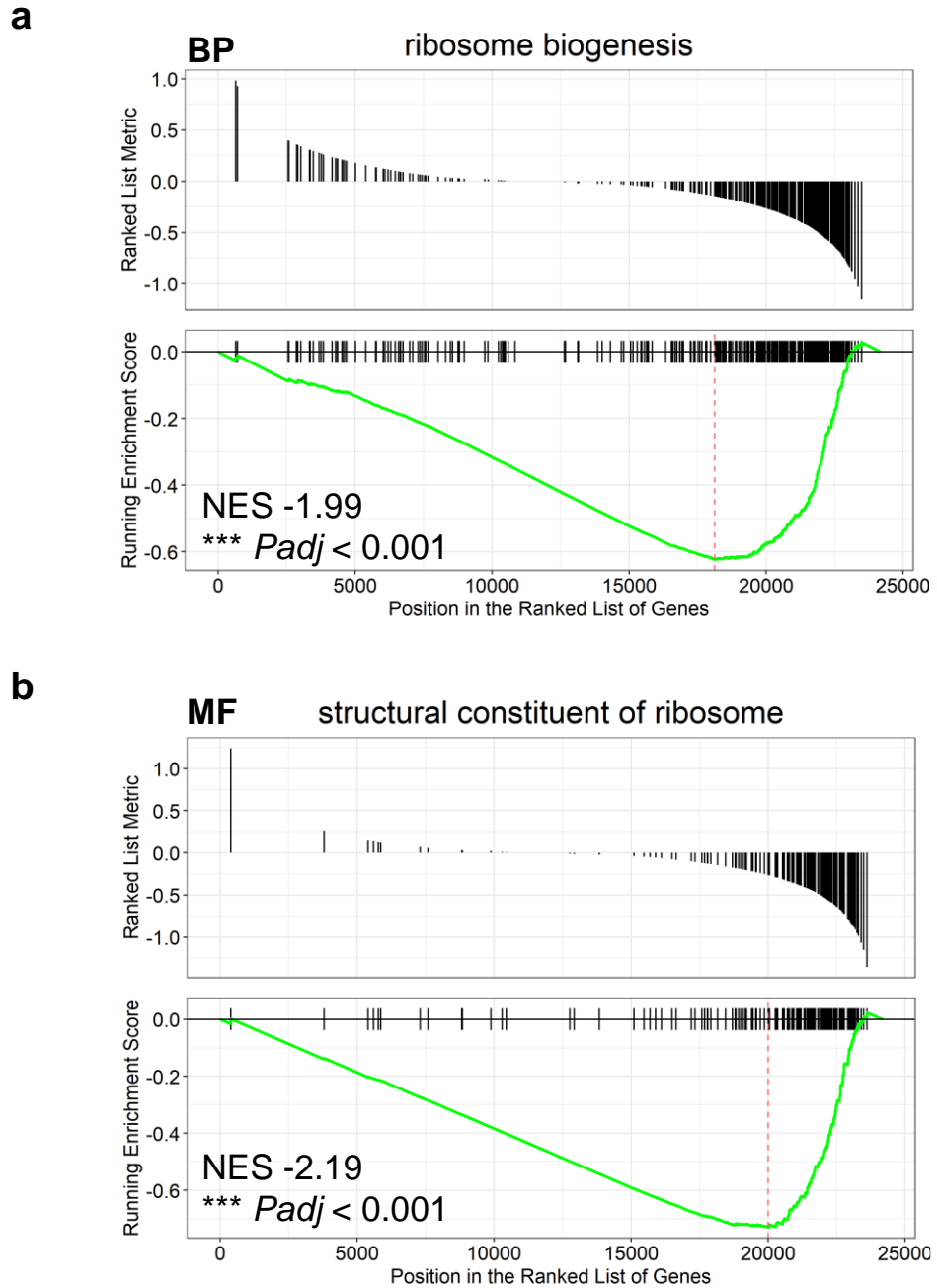


Figure 5.8 Most Enriched GO Terms in T-47D Cells Following ER α Knockdown. GSEA revealing most enriched (a) BP and (b) MF GO gene sets in normoxic T-47D cells treated with fulvestrant compared to vehicle control. Significantly differentially expressed genes were ranked from most positive Log₂FC to most negative Log₂FC for GSEA. *** *padj* < 0.001.

Table 5.4 Most Enriched BP Terms in T-47D Cells Treated with Fulvestrant Compared to Vehicle. GO terms (Description) ranked according to FDR.

Description	NES	Set Size	Leading Edge Tags (%)
Ribonucleoprotein complex biogenesis	-1.87	467	58
Cytoplasmic translation	-2.05	155	61
rRNA processing	-1.96	222	67
rRNA metabolic process	-1.93	261	64
DNA-templated DNA replication	-1.96	160	57
Ribosomal small subunit biogenesis	-1.99	103	76
DNA replication	-1.78	275	48
ncRNA processing	-1.67	431	53
Chromosome segregation	-1.68	418	35
Vacuolar transport	1.80	166	49

Table 5.5 Most Enriched MF Terms in T-47D Cells Treated with Fulvestrant Compared to Vehicle. GO terms (Description) ranked according to FDR.

Description	NES	Set Size	Leading Edge Tags (%)
Receptor ligand activity	-1.63	428	15
Signalling receptor regulator activity	-1.61	467	14
Signalling receptor activator activity	-1.63	433	15
Catalytic activity, acting on DNA	-1.69	242	37
Growth factor activity	-1.76	143	22
Hormone activity	-1.79	106	16
Protein heterodimerization activity	1.46	327	20
ATP-dependent activity, acting on DNA	-1.69	122	41
Integrin binding	-1.62	151	21
Organic acid transmembrane transporter activity	-1.59	163	25

Next, the effect of hypoxia on BPs and MFs in Luminal A cell lines was explored. In MCF-7 cells, hypoxic challenge negatively enriched for 80 BP whereas a striking 480 BPs were positively enriched. As expected, many of the BPs positively enriched in hypoxic MCF-7 cells were those involved in cellular responses to decreased O₂ availability (Table 5.6), including “response to hypoxia” (NES: 1.93; *p*_{adj} < 0.0001) “cellular response to hypoxia” (NES: 1.92; *p*_{adj} < 0.0001) and “response to decreased oxygen levels” (NES: 1.87; *p*_{adj} < 0.0001). Additionally, “positive regulation of epithelial cell proliferation” (NES: 1.82; *p*_{adj} < 0.0001) was amongst the most positively enriched BPs, suggesting hypoxia drives increased proliferation. In contrast, BPs with the smallest *p*_{adj} in hypoxic MCF-7 cells were preferentially negatively enriched and were involved in protein synthesis, including “ribonucleoprotein complex biogenesis” (Figure 5.9a), “ribosome biogenesis” (NES: -2.41; *p*_{adj} < 0.0001), “tRNA processing” (NES: -2.28; *p*_{adj} < 0.0001) and “mitochondrial gene expression” (NES: -2.46; *p*_{adj} < 0.0001). Mitochondrial genes include 13 subunits of the respiratory chain and the ncRNA required for their translation. Negative enrichment of mitochondrial gene expression could be a consequence of impaired oxidative phosphorylation or remodelling of the electron transport chain since O₂ is not available to act as the final electron acceptor (Fuhrmann and Brüne, 2017; Rusecka et al., 2018).

Exploring hypoxia-mediated MFs in MCF-7 cells revealed 19 negatively enriched and 27 positively enriched GO terms. The MF with the smallest *p*_{adj} was “catalytic activity, acting on RNA” (Figure 5.9b), closely followed by “catalytic activity, acting on tRNA” (Table 5.7) which describes gene products that modify RNA (or tRNA) through a mechanism driven by ATP hydrolysis and includes RNA helicases and 3'-5' RNA exonucleases, implicating hypoxia in dysregulated RNA stability, folding and turnover. Conversely, positive enrichment of MF terms including “signalling receptor regulator activity” (NES: 1.69; *p*_{adj} < 0.0001) “DNA-binding transcription activator activity” (NES: 1.62; *p*_{adj} < 0.0001) and “DNA-binding transcription activator activity, RNA polymerase II-specific” (NES: 1.62; *p*_{adj} < 0.0001) was observed and corresponds to the preferential increase in gene expression in MCF-7 cells following O₂ deprivation described in Section 5.2.4.

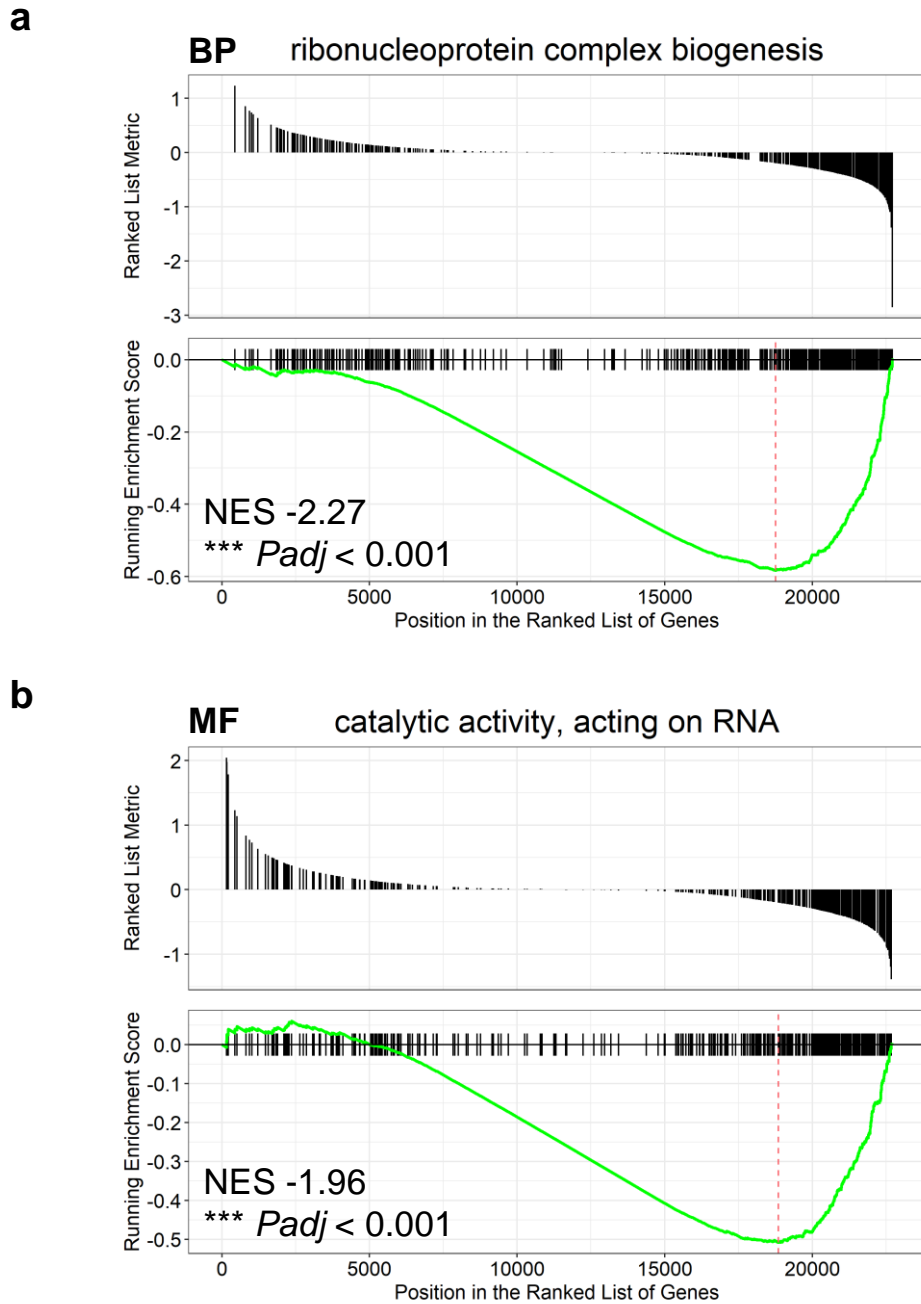


Figure 5.9 Most Enriched GO Terms in Hypoxic vs. Normoxic MCF-7 Cells. GSEA revealing most enriched (a) BP and (b) MF GO gene sets in ER α + MCF-7 cells cultured in hypoxia compared to normoxia. Significantly differentially expressed genes were ranked from most positive Log₂FC to most negative Log₂FC for GSEA. Top box of GSEA plots demonstrates the degree of correlation of genes with a hypoxic phenotype (> 0 for positive correlation, < 0 for negative correlation). *** *p*adj < 0.001.

Table 5.6 Most Enriched BP Terms in MCF-7 Cells Cultured in Hypoxia vs. Normoxia.

GO terms (Description) ranked according to FDR.

Description	NES	Set Size	Leading Edge Tags (%)
ncRNA processing	-2.22	433	54
Ribosome biogenesis	-2.41	323	54
Mitochondrial gene expression	-2.46	163	70
Mitochondrial translation	-2.44	130	72
rRNA processing	-2.30	223	57
rRNA metabolic process	-2.20	262	53
tRNA metabolic process	-2.27	196	58
tRNA processing	-2.28	133	62
Response to hypoxia	1.93	277	31
Response to decreased oxygen levels	1.90	294	33

Table 5.7 Most Enriched MF Terms in MCF-7 Cells Cultured in Hypoxia vs. Normoxia.

GO terms (Description) ranked according to FDR.

Description	NES	Set Size	Leading Edge Tags (%)
Signalling receptor regulator activity	1.69	458	16
Catalytic activity, acting on a tRNA	-2.06	130	65
Signalling receptor activator activity	1.70	425	17
Receptor ligand activity	1.71	420	17
Extracellular matrix structural constituent	1.89	156	27
DNA-binding transcription activator activity	1.61	446	28
DNA-binding transcription activator activity, RNA polymerase II-specific	1.61	442	29
Heparin binding	1.81	157	24
Carbohydrate binding	1.71	247	17
Cytokine activity	1.74	189	21

Investigating hypoxia-dependent effects on BPs in T-47D cells showed 52 negatively enriched BPs and 523 positively enriched BPs due to O₂ deprivation. As in MCF-7 cells, “mitochondrial gene expression” was significantly downregulated in response to hypoxia in T-47D cells (Figure 5.10a). Additionally, “respiratory electron transport chain” (NES: -2.26; *p*_{adj} < 0.0001) and “oxidative phosphorylation” (NES: -2.07; *p*_{adj} < 0.0001) were among the most significant downregulated BPs (Table 5.8), and further support an impaired electron transport chain hypothesis as described for hypoxic MCF-7 cells. As expected, the most positively enriched BPs were those involved in hypoxic response including “response to hypoxia” (NES: 2.05; *p*_{adj} < 0.0001), “response to oxygen levels” (NES: 1.97; *p*_{adj} < 0.0001) and “response to decreased oxygen levels” (NES: 2.00; *p*_{adj} < 0.0001), as was “pyruvate metabolic process” (NES: 1.85; *p*_{adj} < 0.0001) demonstrating the hypoxic-induced shift in energy metabolism in T-47D cells deprived of O₂.

In terms of MFs, 12 were negatively enriched in hypoxic T-47D cells, whereas positive enrichment of 64 MF GO terms was observed. Negative enrichment was again seen in “structural constituent of ribosome” (Figure 5.10b) indicating impaired protein translation due to compromised ribosome assembly. On the contrary, positively enriched MF GO terms included “glycosaminoglycan binding” (NES: 2.04; *p*_{adj} < 0.0001), “heparin binding” (NES: 2.02; *p*_{adj} < 0.0001) and “signalling receptor regulator activity” (NES: 1.68; *p*_{adj} < 0.0001) suggesting altered cell adhesion and motility properties and modulated signalling receptor function in hypoxic T-47D cells (Table 5.9).

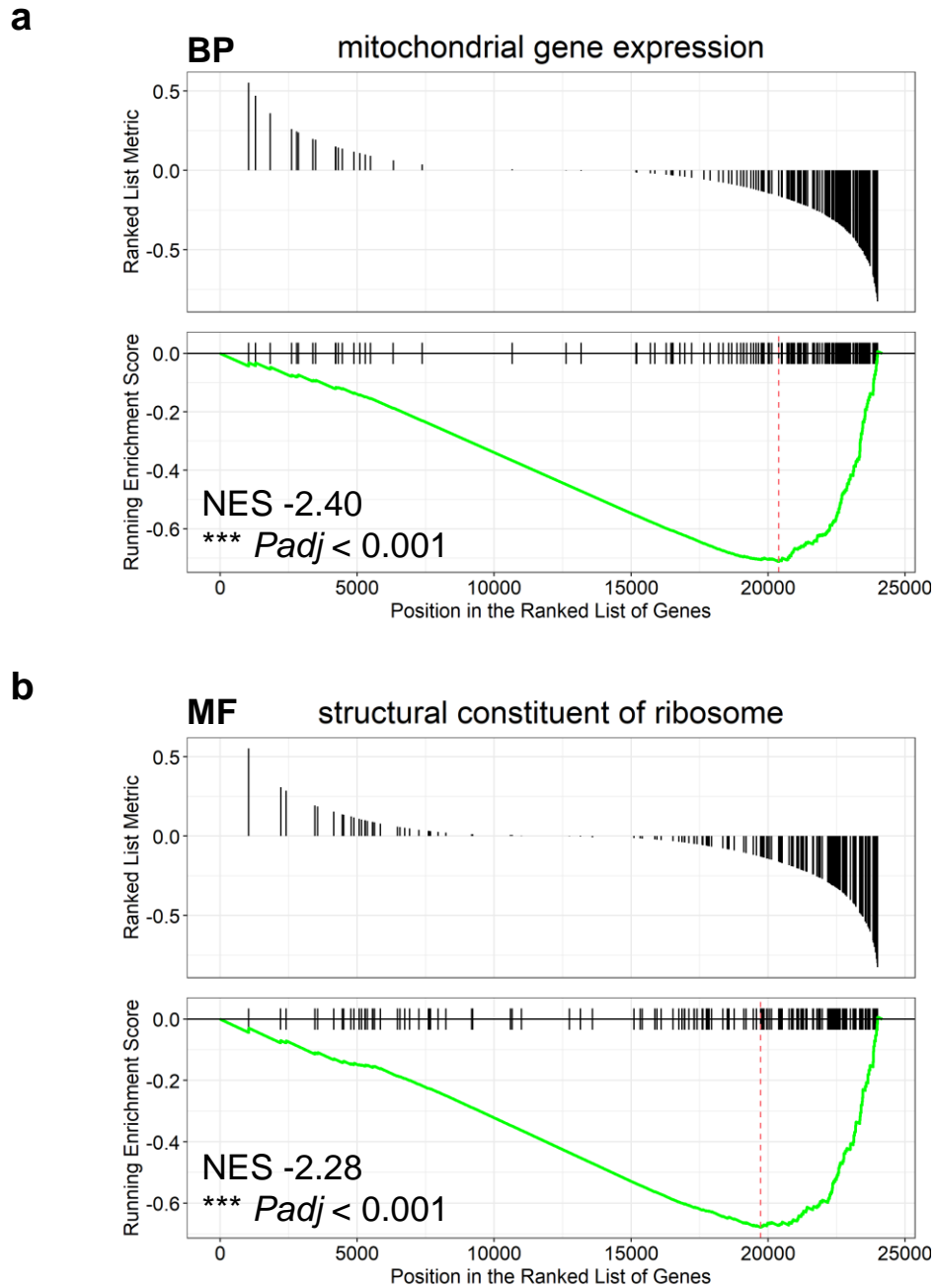


Figure 5.10 Most Enriched GO Terms in Hypoxic vs. Normoxic T-47D Cells. GSEA revealing most enriched (a) BP and (b) MF GO gene sets in ER α + T-47D cells cultured in hypoxia compared to normoxia. Significantly differentially expressed genes were ranked from most positive Log₂FC to most negative Log₂FC for GSEA. *** *p*_{adj} < 0.001.

Table 5.8 Most Enriched BP Terms in T-47D Cells Cultured in Hypoxia vs. Normoxia.

GO terms (Description) ranked according to FDR.

Description	NES	Set Size	Leading Edge Tags (%)
Mitochondrial translation	-2.42	130	71
Response to hypoxia	2.05	279	28
Response to decreased oxygen levels	2.00	296	27
Response to oxygen levels	1.97	321	26
Ribosome biogenesis	-1.98	319	49
Respiratory electron transport chain	-2.26	110	53
Ribonucleoprotein complex biogenesis	-1.75	467	40
ncRNA processing	-1.72	431	48
rRNA processing	-1.95	222	50
Oxidative phosphorylation	-2.07	131	64

Table 5.9 Most Enriched MF Terms in T-47D Cells Cultured in Hypoxia vs. Normoxia.

GO terms (Description) ranked according to FDR.

Description	NES	Set Size	Leading Edge Tags (%)
Glycosaminoglycan binding	2.04	225	23
Heparin binding	2.02	163	23
Signalling receptor regulator activity	1.68	467	15
Receptor ligand activity	1.66	428	15
Oxidoreductase activity	1.85	174	25
Signalling receptor activator activity	1.65	433	15
Sulphur compound binding	1.75	260	20
Carbohydrate binding	1.72	260	22
Cadherin binding	1.66	333	38
Growth factor activity	1.78	143	22

5.2.6 Positive enrichment of Na⁺ transport occurs in Luminal A cell lines cultured in hypoxia

Continuing with GSEA in the RNA-seq data sets, each possible permutation in MCF-7 and T-47D cell lines were studied for perturbations in Na⁺ transport by including a search term of “sodium” in *ClusterProfiler* results. Interrogating MSigDB (available at gsea-msigdb.org) for gene sets that include “sodium” in the gene set name revealed 27 BP and 25 MF gene sets that are involved in Na⁺ handling, including Na⁺ channel clustering, Na⁺ channel function or Na⁺ transport. Directed investigations of GSEA revealed BP or MF gene sets implicated in Na⁺ handling were not significantly enriched in MCF-7 or T-47D cells singularly challenged by ER α knockdown (NV vs. NF, and HV vs. HF). Additionally, Luminal A cells exposed to hypoxia and fulvestrant compared to the normoxic ER α + control (NV vs. HF) did not demonstrate significant alterations in Na⁺ transport. In contrast, culturing ER α + MCF-7 cells in hypoxia (NV vs. HV) significantly upregulated BP “sodium ion transport” (Figure 5.11). T-47D cells under the same experimental test upregulated BPs “sodium ion transmembrane transport” (Figure 5.12a), “sodium ion transport” (Figure 5.12b) and MF “sodium ion transmembrane transporter” (Figure 5.12c). Additionally, in ER α - T-47D cells, but not MCF-7 cells, O₂ deprivation (NF vs. HF) significantly enriched BPs “sodium ion transmembrane transport” (NES: 1.57; *p*_{adj} < 0.01) (Appendix Figure VII a) and “sodium ion transport” (NES: 1.54; *p*_{adj} < 0.01) (Appendix Figure VII b). Therefore, hypoxic culture of Luminal A cell lines in the presence of the ER α , or in T-47D cells that have experienced proteasomal degradation of the hormone receptor significantly enhanced Na⁺ transport. However, ER α was not a significant regulator of Na⁺ handling in the cell lines studied.

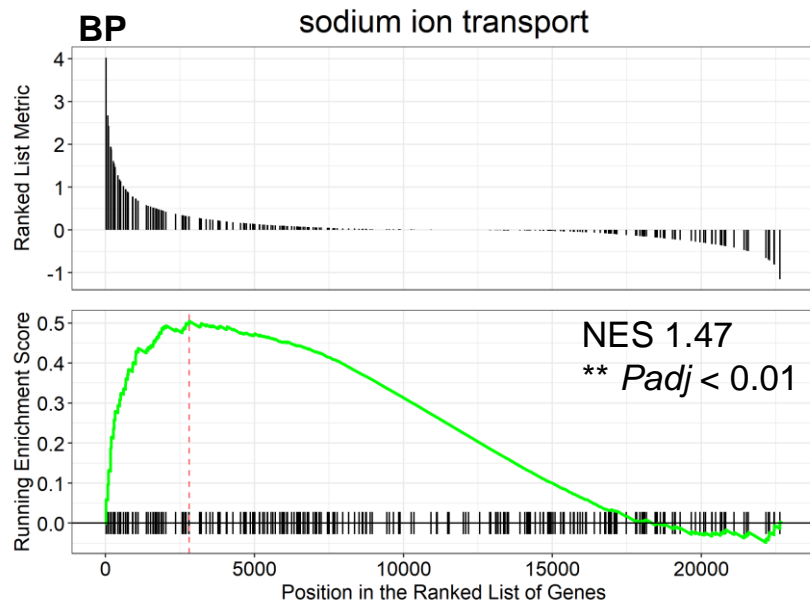
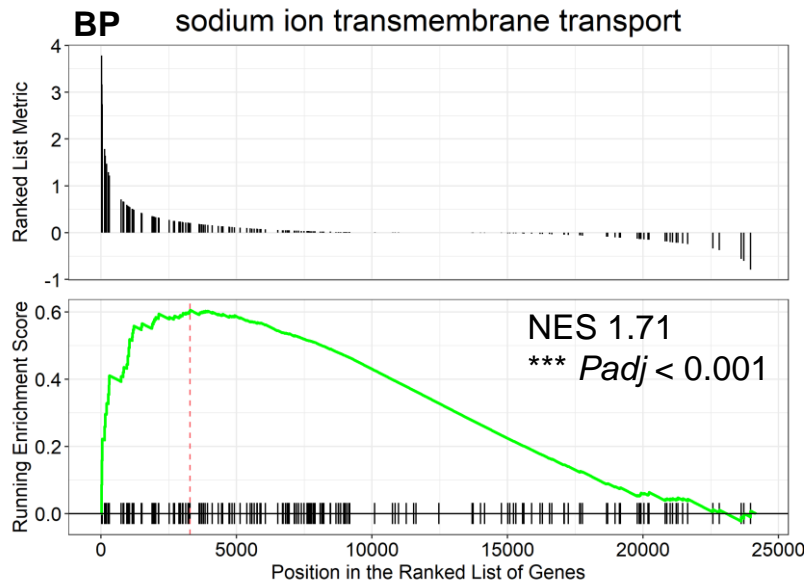
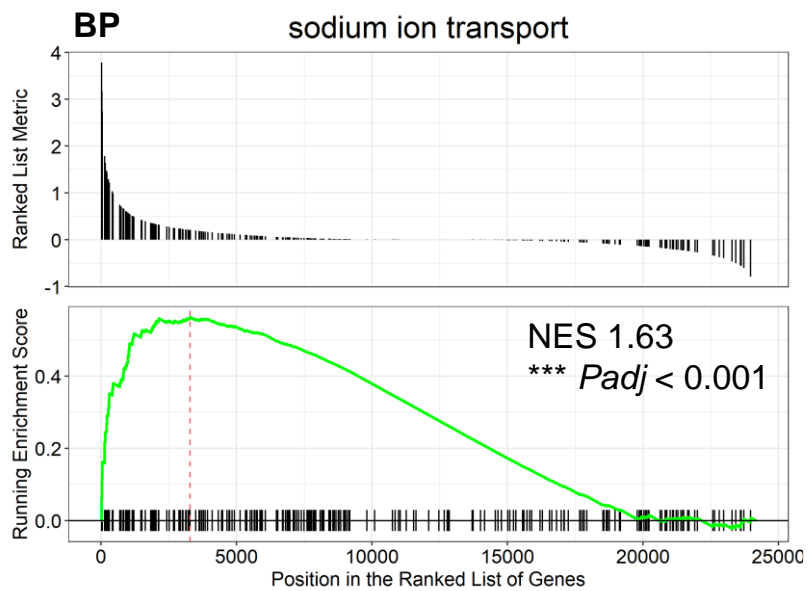


Figure 5.11 GSEA Plot Showing Positive Enrichment of Na⁺ Transporter Genes in Hypoxic vs. Normoxic MCF-7 Cells. Targeted GSEA identified positive enrichment for genes in BP “sodium ion transport” (GO:0006814) in ER α + MCF-7 cells cultured in hypoxia compared to normoxia. Significantly differentially expressed genes were ranked from most positive Log₂FC to most negative Log₂FC for GSEA. ** *padj* < 0.01.

a



b



c

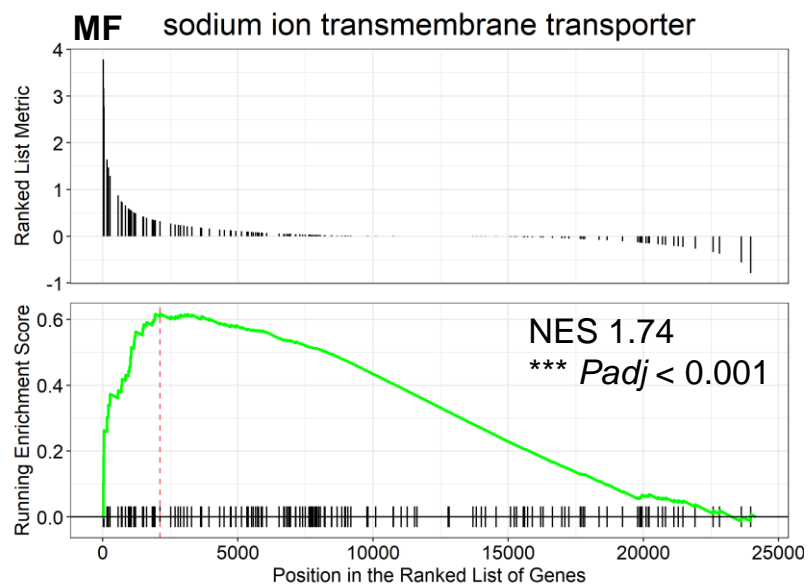


Figure 5.12 GSEA Plot Showing Positive Enrichment of Na⁺ Transporter Genes in Hypoxic vs. Normoxic T-47D Cells. Targeted GSEA identified positive enrichment for genes in **(a)** BPs “sodium ion transmembrane transport” (GO:0035725) and **(b)** “sodium ion transport” (GO:0006814) or **(c)** MF “sodium ion transmembrane transporter” (GO:0015081) in ER α + T-47D cells cultured in hypoxia compared to normoxia. Significantly differentially expressed genes were ranked from most positive Log₂FC to most negative Log₂FC for GSEA. ** *padj* < 0.01.

Next, ion channels that contribute most significantly to the enhanced Na⁺ transport phenotype of hypoxic cell lines was explored in more detail. The “leading edge” of GSEA plots identifies the genes that are most responsible for the NES of a BP or MF (Reimand *et al.*, 2019). Genes present in the leading edge of ER α + normoxic vs. hypoxic Na⁺ transport BPs or MFs were compared against a gene list of 131 Na⁺ channel genes generated from the Human genome organisation gene nomenclature committee (HGNC; available at genenames.org) to distinguish Na⁺ channel genes from “other” genes that affect Na⁺ transport. In total, 173 genes made up the leading edge of all the BP and MF GO terms involved in Na⁺ transport, and 44.51% of these genes were Na⁺ channel genes according to the HGNC Na⁺ channel list (Figure 5.13a). The remaining 55.49% of contributors to the leading edge included growth factor signalling molecules such as *FGF11* and *FGF12*; other types of ion channels including Ca²⁺ transporter *ATP2B4* and Ca²⁺-activated nonselective cation channel *ANO6* or other classes of Na⁺ channel transporters that are not part of the HGNC Na⁺ channel gene list, including the Na⁺/Mg²⁺ exchanger *SLC41A3* or the Na⁺/Pi symporter *SLC20A1*.

Further extrapolating leading edge “HGNC Na⁺ Channel” genes to identify which classes of Na⁺ channels are most strongly associated with hypoxic modulation of Na⁺ transport revealed 15.58% of Na⁺ channel genes enriched in hypoxic Luminal A cell lines belonged to the ENaC family, closely followed by the NKA, the Na⁺-Cl⁻-dependent dopamine transporter DAT1 and NHE1 (Figure 5.13b). Next, overlap between Na⁺ channel genes significantly differentially expressed (*p*_{adj} < 0.05) in hypoxic vs. normoxic MCF-7 and T-47D cells was explored. From DGEA, Luminal A cell lines had a significant overlap of 12 Na⁺ channel genes that were upregulated because of hypoxic challenge (NV vs. HV; Figure 5.13c), and included all major subunits of ENaC, the α and β subunits of the NKA and NHE1. In contrast, of the significantly downregulated Na⁺ channel genes in response to hypoxia, only *NHERF1* and *SLC9A2* (NHE2) was shared between MCF-7 and T-47D cells (Figure 5.13d).

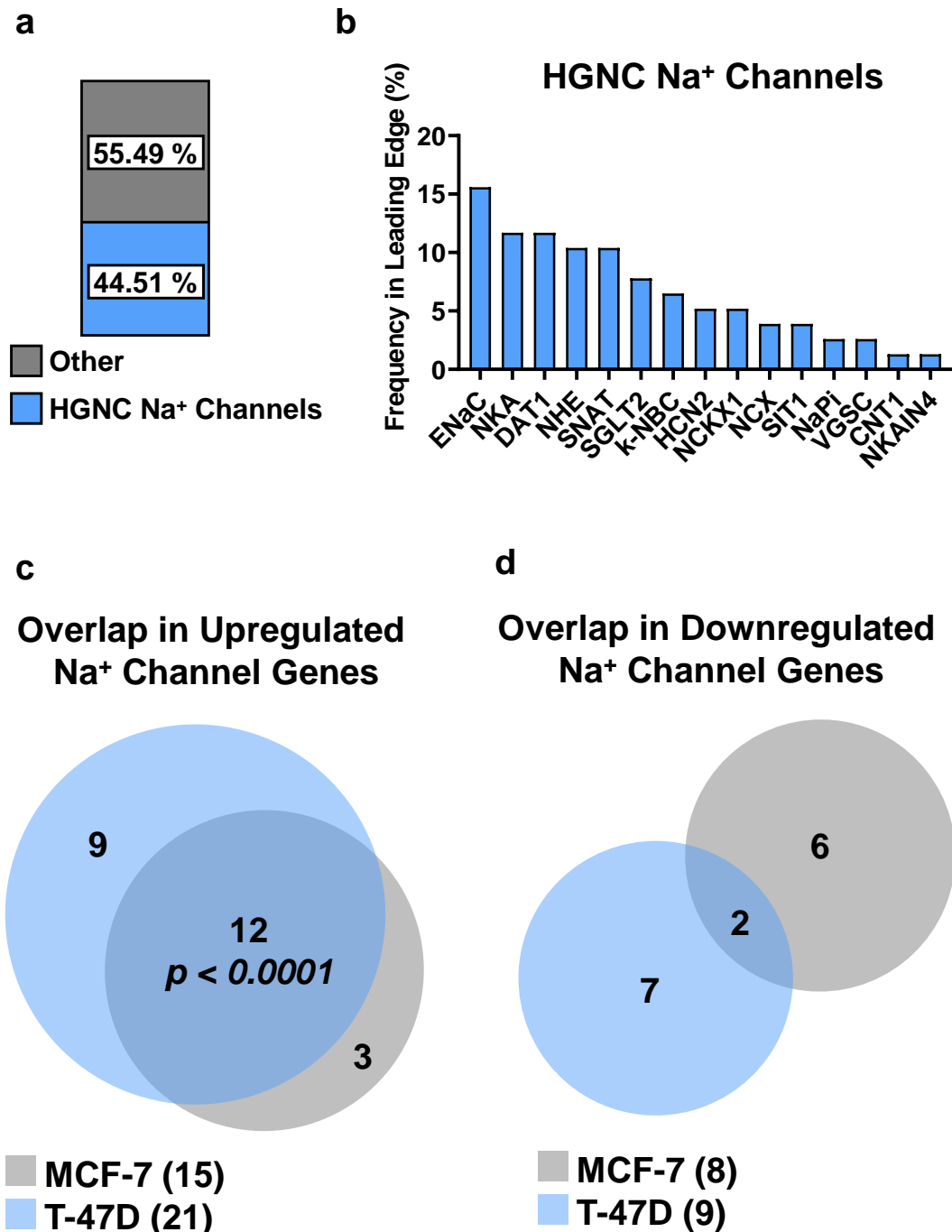


Figure 5.13 Leading Edge and Differentially Expressed Na⁺ Channel Genes in MCF-7 and T-47D Cells Cultured in Hypoxia vs. Normoxia. (a) Stratifying genes in the Leading Edge of Na⁺ transport GO terms as either “HGNC Na⁺ channels” or “other”. (b) Frequency in which a HGNC Na⁺ channel gene appears in the Leading Edge characterised by the Na⁺ channel it encodes. Overlap in significantly differentially expressed Na⁺ channel genes that are (c) upregulated or (d) downregulated in MCF-7 and T-47D cells cultured in hypoxia compared to normoxia. Fisher’s exact test was used to calculate significant overlap in differentially expressed genes. *** $p < 0.001$.

5.2.7 METABRIC analysis reveals significant implications of hypoxia-regulated Na⁺ transporter gene amplification in relapse-free and overall survival

To contextualise major findings of this chapter so far into clinical relevance, gene expression profiles of Na⁺ channel genes differentially regulated in both MCF-7 and T-47D cells cultured in hypoxia were analysed utilising the METABRIC patient cohort of 2,509 primary breast tumours, available at cbioportal.org (Curtis *et al.*, 2012; Dawson *et al.*, 2013; Pereira *et al.*, 2016). Specifically, Na⁺ transporter expression was assessed for the relationship between genomic alteration and overall or relapse-free survival in breast cancer patients. The α subunit of NKA encoded by *ATP1A1* was found to be amplified in 1% of breast cancer patients (n = 26). Amplification of α -NKA was significantly associated with decreased overall survival with a hazard ratio (HR) of 1.59 and FDR < 0.05 (Figure 5.14a). Additionally, α -NKA amplification also increased risk of disease relapse with a HR of 1.70 and FDR < 0.05 (Figure 5.14b). In contrast, the β subunit of NKA encoded by *ATP1B1* was amplified in 21% of breast cancers but had no significant association with relapse-free or overall survival (Table 5.10). Furthermore, genomic alterations in *HCN2* (hyperpolarization-activated cyclic nucleotide gated channel), *SLC28A1* (nucleoside transporter), *SLC6A3* (dopamine transporter), *SLC6A8* (Na⁺-dependent creatine transporter), *IST1* (ESCRT-interacting cargo transport protein) and *SLC9A2* (NHE2) had no relationship with relapse-free or overall survival (Table 5.10).

Interestingly, visualising the OncoPrint revealed genomic alteration in *SCNN1A* (α -ENaC) appeared to be mutually exclusive to alterations in *SCNN1B* (β -ENaC) and *SCNN1G* (γ -ENaC) which were often amplified together in the same patient (Figure 5.14c). α -NKA was also amplified predominantly in breast tumours that did not have an alteration in ENaC subunits (Figure 5.14c). Amplification (or deep deletion) of α -ENaC was not associated with survival metrics (Table 5.10). In contrast, amplification of β -ENaC was associated with improved median relapse-free survival (+ 58.2 months; FDR < 0.05), and amplification of γ -ENaC was associated with improved median relapse-free survival (+ 58.2 months, FDR < 0.05) and improved median overall survival (+ 37.9 months; FDR < 0.05) (Table 5.10, Table 5.11). Investigating NHE dynamics revealed that deep deletion of *SLC9A1* (NHE1) significantly decreased median overall survival (- 130.5 months, FDR < 0.05) and median relapse-free survival (- 214.9 months, FDR < 0.01) for breast cancer patients, but perturbations in *SLC9A2* (NHE2) were not associated with

either survival metric (Table 5.10, Table 5.11). Additionally, amplification of NHE regulatory factor *NHERF1* was correlated to decreased median overall survival (- 53.3 months, FDR < 0.05) and relapse-free survival (- 158.6 months, FDR < 0.001). Finally, amplification of Na⁺-coupled amino acid transporter *SLC38A2* was significantly associated with decreased median overall survival (- 68.2 months, FDR < 0.05) and median relapse-free survival (- 157.8 months. FDR < 0.01) in breast cancer patients (Table 5.10, Table 5.11).

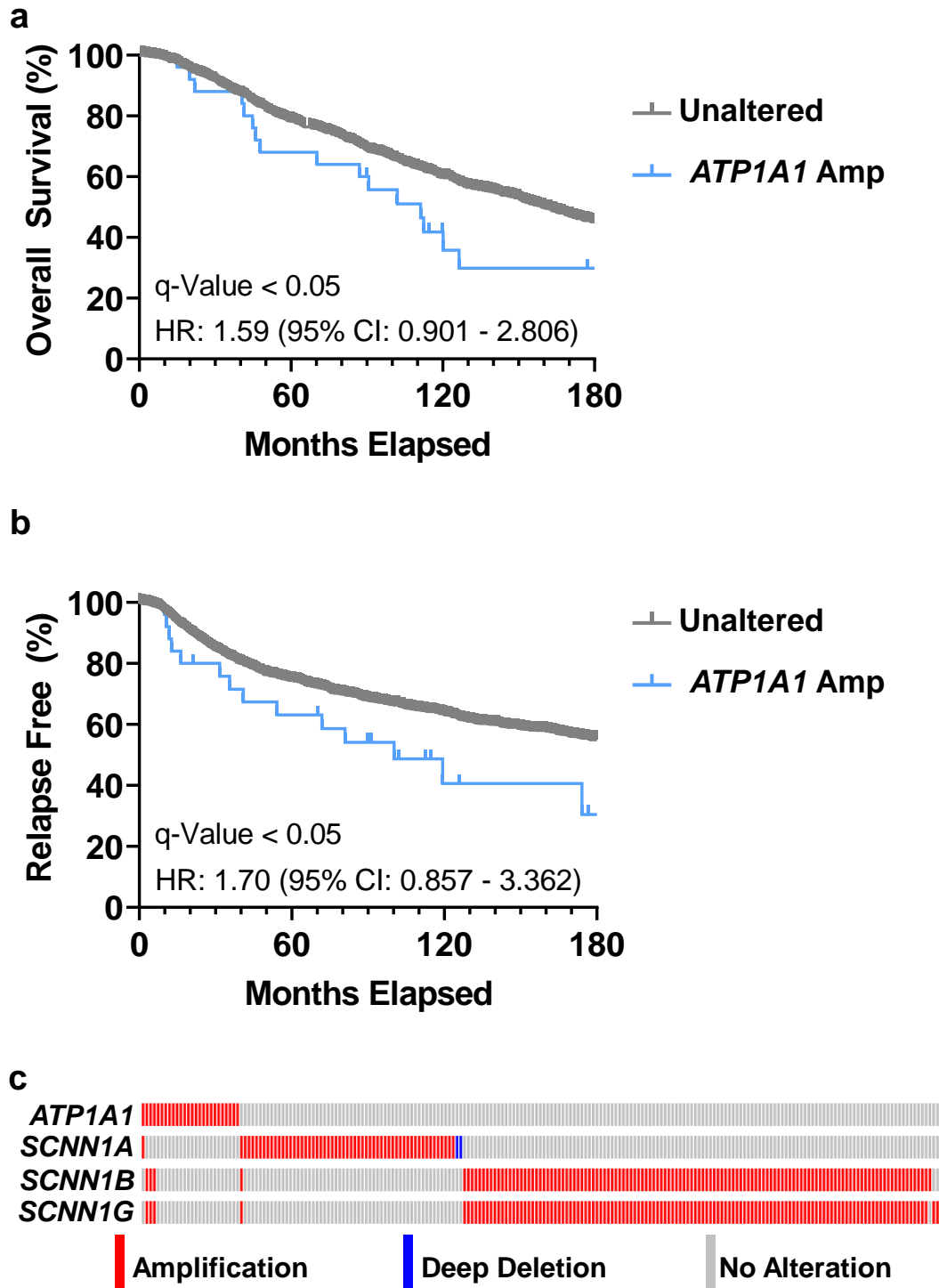


Figure 5.14 Overall and Relapse Free Survival Associated with Amplified *ATP1A1* in Breast Cancer Patients (a METABRIC Analysis). Relationship between amplification of *ATP1A1* (α -NKA) in breast cancer patients and (a) overall survival or (b) relapse free survival from the METABRIC cohort of breast cancer patients available on cBioPortal. *P* value adjusted for FDR (q-Value) < 0.05. (c) Truncated OncoPrint of *ATP1A1*, *SCNN1A* (α -ENaC), *SCNN1B* (β -ENaC) and *SCNN1G* (γ -ENaC) in METABRIC primary tumours showing mutual exclusivity in genome alterations (created with cBioPortal).

Table 5.10 Overall and Relapse-Free Survival in the METABRIC Cohort with Alterations in Na⁺ Transporter Gene Expression. Na⁺ Transporter genes that were upregulated (Up) or downregulated (Down) in both MCF-7 and T-47D cells after chronic (48 hours) hypoxic challenge were studied for the relationship between gene expression alteration and overall survival (OS) or relapse free survival (RFS) using METABRIC breast cancer patient cohort. Alteration types identified were amplification (Amp) or deep deletions (D Del). Where both types of alterations were observed, the major alteration is in **bold**. *P* values corrected for FDR (*q*) are shown. * *q* < 0.05, ** *q* < 0.01 and ****q* < 0.001.

Gene (Up)	Occurrence n / (%)	Alteration type	OS (<i>q</i>)	RFS (<i>q</i>)
<i>ATP1B1</i>	440 / (21)	Amp	0.636	0.643
<i>HCN2</i>	11 / (< 1)	Amp D Del	0.672	0.672
<i>SCNN1A</i>	60 / (3)	Amp D Del	0.794	0.794
<i>SCNN1B</i>	128 / (6)	Amp	0.0641	* 0.0329
<i>SCNN1G</i>	129 / (6)	Amp	* 0.0402	* 0.0150
<i>SLC28A1</i>	26 / (1)	Amp	0.360	0.360
<i>SLC38A2</i>	20 / (< 1)	Amp D Del	* 0.0106	** 0.0020
<i>SLC6A3</i>	88 / (4)	Amp	0.429	0.429
<i>SLC6A8</i>	34 / (2)	Amp D Del	0.572	0.572
<i>SLC9A1</i>	4 / (< 1)	D Del	* 0.0127	** 0.0011
<i>IST1</i>	12 / (< 1)	Amp D Del	0.654	0.654
Gene (Down)	Occurrence n / (%)	Alteration type	OS (<i>q</i>)	RFS (<i>q</i>)
<i>NHERF1</i>	124 / (6)	Amp	* 0.0174	*** < 0.001
<i>SLC9A2</i>	13 / (< 1)	Amp D Del	0.722	0.488

Table 5.11 Median Overall and Relapse-Free Survival in the METABRIC Cohort.

Na⁺ transporter genes that significantly affect patient overall survival (OS) or relapse free survival (RFS), and corresponding difference (Δ) in median OS or median RFS in months, relative to patients with tumours that did not possess the genomic alterations (unaltered).

Gene	Unaltered Median OS	Altered Median OS	ΔOS	Unaltered Median RFS	Altered Median RFS	ΔRFS
<i>SCNN1B</i>	151.2	189.1	+ 37.9	218.7	276.9	+ 58.2
<i>SCNN1G</i>	151.2	189.1	+ 37.9	218.7	276.9	+ 58.2
<i>SLC38A2</i>	153.9	85.7	- 68.2	229.3	71.5	- 157.8
<i>SLC9A1</i>	153.9	23.4	- 130.5	229.3	14.4	- 214.9
<i>NHERF1</i>	157.8	104.5	- 53.3	252.3	93.7	- 158.6

To summarise, expression of Na⁺ transporter genes were significantly altered as a consequence of hypoxia in MCF-7 and T-47D cell lines. Subunits of ENaC and NKA were mostly involved in the increased Na⁺ transport phenotype of hypoxic Luminal A cells owing to significant induction of these genes following O₂ deprivation. Consequently, selective amplification in the expression of *ATP1A1* but not *ATP1B1*, or *SCNN1B* and *SCNN1G* but not *SCNN1A*, was significantly associated with disease burden in breast cancer patients when relapse-free or overall survival metrics are considered. Taken together, the findings discussed in Section 5.2.7 implicated dysregulated Na⁺ transport through several Na⁺ channels in breast cancer progression, potentially in an O₂-dependent manner.

5.2.8 Hypoxia does not significantly affect *ATP1A1* expression when measured by RT-qPCR

Because α -NKA amplification is associated with adverse survival outcomes for patients with breast cancer, and mRNA of this subunit was amplified in response to chronic hypoxia, this channel was explored further in MCF-7 and T-47D cells cultured under an acute or chronic hypoxic time course to investigate which HIF- α isoform may regulate *ATP1A1* transcription. However, RT-qPCR found no significant alteration in *ATP1A1* expression in MCF-7 (Figure 5.15a) or T-47D cells (Figure 5.15b) following either an acute or chronic hypoxic time course. Looking at the DGEA in more detail revealed a small but highly significant ($p_{adj} < 0.0001$) Log₂FC of 0.37 and 0.50 in MCF-7 and T-47D cells, respectively. Different approaches were used to normalise gene expression and perform statistical testing in RNA-seq and RT-qPCR experiments, which could explain the variance in results between the two methods. Furthermore, the small differences in *ATP1A1* expression identified by RNA-seq may not be sufficiently strong enough to identify the same changes when tested using RT-qPCR.

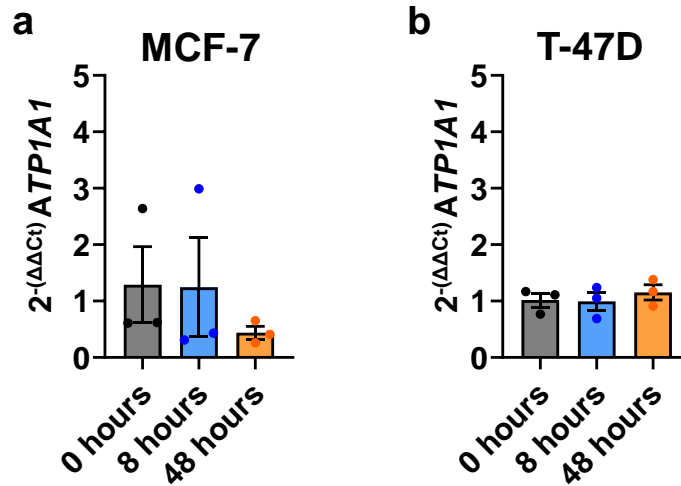


Figure 5.15 RT-qPCR of *ATP1A1* in MCF-7 and T-47D Breast Cancer Cells Following Acute or Chronic Hypoxic Culture. RT-qPCR of *ATP1A1* in (a) MCF-7 and (b) T-47D breast cancer cells. Cell lines were cultured in normoxia (~20% O₂, “0 hours”), acute hypoxia (1% O₂, 8 hours) or chronic hypoxia (1% O₂, 48 hours). Changes in *ATP1A1* expression were determined by the $2^{-\Delta\Delta C_t}$ method, using the geometric mean of RGs *RPLP1* and *RPL27* for normalisation. One-way ANOVA with Dunnett’s multiple comparisons revealed no significant changes in expression. Error bars are \pm SEM. N = 3.

5.2.9 Ouabain inhibition of NKA does not affect normoxic or hypoxic breast cancer cell migration

Since amplification of NKA α subunit *ATP1A1* had significant prognostic effects in breast cancer patients, and expression of NKA has been implicated in cancer cell proliferation, motility and invasion in normoxic breast cancer cells (Khajah *et al.*, 2018), it was expected that NKA activity in hypoxic breast cancer cell lines would further increase migratory capacity, and inhibition of NKA by ouabain would impede motility of hypoxic Luminal A cell lines. Therefore, the migratory index (MI) of MCF-7 and T-47D cells was measured following normoxic vs. hypoxic culture, in addition to treatment with 100 nM ouabain or corresponding vehicle control. Following a 24-hour time course post-wound, neither MCF-7 (Figure 5.16a) or T-47D cells (Figure 5.16b) saw a significant reduction in MI following singular challenge of ouabain or hypoxia, or when cells were cultured in hypoxia and with ouabain. After 48 hours, MCF-7 cells cultured in hypoxia saw a significant reduction in MI compared to normoxic cells (Figure 5.16c). Additionally, hypoxia alone, or in combination with ouabain significantly reduced MI when compared to normoxic ouabain-treated cells. However, no significant change in MI was observed between vehicle and ouabain treated cells cultured in normoxia, or vehicle and ouabain treated cells cultured in hypoxia. Furthermore, 48-hours post wound in T-47D cells, a significant reduction was only observed between normoxic vehicle treated cells, and hypoxic vehicle or hypoxic ouabain treated cells (Figure 5.16d). Therefore, hypoxia significantly inhibited the migratory capacity of MCF-7 and T-47D cells, whereas blocking of the NKA with ouabain had no additional inhibitory affect.

The lack of significant reduction in MI of ouabain-treated cells could be attributed to the concentration of ouabain used. Previous research has demonstrated 100 nM ouabain is sufficient to inhibit cell proliferation of breast cancer cells, and inhibit NKA-dependent Na⁺ efflux (Kometiani *et al.*, 2005; Shandell *et al.*, 2022). In contrast, 1 μ M – 10 μ M ouabain has been shown to significantly inhibit breast cancer cell migration, although a prolonged 48-hour time course also significantly increased apoptosis relative to vehicle treated cells (Khajah *et al.*, 2018). Thus, 100 nM ouabain was chosen as the final concentration, as a compromise between eliciting significant inhibition of NKA and impairing cell function, without jeopardising cell survival.

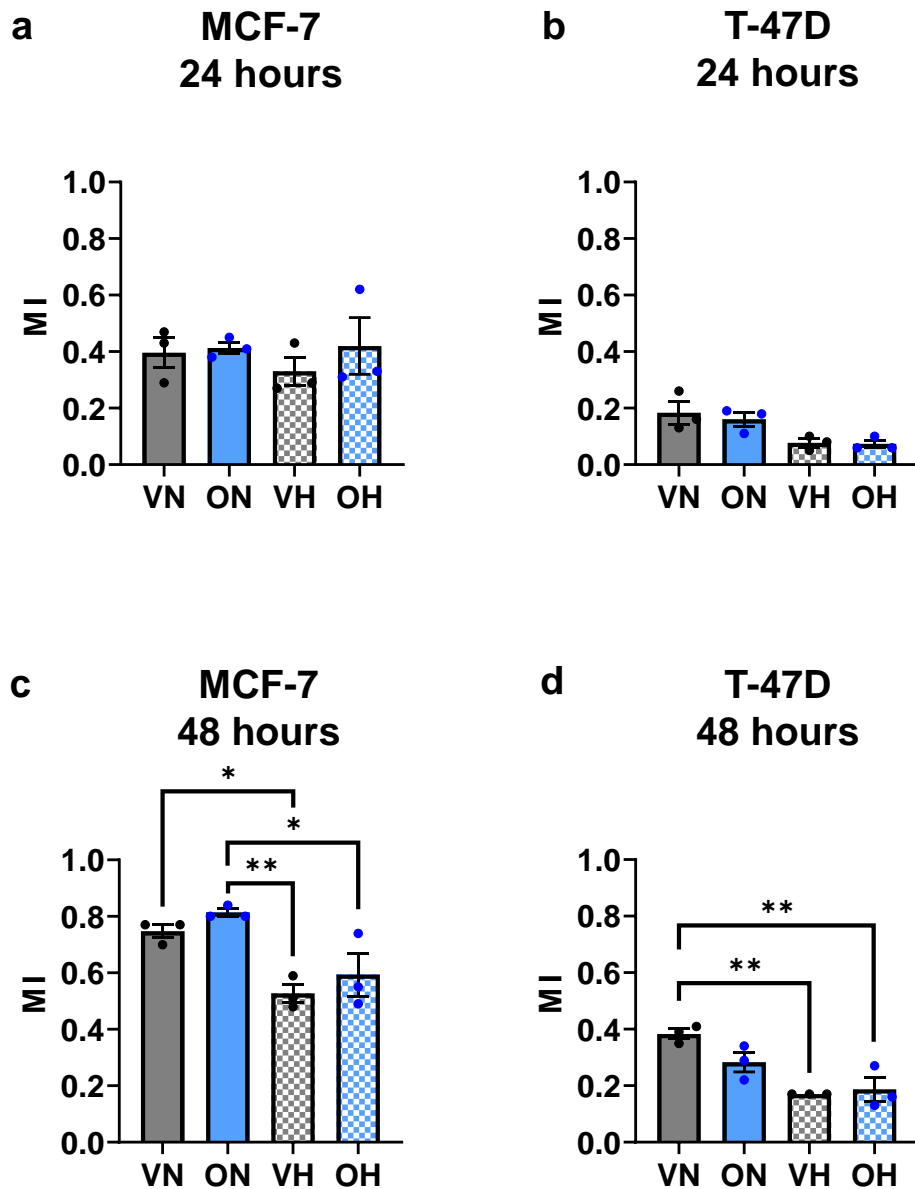


Figure 5.16 Investigating NKA Inhibition on the Migratory Capacity of Normoxic or Hypoxic Breast Cancer Cells. The Migratory Index (MI) was calculated following Ouabain and / or hypoxia culture in (a) MCF-7 or (b) T-47D cells 24 hours post-wound, or (c) MCF-7 or (d) T-47D cells 48 hours post-wound. 100 nM Ouabain (O) or vehicle (V) was applied and / or normoxic (N) or hypoxic (H; 1% O₂) culture was implemented immediately following wound generation and initial (t₀) wound measurement. After 24 or 48 hours, wounds were remeasured (t₁). One-way ANOVA with Tukey's multiple comparisons was performed. * $p < 0.05$, ** $p < 0.01$ and *** $p < 0.001$. Error bars are \pm SEM. N = 3.

5.2.10 Ion transporter genes are significantly affected by O₂ and ER α perturbations in Luminal A cell lines

Following on from the findings of hypoxia and fulvestrant-dependent effects on Na⁺ channel gene expression, the analysis was expanded further to more broadly include ion channel gene expression alterations in MCF-7 and T-47D cells in all RNA-seq permutations described in Section 5.2.2. An ion channel list was generated from HGNC that contained 330 ion channel genes, including Na⁺ channels, Ca²⁺ channels, K⁺ channels, Cl⁻ channels, porins and gap junction proteins (available at genenames.org). DGEA was performed using *DESeq2* and the ion channel list was used to identify significantly differentially expressed ion channel genes (*p*_{adj} < 0.05) in response to hypoxia and/or ER α knockdown. Ion channels that displayed significant alterations in expression in both MCF-7 and T-47D cells, across all RNA-seq comparisons were identified. Out of the 330 ion channels available, only nine ion channels were differentially expressed in both Luminal A cell lines, and in all combinations of analysis (Table 5.12).

ATP1A1 was among the nine shared significantly differentially expressed ion channel genes, with the greatest fold change in expression in normoxia and vehicle vs. hypoxia and fulvestrant comparison (NV vs. HF) of T-47D cells, whereas a moderate induction was seen in MCF-7 cells. However, largest alterations in expression of *AQP3* (aquaporin), *GJA1* (gap junction), *SFXN2* (sideroflexin) and *SLC29A4* (monoamine transporter) occurred in NV vs. HF MCF-7s. Changes occurring in NV vs. HF are of great interest, as this comparison could recapitulate Luminal A disease progression where endocrine resistance and hypoxic signatures are developing in the breast tumour (Jehanno *et al.*, 2022).

NHERF1 and the mitochondrial amino acid transporter *SFXN2* were both significantly downregulated in MCF-7 and T-47D cells, because of O₂ deprivation, fulvestrant treatment, or a combination of experimental challenges (Table 5.12). It is interesting that many genes regulated in one direction in MCF-7 cells had an opposite regulation in T-47Ds, especially where fulvestrant-mediated ER α knockdown was the only test. For example, in normoxic MCF-7 cells, fulvestrant led to upregulated *GJA1*, mitochondrial serine transporter *SFXN3* and NHE *SLC9A4*, and downregulated *ATP1A1*, compared to vehicle. T-47D cells had the opposite differential expression of the same genes. Similarly, in hypoxic MCF-7 cells,

fulvestrant treatment led to upregulated *GJA1* and *SLC9A4*, and downregulated *ATP1A1*, relative to vehicle, and these genes were downregulated in T-47D cells. Such a striking observation could be explained by the differential ER α transcriptome in the two Luminal A cell lines, and highlights the importance of selecting the most appropriate cell model, or utilising more than one cell line to observe differences in biological responses to a condition (Yu *et al.*, 2017). The remaining two genes which were significantly differentially expressed were anoctamin 7 (*ANO7*) and monocarboxylic acid transporter 4 (MCT4; *SLC16A3*), which displayed the same regulatory patterns as each other.

Table 5.12 Log₂FC in Shared Differentially Expressed Ion Transporter Genes. Log₂FC of ion channel genes that are significantly (*p*_{adj} < 0.05) differentially regulated in MCF-7 (M) and T-47D (T) cell lines, in all RNA-Seq permutations available in this chapter: normoxia and vehicle vs. hypoxia and vehicle (NV vs. HV), normoxia and vehicle vs. normoxia and fulvestrant (NV vs. NF), normoxia and vehicle vs. hypoxia and fulvestrant (NV vs. HF), normoxia and fulvestrant vs. hypoxia and fulvestrant (NF vs. HF), normoxia and fulvestrant vs. hypoxia and vehicle (NF vs. HV) and hypoxia and vehicle vs. hypoxia and fulvestrant (HV vs. HF). Significantly upregulated genes are shown by light orange to dark orange colour arrangement. Significantly downregulated genes are shown by light blue to dark blue colour arrangement.

Gene	NV vs. HV		NV vs. NF		NV vs. HF		NF vs. HV		NF vs. HF		HV vs. HF	
	M	T	M	T	M	T	M	T	M	T	M	T
<i>ANO7</i>	0.59	1.47	-3.49	-0.74	-2.22	0.75	-4.14	-2.42	1.17	1.67	-2.87	-0.56
<i>AQP3</i>	1.57	1.03	2.67	2.97	3.51	2.05	1.08	1.81	0.83	-0.82	1.93	0.87
<i>GJA1</i>	2.95	0.75	1.73	-3.45	4.40	-1.73	-1.03	-4.49	2.49	1.50	1.31	-2.78
<i>SFXN2</i>	-1.70	-1.03	-4.40	-1.91	-5.00	-2.24	-2.68	-0.87	-0.54	-0.31	-3.28	-1.20
<i>SFXN3</i>	1.82	0.74	0.44	-0.43	1.22	0.43	-1.36	-1.19	0.75	0.87	-0.58	-0.30
<i>SLC29A4</i>	1.57	1.25	1.89	-1.15	2.54	0.47	0.31	-2.43	0.62	1.64	0.95	-0.76
<i>SLC16A3</i>	0.51	2.42	-1.16	-2.47	-0.61	1.00	-1.71	-4.91	0.50	3.49	-1.15	-1.41
<i>ATP1A1</i>	0.37	0.50	-0.26	0.86	0.20	1.31	-0.63	0.35	0.45	0.45	-0.18	0.81
<i>NHERF1</i>	-0.27	-0.15	-1.13	-0.39	-1.45	-0.69	-0.85	-0.23	-0.30	-0.29	-1.16	-0.52

Next, RT-qPCR was performed to explore a potential HIF-dependent regulation of four shared ion channel genes in hypoxic breast cancer cell lines. MCF-7 cells were cultured under normoxia, or under hypoxia for 8 or 48 hours, and fold change in expression of *SFXN2*, *SFXN3*, *SLC16A2* and *NHERF1* was calculated. Based on the RNA-seq findings, expression of *SFXN2* and *NHERF1* should be significantly downregulated because of chronic (48 hours) hypoxia, whereas expression of *SFXN3* and *SLC16A3* should be induced. RT-qPCR revealed a downward trend in *SFXN2* expression (Figure 5.17a), upregulation of *SFXN3* (Figure 5.17b), and a moderate decrease in *SLC16A2* (Figure 5.17c) and *NHERF1* (Figure 5.17d). Despite clear trends in hypoxia-mediated gene expression, most of which agreed with the RNA-seq expression patterns, none of the RT-qPCR results from MCF-7 lysates were significant (One-way ANOVA with Dunnett's multiple comparisons). A possible reason for this is the large variation seen across samples which may be improved by including additional biological replicates.

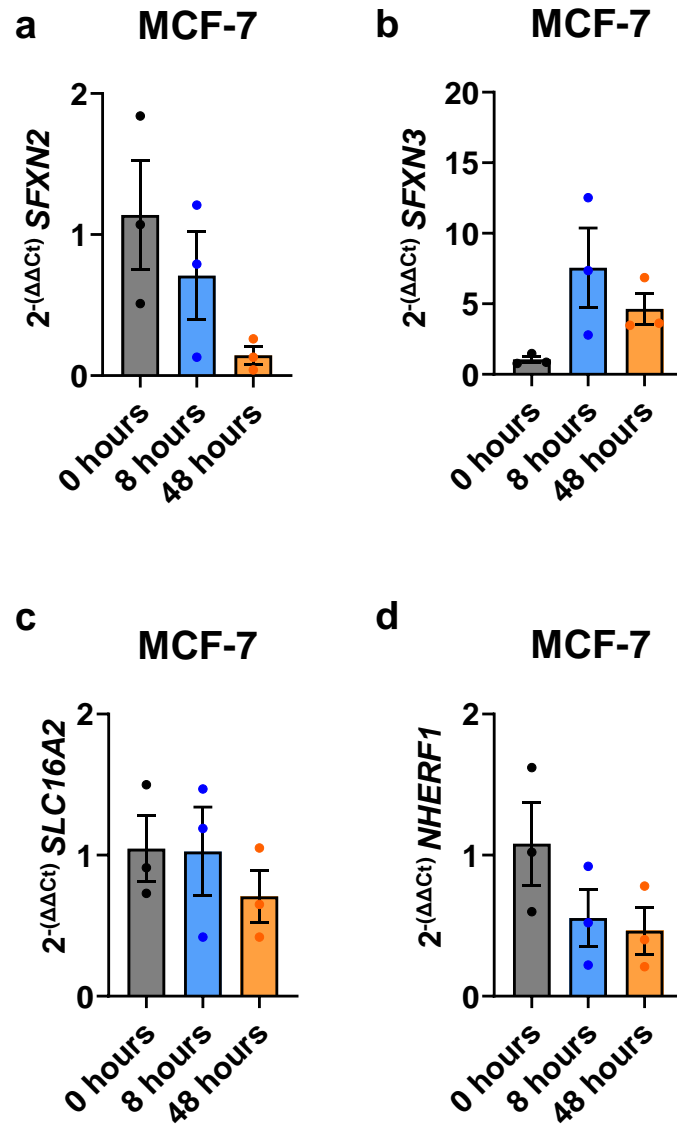


Figure 5.17 RT-qPCR of Ion Transporters Differentially Expressed in All RNA-Seq Comparisons in MCF-7 Cells RT-qPCR of (a) *SFXN2*, (b) *SFXN3*, (c) *SLC16A2* and (d) *NHERF1* in MCF-7 breast cancer cells. Cell lines were cultured in normoxia (~20% O₂, “0 hours”), acute hypoxia (1% O₂, 8 hours) or chronic hypoxia (1% O₂, 48 hours). Changes in ion transporter gene expression was determined by the 2^{-ΔΔCt} method, using the geometric mean of RGs *RPLP1* and *RPL27* for normalisation. One-way ANOVA with Dunnett’s multiple comparisons revealed no significant changes in expression. Error bars are ± SEM. N = 3.

When T-47D cells were studied for changes in the same panel of ion channel genes, *SFXN2* was significantly downregulated after 48 hours, but not 8 hours of hypoxic culture (Figure 5.18a). In contrast, positive induction of *SFXN3* (Figure 5.18b) and *SLC16A2* (Figure 5.18c) following an acute and chronic hypoxic time course was observed. The rapid induction of *SFXN3* and *SLC16A2* observed in T-47D cells implicates HIF-1 α as the transcriptional regulator of these genes. Conversely, no significant change in *NHERF1* was seen as a consequence of hypoxia in T-47D lysate (Figure 5.18d). The RT-qPCR findings are largely in agreement with the RNA-seq findings. Where *NHERF1* is concerned, a very small Log₂FC was seen in T-47D cells following 48 hours of hypoxic challenge (Log₂FC - 0.15; *padj* < 0.5), which could explain the variance between RT-qPCR and RNA-seq results.

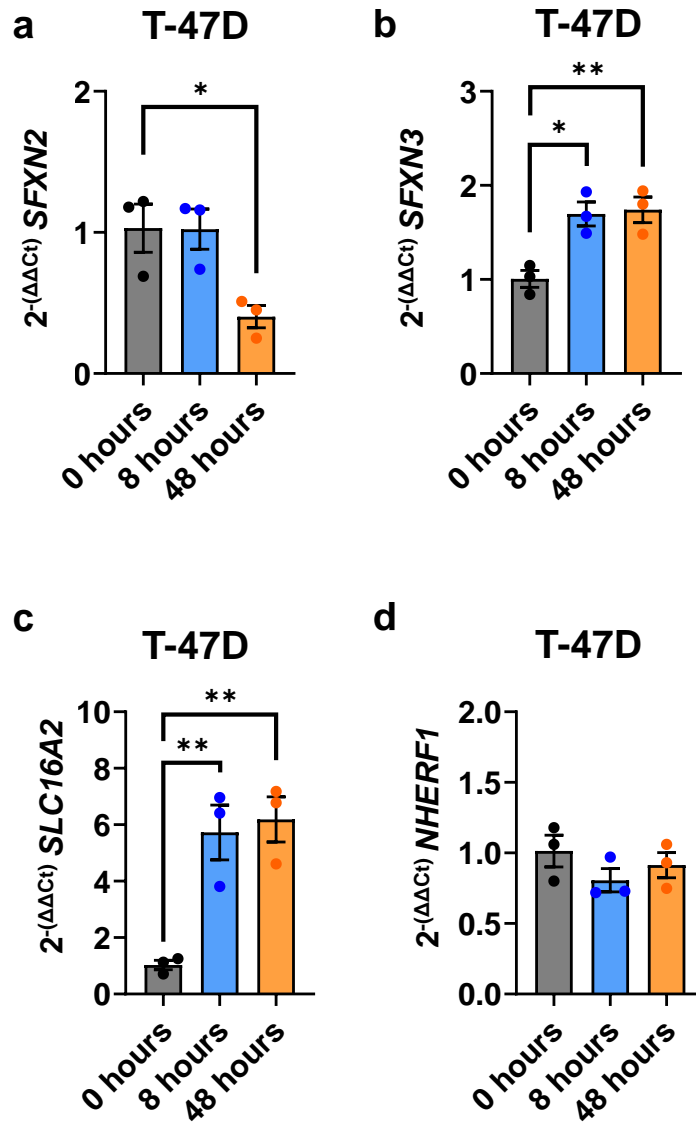


Figure 5.18 RT-qPCR of Ion Transporters Differentially Expressed in All RNA-Seq Comparisons in T-47D Cells. RT-qPCR of (a) *SFXN2*, (b) *SFXN3*, (c) *SLC16A2* and (d) *NHERF1* in T-47D breast cancer cells. Cell lines were cultured in normoxia (~20% O₂, “0 hours”), acute hypoxia (1% O₂, 8 hours) or chronic hypoxia (1% O₂, 48 hours). Changes in ion transporter gene expression was determined by the 2^{-ΔΔCt} method, using the geometric mean of RGs *RPLP1* and *RPL27* for normalisation. One-way ANOVA with Dunnett’s multiple comparisons was performed. * *p* < 0.05 and ** *p* < 0.01. Error bars are ± SEM. N = 3.

5.3 Discussion

Investigations carried out in this chapter were set up to explore potential mechanisms of dysregulated Na⁺ homeostasis in breast cancer by identifying major Na⁺ channel genes most perturbed by O₂ deprivation and/or fulvestrant-mediated ER α knockdown. A primary aim was to understand if hypoxia positively induces expression of, or if ER α negatively regulates expression of key VGSC subunits most implicated in breast cancer progression, particularly nNa_v1.5 which is strongly associated with metastatic TNBC. A secondary aim was to explore the role of hypoxia and ER α in regulating ion homeostasis through a broader range of Na⁺ and other ion channels. RNA-seq was predominantly utilised in this chapter, as it enables highly sensitive investigations of gene alterations on a genome-wide scale. Wet lab experiments included RT-qPCR to test the reproducibility of RNA-seq findings, as well as a wound healing assay to determine potential therapeutic benefit of inhibiting hypoxia-induced NKA activity in breast cancer metastasis.

5.3.1 Summary of main findings

- Widespread transcriptional changes were elicited following chronic hypoxic culture and/or ER α knockdown with fulvestrant in MCF-7 and T-47D cells.
- Acute or chronic hypoxia did not significantly affect expression of α or β VGSC subunits in Luminal A cell lines.
- ER α positively regulated expression of *SCN8A* and *SCN1B* in T-47D cells, whereas ER α attenuated expression of *SCN1A* in T-47D and *SCN1B* in MCF-7 cells.
- Hypoxia and fulvestrant shut down major biosynthetic processes in both MCF-7 and T-47D cells.
- Elevated Na⁺ transport was a feature of a hypoxic signature, whereas ER α did not play a significant part in dysregulated Na⁺ homeostasis in ER α + cell lines.
- Major contributors to enhanced Na⁺ transport in MCF-7 and T-47D cells were hypoxic-induced NKA, ENaC and NHE1 subunits.
- Amplification of *ATP1A1*, *SCNN1B* or *SCNN1G* were significantly associated with disease outcomes for patients with breast cancer.
- 100 nM ouabain was not sufficient to significantly impair Luminal A cell line migration in normoxia or in hypoxia.

5.3.2 Differential regulation of VGSC subunits in two models of Luminal A breast cancer

Neither an acute nor chronic hypoxic time course was able to induce transcription of *nSCN5A*, *SCN8A* or *SCN9A* in MCF-7, T-47D, MDA-MB-231 or MDA-MB-468 breast cancer cell lines, as determined by RT-qPCR. Only MDA-MB-231 cells exhibited detectable levels of *SCN5A* and *SCN9A*, whereas the second model of TNBC and the two Luminal A cell lines had no detectable levels of VGSC transcript. One possible explanation for the difference in VGSC expression observed between two TNBC cell lines could be attributed to differential FOXC1 binding in MDA-MB-231 and MDA-MB-468 cells. Pioneer factor binding has been shown to have small overlap with H3K27ac peaks, which is indicative of active chromatin in the basal-like MDA-MB-468s, whereas a large proportion of FOXC1 binding events in mesenchymal stem-like MDA-MB-231s are associated with an active chromatin signal (Espinosa Fernandez *et al.*, 2020; Ramachandran *et al.*, 2024). An unbiased RNA-seq approach of MCF-7 and T-47D cells cultured in chronic hypoxia did not show significant induction of any VGSC α subunit (*SCN1A* – *SCN11A*) or β subunit (*SCN1B* – *SCN4B*). Therefore, transcription of VGSCs in cell lines studied is not significantly affected by O₂ deprivation. The finding that VGSC expression is unperturbed by hypoxia was unexpected, as a link between O₂ deficiency and mechanisms known to enhance VGSC expression have been reported, including a synergistic role between hypoxia and increased growth factor signalling, and impaired SIK1 activity. (Mallikarjuna *et al.*, 2019; Mamo *et al.*, 2020; Pu *et al.*, 2022). Therefore, additional factors are mediating a hypoxia - growth factor / SIK1 - VGSC regulatory network that need to be explored in greater detail. However, control of VGSC expression in an O₂-dependent manner was not investigated further in this chapter. Instead, functional involvement of the ER α in repression of VGSC expression was studied.

The ER α is estimated to repress expression of between 35 – 50 % of canonical target genes, in a time-dependent manner post-oestradiol stimulation (Carroll *et al.*, 2006). Additionally, a significant negative correlation has recently been reported between ER α status of primary breast tumours and protein levels of Nav1.5 (Leslie *et al.*, 2024). Therefore, VGSC expression in ER α + cell lines were expected to be negatively regulated by ER α activity. RNA-seq analysis of fulvestrant treated MCF-7 and T-47D cells revealed differential expression of some VGSC

subunits in response to ER α knockdown, in a cell type dependent manner. Of the VGSC α subunits, *SCN1A* was significantly upregulated, and *SCN8A* was significantly downregulated following proteasomal degradation of the steroid receptor in T-47D cells, whereas no such differential expression was observed in MCF-7 cells. Additionally, ER α knockdown significantly reduced expression of β 1 subunit *SCN1B* in T-47D cells, whereas transcript levels of this gene were significantly amplified in MCF-7 cells in the same condition. Fulvestrant-dependent differential expression patterns of VGSC subunits suggest that in T-47D cells, ER α enhances expression of *SCN8A* and *SCN1B*, whereas the steroid receptor seems to negatively regulate expression of *SCN1A* in T-47D and *SCN1B* in MCF-7 cells, in agreement with the original hypothesis. Transcript abundance of Nav1.5 was unperturbed by ER α degradation in either cell line studied, suggesting expression of this isoform in TNBC tumours is not due to a lack of negative regulation of gene expression by the hormone receptor.

The channels encoded by *SCN1A* and *SCN8A* are TTX-sensitive Nav1.1 and Nav1.6, respectively. Neither VGSC isoform has of yet been significantly implicated in breast cancer disease. However, mRNA expression of Nav1.1 is elevated in ovarian tumours, where positive expression of ER α and PgR is associated with a better clinical outcome (Gao *et al.*, 2010; Chen *et al.*, 2017). Additionally, intronic single-nucleotide polymorphisms in *SCN1A* that are linked to increased risk of febrile seizures and epilepsy have been implicated in decreased time-to-recurrence (TTS) for patients with colorectal carcinoma (Benhaim *et al.*, 2014). Nav1.6 transcripts are elevated 40-fold in cervical cancer biopsies relative to noncancerous cervical samples, and active Nav1.6 channels on the plasma membrane of cervical cancer cells are responsible for almost one-third of Na⁺ current recorded by whole-cell patch-clamp experiments (Hernandez-Plata *et al.*, 2012). The observation that Nav1.1 and Nav1.6 were responsive to ER α signalling in T-47D breast cancer cells was unexpected, as a hormone link modulating expression of these two channels has not previously been discussed. Thus, impact of altered VGSC transcription in response to hormone receptor perturbation should be further explored, particularly whether protein expression and membrane-trafficking of the channels are also altered in response to ER α knockdown. No inward Na⁺ current has been observed in T-47D cells, suggesting potential Nav1.6 activity in this cell line may be distinct from a canonical role in membrane depolarisation (Leslie *et al.*, 2024). Nav1.6 is expressed in astrocytes and microglia,

where Na⁺ channel activity modulates β -amyloid clearance and microglial phagocytosis and migration (Reese and Caldwell, 1999; Black et al., 2009; Wang et al., 2024). Intracellular localisation of a Nav1.6 splice variant controls invasion and migration of macrophage and melanoma cells by modulating podosome formation (Carrithers *et al.*, 2009). Enhanced Nav1.1 abundance in response to ER α knockdown may also have significant clinical implications for patients with endocrine resistant Luminal A breast cancer, and potentially identifies a population of breast cancer patients who would most benefit from adjuvant VGSC blockers such as rufinamide (Gilchrist *et al.*, 2014).

In contrast to Nav1.1 and Nav1.6, VGSC β 1 subunit encoded by *SCN1B* has been shown to be important in breast cancer progression. The β subunits are auxiliary proteins primarily involved in regulating α subunit trafficking, gating kinetics and post-translational modifications (Haworth *et al.*, 2022). Thus, there may be some form of interplay that exists between β 1 expression and Nav1.6 activity in T-47D cells that should be explored in cell lines and primary and metastatic breast cancer specimens. In addition to α subunit regulation, β subunits are members of the Ig superfamily of CAMs involved in mediating *trans*-homophilic adhesion of ankyrin-dependent cell-cell contacts, and heterophilic contacts with other CAMs including β 2, N-cadherin and tenascin-R (Xiao et al., 1999; Malhotra et al., 2000, 2004; McEwen and Isom, 2004). In breast cancer, expression of β 1 in patient tumour specimens is significantly elevated compared to healthy tissue and is correlated with ER α status in a non-oestrogen dependent manner (Nelson *et al.*, 2014). β 1 mRNA and protein levels are strongly expressed in weakly metastatic MCF-7 cells but not readily detectable in TNBC MDA-MB-231 cells (Chioni *et al.*, 2009). Downregulation of β 1 by siRNA enhances Nav1.5 mRNA and protein expression in MCF-7 cells, whereas stably transfecting β 1 in MDA-MB-231 cells significantly increases cell-cell adhesion and decreases migration and proliferation compared to control cells (Chioni *et al.*, 2009). On the other hand, overexpression of β 1 in an orthotopic mouse model bearing MDA-MB-231 tumours significantly enhances tumour growth by inhibiting apoptosis, and promotes liver and lung metastasis relative to control tumours, highlighting a potential pro-tumorigenic role of β 1 subunit in breast cancer in vivo (Nelson *et al.*, 2014). RNA-seq analysis of T-47D cells described in Section 5.2.5 disagrees with findings described by Chioni *et al.* as fulvestrant-mediated downregulation of *SCN1B* expression was not associated with elevated *SCN5A* transcription. The discrepancy could be a result of

cell line-specific variability in VGSC regulation, or due to contrasting experimental approaches leading to reduced levels of *SCN1B* with different primary molecular targets. However, expression of Nav1.5 was also unresponsive to elevated *SCN1B* in MCF-7 cells according to RNA-seq data, implicating other regulatory factors involved in the β 1-Nav1.5 relationship in Luminal A cell lines. The observation that ER α -degradation had cell type-dependent effects on *SCN1B* expression is contradictory to previous research that showed β 1 is not responsive to ER α activation or attenuation in MCF-7 cells and therefore thought not to be oestrogen-regulated (Nelson *et al.*, 2014). Here, microarray instead suggests that upregulation of β 1 in ER α + breast tumours is correlated with expression of genomic neighbours of *SCN1B* on chromosome 19q (Nelson *et al.*, 2014). Therefore, the RNA-seq finding that *SCN1B* expression is in fact potentially repressed by ER α in MCF-7 cells and enhanced by the hormone receptor in T-47D cells could have significant implications for the treatment of Luminal A breast cancers and highlights the need for investigations into patient-specific VGSC expression signatures and responses to anti-oestrogen therapies. The disparity between published results and the finding of ER α -dependent regulation of β 1 described in this Chapter could be attributed to the differences in fulvestrant-treatment. In Nelson *et al.* proteasomal degradation of ER α was induced by a 24-hour treatment of 1 μ M fulvestrant, whereas ER α attenuation described in this Chapter was the result of a 96-hour treatment of 100 nM fulvestrant. Thus, the differences in working concentration of SERD and treatment length suggest effects in *SCN1B* expression may be a secondary or tertiary response, and not due to direct regulation by ER α . Additional experiments exploring ER α -VGSC axis in breast cancer needs to be implemented to ascertain functional involvement of the steroid receptor in regulating VGSC subunit expression, and clinical implications of such regulations in a cell type and patient-specific manner.

5.3.3 Hypoxia regulates Na⁺ network *in vitro*

Beyond aberrant VGSC activity enhancing pathological Na⁺ influx, RNA-seq datasets analysed in this Chapter aimed to further delineate O₂-dependent and ER α -dependent mechanisms of Na⁺ regulation in a broader context, by exploring perturbations across 131 Na⁺ channel genes in Luminal A breast cancer cell lines. DGEA in MCF-7 and T-47D cells under stress of ER α -knockdown found several Na⁺ channel genes that were significantly differentially expressed as a consequence of

fulvestrant treatment, including NKCC1 (*SLC12A2*), Na⁺-coupled nucleoside transporter (*SLC28A1*) and NDBT (*SLC4A8*). In contrast with previous studies, ER α knockdown also predominantly enhanced expression of NKA subunits, including *ATP1A1*, *ATP1B1* and *ATP1A3*, whereas NKA expression and activity has been reported to be elevated following oestradiol activation of the hormone receptor (Sudar *et al.*, 2008; Obradovic *et al.*, 2015). A possible explanation for the disparity could be due to differences in disease models, as Sudar *et al.* and Obradovic *et al.* are exploring oestrogen-dependent regulation of NKA in heart disease and hypertension, but the role of ER α in pathophysiology of breast cancer was being investigated in Chapter 5. Despite evidence that ER α regulates Na⁺ channels at the gene level, exploring Na⁺ handling on a gene set level with GSEA revealed no significant enhancement of BPs or MFs involved in Na⁺ transport. Thus, alterations in the expression of a few Na⁺ channel genes in response to ER α perturbation does not contribute to a significantly altered Na⁺ transport phenotype in MCF-7 and T-47D cells, and so ER α -dependent effects in Na⁺ handling in these cells were not studied further in this Chapter. Conversely, DGEA in response to chronic O₂ deprivation in Luminal A cell lines found significant alterations in expression of all major ENaC subunits (*SCNN1A*, *SCNN1B* and *SCNN1G*), NKA α and β subunits (*ATP1A1* and *ATP1B1*) and NHE1 (*SLC9A1*). In addition, GSEA found significant positive enrichment of BPs and MFs involved in Na⁺ transport in both cell lines as a consequence of hypoxic culture. Therefore, hypoxic stress significantly elevates Na⁺ transport in MCF-7 and T-47D cells by altering expression of many Na⁺ channel genes.

Overexpression of NKA subunits has been identified in several malignancies, including NSCLC, melanoma, hepatocellular carcinoma and breast cancer (Nilsson *et al.*, 2007; Mathieu *et al.*, 2009; Shibuya *et al.*, 2010; Wang *et al.*, 2018). Researchers are developing novel NKA tracer molecules to stratify NKA+ breast cancer patients through non-invasive imaging of NKA α 1 subunit, and further utilising overexpression of α 1 subunit to enhance targeted delivery of doxorubicin to breast tumours with elevated NKA (Wang *et al.*, 2018; Araste *et al.*, 2020). Analysis of 2,509 primary breast tumours part of the METABRIC project revealed NKA β 1 amplification was more prevalent compared to NKA α 1 (21% β 1 vs. 1% α 1). However, amplification of catalytic NKA α 1 subunit was associated with poor prognostic signatures in relapse-free and overall survival whereas NKA β 1 genomic alteration was not significantly associated with patient outcomes. Independent IHC

analysis of 107 breast tumours further demonstrated poor prognosis for overall and disease-free survival for patients with breast tumours that had high NKA α 1 expression (Wang *et al.*, 2018). Investigating the genomic landscape dictating expression profiles of *ATP1A1* in 764 TCGA samples revealed hypermethylation of α 1 gene was associated with better overall survival in TNBC, whereas high-risk patients had hypomethylated and elevated *ATP1A1* expression and a corresponding decreased overall survival, relapse-free survival and metastasis-free survival (Kim *et al.*, 2024). Adverse effects of increased NKA expression can be attributed to enhanced NKA signalling cascade activity involving Src, increasing cell migration (Ou *et al.*, 2017). Decreased expression of NKA α 1 has been shown to cause cell cycle arrest, induce apoptosis and inhibit migration of HCC cells *in vitro* and further impair tumorigenicity *in vivo* (Zhuang *et al.*, 2015). Therefore, there is strong evidence implicating elevated *ATP1A1* in cancer progression and identifies the catalytic subunit of NKA as a therapeutic biomarker for patients with breast cancer. The finding that both NKA α 1 and NKA β 1 transcripts were amplified following chronic O₂ deprivation has not been reported before. However, a study in rat astrocytes demonstrated transient increase in NKA α 1 and NKA β 1 mRNA during reoxygenation after 24 hours hypoxia (8 mmHg), whereas hypoxia alone was not shown to affect expression of the NKA subunits (Kasai *et al.*, 2003). In contrast, hypoxia is known to downregulate ATP-consuming proteins, including NKA, in a process mediated by mitochondrial ROS production, endocytosis of membrane-bound NKA and subsequent ubiquitination and degradation of the enzyme (Dada *et al.*, 2003; Chen *et al.*, 2006; Comellas *et al.*, 2006). When investigating potential therapeutic benefits of ouabain in reducing migration of hypoxic Luminal A cell lines, no significant difference was observed in MI between vehicle treated and ouabain treated cells cultured in hypoxia, and this could be explained by hypoxia-induced degradation of NKA protein, as only alterations in transcript levels as a result of O₂ deprivation were studied in this Chapter and not corresponding protein levels. However, ouabain was also ineffective in reducing MI of breast cancer cells cultured in normoxia, where an active NKA is expected. This result could be due to the dose of ouabain being too low, as previous studies have used 1 μ M – 10 μ M ouabain to inhibit NKA activity *in vitro* (Khajah *et al.*, 2018). However, the IC₅₀ of ouabain for inhibiting kynurenine production was purported to be 89 nM in MDA-MB-231 cells, with 100 nM significantly inhibiting Na⁺ export via the NKA, further supporting the initial use of 100 nM in this thesis (Shandell *et al.*, 2022). Further investigations into the activity of NKA in normoxic and hypoxic Luminal A cells, and optimisation of

ouabain concentration for inhibiting NKA-dependent effects on breast cancer progression, are therefore warranted.

In addition to NKA, ENaC is an emerging therapeutic target in breast cancer, although the field of ENaC+ breast cancer research is still in its infancy. ENaCs are mechanosensitive channels typically expressed on apical membranes of collecting ducts in kidney tubules, and are essential for Na⁺ and subsequently water reabsorption into cells (Hanukoglu and Hanukoglu, 2016). Luminal A cell lines exposed to chronic hypoxia significantly upregulated mRNA expression of three ENaC subunits, which make up the predominant ENaC trimer. However an *in vivo* model of pulmonary oedema demonstrated polyubiquitination of α -ENaC (*SCNN1A*) and subsequent endocytosis and degradation of the channel as a feature of hypoxia which could suggest elevated ENaC transcript does not correspond to enhanced ENaC on cell membranes (Gille *et al.*, 2014). Analysis of METABRIC data found genomic amplification of β -ENaC and γ -ENaC in 6% of breast cancer patients, compared to no genomic alteration in expression. Such amplification was significantly associated with improved relapse free and overall survival. Genomic alteration of *SCNN1A* (α -ENaC) occurred independent of alterations in β -ENaC and γ -ENaC subunits and had no significant impact on breast cancer patient outcomes, in contrast to previous research implicating α -ENaC in HCC and GBM Na⁺-induced proliferation and migration (Bondarava *et al.*, 2009; Kapoor *et al.*, 2009, 2011). Conversely, a recent study in MCF-7, T-47D, BT549 and MDA-MB-231 cells suggests α -ENaC expression or activity is a negative regulator of breast cancer cell proliferation and is associated with maintaining epithelial over mesenchymal phenotype (Ware *et al.*, 2021). No functional studies into possible protective roles for ENaC β and γ subunits in breast cancer cells have been undertaken, highlighting an important knowledge gap in ENaC breast cancer biology. Nevertheless, controlled activation of ENaC activity may present a novel therapeutic avenue for a cohort of breast cancer patients to improve survival outcomes. The observation that genomic alterations in α -ENaC are independent of alterations in β -ENaC and γ -ENaC in breast tumours was surprising. Single-particle cryo-electron microscopy revealed trimer ENaC assembly occurs in a 1:1:1 stoichiometry of α : β : γ dictating equal expression of ENaC subunits is required for complete trimer formation (Noreng *et al.*, 2018). Non-canonical ENaCs exist as monomers or heterodimers that are responsive to shear force (Baldin *et al.*, 2020). Therefore, 6% of breast cancer patients may express a β : γ -ENaC formation that protects against cancer cell

progression. Such mechanisms behind a beneficial heterodimer channel have not been studied but could be due to a decrease in Na⁺ influx through an incomplete ENaC which will protect against Na⁺-induced proliferation and migration. Specific dimer channel characteristics, including effect on Na⁺ influx and downstream cancer cell progression need to be investigated.

5.3.4 Limitations and Future work

A significant proportion of research carried out in this chapter centred around bioinformatic approaches to explore differences in transcript levels of Na⁺ channel genes in response to chronic hypoxia or ER α knockdown. Three and four biological replicates were carried out for MCF-7 and T-47D cell lines, respectively ensuring high reproducibility of data generated during RNA-seq. Complementary RT-qPCR was carried out in the same cell lines to validate major findings of altered Na⁺ channel gene expression. Similarly, three biological replicates consisting of three technical replicates were used. RT-qPCR did not recapitulate the α -NKA gene induction determined by *DESeq2*. One possible explanation for the discrepancy is that different sets of samples were used for RT-qPCR and RNA-seq experiments, which would introduce a source of variability owing to differences in sample collection and nucleic acid extraction protocols implemented for each method of mRNA quantification. To limit differences associated between RNA-seq and RT-qPCR, uniform processing of samples should be implemented, which includes utilising the same sample for each transcript detection method and diverging sample processing as late as possible (Aguiar *et al.*, 2023).

An important consideration for transcriptional findings in this chapter is that changes in mRNA levels were not compared to subsequent aberrations in protein synthesis, PTMs, channel trafficking to plasma membrane or altered kinetics or activity. As such, elevated α -NKA, α -ENaC, β -ENaC and γ -ENaC transcript does not guarantee a functional Na⁺ channel. As described above, NKA has been shown to be degraded at the protein level when O₂ is limited to conserve energy in the form of ATP (Comellas *et al.*, 2006). The same is also true for α -ENaC in a hypoxic model of pulmonary oedema (Gille *et al.*, 2014). Therefore, protein-level analysis of Na⁺ channel expression following O₂ perturbation either by western blot or ELISA would be instrumental in ascertaining functional consequences of hypoxia-mediated NKA or ENaC transcription in breast cancer cells. In addition, alterations in Na⁺ influx or

efflux could be measured using SBFI AM following hypoxic challenges, in the presence of ouabain or amiloride to block NKA or ENaC activity respectively, which would also confirm if overexpressed channels at the transcript level are subsequently translated into a functional channel. Determining changes in $[Na^+]_i$ may explain why upregulation of a proposed $\beta:\gamma$ -ENaC is beneficial for breast cancer patients. Such an experiment could include stable transfection of $\alpha:\beta:\gamma$ or $\beta:\gamma$ into MCF-7, T-47D, MDA-MB-231 and MDA-MB-468 cells to compare differences in Na^+ influx through different ENaC conformations. Alterations in cancer cell behaviours including proliferation, invasion and migration could be measured in $\alpha:\beta:\gamma$ vs. $\beta:\gamma$ cell lines to further investigate why amplification of *SCNN1B* and *SCNN1G* leads to a significantly improved outcome for breast cancer patients. Accordingly, modulation of NKA and ENaC expression or activity could be tested alongside gold standard TNBC chemotherapies (doxorubicin or cisplatin) or Luminal A endocrine therapies (e.g. aromatase inhibitors or tamoxifen) to assess if there are additional therapeutic benefits by combining ouabain with breast cancer treatments, or if ENaC expression enhances breast cancer cells' sensitivity to treatment. Na^+ channel blockade using Class 1c and Class 1d antiarrhythmics in breast, bowel or prostate cancer has recently shown to associate with improved cancer-specific survival (Fairhurst *et al.*, 2023). Thus, targeting altered Na^+ in malignancies may derive therapeutic benefit via repurposing of existing Na^+ channel inhibitors.

As regards $ER\alpha$ -dependent regulation of VGSC expression, much is still to be addressed. It was not tested if altered transcription of $\beta 1$, $Na_v1.1$ or $Na_v1.6$ corresponds to altered protein levels of these subunits. Thus, western blots should also be considered to determine if protein levels of the VGSCs significantly affected by $ER\alpha$ knockdown are also changed. Na^+ currents have not been detected in Luminal A cell lines (Leslie *et al.*, 2024). Of particular interest is upregulation of $Na_v1.1$ in T-47D cells following treatment with fulvestrant. Whole-cell patch clamp recordings of these cells in the presence of 4.1 nM TTX would discern if expression of $Na_v1.1$ is functional, as this channel is TTX-sensitive and I_{Na} would be blocked at this low concentration of inhibitor. In addition, stable transfection of the hormone receptor into $ER\alpha$ - TNBC cell lines could also be implemented to determine whether $ER\alpha$ affects expression of $Na_v1.5$ in these cells. Only expression of *nSCN5A*, *SCN8A* and *SCN9A* was studied in MDA-MB-231 and MDA-MB-468 cells, whereas RNA-seq in Luminal A cells enabled unbiased pan-VGSC exploration. As VGSC expression is associated with more aggressive, metastatic cancers it would be

interesting to explore expression of all VGSCs in the TNBC cells as well as endocrine resistant Luminal A cells.

To further advance research into Na⁺ channelopathies, primary and metastatic Luminal A and TNBC tumours and matched healthy tissue biopsies would be invaluable. For example, IHC could be conducted to determine relative Na⁺ channel abundance across a broad range of breast tumours. Such studies could stratify breast cancer patients based on Na⁺ channel expression and highlight cohorts of patients who would most benefit from Na⁺ channel blockade in conjunction with chemotherapy / endocrine therapy and surgery.

5.4 Conclusion

Dysregulated Na⁺ transport has been implicated in many hallmarks of cancer, but the mechanism driving altered Na⁺ homeostasis was not known. By carrying out an extensive RNA-seq experiment, the contribution of hypoxia and the ER α was able to be fully investigated into their involvement in perturbed Na⁺ regulation. Chronic hypoxic stress imparted on two Luminal A cell lines significantly enhanced Na⁺ transport through preferential upregulation of NKA, ENaC and NHE, whereas the involvement of the ER α in dysregulated Na⁺ balance was more discrete and less significant on a gene-set level. However, ER α was found to significantly regulate expression of VGSC subunits in a cell type specific manner. The findings of this Chapter may have significant implications for the treatment of breast tumours that have elevated [Na⁺]_i driving disease progression. In particular, existing Na⁺ channel targeting drugs such as ouabain or rufinamide could be repurposed for a subset of breast cancer patients whose tumours are shown to have aberrant expression of NKA or VGSCs.

6. General discussion

This thesis addressed two independent questions, that were motivated by the observation of: (i) elevated tRNA levels and; (ii) raised $[Na^+]_i$ corresponding to adverse disease outcomes for patients with breast cancer (Roger et al., 2003; Fraser et al., 2005; Pavon-Eternod et al., 2009).

Previous work identified a link between oestradiol activation of $ER\alpha$ in MCF-7 cells and significant upregulation of a large proportion of tRNA genes (Hah et al., 2011). However, until now, large-scale investigation into $ER\alpha$ regulation of Pol III transcribed genes had not been conducted. Research had also demonstrated elevated expression of VGSCs in many types of solid malignancies, including breast tumours, which correspondingly raises $[Na^+]_i$ and promotes advanced disease (Brackenbury et al., 2007; Nelson et al., 2015b; Djamgoz et al., 2019). Hypoxia had been considered one such mechanism by which VGSCs are upregulated in breast tumours, owing to similar regulation of these channels in hypoxic cardiomyocytes (Ju et al., 1996; Plant et al., 2020). However, the link between hypoxia and VGSC expression in solid tumours had not been fully explored. Therefore, the focus of this thesis was to address two important knowledge gaps in breast cancer development, namely, to: (i) Understand the mechanism by which $ER\alpha$ is targeted to tRNA genes and the functional significance of such targeted hormone receptor delivery to these promoters; and (ii) Investigate the effect of hypoxia on Na^+ homeostasis in breast cancer cells, with a particular focus on hypoxia-mediated regulation of Na^+ channel genes, including VGSCs. To enable (ii), an additional and equally important goal of this thesis was to identify robust and stably expressed RGs that can be used for studying hypoxia-mediated alterations in gene expression by RT-qPCR. Such identification of RGs in a panel of normoxic vs. hypoxic breast cancer cell lines had not been previously conducted.

6.1 $ER\alpha$ regulation of tRNA expression in breast cancer

The main findings from Chapter 3 show that $ER\alpha$ was strongly enriched with 30-50% of tRNA genes in breast cancer cell lines, and primary and secondary patient $ER\alpha+$ breast tumours as determined by CHIP-seq and CHIP-qPCR. GRO-seq of oestradiol-stimulated MCF-7 cells demonstrated rapid induction in expression of 32% of tRNA genes (Hah et al., 2011). As such, results from Chapter 3 suggest

such rapid hormone-mediated tRNA transcription is a result of direct ER α associations at these promoters, in agreement with previous ChIP-qPCR of ER α at tRNA^{Leu} (Fang et al., 2017). As GRO-seq is a measure of nascent transcription and does not capture steady state RNA, including processing and degradation of RNA in response to stimuli, further quantification of tRNA abundance mediated by ER α activity is necessary (Tzerpos et al., 2021). FOXA1 was also associated at many of the same tRNA genes as ER α in MCF-7 cells. As such, ER α association at tRNA loci indicates that the hormone receptor may orchestrate transcription of Pol III genes by recruiting necessary transcription factors to promoters, or stabilising transcription complexes, though more work is required to confirm this potential role. TFIIC was found to make strong connections with ER α by qPLEX-RIME and co-immunoprecipitation, suggesting a protein-protein tethering mechanism recruiting ER α to target tDNA. ER α was previously shown to co-immunoprecipitate with Brf1 of TFIIB, further supporting a mechanism of ER α stabilising PIC assembly through protein-protein interactions with Pol III transcription factors (Fang et al., 2017). Fulvestrant-mediated knockdown of ER α in MCF-7 cells slightly decreased occupancy of FOXA1 and Pol III and tRNA promoters, but did not affect TFIIC binding to these loci, suggesting ER α may influence Pol III loading to target genes after TFIIC binds to tRNA A and B boxes. Therefore, Chapter 3 has provided significant evidence that ER α can directly associate with tRNA genes in MCF-7 cells and Luminal A breast tumours, demonstrating that ER α can promote tumorigenesis by mediating expression of Pol III transcribed genes, in addition to indirectly affecting tRNA modifications (Delaunay et al., 2016; Lorent et al., 2019). The proposed model of ER α regulation of tRNA expression, modification and enhanced malignant capacity is shown in Figure 6.1.

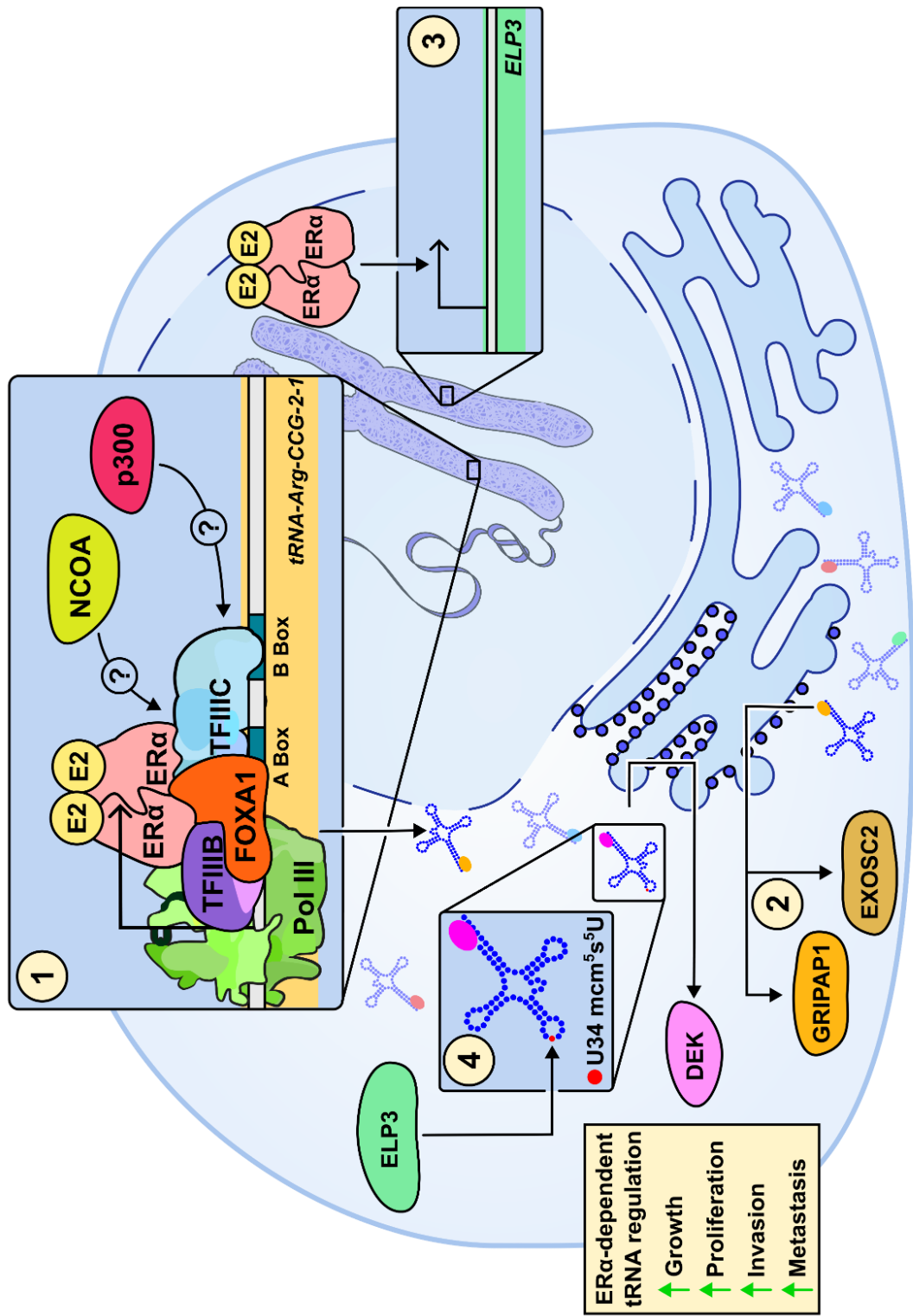


Figure 6.1 Hypothetical Mechanism of ER α Activity in Luminal A Breast Cancer Cells Discussed in this Thesis. 1. In hormone responsive breast cancer cells, the ER α is directed to target tRNA genes through a robust protein-protein interaction with Pol III transcription factor TFIIIC. Once primed at target tRNA loci, ER α may facilitate complete PIC assembly by honing FOXA1 to these promoters which could help unravel tightly bound chromatin such that TFIIIB and Pol III have easier access to regulatory elements. In complex, ER α may strengthen stability of Pol III PIC to enable effective transcription of target genes. Additional recruitment of NCOAs or HATs associated with ER α could also enhance Pol III transcription and should be investigated. 2. Some tRNA targets of ER α are preferentially upregulated in transformed cells where they are essential for translation of oncoproteins, such as tRNA-Arg-CCG-2-1 which is necessary for protein synthesis of pro-metastatic GRIPAP1 and EXOSC2. ER α was strongly associated with tRNA-Arg-CCG-2-1 in breast cancer cells. 3. ER α mediates transcription of tRNA modifying enzymes, such as *ELP3*. 4. ELP3 is essential for a mcm⁵s⁵U modification at position U34 in tRNA anticodon loop, which enables efficient translation of oncoprotein DEK. The sum of ER α regulation of tRNA transcription and modification in breast cancer cells is increased growth, proliferation, invasion and metastasis.

6.2 Role of hypoxia in progressing breast cancer development by modulating Na⁺ transport

The aim of Chapter 4 was to identify stably expressed RGs that could be used to investigate important transcriptional changes occurring in MCF-7, T-47D, MDA-MB-231 and MDA-MB-468 breast cancer cell lines cultured in acute or chronic hypoxia, versus normoxia. The timepoints were determined based on abundance of HIF-1 α and HIF-2 α which corresponds to the HIF switch. The HIF switch is thought to be mediated by HIF-1 α mRNA instability and reactivation of PHD enzymes (Jaśkiewicz et al., 2022). Due to cell type-dependent differences in HIF protein expression timings, it was important to elucidate a suitable time course that accommodates the four breast cancer cell lines ubiquitously (Zhou et al., 2011). Western blot analysis of HIF-1 α and HIF-2 α suggests the HIF switch occurs in an 8- and 48-hour time course at 1% O₂. Next, a comprehensive study of a large panel of RG candidates revealed ribosomal proteins *RPL27* and *RPLP1* to be least variable in expression in the four breast cancer cell lines in all O₂ conditions, which is a valuable and important finding necessary for accurate normalisation of gene expression quantification. Alongside positive identification of RGs, certain exclusion criteria were implemented that were predominantly centred around primer quality (i.e. primer-dimer formation and primer efficiency) as well as baseline gene expression.

In Chapter 5, chronic exposure to low O₂ tension was initially used to determine major changes in Na⁺ transporter expression by RNA-seq analysis, followed by an acute and chronic time course of hypoxia to identify the HIF isoform driving such transcriptional changes by RT-qPCR using RGs identified in Chapter 4. Chronic hypoxia had a significant positive effect on Na⁺ transport according to GSEA, which was independent of alterations in VGSC expression as determined by DGEA. In contrast, mRNA levels of NKA, ENaC and NHE1 subunits were most upregulated by low O₂ tension and significantly contributed to Na⁺ transport BPs and MFs, possibly leading to increased [Na⁺]_i. Recent work in Langendorff perfused rat hearts demonstrated elevated [Na⁺]_i enhances NCX activity in mitochondrial membranes leading to significant Ca²⁺ export into cytosol and inhibition of the TCA cycle and OXPHOS, amplifying ROS production and stabilising HIF- α in a process termed “Na⁺-induced pseudohypoxia”, suggesting a positive feedback mechanism between [Na⁺]_i and HIF- α transcriptional activity (Chung et al., 2024).

Amplification of the α subunit of NKA was shown to be an indicator of poor prognosis in breast cancer according to the METABRIC study, whereas amplification of the β subunit of NKA was not significantly correlated with breast cancer outcome. In contrast, amplification of β -ENaC and γ -ENaC conferred a better prognosis for breast cancer patients compared to those who had unaltered expression of these subunits. The cardiac glycoside ouabain, which specifically blocks NKA activity, was shown to not be an effective inhibitor of MCF-7 cell migration in normoxia or in hypoxia. Corresponding protein levels of Na^+ transporters upregulated at the mRNA level in hypoxia were not studied and may be one possible explanation as to why ouabain was ineffective at decreasing MI of breast cancer cells. In particular, hypoxia has been shown to induce proteasomal degradation of NKA, which warrants further investigation in breast cancer cell lines (Comellas et al., 2006). A hypothetical model of Na^+ transporter expression in hypoxic breast cancer cells, and corresponding alterations in $[\text{Na}^+]_i$ and pH_e is shown in Figure 6.2.

6.2.1 Potential role of $\text{ER}\alpha$ in mediating VGSC expression in breast cancer

$\text{ER}\alpha$ was shown to modulate expression of some VGSC subunits by DGEA following proteasomal degradation of the hormone receptor in Luminal A breast cancer cells. Transcription of *SCN1A*, *SCN8A* and *SCN1B* was significantly affected by $\text{ER}\alpha$ perturbation, which appeared to be cell type dependent. Specifically, *SCN1A* which encodes $\text{Na}_v1.1$ was significantly upregulated, and *SCN8A* and *SCN1B* which encode $\text{Na}_v1.6$ and $\beta1$, respectively, were significantly downregulated in T-47D cells treated with fulvestrant for 48 hours. Conversely, Na_v subunits were not affected by fulvestrant-mediated $\text{ER}\alpha$ knockdown in MCF-7 cells, whereas $\beta1$ mRNA was significantly elevated. Whether or not changes in VGSC transcription by $\text{ER}\alpha$ knockdown significantly alters protein levels of these channels, or numbers of these VGSCs on the plasma membrane, is a question that was not addressed in this thesis and warrants further exploration.

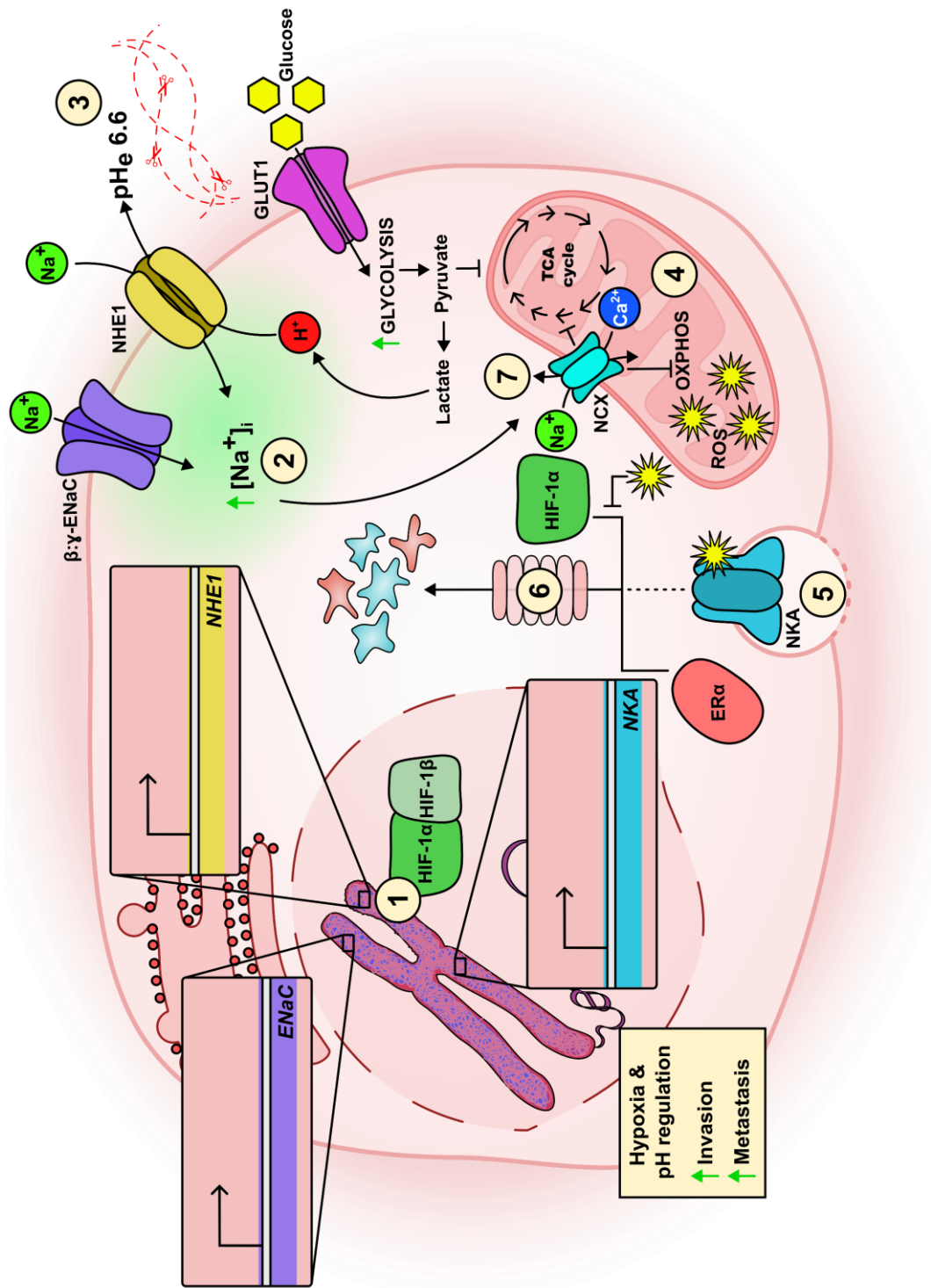


Figure 6.2 Proposed Model of Hypoxia-Driven Na⁺ Transport. 1. Hypoxic breast cancer cells have abundant protein levels of HIF- α , which form heterodimers with O₂-independent HIF-1 β , translocate into the nucleus and regulate expression of target genes which may have a survival advantage in unfavourable conditions. Na⁺ transporter genes that are significantly upregulated in hypoxia include those encoding for NKA, ENaC and NHE1. Whether NKA or ENaC genes are upregulated by HIF activity is unknown. 2. Ion transport conducted by NHE1 raises [Na⁺]_i and significantly contributes to the acidification of ECM. Heightened ENaC expression at plasma membranes would further contribute to increased [Na⁺]_i. 3. Glucose transporters such as GLUT1 are upregulated in hypoxia, which feed more glucose into the glycolytic pathway. Lactate levels are enhanced which results in H⁺ extrusion through NHE1, further acidifying ECM to pH 6.6 which is the optimal pH for MMPs and cathepsins to effectively degrade surrounding stroma. 4. Despite elevated glucose transport, glycolysis does not feed into TCA cycle and OXPHOS is also inhibited as no O₂ is available to act as the final electron acceptor in the ETC. ROS build up in mitochondria, destabilising PHD enzymes. HIF- α proteins are therefore not degraded by the proteasome, and a positive feedback loop is established between hypoxia, HIF- α and ROS. 5. Elevated ROS has been shown to induce endocytosis of NKA at plasma membranes in hypoxia, rendering cardiac glycosides ineffective. 6. Hypoxia induces proteasomal degradation of ER α in breast cancer cells and may also cause proteasomal degradation of NKA if present at the protein level. 7. Elevated [Na⁺]_i increases NCX activity on the mitochondria membrane, leading to Ca²⁺ efflux from the mitochondrial matrix into the cytosol and inhibition of Ca²⁺-dependent enzymes of the TCA and OXPHOS, further driving ROS production and HIF- α stabilisation. This Na⁺-mediated mechanism occurs independent of O₂ availability and is correspondingly termed “Na⁺-induced pseudohypoxia” (Chung et al., 2024).

6.3 Future directions

The future vision for work carried out in Chapter 3 would be to fully delineate the importance of ER α regulation of tRNA gene expression in breast tumours, to understand the potential of targeting Pol III transcription for a cohort of breast cancer patients with endocrine resistant disease. Missense mutations of *ESR1* are found in 60% of metastatic breast tumours that have progressed with endocrine therapy, and of these mutations, more than 70% are located in the LBD of *ESR1* which promote constitutive oestrogen-independent ER α transcriptional activities (Jeselson et al., 2015; Tolaney et al., 2022). As such, downstream targets of ER α that promote tumorigenesis are of great importance when considering therapeutic options for metastatic tumours. If ER α drives tRNA expression in Luminal breast cancers, it may be that novel therapeutics which shut down Pol III transcription in advanced endocrine resistant disease will significantly improve patient outcomes. Pol III antagonists exist but would not be well tolerated if delivered systemically, owing to Pol III-transcribed genes being essential in all cell types (Dumay-Odelot et al., 2010; Turowski and Tollervey, 2016). Therefore, tumour-targeting drug delivery mechanisms including antibody-drug conjugates with Pol III inhibitors such as triptolide may be of great therapeutic benefit (Liang et al., 2019; Dannheim et al., 2022). For this vision to be realised extensive further work needs to be carried out to expand on the findings of Chapter 3. Disseminating oestrogen-ER α modulation of tRNA expression in primary and metastatic human breast tumours could involve culturing primary cell lines in combination with Pol III inhibitors and determining effects on cell viability, proliferation, migration and invasion, before moving forward to *in vivo* studies exploring mechanisms of safely delivering Pol III inhibitors to tumour-bearing mice.

In addition to ER α modulation of tRNA expression, *SCN1A*, *SCN8A* and *SCN1B* were identified to be differentially regulated at the transcription level by the hormone receptor in two Luminal A cell lines in Chapter 5. The implications of altered VGSC α and β subunit expression because of ER α knockdown by fulvestrant was not studied beyond transcriptional aberrations. However, all VGSC α subunits have been identified in many solid tumours, and some subunits are associated with disease progression and poor patient outcomes (Malcolm et al., 2023). The different expression of VGSC subunits between MCF-7 and T-47D cells further highlights importance of considering cell-type and patient heterogeneity. If

VGSCs identified to be regulated at the mRNA level by ER α are subsequently translated and trafficked to plasma membranes where they are functional, a sub-population of patients with Luminal A breast tumours may significantly benefit from pharmacological inhibition of active α subunits. Many VGSC inhibitors are routinely used to treat a variety of channelopathies. As such, repurposing such drugs could save a significant amount of money and importantly time in developing new treatment strategies, and provide a population of breast cancer patients most at risk of adverse outcomes with better survival opportunities (Fairhurst et al., 2015, 2016, 2023).

More aggressive breast tumours are significantly associated with hypoxic signatures (Vaupel et al., 2007; Shamis et al., 2022). In endocrine resistant breast cancer, hypoxia induces proteasomal degradation of ER α and gene silencing of *ESR1* by promoting hypermethylation of this promoter (Stoner et al., 2002; Ryu et al., 2011; Wolff et al., 2017). In such cases of advanced disease, additional therapeutics are desperately needed to overcome treatment resistance and improve patient survival. Therefore, results from Chapter 5 aim to ultimately expand treatment options for women with breast cancer who are no longer responsive to conventional anti-oestrogen or chemotherapies. In the case of hypoxia-driven Na⁺ transport aberrations, methods of delivering cardiac glycosides to patient tumours overexpressing NKA α -subunit may be of significant therapeutic benefit. For many solid tumours and haematological malignancies, NKA has been proposed as an attractive therapeutic target, particularly governed by selective expression of alternative α and β subunit isoforms which are seldom expressed in normal tissues (Sakai et al., 2004; Lefranc and Kiss, 2008; Mijatovic et al., 2008; Mathieu et al., 2009; Schneider et al., 2024). Consequently, NKA-inhibiting agents such as bufalin, or ouabain with berbamine significantly inhibit tumorigenesis (Yang et al., 2021b; Soumoy et al., 2024). To fully understand the therapeutic potential of targeting NKA in advanced hypoxic breast tumours, NKA expression needs to be further characterised beyond elevated transcription in hypoxic breast cancer cell lines discussed in Chapter 5. Analysis of protein expression and cellular localisation of NKA is necessary, along with assessment of the pump activity. Corresponding effects of NKA expression and activity on cell growth, proliferation, invasion and migration should be explored *in vitro* and *in vivo*. Importantly, hypoxia has been significantly linked to endocytosis and proteasomal degradation of NKA, further

highlighting the critical need for characterising NKA expression at the protein level both in normoxia and in hypoxia (Dada et al., 2003; Gusarova et al., 2009).

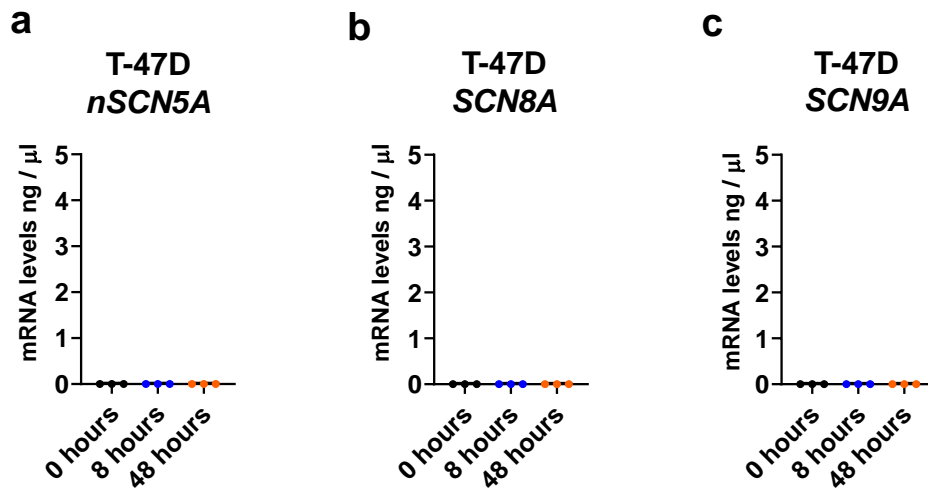
ENaC subunits were also identified to be significantly elevated at the mRNA level in hypoxic breast cancer cell lines. Similarly, protein expression and functional characterisation of ENaC in breast cancer should be further explored *in vitro* and *in vivo*. Interestingly, amplification of β -ENaC and γ -ENaC in patient breast tumours is associated with improved disease outcomes and seems to be mutually exclusive to amplification events of α -ENaC and α -NKA. Studying downstream effects of β : γ -ENaC may identify novel anti-tumorigenic molecules that could be targeted pharmacologically to improve survival for patients who do not exhibit β : γ -ENaC amplification. For example, ENaC has been shown to be crucial for mediating Na^+ / Ca^{2+} exchange through NCX, with significant effects on downstream Ca^{2+} signalling pathways involved in inflammation (Chen et al., 2023b). As such, ENaC expression in breast tumours may impose improved survival advantages by regulating activity of other ion channels or affecting ion-mediated signalling cascades. Where VGSC, ENaC and NKA are concerned, corresponding effects of Na^+ channel activity on $[\text{Na}^+]_i$ and pH_e should be explored using an SBFI AM assay and a Seahorse analyser, respectively. Such studies would provide insight into important physiological changes occurring because of aberrant Na^+ transport, and further determine NKA function. Additionally, measurement of $[\text{Na}^+]_i$ and pH_e could distinguish potentially beneficial Na^+ currents carried by β : γ -ENaC versus potentially pathological Na^+ currents carried by VGSCs or α : β : γ -ENaC.

6.4 Conclusion

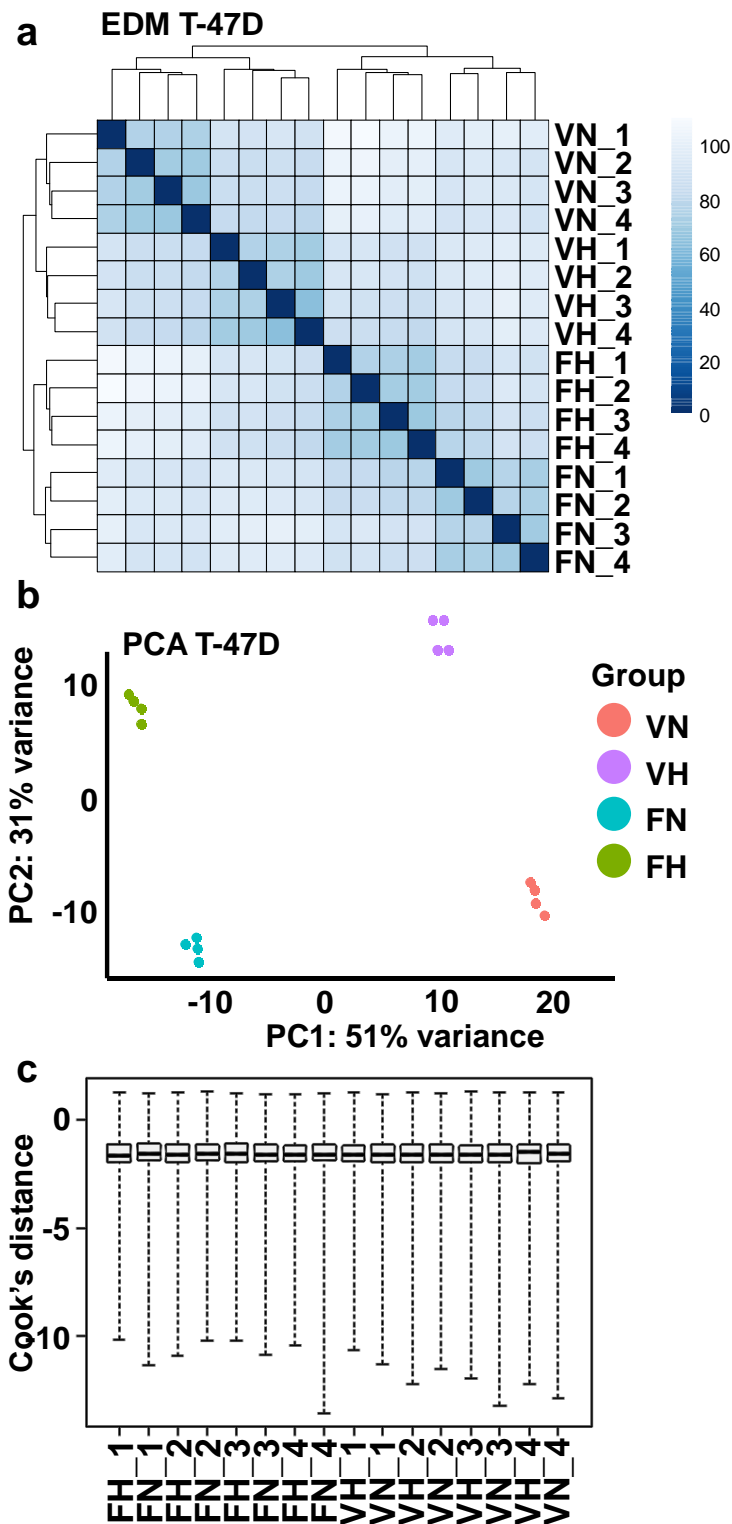
This thesis aimed to investigate ER α -Pol III transcriptome, delineate the mechanism by which ER α is recruited to such targets and understand how ER α mediates changes in tRNA expression in response to hormone. Significant evidence from Chapter 3 shows ER α is specifically targeted to tRNA through a protein-protein interaction with Pol III transcription factors, both *in vitro* and *in vivo*, where it may elicit immediate transcriptional responses following hormone activation. Interestingly, FOXA1 appears to be recruited to some Pol III promoters secondary to ER α recruitment. To date, no such studies exploring ER α regulation of Pol III-transcribed genes has been carried out to such an extent. Additionally, work in this thesis was set up to explore alterations in Na^+ transport because of low O_2

availability, or reduction in ER α abundance. Importantly, *RPLP1* and *RPL27* were identified as stably expressed RGs in Chapter 4, allowing accurate determination of gene expression changes in hypoxic breast cancer cell lines by RT-qPCR. In Chapter 5, hypoxia was shown to significantly affect Na⁺ transport in breast cancer cell lines by preferentially upregulating NKA and ENaC. Amplification of the NKA catalytic α subunit is associated with a poor overall survival for patients with breast cancer, whereas amplification of some ENaC subunits is correlated with a more favourable outcome. Together, the findings discussed in this thesis highlight potential new mechanisms by which ER α and hypoxia contribute to breast cancer progression and therapy resistance. As a result, future new breast cancer treatment strategies should focus on attenuating Pol III transcription of tRNA in endocrine resistant disease, or similarly be directed to inhibiting aberrant NKA activity in patient tumours with elevated α -subunit expression.

Appendix

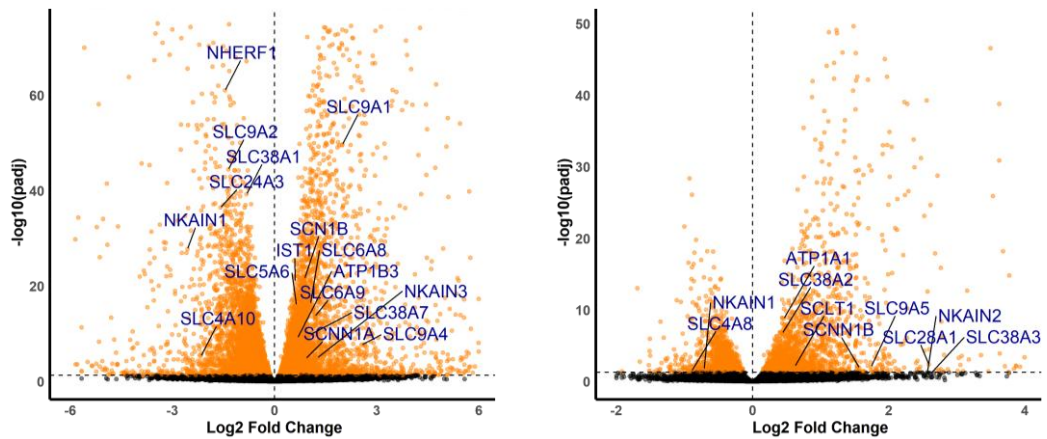


Appendix Figure I Effect of Acute or Chronic Hypoxia on VGSC Subunit mRNA Expression in T-47D cells. RT-qPCR of VGSC subunits (a) *nSCN5A*, (b) *SCN8A* and (c) *SCN9A* in T-47D breast cancer cells. Cell lines were cultured in normoxia (~20% O₂, “0 hours”), acute hypoxia (1% O₂, 8 hours) or chronic hypoxia (1% O₂, 48 hours). No detectable mRNA was seen for each VGSC gene.

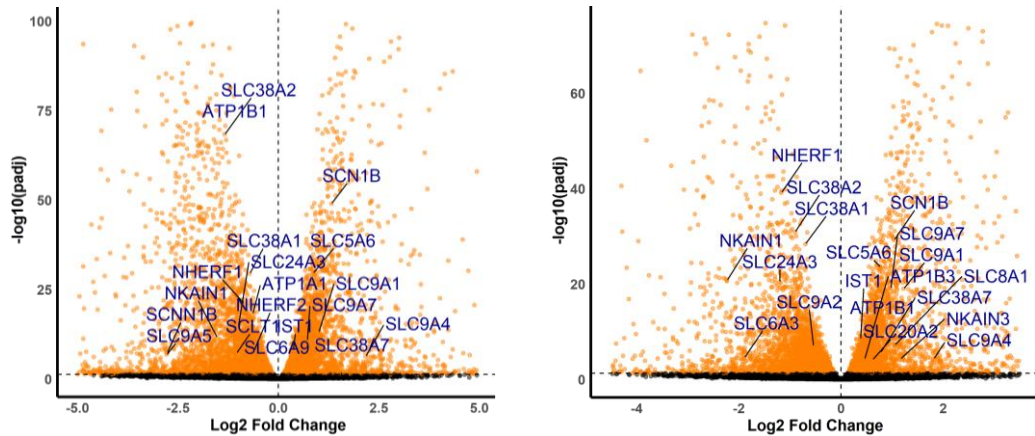


Appendix Figure II. Data Quality of RNA-seq from T-47D Breast Cancer Cells (a) EDM of squared distances between each sample from the T-47D RNA-seq. Experimental conditions for samples are vehicle and normoxia” (V_N), vehicle and hypoxia (V_H), fulvestrant and normoxia (F_N) and fulvestrant and hypoxia (V_H). N = 4. **(b)** Principal component analysis (PCA) plot with a PC1 variance of 51% and a PC2 variance of 31% for the 16 T-47D samples. **(c)** Boxplot of Cook's distances for outlier detection, calculated for each gene within each T-47D sample.

a Normoxia (ER α +) vs. Hypoxia (ER α -) **b** Normoxia vs Hypoxia (ER α -)

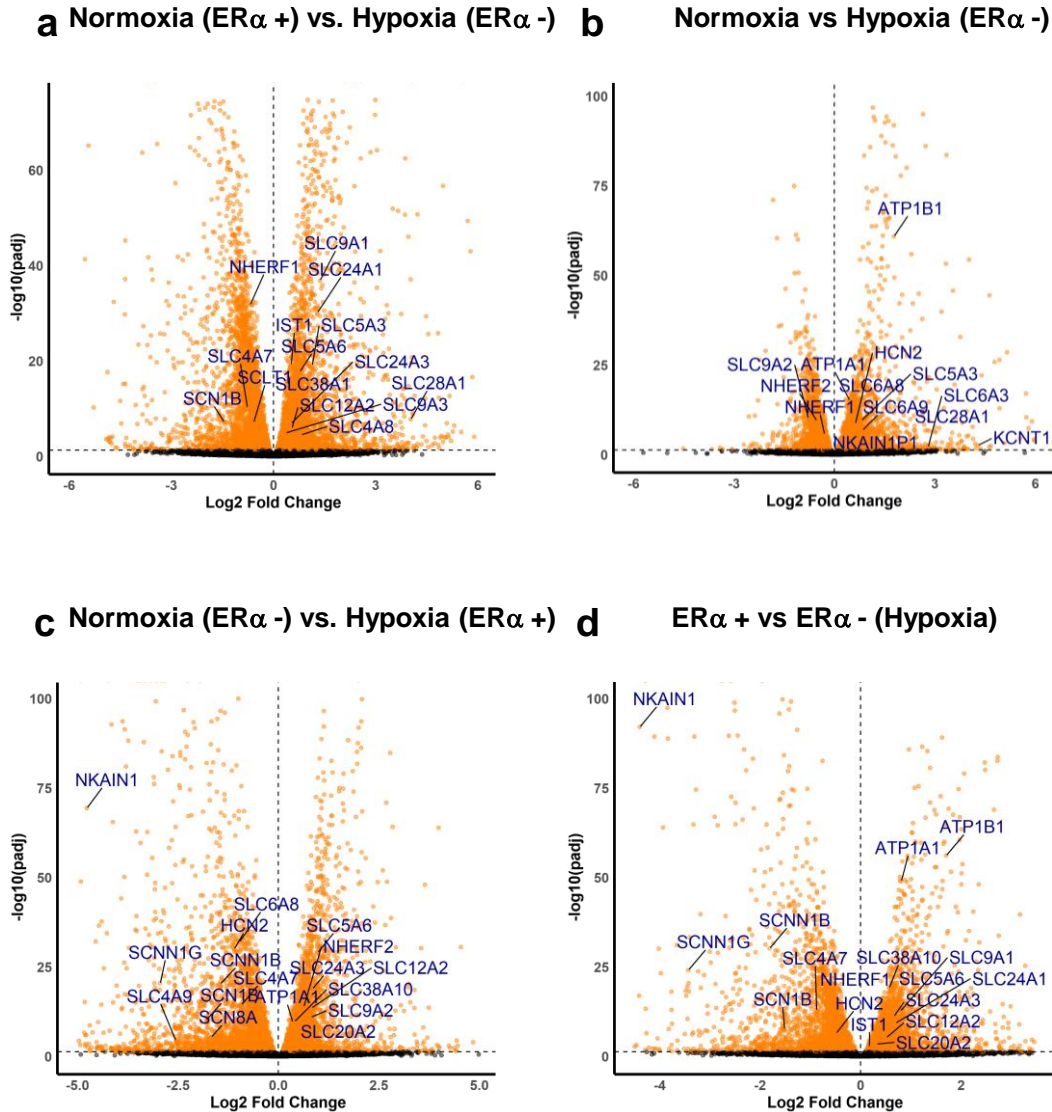


c Normoxia (ER α -) vs. Hypoxia (ER α +) **d** ER α + vs ER α - (Hypoxia)



Appendix Figure III Transcriptome-Wide Expression Changes in MCF-7 Cells

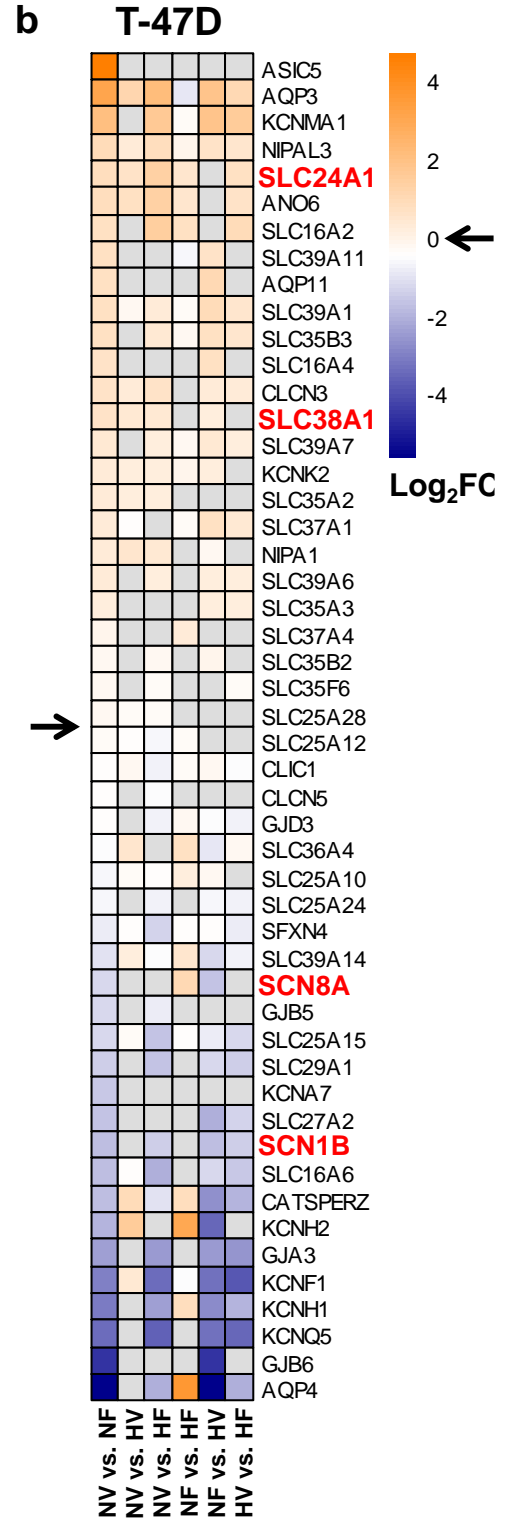
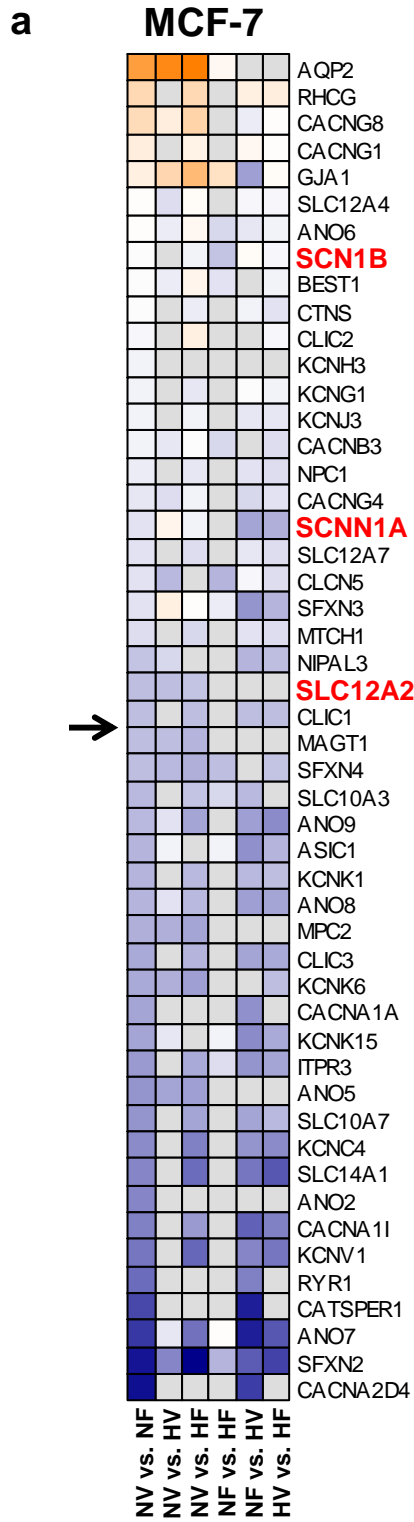
Following Different Oxygen and ER α Perturbations. Volcano plots of differentially expressed genes in MCF-7 cells **(a)** cultured in normoxia with vehicle vs. hypoxia with fulvestrant, **(b)** cultured in normoxia with fulvestrant vs. hypoxia with fulvestrant, **(c)** normoxia with fulvestrant vs. hypoxia with vehicle or **(d)** in hypoxia with vehicle or fulvestrant. Orange symbols above horizontal dashed line show significant differentially expressed genes ($padj < 0.05$). Orange symbols on the left of the vertical dashed line are significantly downregulated (negative Log_2 FoldChange). Orange symbols on the right of the vertical dashed line are significantly upregulated (positive Log_2 FoldChange). Black symbols are genes which were not significantly differentially expressed ($padj > 0.05$). Gene annotations are significant differentially expressed Na⁺ channel genes with the smallest $padj$.



Appendix Figure IV Transcriptome-Wide Expression Changes in T-47D Cells

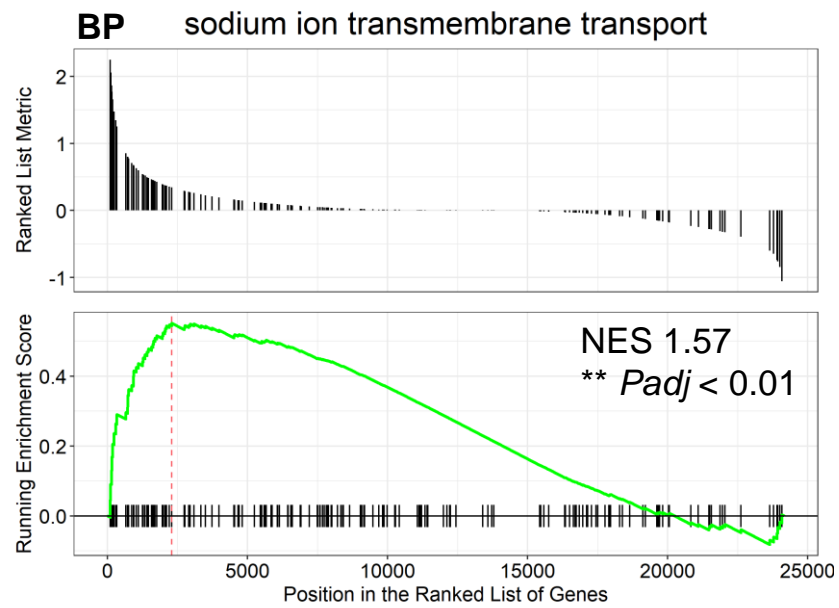
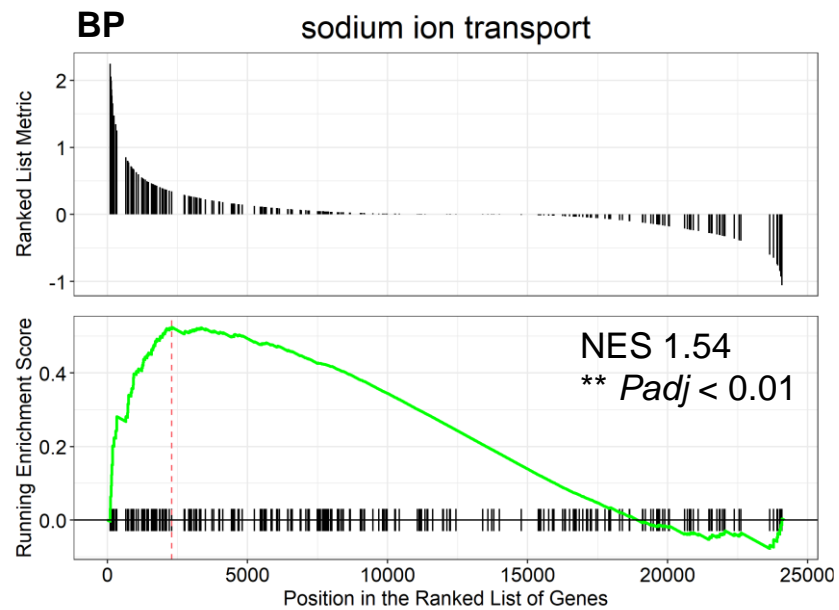
Following Different Oxygen and ER α Perturbations. Volcano plots of differentially expressed genes in T-47D cells **(a)** cultured in normoxia with vehicle vs. hypoxia with fulvestrant, **(b)** cultured in normoxia with fulvestrant vs. hypoxia with fulvestrant, **(c)** normoxia with fulvestrant vs. hypoxia with vehicle or **(d)** in hypoxia with vehicle or fulvestrant. Orange symbols above horizontal dashed line show significant differentially expressed genes ($padj < 0.05$). Orange symbols on the left of the vertical dashed line are significantly downregulated (negative Log_2 FoldChange). Orange symbols on the right of the vertical dashed line are significantly upregulated (positive Log_2 FoldChange). Black symbols are genes which were not significantly differentially expressed ($padj > 0.05$). Gene annotations are significant differentially expressed Na⁺ channel genes with the smallest $padj$.

Appendix Figure V Heatmaps of Ion Channel Genes with Greatest Significant Log₂ Fold Change in Expression Following 48 Hours of Hypoxic Culture. DGEA of RNA-seq data showing significant ($p_{adj} < 0.05$) top 25 most upregulated (light to dark orange contrast) and bottom 25 most downregulated (light to dark blue contrast) ion channel genes according to Log₂FC in ER α + normoxic vs. hypoxic (NV vs. HV) **(a)** MCF-7 and **(b)** T-47D breast cancer cells. Corresponding alterations in ion channel gene expression in; normoxia and vehicle vs. normoxia and fulvestrant (NV vs. NF), normoxia and vehicle vs. hypoxia and fulvestrant (NV vs. HF), normoxia and fulvestrant vs. hypoxia and fulvestrant (NF vs. HF), normoxia and fulvestrant vs. hypoxia and vehicle (NF vs. HV) and hypoxia and vehicle vs. hypoxia and fulvestrant (HV vs. HF) is shown. Black arrows indicate up- and down-regulated divergence. Grey indicated an ion channel gene that is not significantly differentially expressed in the comparison ($p_{adj} > 0.05$). Gene names highlighted in red are Na⁺ channel genes.



Appendix Figure VI Heatmaps of Ion Channel Genes with Greatest Significant Log₂

Fold Change in Expression Following ER α Knockdown. DGEA of RNA-seq data showing significant ($p_{adj} < 0.05$) top 25 most upregulated (light to dark orange contrast) and bottom 25 most downregulated (light to dark blue contrast) ion channel genes according to Log₂FC in ER α ⁺ vs. ER α ⁻ normoxic (NV vs. NF) **(a)** MCF-7 and **(b)** T-47D breast cancer cells. Corresponding alterations in ion channel gene expression in; normoxia and vehicle vs. hypoxia and vehicle (NV vs. HV), normoxia and vehicle vs. hypoxia and fulvestrant (NV vs. HF), normoxia and fulvestrant vs. hypoxia and fulvestrant (NF vs. HF), normoxia and fulvestrant vs. hypoxia and vehicle (NF vs. HV) and hypoxia and vehicle vs. hypoxia and fulvestrant (HV vs. HF) is shown. Black arrows indicate up- and down-regulated divergence. Grey indicated an ion channel gene that is not significantly differentially expressed in the comparison ($p_{adj} > 0.05$). Gene names highlighted in red are Na⁺ channel genes.

a**b**

Appendix Figure VII GSEA Plot Showing Positive Enrichment of Na⁺ Transporter Genes in ER α - Hypoxic vs. Normoxic T-47D Cells. Targeted GSEA identified positive enrichment for genes in **(a)** BPs “sodium ion transmembrane transport” (GO:0035725) and **(b)** “sodium ion transport” (GO:0006814) in ER α - T-47D cells cultured in hypoxia compared to normoxia. Significantly differentially expressed genes were ranked from most positive Log₂FC to most negative Log₂FC for GSEA. ** *p*_{adj} < 0.01.

Appendix Table I Most Upregulated Genes According to Log₂FC in Normoxic vs. Hypoxic MCF-7 Cells. Gene function descriptions are from UniProtKB (available at uniprot.org) or GeneCards (available at genecards.org).

Gene Symbol	Log ₂ FC	<i>P</i> adj	Function
<i>CA9</i>	7.75	3.65E-75	Catalyses interconversion between carbon dioxide and water and the dissociated ions of carbonic acid
<i>PTPRN</i>	6.66	2.12E-08	Important for vesicle-mediated secretory processes in hippocampus, pituitary and pancreatic islets
<i>AQP2</i>	6.52	5.79E-08	Essential for maintaining an osmotic gradient in renal collecting ducts by forming a water-specific channel on the plasma membrane.
<i>TRNFRSF6B</i>	5.91	2.91E-05	Proposed to play a role in suppressing FasL- and LIGHT-mediated cell death.
<i>CASP14</i>	5.88	1.23E-51	Non-apoptotic caspase involved in epidermal differentiation. Is the predominant caspase in epidermal stratum corneum
<i>EGR4</i>	5.77	2.86E-26	Transcriptional regulator that activates target genes required for mitogenesis and differentiation.
<i>PPP1R3G</i>	5.68	1.39E-24	Glycogen-targeting subunit for protein phosphatase 1 (PP1). Involved in the regulation of hepatic glycogenesis.
<i>S100A3</i>	5.58	0.00013	Binds calcium and zinc. May be involved in calcium-dependent cuticle cell differentiation, hair shaft and hair cuticular barrier formation
<i>FOSB</i>	5.16	1.32E-237	Forms part of the AP-1 complex, binding promoters containing AP-1 ssequences and enhancing transcriptional activity.
<i>S100A4</i>	4.84	6.34E-152	Calcium-binding protein involved in motility, angiogenesis, cell differentiation, apoptosis, and autophagy
<i>SLC28A1</i>	4.83	3.24E-05	Na ⁺ and pyrimidine nucleoside symporter that imports pyrimidines into cells by coupling transport to transmembrane Na ⁺ gradient.
<i>EGR2</i>	4.81	8.69E-64	Sequence-specific DNA-binding transcription factor involved in hindbrain segmentation by regulating homeobox containing genes.

Appendix Table II Most Downregulated Genes According to Log₂FC in Normoxic vs. Hypoxic MCF-7 Cells. Gene function descriptions are from UniProtKB (available at uniprot.org) or GeneCards (available at genecards.org).

Gene Symbol	Log ₂ FC	<i>P</i> adj	Function
<i>SPDYE2B</i>	-4.27	2.00E-05	Predicted to enable kinase binding activity.
<i>GP2</i>	-4.09	0.00051	Functions as an intestinal M-cell transcytotic receptor in the mucosal immune response toward type-I-piliated bacteria.
<i>RPL32P24</i>	-3.66	0.005614	Ribosomal Protein L32 Pseudogene 24.
<i>MYBPH</i>	-3.60	0.006257	Predicted to be a structural constituent of muscle, involved in regulation of striated muscle contraction.
<i>THRSP</i>	-3.02	0.00193	Plays a role in the regulation of lipogenesis, especially in lactating mammary gland.
<i>MCTS2</i>	-2.85	0.000465	Malignant T-cell-amplified sequence 2: Imprinted gene expressed from the paternal allele in foetal spinal cord.
<i>AOX1</i>	-2.78	6.81E-23	Oxidase with broad substrate specificity. Probably involved in regulation of ROS homeostasis.
<i>FSIP1</i>	-2.44	8.40E-08	May play a role in tumorigenesis and invasion of breast cancer and is a potential biomarker for breast cancer diagnosis or prognosis.
<i>CYP26B1</i>	-2.30	2.67E-11	A cytochrome P450 monooxygenase involved in the metabolism of retinoates (RAs), the active metabolites of vitamin A.
<i>ACOX2</i>	-2.23	0.002142	Oxidizes the CoA esters of the bile acid intermediates di- and tri-hydroxycholestanic acids.
<i>ENTREP2</i>	-2.17	0.014111	Predicted to be an integral component of the membrane.
<i>VXN</i>	-2.08	2.48E-06	Required for neurogenesis in the neural plate and retina. Strongly cooperates with neural bHLH factors to promote neurogenesis.

Appendix Table III Most Upregulated Genes According to Log₂FC in Normoxic vs. Hypoxic T-47D Cells. Gene function descriptions are from UniProtKB (available at uniprot.org) or GeneCards (available at genecards.org).

Gene Symbol	Log₂FC	<i>P</i>adj	Function
<i>CA9</i>	6.57	5.74E-22	Catalyses interconversion between carbon dioxide and water and the dissociated ions of carbonic acid
<i>PTPRN</i>	5.90	2.72E-07	Important for vesicle-mediated secretory processes in hippocampus, pituitary and pancreatic islets
<i>KRT3</i>	5.73	9.63E-05	Member of the keratin gene family. Type II keratin expressed in corneal epithelium with KRT12.
<i>PPFIA4</i>	5.06	2.23E-38	May regulate disassembly of focal adhesions. May localise phosphatases on plasma membrane, regulating interaction with ECM.
<i>KCNQ2</i>	4.90	0.000429	Associates with KCNQ3 to form a potassium channel important in the regulation of neuronal excitability.
<i>NDRG1</i>	4.80	1.57E-27	Stress-responsive protein involved in cell growth and differentiation. Tumour suppressor in many cell types.
<i>BPIFB2</i>	4.64	0.000471	A member of the lipid transfer / lipopolysaccharide binding protein (LT/LBP) gene family.
<i>EPO</i>	4.56	5.96E-05	Involved in regulation of erythrocyte proliferation and differentiation and maintenance of circulating erythrocyte mass
<i>MAP7D2</i>	4.41	3.25E-20	Predicted to be involved in microtubule cytoskeleton organisation.
<i>LRRC15</i>	4.20	1.02E-40	Enables collagen, fibronectin and laminin binding activity. Involved in positive regulation of cell migration.
<i>CASP14</i>	4.13	1.95E-22	Non-apoptotic caspase involved in epidermal differentiation. Is the predominant caspase in epidermal stratum corneum.
<i>NRG2</i>	4.04	0.001671	Direct ligand for ERBB3 and ERBB4 tyrosine kinase receptors. May also promote the heterodimerization with the EGF receptor.

Appendix Table IV Most Downregulated Genes According to Log₂FC in Normoxic vs. Hypoxic T-47D Cells. Gene function descriptions are from UniProtKB (available at uniprot.org) or GeneCards (available at genecards.org).

Gene Symbol	Log₂FC	P_{adj}	Function
<i>GLYATL3</i>	-2.73	0.000531	Catalyses conjugation of long-chain fatty acyl-CoA thioester and glycine to produce long-chain N-(fatty acyl)glycine.
<i>RNA5-8SP6</i>	-2.52	0.000274	RNA, 5.8S Ribosomal Pseudogene 6.
<i>IGKV2OR2-10</i>	-2.34	0.012728	Immunoglobulin Kappa Variable 2/OR2-10 Pseudogene.
<i>OR11H7</i>	-2.09	0.000546	Olfactory receptors interact with odorant molecules in the nose, to initiate a neuronal response that triggers perception of smell.
<i>ASNSP1</i>	-2.06	5.13E-13	Asparagine Synthetase Pseudogene 1.
<i>SINHCAFP3</i>	-2.03	0.00117	Family With Sequence Similarity 60 Member D, Pseudogene.
<i>GPR174</i>	-1.98	0.004715	G-protein-coupled receptor of lysophosphatidylserine (LysoPS) that plays different roles in immune response.
<i>GLRA3</i>	-1.98	0.000145	Glycine receptors are ligand-gated chloride channels. Channel opening is triggered by extracellular glycine.
<i>ANKRD30BL</i>	-1.80	8.52E-09	Ankyrin Repeat Domain 30B Pseudogene 3.
<i>POU3F3</i>	-1.78	0.000191	Encodes a POU-domain containing protein that functions as a transcription factor that may be involved in nervous system development.
<i>SP8</i>	-1.77	0.000379	Transcription factor which positively regulates FGF8 expression in apical ectodermal ridge and contributes to limb outgrowth in embryos.
<i>UGT2B11</i>	-1.70	0.017192	Enables glucuronosyltransferase activity. Involved in oestrogen metabolic process and xenobiotic glucuronidation.

Appendix Table V Most Upregulated Genes According to Log₂FC in Vehicle vs. Fulvestrant Treated MCF-7 Cells. Gene function descriptions are from UniProtKB (available at uniprot.org) or GeneCards (available at genecards.org).

Gene Symbol	Log₂FC	P_{adj}	Function
<i>AQP10</i>	9.47	3.80E-11	Water channel that mediates water transport across cell membranes irrespective of the cytosolic pH. Also permeable to glycerol.
<i>UBD</i>	8.21	3.53E-08	Ubiquitin-like protein modifier which can be covalently attached to target protein and leads to protein degradation by the 26S proteasome.
<i>SLC4A4</i>	7.91	8.77E-08	Electrogenic sodium/bicarbonate cotransporter with a Na ⁺ :HCO ₃ ⁻ stoichiometry, May regulate bicarbonate influx/efflux and regulate pH _i .
<i>REG4</i>	7.65	2.38E-40	Calcium-independent lectin. Maintains carbohydrate recognition activity in acidic environment.
<i>CNR1</i>	7.37	1.07E-44	G-protein coupled receptor for endogenous cannabinoids.
<i>ABCA4</i>	7.33	4.97E-09	Flippase that catalyses transport of retinal-phosphatidylethanolamine conjugates to cytoplasmic leaflet of photoreceptors.
<i>DHRS3</i>	7.12	0	Catalyses the reduction of all-trans-retinal to all-trans-retinol in the presence of NADPH.
<i>VSIR</i>	6.98	5.00E-17	Immunoregulatory receptor which inhibits the T-cell response. May promote differentiation of embryonic stem cells.
<i>TMEM238L</i>	6.97	7.00E-09	May play a role in inducing apoptosis during endoplasmic reticulum (ER) stress and in the inhibition of proliferation and tumorigenicity.
<i>ANAPC1P3</i>	6.49	5.06E-05	Anaphase Promoting Complex Subunit 1 Pseudogene.
<i>BPIFA4P</i>	6.39	1.90E-07	Predicted to enable lipid binding activity and to be involved in regulation of liquid surface tension.
<i>GABBR2</i>	6.30	9.84E-15	Component of G-protein coupled receptor for GABA. Signalling activates K ⁺ channels, inactivates voltage-dependent Ca ²⁺ -channels

Appendix Table V Most Downregulated Genes According to Log₂FC in Vehicle vs. Fulvestrant Treated MCF-7 Cells. Gene function descriptions are from UniProtKB (available at uniprot.org) or GeneCards (available at genecards.org).

Gene Symbol	Log₂FC	P_{adj}	Function
<i>RAMP3</i>	-8.28	6.69E-36	Plays a role in cardioprotection by reducing cardiac hypertrophy and perivascular fibrosis in a GPER1-dependent manner.
<i>AGR3</i>	-7.83	3.44E-109	Required for Ca ²⁺ -mediated regulation of ciliary beat frequency in the airway. Might be involved in regulation of intracellular Ca ²⁺ .
<i>IGSF1</i>	-7.38	1.78E-38	Seems to be a coreceptor in inhibin signalling but seems not to be a high-affinity inhibin receptor.
<i>FAM72C</i>	-7.36	6.37E-06	Novel neuronal progenitor cell protein with potential tumorigenic effects.
<i>ASCL1</i>	-7.31	1.09E-42	bHLH transcription factor involved in neuronal commitment and differentiation of olfactory and autonomic neurons.
<i>VCAN</i>	-7.30	9.68E-12	Chondroitin sulphate proteoglycan of the ECM. Involved in cell adhesion, proliferation, migration and angiogenesis.
<i>TMPRSS3</i>	-7.19	3.31E-09	Probable serine protease. Acts as a permissive factor for cochlear hair cell survival and activation at the onset of hearing.
<i>HMGA1P7</i>	-7.03	5.19E-06	High Mobility Group AT-Hook 1 Pseudogene 7
<i>BFSP2</i>	-7.00	3.86E-11	Plays a role in maintenance of retinal lens optical clarity.
<i>ARHGAP36</i>	-6.95	2.53E-36	GTPase activator for the Rho-type GTPases by converting them to an inactive GDP-bound state.
<i>SLC16A14</i>	-6.42	1.73E-82	Proton-linked monocarboxylate transporter. May catalyse transport of monocarboxylates across the plasma membrane.
<i>FGFBP2</i>	-6.38	3.03E-07	Serum protein that is selectively secreted by cytotoxic lymphocytes and may be involved in cytotoxic lymphocyte-mediated immunity.

Appendix Table VII Most Upregulated Genes According to Log₂FC in Vehicle vs. Fulvestrant Treated T-47D Cells. Gene function descriptions are from UniProtKB (available at uniprot.org) or GeneCards (available at genecards.org).

Gene Symbol	Log₂FC	P_{adj}	Function
<i>SFT2D3</i>	6.855441	0.009904	May be involved in fusion of retrograde transport vesicles derived from an endocytic compartment with the Golgi complex.
<i>LIPF</i>	6.836711	1.67E-06	Catalyses the hydrolysis of triacylglycerols to yield free fatty acids, diacylglycerol, monoacylglycerol, and glycerol.
<i>KRT223P</i>	5.855767	9.23E-12	Keratin 223 Pseudogene
<i>PLEKHG7</i>	5.113326	1.17E-12	Predicted to enable guanyl-nucleotide exchange factor activity. Predicted to be involved in Rho protein signal transduction.
<i>CCR2</i>	4.711062	5.21E-12	Functional receptor for CCL2. Mediates chemotaxis and migration induction through activation of the PI3K cascade.
<i>GLRA2</i>	4.647974	2.63E-05	Glycine receptors are ligand-gated chloride channels. Contributes to the generation of inhibitory postsynaptic currents.
<i>FPR3</i>	4.485134	1.45E-31	Low affinity receptor for neutrophils chemotactic factors. Binding of FMLP to the receptor causes activation of neutrophils.
<i>MS4A7</i>	4.116863	8.06E-21	May be involved in signal transduction as a component of a multimeric receptor complex.
<i>ANOS1</i>	4.085046	3.70E-10	Chemoattractant for foetal olfactory epithelial cells.
<i>NDP</i>	4.083664	2.99E-18	Activates canonical Wnt signalling pathway through FZD4 and LRP5 coreceptor. Plays a central role in retinal vascularisation.
<i>LTF</i>	4.082233	0.000219	Iron binding transport protein which can bind two Fe ³⁺ ions in association with the binding of an anion, usually bicarbonate.
<i>CLCA2</i>	3.958383	2.74E-22	Plays a role in modulating Cl ⁻ current across the plasma membrane. May act as a tumour suppressor in breast and colorectal cancer.

Appendix Table VIII Most Downregulated Genes According to Log₂FC in Vehicle vs. Fulvestrant Treated T-47D Cells. Gene function descriptions are from UniProtKB (available at uniprot.org) or GeneCards (available at genecards.org).

Gene Symbol	Log₂FC	P_{adj}	Function
<i>FGFBP2</i>	-9.96	3.34E-15	Serum protein that is selectively secreted by cytotoxic lymphocytes and may be involved in cytotoxic lymphocyte-mediated immunity.
<i>SPINK4</i>	-9.33	9.68E-19	Predicted to be involved in negative regulation of endopeptidase activity and response to xenobiotic stimulus.
<i>WARS2P1</i>	-7.24	1.99E-07	Tryptophanyl TRNA Synthetase 2, Mitochondrial Pseudogene.
<i>GATA4</i>	-6.40	1.21E-19	Transcriptional activator that plays a key role in cardiac development and function.
<i>DOK7</i>	-6.12	2.24E-91	Probable muscle-intrinsic activator of MUSK that plays an essential role in neuromuscular synaptogenesis.
<i>ACOX2</i>	-5.92	2.43E-51	Oxidizes the CoA esters of the bile acid intermediates di- and tri-hydroxycholestanic acids.
<i>PDZK1</i>	-5.82	1.47E-206	Scaffold protein may be involved in coordination of regulator processes for ion transport and second messenger cascades.
<i>WSCD2</i>	-5.67	2.55E-06	Sialate:O-sulfotransferase which catalyzes 8-O-sulfation at the Sia-glycan level.
<i>IL20</i>	-5.36	0.00034	Pro-inflammatory and angiogenic cytokine secreted by monocytes and skin keratinocytes that plays crucial roles in immune responses.
<i>AQP4</i>	-5.34	1.35E-05	Plays an important role in brain water homeostasis and is required for normal water exchange across the blood brain interface.
<i>CD34</i>	-5.23	6.90E-36	Possible adhesion molecule in haematopoiesis mediating attachment of stem cells to bone marrow ECM or stromal cells.
<i>SPRY4</i>	-5.16	1.89E-08	Suppresses the insulin receptor and EGFR-transduced MAPK signalling pathway. Inhibits Ras-independent RAF1 activation.

References

- Abal M, Andreu JM, Barasoain I (2003) Taxanes: microtubule and centrosome targets, and cell cycle dependent mechanisms of action. *Curr Cancer Drug Targets* 3:193–203.
- Abdelmohsen K, Panda AC, Kang M-J, Guo R, Kim J, Grammatikakis I, Yoon J-H, Dudekula DB, Noh JH, Yang X, Martindale JL, Gorospe M (2014) 7SL RNA represses p53 translation by competing with HuR. *Nucleic Acids Res* 42:10099–10111.
- Abdul M, Hoosein N (2002) Voltage-gated sodium ion channels in prostate cancer: expression and activity. *Anticancer Res* 22:1727–1730.
- Abubakar M, Figueroa J, Ali HR, Blows F, Lissowska J, Caldas C, Easton DF, Sherman ME, Garcia-Closas M, Dowsett M, Pharoah PD (2019) Combined quantitative measures of ER, PR, HER2, and KI67 provide more prognostic information than categorical combinations in luminal breast cancer. *Mod Pathol* 32:1244–1256.
- Aguiar VRC, Castelli EC, Single RM, Bashirova A, Ramsuran V, Kulkarni S, Augusto DG, Martin MP, Gutierrez-Arcelus M, Carrington M, Meyer D (2023) Comparison between qPCR and RNA-seq reveals challenges of quantifying HLA expression. *Immunogenetics* 75:249–262.
- Ahmad T, Ertuglu LA, Masenga SK, Kleyman TR, Kirabo A (2023) The epithelial sodium channel in inflammation and blood pressure modulation. *Front Cardiovasc Med* 10:1130148.
- Ai Y, Zhang X, Hu X, Gao J, Liu J, Ou S, Wang J (2023) Role of the voltage-gated sodium channel Nav1.6 in glioma and candidate drugs screening. *Int J Mol Med* 51 Available at: <https://pubmed.ncbi.nlm.nih.gov/37052249/> [Accessed September 21, 2024].
- Akiba I, Seki T, Mori M, Iizuka M, Nishimura S, Sasaki S, Imoto K, Barsoumian EL (2003) Stable expression and characterization of human PN1 and PN3 sodium channels. *Receptors Channels* 9:291–299.
- Alla RK, Cairns BR (2014) RNA polymerase III transcriptomes in human embryonic stem cells and induced pluripotent stem cells, and relationships with pluripotency transcription factors. *PLoS One* 9:e85648.
- Allen DH, Lepple-Wienhues A, Cahalan MD (1997) Ion channel phenotype of melanoma cell lines. *J Membr Biol* 155:27–34.
- Altucci L, Addeo R, Cicatiello L, Dauvois S, Parker MG, Truss M, Beato M, Sica V, Bresciani F, Weisz A (1996) 17beta-Estradiol induces cyclin D1 gene transcription, p36D1-p34cdk4 complex activation and p105Rb phosphorylation during mitogenic stimulation of G(1)-arrested human breast cancer cells. *Oncogene* 12:2315–2324.
- Altwegg KA, Vadlamudi RK (2021) Role of estrogen receptor coregulators in endocrine resistant breast cancer. *Explor Target Antitumor Ther* 2:385–400.

- An WG, Kanekal M, Simon MC, Maltepe E, Blagosklonny MV, Neckers LM (1998) Stabilization of wild-type p53 by hypoxia-inducible factor 1alpha. *Nature* 392:405–408.
- Anders S, Huber W (2010) Differential expression analysis for sequence count data. *Genome Biol* 11:R106.
- Andersen CL, Jensen JL, Ørntoft TF (2004) Normalization of real-time quantitative reverse transcription-PCR data: a model-based variance estimation approach to identify genes suited for normalization, applied to bladder and colon cancer data sets. *Cancer Res* 64:5245–5250.
- Anderson JD, Hansen TP, Lenkowski PW, Walls AM, Choudhury IM, Schenck HA, Friehling M, Höll GM, Patel MK, Sikes RA, Brown ML (2003) Voltage-gated sodium channel blockers as cytostatic inhibitors of the androgen-independent prostate cancer cell line PC-3. *Mol Cancer Ther* 2:1149–1154.
- Angelucci A, Valentini A, Millimaggi D, Gravina GL, Miano R, Dolo V, Vicentini C, Bologna M, Federici G, Bernardini S (2006) Valproic acid induces apoptosis in prostate carcinoma cell lines by activation of multiple death pathways. *Anticancer Drugs* 17:1141–1150.
- Angus M, Ruben P (2019) Voltage gated sodium channels in cancer and their potential mechanisms of action. *Channels* 13:400–409.
- Anurag M, Ellis MJ, Haricharan S (2018) DNA damage repair defects as a new class of endocrine treatment resistance driver. *Oncotarget* 9:36252–36253.
- Anzai E, Hirata K, Shibazaki M, Yamada C, Morii M, Honda T, Yamaguchi N, Yamaguchi N (2017) FOXA1 induces E-cadherin expression at the protein level via suppression of Slug in epithelial breast cancer cells. *Biol Pharm Bull* 40:1483–1489.
- Araste F, Abnous K, Hashemi M, Dehshahri A, Detampel P, Alibolandi M, Ramezani M (2020) Na⁺/K⁺ ATPase-targeted delivery to metastatic breast cancer models. *Eur J Pharm Sci* 143:105207.
- Arimbasseri AG, Maraia RJ (2016) RNA Polymerase III Advances: Structural and tRNA Functional Views. *Trends Biochem Sci* 41:546–559.
- Armstrong CM, Bezanilla F (1977) Inactivation of the sodium channel. II. Gating current experiments. *J Gen Physiol* 70:567–590.
- Arponen O, McLean MA, Nanaa M, Manavaki R, Baxter GC, Gill AB, Riemer F, Kennerley AJ, Woitek R, Kaggie JD, Brackenbury WJ, Gilbert FJ (2024) ²³Na MRI: inter-reader reproducibility of normal fibroglandular sodium concentration measurements at 3 T. *Eur Radiol Exp* 8:75.
- Arts GJ, Fornerod M, Mattaj IW (1998) Identification of a nuclear export receptor for tRNA. *Curr Biol* 8:305–314.
- Asghari A, Wall K, Gill M, Vecchio ND, Allahbakhsh F, Wu J, Deng N, Zheng WJ, Wu H, Umetani M, Maroufy V (2022) A novel group of genes that cause endocrine resistance in breast cancer identified by dynamic gene expression analysis. *Oncotarget* 13:600–613.

- Attwell D, Laughlin SB (2001) An energy budget for signaling in the grey matter of the brain. *J Cereb Blood Flow Metab* 21:1133–1145.
- Bae YJ, Yoo J-C, Park N, Kang D, Han J, Hwang E, Park J-Y, Hong S-G (2013) Acute hypoxia activates an ENaC-like channel in rat pheochromocytoma (PC12) cells. *Korean J Physiol Pharmacol* 17:57–64.
- Baker Bechmann M, Rotoli D, Morales M, Maeso MDC, García MDP, Ávila J, Mobasher A, Martín-Vasallo P (2016) Na,K-ATPase isozymes in colorectal cancer and liver metastases. *Front Physiol* 7:9.
- Baldin J-P, Barth D, Fronius M (2020) Epithelial Na⁺ channel (ENaC) formed by one or two subunits forms functional channels that respond to shear force. *Front Physiol* 11:141.
- Baloglu E, Nonnenmacher G, Seleninova A, Berg L, Velineni K, Ermis-Kaya E, Mairbäurl H (2020) The role of hypoxia-induced modulation of alveolar epithelial Na⁺- transport in hypoxemia at high altitude. *Pulm Circ* 10:50–58.
- Baptista-Hon DT, Robertson FM, Robertson GB, Owen SJ, Rogers GW, Lydon EL, Lee NH, Hales TG (2014) Potent inhibition by ropivacaine of metastatic colon cancer SW620 cell invasion and NaV1.5 channel function. *Br J Anaesth* 113 Suppl 1:i39–i48.
- Barrett T, Riemer F, McLean MA, Kaggie J, Robb F, Tropp JS, Warren A, Bratt O, Shah N, Gnanapragasam VJ, Gilbert FJ, Graves MJ, Gallagher FA (2018) Quantification of Total and Intracellular Sodium Concentration in Primary Prostate Cancer and Adjacent Normal Prostate Tissue With Magnetic Resonance Imaging. *Invest Radiol* 53:450–456.
- Belton J-M, McCord RP, Gibcus JH, Naumova N, Zhan Y, Dekker J (2012) Hi-C: a comprehensive technique to capture the conformation of genomes. *Methods* 58:268–276.
- Ben-David U et al. (2018) Genetic and transcriptional evolution alters cancer cell line drug response. *Nature* 560:325–330.
- Benhaim L, Gerger A, Bohanes P, Paez D, Wakatsuki T, Yang D, Labonte MJ, Ning Y, El-Khoueiry R, Loupakis F, Zhang W, Laurent-Puig P, Lenz HJ (2014) Gender-specific profiling in SCN1A polymorphisms and time-to-recurrence in patients with stage II/III colorectal cancer treated with adjuvant 5-fluoruracil chemotherapy. *Pharmacogenomics J* 14:135–141.
- Benjamini Y, Hochberg Y (1995) Controlling the false discovery rate: A practical and powerful approach to multiple testing. *J R Stat Soc Series B Stat Methodol* 57:289–300.
- Bennett ES, Smith BA, Harper JM (2004) Voltage-gated Na⁺ channels confer invasive properties on human prostate cancer cells. *Pflugers Arch* 447:908–914.
- Berg MD, Brandl CJ (2021) Transfer RNAs: diversity in form and function. *RNA Biol* 18:316–339.

- Bergers G, Brekken R, McMahon G, Vu TH, Itoh T, Tamaki K, Tanzawa K, Thorpe P, Itohara S, Werb Z, Hanahan D (2000) Matrix metalloproteinase-9 triggers the angiogenic switch during carcinogenesis. *Nat Cell Biol* 2:737–744.
- Bernardo GM, Keri RA (2012) FOXA1: a transcription factor with parallel functions in development and cancer. *Biosci Rep* 32:113–130.
- Bezanilla F, Armstrong CM (1977) Inactivation of the sodium channel. I. Sodium current experiments. *J Gen Physiol* 70:549–566.
- Bharti SK, Kakkad S, Danhier P, Wildes F, Penet M-F, Krishnamachary B, Bhujwalla ZM (2019) Hypoxia patterns in primary and metastatic prostate cancer environments. *Neoplasia* 21:239–246.
- Bian Y, Tuo J, He L, Li W, Li S, Chu H, Zhao Y (2023) Voltage-gated sodium channels in cancer and their specific inhibitors. *Pathol Res Pract* 251:154909.
- Birch J, Clarke CJ, Campbell AD, Campbell K, Mitchell L, Liko D, Kalna G, Strathdee D, Sansom OJ, Neilson M, Blyth K, Norman JC (2016) The initiator methionine tRNA drives cell migration and invasion leading to increased metastatic potential in melanoma. *Biol Open* 5:1371–1379.
- Björnström L, Sjöberg M (2002) Mutations in the estrogen receptor DNA-binding domain discriminate between the classical mechanism of action and cross-talk with Stat5b and activating protein 1 (AP-1). *J Biol Chem* 277:48479–48483.
- Black JA, Liu S, Waxman SG (2009) Sodium channel activity modulates multiple functions in microglia. *Glia* 57:1072–1081.
- Blanco G, Koster JC, Mercer RW (1994) The alpha subunit of the Na,K-ATPase specifically and stably associates into oligomers. *Proc Natl Acad Sci U S A* 91:8542–8546.
- Blandino JK, Viglione MP, Bradley WA, Oie HK, Kim YI (1995) Voltage-dependent sodium channels in human small-cell lung cancer cells: role in action potentials and inhibition by Lambert-Eaton syndrome IgG. *J Membr Biol* 143:153–163.
- Bogdanov A, Moiseenko F, Dubina M (2017) Abnormal expression of ATP1A1 and ATP1A2 in breast cancer. *F1000Res* 6:10.
- Boivin V, Deschamps-Francoeur G, Couture S, Nottingham RM, Bouchard-Bourelle P, Lambowitz AM, Scott MS, Abou-Elela S (2018) Simultaneous sequencing of coding and noncoding RNA reveals a human transcriptome dominated by a small number of highly expressed noncoding genes. *RNA* 24:950–965.
- Bon E et al. (2016) SCN4B acts as a metastasis-suppressor gene preventing hyperactivation of cell migration in breast cancer. *Nat Commun* 7:13648.
- Bondarava M, Li T, Endl E, Wehner F (2009) alpha-ENaC is a functional element of the hypertonicity-induced cation channel in HepG2 cells and it mediates proliferation. *Pflugers Arch* 458:675–687.

- Bonhoure N, Praz V, Moir RD, Willemin G, Mange F, Moret C, Willis IM, Hernandez N (2020) MAF1 is a chronic repressor of RNA polymerase III transcription in the mouse. *Sci Rep* 10:11956.
- Bourque CW (2008) Central mechanisms of osmosensation and systemic osmoregulation. *Nat Rev Neurosci* 9:519–531.
- Brackenbury WJ (2012) Voltage-gated sodium channels and metastatic disease. *Channels* 6:352–361.
- Brackenbury WJ, Chioni A-M, Diss JKJ, Djamgoz MBA (2007) The neonatal splice variant of Nav1.5 potentiates in vitro invasive behaviour of MDA-MB-231 human breast cancer cells. *Breast Cancer Res Treat* 101:149–160.
- Brackenbury WJ, Isom LL (2008) Voltage-gated Na⁺ channels: potential for beta subunits as therapeutic targets. *Expert Opin Ther Targets* 12:1191–1203.
- Brackenbury WJ, Isom LL (2011) Na Channel β Subunits: Overachievers of the Ion Channel Family. *Front Pharmacol* 2:53.
- Bray F, Laversanne M, Sung H, Ferlay J, Siegel RL, Soerjomataram I, Jemal A (2024) Global cancer statistics 2022: GLOBOCAN estimates of incidence and mortality worldwide for 36 cancers in 185 countries. *CA Cancer J Clin* 74:229–263.
- Bray NL, Pimentel H, Melsted P, Pachter L (2016) Near-optimal probabilistic RNA-seq quantification. *Nat Biotechnol* 34:525–527.
- Brisson L, Driffort V, Benoist L, Poet M, Counillon L, Antelmi E, Rubino R, Besson P, Labbal F, Chevalier S, Reshkin SJ, Gore J, Roger S (2013) NaV1.5 Na⁺ channels allosterically regulate the NHE-1 exchanger and promote the activity of breast cancer cell invadopodia. *J Cell Sci* 126:4835–4842.
- Brisson L, Gillet L, Calaghan S, Besson P, Le Guennec J-Y, Roger S, Gore J (2011) Na(V)1.5 enhances breast cancer cell invasiveness by increasing NHE1-dependent H(+) efflux in caveolae. *Oncogene* 30:2070–2076.
- Britschgi A, Andraos R, Brinkhaus H, Klebba I, Romanet V, Müller U, Murakami M, Radimerski T, Bentires-Alj M (2012) JAK2/STAT5 inhibition circumvents resistance to PI3K/mTOR blockade: a rationale for cotargeting these pathways in metastatic breast cancer. *Cancer Cell* 22:796–811.
- Bruick RK, McKnight SL (2001) A conserved family of prolyl-4-hydroxylases that modify HIF. *Science* 294:1337–1340.
- Bustin SA, Benes V, Garson JA, Hellems J, Huggett J, Kubista M, Mueller R, Nolan T, Pfaffl MW, Shipley GL, Vandesompele J, Wittwer CT (2009) The MIQE guidelines: minimum information for publication of quantitative real-time PCR experiments. *Clin Chem* 55:611–622.
- Cairns CA, White RJ (1998) p53 is a general repressor of RNA polymerase III transcription. *EMBO J* 17:3112–3123.
- Caizzi L, Ferrero G, Cutrupi S, Cordero F, Ballaré C, Miano V, Reineri S, Ricci L, Friard O, Testori A, Corà D, Caselle M, Di Croce L, De Bortoli M (2014)

- Genome-wide activity of unliganded estrogen receptor- α in breast cancer cells. *Proc Natl Acad Sci U S A* 111:4892–4897.
- Calderón-Montaña JM, Burgos-Morón E, Orta ML, Maldonado-Navas D, García-Domínguez I, López-Lázaro M (2014) Evaluating the cancer therapeutic potential of cardiac glycosides. *Biomed Res Int* 2014:794930.
- Campbell TM, Main MJ, Fitzgerald EM (2013) Functional expression of the voltage-gated Na⁺-channel Nav1.7 is necessary for EGF-mediated invasion in human non-small cell lung cancer cells. *J Cell Sci* 126:4939–4949.
- Cancer Genome Atlas Network (2012) Comprehensive molecular portraits of human breast tumours. *Nature* 490:61–70.
- Canella D, Praz V, Reina JH, Cousin P, Hernandez N (2010) Defining the RNA polymerase III transcriptome: Genome-wide localization of the RNA polymerase III transcription machinery in human cells. *Genome Res* 20:710–721.
- Canessa CM, Merillat AM, Rossier BC (1994a) Membrane topology of the epithelial sodium channel in intact cells. *Am J Physiol* 267:C1682-90.
- Canessa CM, Schild L, Buell G, Thorens B, Gautschi I, Horisberger JD, Rossier BC (1994b) Amiloride-sensitive epithelial Na⁺ channel is made of three homologous subunits. *Nature* 367:463–467.
- Capatina AL, Malcolm JR, Stenning J, Moore RL, Bridge KS, Brackenbury WJ, Holding AN (2024) Hypoxia-induced epigenetic regulation of breast cancer progression and the tumour microenvironment. *Front Cell Dev Biol* 12:1421629.
- Caradec J, Sirab N, Keumeugni C, Moutereau S, Chimingqi M, Matar C, Revaud D, Bah M, Manivet P, Conti M, Loric S (2010) “Desperate house genes”: the dramatic example of hypoxia. *Br J Cancer* 102:1037–1043.
- Carmeci C, Thompson DA, Ring HZ, Francke U, Weigel RJ (1997) Identification of a gene (GPR30) with homology to the G-protein-coupled receptor superfamily associated with estrogen receptor expression in breast cancer. *Genomics* 45:607–617.
- Carmeliet P (2005) VEGF as a key mediator of angiogenesis in cancer. *Oncology* 69 Suppl 3:4–10.
- Carreira VS, Fan Y, Wang Q, Zhang X, Kurita H, Ko C-I, Naticchioni M, Jiang M, Koch S, Medvedovic M, Xia Y, Rubinstein J, Puga A (2015) Ah receptor signaling controls the expression of cardiac development and homeostasis genes. *Toxicol Sci* 147:425–435.
- Carrithers MD, Chatterjee G, Carrithers LM, Offoha R, Iheagwara U, Rahner C, Graham M, Waxman SG (2009) Regulation of podosome formation in macrophages by a splice variant of the sodium channel SCN8A. *J Biol Chem* 284:8114–8126.
- Carroll CP, Bolland H, Vancauwenberghe E, Collier P, Ritchie AA, Clarke PA, Grabowska AM, Harris AL, McIntyre A (2022) Targeting hypoxia regulated

sodium driven bicarbonate transporters reduces triple negative breast cancer metastasis. *Neoplasia* 25:41–52.

- Carroll JS, Liu XS, Brodsky AS, Li W, Meyer CA, Szary AJ, Eeckhoute J, Shao W, Hestermann EV, Geistlinger TR, Fox EA, Silver PA, Brown M (2005) Chromosome-wide mapping of estrogen receptor binding reveals long-range regulation requiring the forkhead protein FoxA1. *Cell* 122:33–43.
- Carroll JS, Meyer CA, Song J, Li W, Geistlinger TR, Eeckhoute J, Brodsky AS, Keeton EK, Fertuck KC, Hall GF, Wang Q, Bekiranov S, Sementchenko V, Fox EA, Silver PA, Gingeras TR, Liu XS, Brown M (2006) Genome-wide analysis of estrogen receptor binding sites. *Nat Genet* 38:1289–1297.
- Catterall WA (2012) Voltage-gated sodium channels at 60: structure, function and pathophysiology. *J Physiol* 590:2577–2589.
- Cavadas MA, Mesnieres M, Crifo B, Manresa MC, Selfridge AC, Keogh CE, Fabian Z, Scholz CC, Nolan KA, Rocha LM, Tambuwala MM, Brown S, Wdowicz A, Corbett D, Murphy KJ, Godson C, Cummins EP, Taylor CT, Cheong A (2016) REST is a hypoxia-responsive transcriptional repressor. *Scientific reports* 6 Available at: <https://pubmed.ncbi.nlm.nih.gov/27531581/> [Accessed September 1, 2024].
- Cavaillès V, Augereau P, Rochefort H (1993) Cathepsin D gene is controlled by a mixed promoter, and estrogens stimulate only TATA-dependent transcription in breast cancer cells. *Biochemistry* 90:203–207.
- Chan CW, Chetnani B, Mondragón A (2013) Structure and function of the T-loop structural motif in noncoding RNAs: Structure and function of the T-loop structural motif. *Wiley Interdiscip Rev RNA* 4:507–522.
- Chen C, Pore N, Behrooz A, Ismail-Beigi F, Maity A (2001) Regulation of glut1 mRNA by Hypoxia-inducible Factor-1: INTERACTION BETWEEN H-ras AND HYPOXIA *. *J Biol Chem* 276:9519–9525.
- Chen Q, Liu Y, Zhu X-L, Feng F, Yang H, Xu W (2019) Increased NHE1 expression is targeted by specific inhibitor cariporide to sensitize resistant breast cancer cells to doxorubicin in vitro and in vivo. *BMC Cancer* 19:211.
- Chen S, Dai X, Gao Y, Shen F, Ding J, Chen Q (2017) The positivity of estrogen receptor and progesterone receptor may not be associated with metastasis and recurrence in epithelial ovarian cancer. *Sci Rep* 7:16922.
- Chen SY, Bhargava A, Mastroberardino L, Meijer OC, Wang J, Buse P, Firestone GL, Verrey F, Pearce D (1999) Epithelial sodium channel regulated by aldosterone-induced protein sgk. *Proc Natl Acad Sci U S A* 96:2514–2519.
- Chen W, Böcker W, Brosius J, Tiedge H (1997) Expression of neural BC200 RNA in human tumours. *J Pathol* 183:345–351.
- Chen X, Jin S, Chen M, Bueno C, Wolynes PG (2023a) The marionette mechanism of domain-domain communication in the antagonist, agonist, and coactivator responses of the estrogen receptor. *Proc Natl Acad Sci U S A* 120:e2216906120.

- Chen Y, Yu X, Yan Z, Zhang S, Zhang J, Guo W (2023b) Role of epithelial sodium channel-related inflammation in human diseases. *Front Immunol* 14:1178410.
- Chen Z, Krmar RT, Dada L, Efendiev R, Leibiger IB, Pedemonte CH, Katz AI, Sznajder JI, Bertorello AM (2006) Phosphorylation of adaptor protein-2 mu2 is essential for Na⁺,K⁺-ATPase endocytosis in response to either G protein-coupled receptor or reactive oxygen species. *Am J Respir Cell Mol Biol* 35:127–132.
- Chioni A-M, Brackenbury WJ, Calhoun JD, Isom LL, Djamgoz MBA (2009) A novel adhesion molecule in human breast cancer cells: voltage-gated Na⁺ channel beta1 subunit. *Int J Biochem Cell Biol* 41:1216–1227.
- Chioni A-M, Shao D, Grose R, Djamgoz MBA (2010) Protein kinase A and regulation of neonatal Nav1.5 expression in human breast cancer cells: activity-dependent positive feedback and cellular migration. *Int J Biochem Cell Biol* 42:346–358.
- Choi SYC, Lin D, Gout PW, Collins CC, Xu Y, Wang Y (2014) Lessons from patient-derived xenografts for better in vitro modeling of human cancer. *Adv Drug Deliv Rev* 79–80:222–237.
- Chung YJ, Hoare Z, Baark F, Yu CS, Guo J, Fuller W, Southworth R, Katschinski DM, Murphy MP, Eykyn TR, Shattock MJ (2024) Elevated Na is a dynamic and reversible modulator of mitochondrial metabolism in the heart. *Nat Commun* 15:4277.
- Cicatiello L, Addeo R, Sasso A, Altucci L, Petrizzi VB, Borgo R, Cancemi M, Caporali S, Caristi S, Scafoglio C, Teti D, Bresciani F, Perillo B, Weisz A (2004) Estrogens and progesterone promote persistent CCND1 gene activation during G1 by inducing transcriptional derepression via c-Jun/c-Fos/estrogen receptor (progesterone receptor) complex assembly to a distal regulatory element and recruitment of cyclin D1 to its own gene promoter. *Mol Cell Biol* 24:7260–7274.
- Clare JJ, Tate SN, Nobbs M, Romanos MA (2000) Voltage-gated sodium channels as therapeutic targets. *Drug Discov Today* 5:506–520.
- Clarke CJ et al. (2016) The Initiator Methionine tRNA Drives Secretion of Type II Collagen from Stromal Fibroblasts to Promote Tumor Growth and Angiogenesis. *Curr Biol* 26:755–765.
- Clausen MV, Hilbers F, Poulsen H (2017) The structure and function of the Na,K-ATPase isoforms in health and disease. *Front Physiol* 8:371.
- Clusan L, Ferrière F, Flouriot G, Pakdel F (2023) A basic review on estrogen receptor signaling pathways in breast cancer. *Int J Mol Sci* 24:6834.
- Comellas AP, Dada LA, Lecuona E, Pesce LM, Chandel NS, Quesada N, Budinger GRS, Strous GJ, Ciechanover A, Sznajder JI (2006) Hypoxia-mediated degradation of Na,K-ATPase via mitochondrial reactive oxygen species and the ubiquitin-conjugating system. *Circ Res* 98:1314–1322.
- Connolly E, Braunstein S, Formenti S, Schneider RJ (2006) Hypoxia inhibits protein synthesis through a 4E-BP1 and elongation factor 2 kinase pathway

- controlled by mTOR and uncoupled in breast cancer cells. *Mol Cell Biol* 26:3955–3965.
- Cook AG, Fukuhara N, Jinek M, Conti E (2009) Structures of the tRNA export factor in the nuclear and cytosolic states. *Nature* 461:60–65.
- Corbet C, Feron O (2017) Tumour acidosis: from the passenger to the driver's seat. *Nat Rev Cancer* 17:577–593.
- Corry B (2018) Physical basis of specificity and delayed binding of a subtype selective sodium channel inhibitor. *Sci Rep* 8:1356.
- Cortes J et al. (2022) Pembrolizumab plus chemotherapy in advanced triple-negative breast cancer. *N Engl J Med* 387:217–226.
- Coussens LM, Werb Z (2002) Inflammation and cancer. *Nature* 420:860–867.
- Cramer P (2002) Multisubunit RNA polymerases. *Curr Opin Struct Biol* 12:89–97.
- Creighton CJ, Massarweh S, Huang S, Tsimelzon A, Hilsenbeck SG, Osborne CK, Shou J, Malorni L, Schiff R (2008) Development of resistance to targeted therapies transforms the clinically associated molecular profile subtype of breast tumor xenografts. *Cancer Res* 68:7493–7501.
- Curtis C et al. (2012) The genomic and transcriptomic architecture of 2,000 breast tumours reveals novel subgroups. *Nature* 486:346–352.
- Dada LA, Chandel NS, Ridge KM, Pedemonte C, Bertorello AM, Sznajder JI (2003) Hypoxia-induced endocytosis of Na,K-ATPase in alveolar epithelial cells is mediated by mitochondrial reactive oxygen species and PKC-zeta. *J Clin Invest* 111:1057–1064.
- Dai X, Cheng H, Bai Z, Li J (2017) Breast Cancer Cell Line Classification and Its Relevance with Breast Tumor Subtyping. *J Cancer* 8:3131–3141.
- Dana A, Tuller T (2014) The effect of tRNA levels on decoding times of mRNA codons. *Nucleic Acids Res* 42:9171–9181.
- Dannheim FM, Walsh SJ, Orozco CT, Hansen AH, Bargh JD, Jackson SE, Bond NJ, Parker JS, Carroll JS, Spring DR (2022) All-in-one disulfide bridging enables the generation of antibody conjugates with modular cargo loading. *Chem Sci* 13:8781–8790.
- Darby SC, Ewertz M, McGale P, Bennet AM, Blom-Goldman U, Brønnum D, Correa C, Cutter D, Gagliardi G, Gigante B, Jensen M-B, Nisbet A, Peto R, Rahimi K, Taylor C, Hall P (2013) Risk of ischemic heart disease in women after radiotherapy for breast cancer. *N Engl J Med* 368:987–998.
- Davanloo P, Sprinzl M, Watanabe K, Albani M, Kersten H (1979) Role of ribothymidine in the thermal stability of transfer RNA as monitored by proton magnetic resonance. *Nucleic Acids Res* 6:1571–1581.
- Dawson S-J, Rueda OM, Aparicio S, Caldas C (2013) A new genome-driven integrated classification of breast cancer and its implications. *EMBO J* 32:617–628.

- de Jonge HJM, Fehrmann RSN, de Bont ESJM, Hofstra RMW, Gerbens F, Kamps WA, de Vries EGE, van der Zee AGJ, te Meerman GJ, ter Elst A (2007) Evidence based selection of housekeeping genes. *PLoS One* 2:e898.
- de Llobet Cucalon L, Di Vona C, Morselli M, Vezzoli M, Montanini B, Teichmann M, de la Luna S, Ferrari R (2022) An RNA polymerase III general transcription factor engages in cell type-specific chromatin looping. *Int J Mol Sci* 23:2260.
- de Souza WF, Barbosa LA, Liu L, de Araujo WM, de-Freitas-Junior JCM, Fortunato-Miranda N, Fontes CFL, Morgado-Díaz JA (2014) Ouabain-induced alterations of the apical junctional complex involve α 1 and β 1 Na,K-ATPase downregulation and ERK1/2 activation independent of caveolae in colorectal cancer cells. *J Membr Biol* 247:23–33.
- deGraffenried LA, Hilsenbeck SG, Fuqua SAW (2002) Sp1 is essential for estrogen receptor α gene transcription. *J Steroid Biochem Mol Biol* 82:7–18.
- Dehesh T, Fadaghi S, Seyedi M, Abolhadi E, Ilaghi M, Shams P, Ajam F, Mosleh-Shirazi MA, Dehesh P (2023) The relation between obesity and breast cancer risk in women by considering menstruation status and geographical variations: a systematic review and meta-analysis. *BMC Womens Health* 23:392.
- Delaunay S, Rapino F, Tharun L, Zhou Z, Heukamp L, Termathe M, Shostak K, Klevernic I, Florin A, Desmecht H, Desmet CJ, Nguyen L, Leidel SA, Willis AE, Büttner R, Chariot A, Close P (2016) Elp3 links tRNA modification to IRES-dependent translation of LEF1 to sustain metastasis in breast cancer. *J Exp Med* 213:2503–2523.
- Dembinski TC, Leung CK, Shiu RP (1985) Evidence for a novel pituitary factor that potentiates the mitogenic effect of estrogen in human breast cancer cells. *Cancer Res* 45:3083–3089.
- Denkert C, Loibl S, Noske A, Roller M, Müller BM, Komor M, Budczies J, Darb-Esfahani S, Kronenwett R, Hanusch C, von Törne C, Weichert W, Engels K, Solbach C, Schrader I, Dietel M, von Minckwitz G (2010) Tumor-associated lymphocytes as an independent predictor of response to neoadjuvant chemotherapy in breast cancer. *J Clin Oncol* 28:105–113.
- Denomme N, Hull JM, Mashour GA (2019) Role of voltage-gated sodium channels in the mechanism of ether-induced unconsciousness. *Pharmacol Rev* 71:450–466.
- Desai N, Lee J, Upadhyya R, Chu Y, Moir RD, Willis IM (2005) Two steps in Maf1-dependent repression of transcription by RNA polymerase III. *J Biol Chem* 280:6455–6462.
- Devin-Leclerc J, Meng X, Delahaye F, Leclerc P, Baulieu EE, Catelli MG (1998) Interaction and dissociation by ligands of estrogen receptor and Hsp90: the antiestrogen RU 58668 induces a protein synthesis-dependent clustering of the receptor in the cytoplasm. *Mol Endocrinol* 12:842–854.
- Dewadas HD, Kamarulzaman NS, Yaacob NS, Che Has AT, Mokhtar NF (2019) The role of HIF-1 α , CBP and p300 in the regulation of Nav1.5 expression in breast cancer cells. *Gene Reports* 16:100405.

- Dheda K, Huggett JF, Bustin SA, Johnson MA, Rook G, Zumla A (2004) Validation of housekeeping genes for normalizing RNA expression in real-time PCR. *Biotechniques* 37:112–114, 116, 118–119.
- Diaz D, Delgadillo DM, Hernández-Gallegos E, Ramírez-Domínguez ME, Hinojosa LM, Ortiz CS, Berumen J, Camacho J, Gomora JC (2007) Functional expression of voltage-gated sodium channels in primary cultures of human cervical cancer. *J Cell Physiol* 210:469–478.
- Dieci G, Fiorino G, Castelnuovo M, Teichmann M, Pagano A (2007) The expanding RNA polymerase III transcriptome. *Trends Genet* 23:614–622.
- Diss JK, Archer SN, Hirano J, Fraser SP, Djamgoz MB (2001) Expression profiles of voltage-gated Na(+) channel alpha-subunit genes in rat and human prostate cancer cell lines. *Prostate* 48:165–178.
- Diss JKJ, Fraser SP, Walker MM, Patel A, Latchman DS, Djamgoz MBA (2008) Beta-subunits of voltage-gated sodium channels in human prostate cancer: quantitative in vitro and in vivo analyses of mRNA expression. *Prostate Cancer Prostatic Dis* 11:325–333.
- Diss JKJ, Stewart D, Pani F, Foster CS, Walker MM, Patel A, Djamgoz MBA (2005) A potential novel marker for human prostate cancer: voltage-gated sodium channel expression in vivo. *Prostate Cancer Prostatic Dis* 8:266–273.
- Djamgoz M, Onkal R (2013) Persistent Current Blockers of Voltage-Gated Sodium Channels: A Clinical Opportunity for Controlling Metastatic Disease. *Recent Pat Anticancer Drug Discov* 8:66–84.
- Djamgoz MBA, Fraser SP, Brackenbury WJ (2019) In Vivo Evidence for Voltage-Gated Sodium Channel Expression in Carcinomas and Potentiation of Metastasis. *Cancers* 11 Available at: <https://www.ncbi.nlm.nih.gov/pmc/articles/PMC6895836/>.
- Dong Q, Zhao N, Xia C-K, Du L-L, Fu X-X, Du Y-M (2012) Hypoxia induces voltage-gated K⁺ (Kv) channel expression in pulmonary arterial smooth muscle cells through hypoxia-inducible factor-1 (HIF-1). *Bosn J Basic Med Sci* 12:158–163.
- Driffort V, Gillet L, Bon E, Marionneau-Lambot S, Oullier T, Joulin V, Collin C, Pagès J-C, Jourdan M-L, Chevalier S, Bougnoux P, Le Guennec J-Y, Besson P, Roger S (2014) Ranolazine inhibits NaV1.5-mediated breast cancer cell invasiveness and lung colonization. *Mol Cancer* 13:264.
- Duc C, Farman N, Canessa CM, Bonvalet JP, Rossier BC (1994) Cell-specific expression of epithelial sodium channel alpha, beta, and gamma subunits in aldosterone-responsive epithelia from the rat: localization by in situ hybridization and immunocytochemistry. *J Cell Biol* 127:1907–1921.
- Dumay-Odelot H, Durrieu-Gaillard S, Da Silva D, Roeder RG, Teichmann M (2010) Cell growth- and differentiation-dependent regulation of RNA polymerase III transcription. *Cell Cycle* 9:3687–3699.
- Durrieu-Gaillard S et al. (2018) Regulation of RNA polymerase III transcription during transformation of human IMR90 fibroblasts with defined genetic elements. *Cell Cycle* 17:605–615.

- Dutta S, Lopez Charcas O, Tanner S, Gradek F, Driffort V, Roger S, Selander K, Velu SE, Brouillette W (2018) Discovery and evaluation of nNav1.5 sodium channel blockers with potent cell invasion inhibitory activity in breast cancer cells. *Bioorg Med Chem* 26:2428–2436.
- Ebright RY, Zachariah MA, Micalizzi DS, Wittner BS, Niederhoffer KL, Nieman LT, Chirn B, Wiley DF, Wesley B, Shaw B, Nieblas-Bedolla E, Atlas L, Szabolcs A, Iafrate AJ, Toner M, Ting DT, Brastianos PK, Haber DA, Maheswaran S (2020) HIF1A signaling selectively supports proliferation of breast cancer in the brain. *Nat Commun* 11:6311.
- El Mernissi G, Doucet A (1984) Quantitation of [³H]ouabain binding and turnover of Na-K-ATPase along the rabbit nephron. *Am J Physiol* 247:F158-67.
- Ema M, Taya S, Yokotani N, Sogawa K, Matsuda Y, Fujii-Kuriyama Y (1997) A novel bHLH-PAS factor with close sequence similarity to hypoxia-inducible factor 1 α regulates the VEGF expression and is potentially involved in lung and vascular development. *Proc Natl Acad Sci U S A* 94:4273–4278.
- ENCODE Project Consortium (2012) An integrated encyclopedia of DNA elements in the human genome. *Nature* 489:57–74.
- Enver T, Soneji S, Joshi C, Brown J, Iborra F, Orntoft T, Thykjaer T, Maltby E, Smith K, Abu Dawud R, Jones M, Matin M, Gokhale P, Draper J, Andrews PW (2005) Cellular differentiation hierarchies in normal and culture-adapted human embryonic stem cells. *Hum Mol Genet* 14:3129–3140.
- Erdogan MA, Yuca E, Ashour A, Gurbuz N, Sencan S, Ozpolat B (2023) SCN5A promotes the growth and lung metastasis of triple-negative breast cancer through EF2-kinase signaling. *Life Sci* 313:121282.
- Espineda CE, Chang JH, Twiss J, Rajasekaran SA, Rajasekaran AK (2004) Repression of Na,K-ATPase beta1-subunit by the transcription factor snail in carcinoma. *Mol Biol Cell* 15:1364–1373.
- Espinosa Fernandez JR, Eckhardt BL, Lee J, Lim B, Pearson T, Seitz RS, Hout DR, Schweitzer BL, Nielsen TJ, Lawrence OR, Wang Y, Rao A, Ueno NT (2020) Identification of triple-negative breast cancer cell lines classified under the same molecular subtype using different molecular characterization techniques: Implications for translational research. *PLoS One* 15:e0231953.
- Fairhurst C, Martin F, Watt I, Bland M, Doran T, Brackenbury WJ (2023) Sodium channel-inhibiting drugs and cancer-specific survival: a population-based study of electronic primary care data. *BMJ Open* 13:e064376.
- Fairhurst C, Martin F, Watt I, Doran T, Bland M, Brackenbury WJ (2016) Sodium channel-inhibiting drugs and cancer survival: protocol for a cohort study using the CPRD primary care database. *BMJ Open* 6:e011661.
- Fairhurst C, Watt I, Martin F, Bland M, Brackenbury WJ (2015) Sodium channel-inhibiting drugs and survival of breast, colon and prostate cancer: a population-based study. *Sci Rep* 5:16758.
- Fang Z, Yi Y, Shi G, Li S, Chen S, Lin Y, Li Z, He Z, Li W, Zhong S (2017) Role of Brf1 interaction with ER α , and significance of its overexpression, in human breast cancer. *Mol Oncol* 11:1752–1767.

- Feraille E, Dizin E (2016) Coordinated control of ENaC and Na⁺,K⁺-ATPase in renal collecting duct. *J Am Soc Nephrol* 27:2554–2563.
- Filardo EJ, Quinn JA, Bland KI, Frackelton AR Jr (2000) Estrogen-induced activation of Erk-1 and Erk-2 requires the G protein-coupled receptor homolog, GPR30, and occurs via trans-activation of the epidermal growth factor receptor through release of HB-EGF. *Mol Endocrinol* 14:1649–1660.
- Finlay-Schultz J, Gillen AE, Brechbuhl HM, Ivie JJ, Matthews SB, Jacobsen BM, Bentley DL, Kabos P, Sartorius CA (2017) Breast Cancer Suppression by Progesterone Receptors Is Mediated by Their Modulation of Estrogen Receptors and RNA Polymerase III. *Cancer Res* 77:4934–4946.
- Firth JD, Ebert BL, Pugh CW, Ratcliffe PJ (1994) Oxygen-regulated control elements in the phosphoglycerate kinase 1 and lactate dehydrogenase A genes: similarities with the erythropoietin 3' enhancer. *Proc Natl Acad Sci U S A* 91:6496–6500.
- Fischle W, Dequiedt F, Hendzel MJ, Guenther MG, Lazar MA, Voelter W, Verdin E (2002) Enzymatic activity associated with class II HDACs is dependent on a multiprotein complex containing HDAC3 and SMRT/N-CoR. *Mol Cell* 9:45–57.
- Foo J, Gentile F, Massah S, Morin H, Singh K, Lee J, Smith J, Ban F, LeBlanc E, Young R, Strynadka N, Lallous N, Cherkasov A (2024) Characterization of novel small molecule inhibitors of estrogen receptor-activation function 2 (ER-AF2). *Breast Cancer Res* 26:168.
- Forsythe JA, Jiang BH, Iyer NV, Agani F, Leung SW, Koos RD, Semenza GL (1996) Activation of vascular endothelial growth factor gene transcription by hypoxia-inducible factor 1. *Mol Cell Biol* 16:4604–4613.
- Fortunati N, Bertino S, Costantino L, Bosco O, Vercellinato I, Catalano MG, Boccuzzi G (2008) Valproic acid is a selective antiproliferative agent in estrogen-sensitive breast cancer cells. *Cancer Lett* 259:156–164.
- Franovic A, Holterman CE, Payette J, Lee S (2009) Human cancers converge at the HIF-2alpha oncogenic axis. *Proc Natl Acad Sci U S A* 106:21306–21311.
- Fraser SP et al. (2005) Voltage-gated sodium channel expression and potentiation of human breast cancer metastasis. *Clin Cancer Res* 11:5381–5389.
- Fraser SP, Ozerlat-Gunduz I, Brackenbury WJ, Fitzgerald EM, Campbell TM, Coombes RC, Djamgoz MBA (2014a) Regulation of voltage-gated sodium channel expression in cancer: hormones, growth factors and auto-regulation. *Philos Trans R Soc Lond B Biol Sci* 369:20130105.
- Fraser SP, Peters A, Fleming-Jones S, Mukhey D, Djamgoz MBA (2014b) Resveratrol: inhibitory effects on metastatic cell behaviors and voltage-gated Na⁺ channel activity in rat prostate cancer in vitro. *Nutr Cancer* 66:1047–1058.
- Freudenheim JL (2020) Alcohol's effects on breast cancer in women. *Alcohol Res* 40:11.

- Fu X et al. (2016) FOXA1 overexpression mediates endocrine resistance by altering the ER transcriptome and IL-8 expression in ER-positive breast cancer. *Proc Natl Acad Sci U S A* 113:E6600–E6609.
- Fu X et al. (2019) FOXA1 upregulation promotes enhancer and transcriptional reprogramming in endocrine-resistant breast cancer. *Proc Natl Acad Sci U S A* 116:26823–26834.
- Fuhrmann DC, Brüne B (2017) Mitochondrial composition and function under the control of hypoxia. *Redox Biol* 12:208–215.
- Fujisawa-Sehara A, Sogawa K, Yamane M, Fujii-Kuriyama Y (1987) Characterization of xenobiotic responsive elements upstream from the drug-metabolizing cytochrome P-450c gene: a similarity to glucocorticoid regulatory elements. *Nucleic Acids Res* 15:4179–4191.
- Fulgenzi G, Graciotti L, Faronato M, Soldovieri MV, Miceli F, Amoroso S, Annunziato L, Procopio A, Tagliatela M (2006) Human neoplastic mesothelial cells express voltage-gated sodium channels involved in cell motility. *Int J Biochem Cell Biol* 38:1146–1159.
- Galli F, Aguilera JV, Palermo B, Markovic SN, Nisticò P, Signore A (2020) Relevance of immune cell and tumor microenvironment imaging in the new era of immunotherapy. *J Exp Clin Cancer Res* 39:89.
- Gao N, Zhang J, Rao MA, Case TC, Mirosevich J, Wang Y, Jin R, Gupta A, Rennie PS, Matusik RJ (2003) The role of hepatocyte nuclear factor-3 alpha (Forkhead Box A1) and androgen receptor in transcriptional regulation of prostatic genes. *Mol Endocrinol* 17:1484–1507.
- Gao R, Shen Y, Cai J, Lei M, Wang Z (2010) Expression of voltage-gated sodium channel alpha subunit in human ovarian cancer. *Oncol Rep* 23:1293–1299.
- Gatenby RA, Smallbone K, Maini PK, Rose F, Averill J, Nagle RB, Worrall L, Gillies RJ (2007) Cellular adaptations to hypoxia and acidosis during somatic evolution of breast cancer. *Br J Cancer* 97:646–653.
- Gay L, Baker A-M, Graham TA (2016) Tumour cell heterogeneity. *F1000Res* 5:238.
- Geering K (2001) The Functional Role of β Subunits in Oligomeric P-Type ATPases. *J Bioenerg Biomembr* 33:425–438.
- Geering K (2005) Function of FXYD proteins, regulators of Na, K-ATPase. *J Bioenerg Biomembr* 37:387–392.
- Geisberg CA, Sawyer DB (2010) Mechanisms of anthracycline cardiotoxicity and strategies to decrease cardiac damage. *Curr Hypertens Rep* 12:404–410.
- Gerdes J, Li L, Schlueter C, Duchrow M, Wohlenberg C, Gerlach C, Stahmer I, Kloth S, Brandt E, Flad HD (1991) Immunobiochemical and molecular biologic characterization of the cell proliferation-associated nuclear antigen that is defined by monoclonal antibody Ki-67. *Am J Pathol* 138:867–873.
- Gerdes J, Schwab U, Lemke H, Stein H (1983) Production of a mouse monoclonal antibody reactive with a human nuclear antigen associated with cell proliferation. *Int J Cancer* 31:13–20.

- Ghosh MG, Thompson DA, Weigel RJ (2000) PDZK1 and GREB1 are estrogen-regulated genes expressed in hormone-responsive breast cancer. *Cancer Res* 60:6367–6375.
- Gilchrist J, Dutton S, Diaz-Bustamante M, McPherson A, Olivares N, Kalia J, Escayg A, Bosmans F (2014) Nav1.1 modulation by a novel triazole compound attenuates epileptic seizures in rodents. *ACS Chem Biol* 9:1204–1212.
- Gille T, Randrianarison-Pellan N, Goolaerts A, Dard N, Uzunhan Y, Ferrary E, Hummler E, Clerici C, Planès C (2014) Hypoxia-induced inhibition of epithelial Na⁽⁺⁾ channels in the lung. Role of Nedd4-2 and the ubiquitin-proteasome pathway. *Am J Respir Cell Mol Biol* 50:526–537.
- Gillet L, Roger S, Besson P, Lecaille F, Gore J, Bougnoux P, Lalmanach G, Le Guennec J-Y (2009) Voltage-gated Sodium Channel Activity Promotes Cysteine Cathepsin-dependent Invasiveness and Colony Growth of Human Cancer Cells *. *J Biol Chem* 284:8680–8691.
- Gingold H et al. (2014) A dual program for translation regulation in cellular proliferation and differentiation. *Cell* 158:1281–1292.
- Gingold H, Dahan O, Pilpel Y (2012) Dynamic changes in translational efficiency are deduced from codon usage of the transcriptome. *Nucleic Acids Res* 40:10053–10063.
- Ginzinger DG (2002) Gene quantification using real-time quantitative PCR: an emerging technology hits the mainstream. *Exp Hematol* 30:503–512.
- Girbig M, Misiaszek AD, Vorländer MK, Lafita A, Grötsch H, Baudin F, Bateman A, Müller CW (2021) Cryo-EM structures of human RNA polymerase III in its unbound and transcribing states. *Nat Struct Mol Biol* 28:210–219.
- Giusti I, D’Ascenzo S, Millimaggi D, Taraboletti G, Carta G, Franceschini N, Pavan A, Dolo V (2008) Cathepsin B mediates the pH-dependent proinvasive activity of tumor-shed microvesicles. *Neoplasia* 10:481–488.
- Glont S-E, Chernukhin I, Carroll JS (2019) Comprehensive Genomic Analysis Reveals that the Pioneering Function of FOXA1 Is Independent of Hormonal Signaling. *Cell Rep* 26:2558-2565.e3.
- Godet I, Shin YJ, Ju JA, Ye IC, Wang G, Gilkes DM (2019) Fate-mapping post-hypoxic tumor cells reveals a ROS-resistant phenotype that promotes metastasis. *Nat Commun* 10:4862.
- Goldfarb KC, Cech TR (2017) Targeted CRISPR disruption reveals a role for RNase MRP RNA in human preribosomal RNA processing. *Genes Dev* 31:59–71.
- Gomez-Roman N, Grandori C, Eisenman RN, White RJ (2003) Direct activation of RNA polymerase III transcription by c-Myc. *Nature* 421:290–294.
- Gonçalves-de-Albuquerque CF, Ribeiro Silva A, Ignácio da Silva C, Caire Castro-Faria-Neto H, Burth P (2017) Na/K pump and beyond: Na/K-ATPase as a modulator of apoptosis and autophagy. *Molecules* 22:578.

- Gong Y, Yang J, Wu W, Liu F, Su A, Li Z, Zhu J, Wei T (2018) Preserved SCN4B expression is an independent indicator of favorable recurrence-free survival in classical papillary thyroid cancer. *PLoS One* 13:e0197007.
- González-González L, González-Ramírez R, Flores A, Avelino-Cruz JE, Felix R, Monjaraz E (2019) Epidermal Growth Factor Potentiates Migration of MDA-MB 231 Breast Cancer Cells by Increasing Nav1.5 Channel Expression. *Oncology* 97:373–382.
- Goodarzi E, Beiranvand R, Naemi H, Rahimi PS, Khazaei Z (2020) Geographical distribution incidence and mortality of breast cancer and its relationship with the Human Development Index (HDI): an ecology study in 2018. *WCRJ*:e1468.
- Goodarzi H, Nguyen HCB, Zhang S, Dill BD, Molina H, Tavazoie SF (2016) Modulated Expression of Specific tRNAs Drives Gene Expression and Cancer Progression. *Cell* 165:1416–1427.
- Gote V, Nookala AR, Bolla PK, Pal D (2021) Drug Resistance in Metastatic Breast Cancer: Tumor Targeted Nanomedicine to the Rescue. *Int J Mol Sci* 22 Available at: <http://dx.doi.org/10.3390/ijms22094673>.
- Gouge J, Guthertz N, Kramm K, Dergai O, Abascal-Palacios G, Satia K, Cousin P, Hernandez N, Grohmann D, Vannini A (2017) Molecular mechanisms of Bdp1 in TFIIIB assembly and RNA polymerase III transcription initiation. *Nat Commun* 8:130.
- Gouge J, Satia K, Guthertz N, Widya M, Thompson AJ, Cousin P, Dergai O, Hernandez N, Vannini A (2015) Redox signaling by the RNA polymerase III TFIIIB-related factor Brf2. *Cell* 163:1375–1387.
- Gradek F, Lopez-Charcas O, Chadet S, Poisson L, Ouldamer L, Goupille C, Jourdan M-L, Chevalier S, Moussata D, Besson P, Roger S (2019) Sodium Channel Nav1.5 Controls Epithelial-to-Mesenchymal Transition and Invasiveness in Breast Cancer Cells Through its Regulation by the Salt-Inducible Kinase-1. *Sci Rep* 9:18652.
- Gray LH, Conger AD, Ebert M, Hornsey S, Scott OC (1953) The concentration of oxygen dissolved in tissues at the time of irradiation as a factor in radiotherapy. *Br J Radiol* 26:638–648.
- Greer CL, Peebles CL, Gegenheimer P, Abelson J (1983) Mechanism of action of a yeast RNA ligase in tRNA splicing. *Cell* 32:537–546.
- Grewal SS (2015) Why should cancer biologists care about tRNAs? tRNA synthesis, mRNA translation and the control of growth. *Biochim Biophys Acta* 1849:898–907.
- Grober OMV, Mutarelli M, Giurato G, Ravo M, Cicatiello L, De Filippo MR, Ferraro L, Nassa G, Papa MF, Paris O, Tarallo R, Luo S, Schroth GP, Benes V, Weisz A (2011) Global analysis of estrogen receptor beta binding to breast cancer cell genome reveals an extensive interplay with estrogen receptor alpha for target gene regulation. *BMC Genomics* 12:36.
- Groenendijk FH, Treece T, Yoder E, Baron P, Beitsch P, Audeh W, Dinjens WNM, Bernards R, Whitworth P (2019) Estrogen receptor variants in ER-positive

basal-type breast cancers responding to therapy like ER-negative breast cancers. *NPJ Breast Cancer* 5:15.

- Gu YZ, Moran SM, Hogenesch JB, Wartman L, Bradfield CA (1998) Molecular characterization and chromosomal localization of a third alpha-class hypoxia inducible factor subunit, HIF3alpha. *Gene Expr* 7:205–213.
- Gubern C, Hurtado O, Rodríguez R, Morales JR, Romera VG, Moro MA, Lizasoain I, Serena J, Mallolas J (2009) Validation of housekeeping genes for quantitative real-time PCR in in-vivo and in-vitro models of cerebral ischaemia. *BMC Mol Biol* 10:57.
- Guestini F, Ono K, Miyashita M, Ishida T, Ohuchi N, Nakagawa S, Hirakawa H, Tamaki K, Ohi Y, Rai Y, Sagara Y, Sasano H, McNamara KM (2019) Impact of Topoisomerase II α , PTEN, ABCC1/MRP1, and KI67 on triple-negative breast cancer patients treated with neoadjuvant chemotherapy. *Breast Cancer Res Treat* 173:275–288.
- Guimaraes JC, Zavolan M (2016) Patterns of ribosomal protein expression specify normal and malignant human cells. *Genome Biol* 17:236.
- Gündoğdu AÇ, Özyurt R (2023) Resveratrol downregulates ENaCs through the activation of AMPK in human colon cancer cells. *Tissue Cell* 82:102071.
- Gusarova GA, Dada LA, Kelly AM, Brodie C, Witters LA, Chandel NS, Sznajder JI (2009) Alpha1-AMP-activated protein kinase regulates hypoxia-induced Na,K-ATPase endocytosis via direct phosphorylation of protein kinase C zeta. *Mol Cell Biol* 29:3455–3464.
- Guy Hr Seetharamulu P (1986) Molecular model of the action potential sodium channel. *Proc Natl Acad Sci U S A* 83:508–512.
- Guzel RM, Ogmen K, Ilieva KM, Fraser SP, Djamgoz MBA (2019) Colorectal cancer invasiveness in vitro: Predominant contribution of neonatal Nav1.5 under normoxia and hypoxia. *J Cell Physiol* 234:6582–6593.
- Hah N, Danko CG, Core L, Waterfall JJ, Siepel A, Lis JT, Kraus WL (2011) A rapid, extensive, and transient transcriptional response to estrogen signaling in breast cancer cells. *Cell* 145:622–634.
- Haidar R, Henkler F, Kugler J, Rosin A, Genkinger D, Laux P, Luch A (2021) The role of DNA-binding and ARNT dimerization on the nucleo-cytoplasmic translocation of the aryl hydrocarbon receptor. *Sci Rep* 11:18194.
- Hall JM, McDonnell DP (2005) Coregulators in nuclear estrogen receptor action: from concept to therapeutic targeting. *Mol Interv* 5:343–357.
- Hammarström AKM, Gage PW (2002) Hypoxia and persistent sodium current. *Eur Biophys J* 31:323–330.
- Hanahan D, Weinberg RA (2000) The hallmarks of cancer. *Cell* 100:57–70.
- Hanahan D, Weinberg RA (2011) Hallmarks of cancer: the next generation. *Cell* 144:646–674.
- Hanker AB, Sudhan DR, Arteaga CL (2020) Overcoming endocrine resistance in breast cancer. *Cancer Cell* 37:496–513.

- Hanstein B, Eckner R, DiRenzo J, Halachmi S, Liu H, Searcy B, Kurokawa R, Brown M (1996) p300 is a component of an estrogen receptor coactivator complex. *Proc Natl Acad Sci U S A* 93:11540–11545.
- Hanukoglu I, Hanukoglu A (2016) Epithelial sodium channel (ENaC) family: Phylogeny, structure-function, tissue distribution, and associated inherited diseases. *Gene* 579:95–132.
- Hara S, Hamada J, Kobayashi C, Kondo Y, Imura N (2001) Expression and characterization of hypoxia-inducible factor (HIF)-3 α in human kidney: suppression of HIF-mediated gene expression by HIF-3 α . *Biochem Biophys Res Commun* 287:808–813.
- Hardt WD, Schlegl J, Erdmann VA, Hartmann RK (1993) Role of the D arm and the anticodon arm in tRNA recognition by eubacterial and eukaryotic RNase P enzymes. *Biochemistry* 32:13046–13053.
- Harvey JM, Clark GM, Osborne CK, Allred DC (1999) Estrogen receptor status by immunohistochemistry is superior to the ligand-binding assay for predicting response to adjuvant endocrine therapy in breast cancer. *J Clin Oncol* 17:1474–1481.
- Hauck T, Kadam S, Heinz K, Garcia Peraza M, Schmid R, Kremer AE, Wolf K, Bauer A, Horch RE, Arkudas A, Kengelbach-Weigand A (2022) Influence of the autotaxin-lysophosphatidic acid axis on cellular function and cytokine expression in different breast cancer cell lines. *Sci Rep* 12:5565.
- Haurie V, Durrieu-Gaillard S, Dumay-Odelot H, Da Silva D, Rey C, Prochazkova M, Roeder RG, Besser D, Teichmann M (2010) Two isoforms of human RNA polymerase III with specific functions in cell growth and transformation. *Proc Natl Acad Sci U S A* 107:4176–4181.
- Haworth AS, Hodges SL, Capatina AL, Isom LL, Baumann CG, Brackenbury WJ (2022) Subcellular dynamics and functional activity of the cleaved intracellular domain of the Na⁺ channel β 1 subunit. *J Biol Chem* 298:102174.
- Hayashi M, Sakata M, Takeda T, Yamamoto T, Okamoto Y, Sawada K, Kimura A, Minekawa R, Tahara M, Tasaka K, Murata Y (2004) Induction of glucose transporter 1 expression through hypoxia-inducible factor 1 α under hypoxic conditions in trophoblast-derived cells. *J Endocrinol* 183:145–154.
- Heinzel T, Lavinsky RM, Mullen TM, Söderstrom M, Laherty CD, Torchia J, Yang WM, Brard G, Ngo SD, Davie JR, Seto E, Eisenman RN, Rose DW, Glass CK, Rosenfeld MG (1997) A complex containing N-CoR, mSin3 and histone deacetylase mediates transcriptional repression. *Nature* 387:43–48.
- Heldring N, Isaacs GD, Diehl AG, Sun M, Cheung E, Ranish JA, Kraus WL (2011) Multiple sequence-specific DNA-binding proteins mediate estrogen receptor signaling through a tethering pathway. *Mol Endocrinol* 25:564–574.
- Hernandez-Alias X, Katanski CD, Zhang W, Assari M, Watkins CP, Schaefer MH, Serrano L, Pan T (2023) Single-read tRNA-seq analysis reveals coordination of tRNA modification and aminoacylation and fragmentation. *Nucleic Acids Res* 51:e17.

- Hernandez-Plata E, Ortiz CS, Marquina-Castillo B, Medina-Martinez I, Alfaro A, Berumen J, Rivera M, Gomora JC (2012) Overexpression of NaV 1.6 channels is associated with the invasion capacity of human cervical cancer. *Int J Cancer* 130:2013–2023.
- Higashimura Y, Nakajima Y, Yamaji R, Harada N, Shibasaki F, Nakano Y, Inui H (2011) Up-regulation of glyceraldehyde-3-phosphate dehydrogenase gene expression by HIF-1 activity depending on Sp1 in hypoxic breast cancer cells. *Arch Biochem Biophys* 509:1–8.
- Higuchi R, Fockler C, Dollinger G, Watson R (1993) Kinetic PCR analysis: real-time monitoring of DNA amplification reactions. *Biotechnology* 11:1026–1030.
- Hille B (1984) Ionic channels of excitable membranes. South Yarra, Australia: Macmillan Education.
- Hirota K (2020) Basic biology of hypoxic responses mediated by the transcription factor HIFs and its implication for medicine. *Biomedicines* 8:32.
- Holmquist-Mengelbier L, Fredlund E, Löfstedt T, Noguera R, Navarro S, Nilsson H, Pietras A, Vallon-Christersson J, Borg A, Gradin K, Poellinger L, Pålman S (2006) Recruitment of HIF-1 α and HIF-2 α to common target genes is differentially regulated in neuroblastoma: HIF-2 α promotes an aggressive phenotype. *Cancer Cell* 10:413–423.
- Horsman MR, Mortensen LS, Petersen JB, Busk M, Overgaard J (2012) Imaging hypoxia to improve radiotherapy outcome. *Nat Rev Clin Oncol* 9:674–687.
- Hossain MM, Sonsalla PK, Richardson JR (2013) Coordinated role of voltage-gated sodium channels and the Na⁺/H⁺ exchanger in sustaining microglial activation during inflammation. *Toxicol Appl Pharmacol* 273:355–364.
- Hou P, Kuo C-Y, Cheng C-T, Liou J-P, Ann DK, Chen Q (2014) Intermediary metabolite precursor dimethyl-2-ketoglutarate stabilizes hypoxia-inducible factor-1 α by inhibiting prolyl-4-hydroxylase PHD2. *PLoS One* 9:e113865.
- House CD, Vaske CJ, Schwartz AM, Obias V, Frank B, Luu T, Sarvazyan N, Irby R, Strausberg RL, Hales TG, Stuart JM, Lee NH (2010) Voltage-gated Na⁺ channel SCN5A is a key regulator of a gene transcriptional network that controls colon cancer invasion. *Cancer Res* 70:6957–6967.
- House CD, Wang B-D, Ceniccola K, Williams R, Simaan M, Olender J, Patel V, Baptista-Hon DT, Annunziata CM, Gutkind JS, Hales TG, Lee NH (2015) Voltage-gated Na⁺ Channel Activity Increases Colon Cancer Transcriptional Activity and Invasion Via Persistent MAPK Signaling. *Sci Rep* 5:11541.
- Hsiao LL et al. (2001) A compendium of gene expression in normal human tissues. *Physiol Genomics* 7:97–104.
- Hu C-J, Wang L-Y, Chodosh LA, Keith B, Simon MC (2003) Differential roles of hypoxia-inducible factor 1 α (HIF-1 α) and HIF-2 α in hypoxic gene regulation. *Mol Cell Biol* 23:9361–9374.
- Hu H-J, Wang S-S, Wang Y-X, Liu Y, Feng X-M, Shen Y, Zhu L, Chen H-Z, Song M (2019) Blockade of the forward Na⁺ /Ca²⁺ exchanger suppresses the

- growth of glioblastoma cells through Ca²⁺ -mediated cell death. *Br J Pharmacol* 176:2691–2707.
- Huang W, Peng Y, Kiselar J, Zhao X, Albaqami A, Mendez D, Chen Y, Chakravarthy S, Gupta S, Ralston C, Kao H-Y, Chance MR, Yang S (2018) Multidomain architecture of estrogen receptor reveals interfacial cross-talk between its DNA-binding and ligand-binding domains. *Nat Commun* 9:3520.
- Hurtado A, Holmes KA, Ross-Innes CS, Schmidt D, Carroll JS (2011) FOXA1 is a key determinant of estrogen receptor function and endocrine response. *Nat Genet* 43:27–33.
- Husni Cangara M, Miskad UA, Masadah R, Nelwan BJ, Wahid S (2021) Gata-3 and KI-67 expression in correlation with molecular subtypes of breast cancer. *Breast Dis* 40:S27–S31.
- Iacoangeli A, Lin Y, Morley EJ, Muslimov IA, Bianchi R, Reilly J, Weedon J, Diallo R, Böcker W, Tiedge H (2004) BC200 RNA in invasive and preinvasive breast cancer. *Carcinogenesis* 25:2125–2133.
- Ikeda K, Horie-Inoue K, Inoue S (2015) Identification of estrogen-responsive genes based on the DNA binding properties of estrogen receptors using high-throughput sequencing technology. *Acta Pharmacol Sin* 36:24–31.
- Indukuri R, Damdimopoulos A, Williams C (2022) An optimized ChIP-Seq protocol to determine chromatin binding of estrogen receptor beta. *Methods Mol Biol* 2418:203–221.
- Isom LL (2001) Sodium channel beta subunits: anything but auxiliary. *Neuroscientist* 7:42–54.
- Jafari H, Ahmadian S, Soleimani M (2014) The enhanced apoptosis and antiproliferative response to combined treatment with valproate and nicotinamide in MCF-7 breast cancer cells. *Tumour Biol* 35:2701–2710.
- Jahroudi N, Greenberger JS (1995) The role of endothelial cells in tumor invasion and metastasis. *J Neurooncol* 23:99–108.
- Jain N, Nitisa D, Pirsko V, Cakstina I (2020) Selecting suitable reference genes for qPCR normalization: a comprehensive analysis in MCF-7 breast cancer cell line. *BMC Mol Cell Biol* 21:68.
- James Faresse N, Canella D, Praz V, Michaud J, Romascano D, Hernandez N (2012) Genomic study of RNA polymerase II and III SNAPc-bound promoters reveals a gene transcribed by both enzymes and a broad use of common activators. *PLoS Genet* 8:e1003028.
- Jansson KH, Castillo DG, Morris JW, Boggs ME, Czymmek KJ, Adams EL, Schramm LP, Sikes RA (2014) Identification of beta-2 as a key cell adhesion molecule in PCa cell neurotropic behavior: a novel ex vivo and biophysical approach. *PLoS One* 9:e98408.
- Jansson KH, Lynch JE, Lepori-Bui N, Czymmek KJ, Duncan RL, Sikes RA (2012) Overexpression of the VSSC-associated CAM, β -2, enhances LNCaP cell metastasis associated behavior. *Prostate* 72:1080–1092.

- Jaśkiewicz M, Moszyńska A, Króliczewski J, Cabaj A, Bartoszewska S, Charzyńska A, Gebert M, Dąbrowski M, Collawn JF, Bartoszewski R (2022) The transition from HIF-1 to HIF-2 during prolonged hypoxia results from reactivation of PHDs and HIF1A mRNA instability. *Cell Mol Biol Lett* 27:109.
- Jehanno C, Le Goff P, Habauzit D, Le Page Y, Lecomte S, Lecluze E, Percevault F, Avner S, Métivier R, Michel D, Flouriot G (2022) Hypoxia and ER α Transcriptional Crosstalk Is Associated with Endocrine Resistance in Breast Cancer. *Cancers* 14 Available at: <http://dx.doi.org/10.3390/cancers14194934>.
- Jensen RL, Mumert ML, Gillespie DL, Kinney AY, Schabel MC, Salzman KL (2014) Preoperative dynamic contrast-enhanced MRI correlates with molecular markers of hypoxia and vascularity in specific areas of intratumoral microenvironment and is predictive of patient outcome. *Neuro Oncol* 16:280–291.
- Jeselsohn R, Buchwalter G, De Angelis C, Brown M, Schiff R (2015) ESR1 mutations—a mechanism for acquired endocrine resistance in breast cancer. *Nat Rev Clin Oncol* 12:573–583.
- Jewell UR, Kvietikova I, Scheid A, Bauer C, Wenger RH, Gassmann M (2001) Induction of HIF-1 α in response to hypoxia is instantaneous. *FASEB J* 15:1312–1314.
- Jia M, Dahlman-Wright K, Gustafsson J-Å (2015) Estrogen receptor alpha and beta in health and disease. *Best Pract Res Clin Endocrinol Metab* 29:557–568.
- Jiang Y, Zhang Y, Luan J, Duan H, Zhang F, Yagasaki K, Zhang G (2010) Effects of bufalin on the proliferation of human lung cancer cells and its molecular mechanisms of action. *Cytotechnology* 62:573–583.
- Jögi A, Øra I, Nilsson H, Lindeheim A, Makino Y, Poellinger L, Axelson H, Pålman S (2002) Hypoxia alters gene expression in human neuroblastoma cells toward an immature and neural crest-like phenotype. *Proc Natl Acad Sci U S A* 99:7021–7026.
- Johansson ALV, Trewin CB, Fredriksson I, Reinertsen KV, Russnes H, Ursin G (2021) In modern times, how important are breast cancer stage, grade and receptor subtype for survival: a population-based cohort study. *Breast Cancer Res* 23:17.
- Johansson MJO, Esberg A, Huang B, Björk GR, Byström AS (2008) Eukaryotic wobble uridine modifications promote a functionally redundant decoding system. *Mol Cell Biol* 28:3301–3312.
- Johnson SA, Mandavia N, Wang HD, Johnson DL (2000) Transcriptional regulation of the TATA-binding protein by Ras cellular signaling. *Mol Cell Biol* 20:5000–5009.
- Ju YK, Saint DA, Gage PW (1996) Hypoxia increases persistent sodium current in rat ventricular myocytes. *J Physiol* 497 (Pt 2):337–347.
- Jung S et al. (2016) Alcohol consumption and breast cancer risk by estrogen receptor status: in a pooled analysis of 20 studies. *Int J Epidemiol* 45:916–928.

- Kaelin WG Jr (2008) The von Hippel-Lindau tumour suppressor protein: O₂ sensing and cancer. *Nat Rev Cancer* 8:865–873.
- Kakani P, Dhamdhare SG, Pant D, Joshi R, Mishra J, Samaiya A, Shukla S (2024) Hypoxia-induced CTCF promotes EMT in breast cancer. *Cell Rep* 43:114367.
- Kamarulzaman NS, Dewadas HD, Leow CY, Yaacob NS, Mokhtar NF (2017) The role of REST and HDAC2 in epigenetic dysregulation of Nav1.5 and nNav1.5 expression in breast cancer. *Cancer Cell Int* 17:74.
- Kaneko H, Kaitsuka T, Tomizawa K (2020) Response to Stimulations Inducing Circadian Rhythm in Human Induced Pluripotent Stem Cells. *Cells* 9 Available at: <http://dx.doi.org/10.3390/cells9030620>.
- Kang IN, Lee CY, Tan SC (2019) Selection of best reference genes for qRT-PCR analysis of human neural stem cells preconditioned with hypoxia or baicalein-enriched fraction extracted from *Oroxylum indicum* medicinal plant. *Heliyon* 5:e02156.
- Kang Y, Li J (2022) The heterogeneous subclones might be induced by cycling hypoxia which was aggravated along with the luminal A tumor growth. *Tissue Cell* 77:101844.
- Kantidakis T, Ramsbottom BA, Birch JL, Dowding SN, White RJ (2010) mTOR associates with TFIIIC, is found at tRNA and 5S rRNA genes, and targets their repressor Maf1. *Proc Natl Acad Sci U S A* 107:11823–11828.
- Kapoor N, Bartoszewski R, Qadri YJ, Bebok Z, Bubien JK, Fuller CM, Benos DJ (2009) Knockdown of ASIC1 and epithelial sodium channel subunits inhibits glioblastoma whole cell current and cell migration. *J Biol Chem* 284:24526–24541.
- Kapoor N, Lee W, Clark E, Bartoszewski R, McNicholas CM, Latham CB, Bebok Z, Parpura V, Fuller CM, Palmer CA, Benos DJ (2011) Interaction of ASIC1 and ENaC subunits in human glioma cells and rat astrocytes. *Am J Physiol Cell Physiol* 300:C1246-59.
- Kasai K, Yamashita T, Yamaguchi A, Yoshiya K, Kawakita A, Tanaka H, Sugimoto H, Tohyama M (2003) Induction of mRNAs and proteins for Na/K ATPase alpha1 and beta1 subunits following hypoxia/reoxygenation in astrocytes. *Brain Res Mol Brain Res* 110:38–44.
- Kashlan OB, Kleyman TR (2011) ENaC structure and function in the wake of a resolved structure of a family member. *Am J Physiol Renal Physiol* 301:F684-96.
- Kassavetis GA, Braun BR, Nguyen LH, Geiduschek EP (1990) *S. cerevisiae* TFIIIB is the transcription initiation factor proper of RNA polymerase III, while TFIIIA and TFIIIC are assembly factors. *Cell* 60:235–245.
- Kassavetis GA, Letts GA, Geiduschek EP (2001) The RNA polymerase III transcription initiation factor TFIIIB participates in two steps of promoter opening. *EMBO J* 20:2823–2834.

- Kato A, Romero MF (2011) Regulation of electroneutral NaCl absorption by the small intestine. *Annu Rev Physiol* 73:261–281.
- Kazarinova-Noyes K, Malhotra JD, McEwen DP, Mattei LN, Berglund EO, Ranscht B, Levinson SR, Schachner M, Shrager P, Isom LL, Xiao ZC (2001) Contactin associates with Na⁺ channels and increases their functional expression. *J Neurosci* 21:7517–7525.
- Keeton EK, Brown M (2005) Cell cycle progression stimulated by tamoxifen-bound estrogen receptor-alpha and promoter-specific effects in breast cancer cells deficient in N-CoR and SMRT. *Mol Endocrinol* 19:1543–1554.
- Khajah MA, Mathew PM, Luqmani YA (2018) Na⁺/K⁺ ATPase activity promotes invasion of endocrine resistant breast cancer cells. *PLoS One* 13:e0193779.
- Kim J-W, Tchernyshyov I, Semenza GL, Dang CV (2006) HIF-1-mediated expression of pyruvate dehydrogenase kinase: a metabolic switch required for cellular adaptation to hypoxia. *Cell Metab* 3:177–185.
- Kim Y, Ko JY, Kong HK, Lee M, Chung W, Lim S, Son D, Oh S, Park JW, Kim DY, Lee M, Han W, Park W-Y, Yoo KH, Park JH (2024) Hypomethylation of ATP1A1 is associated with poor prognosis and cancer progression in triple-negative breast cancer. *Cancers (Basel)* 16:1666.
- King GS, Goyal A, Grigorova Y, Patel P, Hashmi MF (2024) Antiarrhythmic medications. In: *StatPearls*. Treasure Island (FL): StatPearls Publishing.
- Kinslow CJ, Tang A, Chaudhary KR, Cheng SK (2022) Prevalence of estrogen receptor alpha (ESR1) somatic mutations in breast cancer. *JNCI Cancer Spectr* 6 Available at: <http://dx.doi.org/10.1093/jncics/pkac060>.
- Klein-Hitpass L, Tsai SY, Greene GL, Clark JH, Tsai MJ, O'Malley BW (1989) Specific binding of estrogen receptor to the estrogen response element. *Molecular and Cellular Biology* 9:43–49.
- Klemba A, Bodnar L, Was H, Brodaczewska KK, Wcislo G, Szczylik CA, Kieda C (2020) Hypoxia-mediated decrease of ovarian cancer cells reaction to treatment: Significance for chemo- and immunotherapies. *Int J Mol Sci* 21:9492.
- Koh MY, Powis G (2012) Passing the baton: the HIF switch. *Trends Biochem Sci* 37:364–372.
- Kometiani P, Liu L, Askari A (2005) Digitalis-induced signaling by Na⁺/K⁺-ATPase in human breast cancer cells. *Mol Pharmacol* 67:929–936.
- Kondoh M, Ohga N, Akiyama K, Hida Y, Maishi N, Towfik AM, Inoue N, Shindoh M, Hida K (2013) Hypoxia-induced reactive oxygen species cause chromosomal abnormalities in endothelial cells in the tumor microenvironment. *PLoS One* 8:e80349.
- Kraus WL, Kadonaga JT (1998) P300 and estrogen receptor cooperatively activate transcription via differential enhancement of initiation and reinitiation. *Genes Dev* 12:331–342.

- Kravtsova VV, Fedorova AA, Tishkova MV, Livanova AA, Matytsin VO, Ganapolsky VP, Vetrovoy OV, Krivoi II (2022) Short-term mild hypoxia modulates Na,K-ATPase to maintain membrane electrogenesis in rat skeletal muscle. *Int J Mol Sci* 23:11869.
- Krishnan P, Ghosh S, Wang B, Heyns M, Li D, Mackey JR, Kovalchuk O, Damaraju S (2016) Genome-wide profiling of transfer RNAs and their role as novel prognostic markers for breast cancer. *Sci Rep* 6:32843.
- Kuiper GG, Enmark E, Peltö-Huikko M, Nilsson S, Gustafsson JA (1996) Cloning of a novel receptor expressed in rat prostate and ovary. *Proc Natl Acad Sci U S A* 93:5925–5930.
- Kumar R, Zakharov MN, Khan SH, Miki R, Jang H, Toraldo G, Singh R, Bhasin S, Jasuja R (2011) The dynamic structure of the estrogen receptor. *J Amino Acids* 2011:812540.
- Kumar RS, Goyal N (2021) Estrogens as regulator of hematopoietic stem cell, immune cells and bone biology. *Life Sci* 269:119091.
- Kumar U, Ardasheva A, Mahmud Z, Coombes RC, Yagüe E (2021) FOXA1 is a determinant of drug resistance in breast cancer cells. *Breast Cancer Res Treat* 186:317–326.
- Kuper H, Adami HO, Trichopoulos D (2000) Infections as a major preventable cause of human cancer. *J Intern Med* 248:171–183.
- Lando D, Peet DJ, Gorman JJ, Whelan DA, Whitelaw ML, Bruick RK (2002) FIH-1 is an asparaginyl hydroxylase enzyme that regulates the transcriptional activity of hypoxia-inducible factor. *Genes Dev* 16:1466–1471.
- Lastraioli E, Fraser SP, Guzel RM, Iorio J, Bencini L, Scarpi E, Messerini L, Villanacci V, Cerino G, Ghezzi N, Perrone G, Djamgoz MBA, Arcangeli A (2021) Neonatal Nav1.5 protein expression in human colorectal cancer: Immunohistochemical characterization and clinical evaluation. *Cancers (Basel)* 13:3832.
- Lautré W, Richard E, Feugeas J-P, Dumay-Odelot H, Teichmann M (2022) The POLR3G subunit of human RNA polymerase III regulates tumorigenesis and metastasis in triple-negative breast cancer. *Cancers (Basel)* 14:5732.
- Lee BT et al. (2022) The UCSC Genome Browser database: 2022 update. *Nucleic Acids Res* 50:D1115–D1122.
- Lee E, McKean-Cowdin R, Ma H, Spicer DV, Van Den Berg D, Bernstein L, Ursin G (2011) Characteristics of triple-negative breast cancer in patients with a BRCA1 mutation: results from a population-based study of young women. *J Clin Oncol* 29:4373–4380.
- Lee SC, Deutsch C, Beck WT (1988) Comparison of ion channels in multidrug-resistant and -sensitive human leukemic cells. *Proc Natl Acad Sci U S A* 85:2019–2023.
- Lee W-L, Cheng M-H, Chao H-T, Wang P-H (2008) The role of selective estrogen receptor modulators on breast cancer: from tamoxifen to raloxifene. *Taiwan J Obstet Gynecol* 47:24–31.

- Lefranc F, Kiss R (2008) The sodium pump alpha1 subunit as a potential target to combat apoptosis-resistant glioblastomas. *Neoplasia* 10:198–206.
- Lei H-T, Wang Z-H, Li B, Sun Y, Mei S-Q, Yang J-H, Qu L-H, Zheng L-L (2023) tModBase: deciphering the landscape of tRNA modifications and their dynamic changes from epitranscriptome data. *Nucleic Acids Res* 51:D315–D327.
- Lerdrup M, Johansen JV, Agrawal-Singh S, Hansen K (2016) An interactive environment for agile analysis and visualization of ChIP-sequencing data. *Nat Struct Mol Biol* 23:349–357.
- Leslie TK et al. (2024) A novel Nav1.5-dependent feedback mechanism driving glycolytic acidification in breast cancer metastasis. *Oncogene* 43:2578–2594.
- Leslie TK, Brackenbury WJ, Na N+, Na H+, Leslie TK, Brackenbury WJ, York :. (2022) Sodium channels and the ionic microenvironment of breast tumours. *J Physiol* 0:1–11.
- Leslie TK, James AD, Zaccagna F, Grist JT, Deen S, Kennerley A, Riemer F, Kaggie JD, Gallagher FA, Gilbert FJ, Brackenbury WJ (2019) Sodium homeostasis in the tumour microenvironment. *Biochim Biophys Acta Rev Cancer* 1872:188304.
- Li G-F, Qian T-L, Li G-S, Yang C-X, Qin M, Huang J, Sun M, Han Y-Q (2012) Sodium valproate inhibits MDA-MB-231 breast cancer cell migration by upregulating NM23H1 expression. *Genet Mol Res* 11:77–86.
- Li H, Liu J, Fan N, Wang H, Thomas AM, Yan Q, Li S, Qin H (2022a) Nav1.6 promotes the progression of human follicular thyroid carcinoma cells via JAK-STAT signaling pathway. *Pathol Res Pract* 236:153984.
- Li H, Sun X, Li J, Liu W, Pan G, Mao A, Liu J, Zhang Q, Rao L, Xie X, Sheng X (2022b) Hypoxia induces docetaxel resistance in triple-negative breast cancer via the HIF-1 α /miR-494/Survivin signaling pathway. *Neoplasia* 32:100821.
- Li L, Zhang F, Liu Z, Fan Z (2023) Immunotherapy for triple-negative breast cancer: Combination strategies to improve outcome. *Cancers (Basel)* 15:321.
- Li S, Han J, Guo G, Sun Y, Zhang T, Zhao M, Xu Y, Cui Y, Liu Y, Zhang J (2020) Voltage-gated sodium channels β 3 subunit promotes tumorigenesis in hepatocellular carcinoma by facilitating p53 degradation. *FEBS Lett* 594:497–508.
- Liang X, Xie R, Su J, Ye B, Wei S, Liang Z, Bai R, Chen Z, Li Z, Gao X (2019) Inhibition of RNA polymerase III transcription by Triptolide attenuates colorectal tumorigenesis. *J Exp Clin Cancer Res* 38:217.
- Lindström LS et al. (2018) Intratumor Heterogeneity of the Estrogen Receptor and the Long-term Risk of Fatal Breast Cancer. *J Natl Cancer Inst* 110:726–733.
- Lindström LS, Karlsson E, Wilking UM, Johansson U, Hartman J, Lidbrink EK, Hatschek T, Skoog L, Bergh J (2012) Clinically used breast cancer markers such as estrogen receptor, progesterone receptor, and human epidermal

- growth factor receptor 2 are unstable throughout tumor progression. *J Clin Oncol* 30:2601–2608.
- Liotta LA, Tryggvason K, Garbisa S, Hart I, Foltz CM, Shafie S (1980) Metastatic potential correlates with enzymatic degradation of basement membrane collagen. *Nature* 284:67–68.
- Liskova V, Hudecova S, Lencesova L, Iuliano F, Sirova M, Ondrias K, Pastorekova S, Krizanova O (2019) Type 1 Sodium Calcium Exchanger Forms a Complex with Carbonic Anhydrase IX and Via Reverse Mode Activity Contributes to pH Control in Hypoxic Tumors. *Cancers* 11 Available at: <http://dx.doi.org/10.3390/cancers11081139>.
- Liu C, Zhu L-L, Xu S-G, Ji H-L, Li X-M (2016) ENaC/DEG in tumor development and progression. *J Cancer* 7:1888–1891.
- Liu J, Tan H, Yang W, Yao S, Hong L (2019) The voltage-gated sodium channel Nav1.7 associated with endometrial cancer. *J Cancer* 10:4954–4960.
- Liu L, Bai J, Hu L, Jiang D (2023) Hypoxia-mediated activation of hypoxia-inducible factor-1 α in triple-negative breast cancer: A review. *Medicine (Baltimore)* 102:e35493.
- Liu X, Zhang W, Wang H, Lai C-H, Xu K, Hu H (2020) Increased expression of POLR3G predicts poor prognosis in transitional cell carcinoma. *PeerJ* 8:e10281.
- Liu X-B, Wang J-A, Ogle ME, Wei L (2009a) Prolyl hydroxylase inhibitor dimethylxalylglycine enhances mesenchymal stem cell survival. *J Cell Biochem* 106:903–911.
- Liu Y, Gao H, Marstrand TT, Ström A, Valen E, Sandelin A, Gustafsson J-A, Dahlman-Wright K (2008) The genome landscape of ER α - and ER β -binding DNA regions. *Proc Natl Acad Sci U S A* 105:2604–2609.
- Liu Y, Li Y-M, Tian R-F, Liu W-P, Fei Z, Long Q-F, Wang X-A, Zhang X (2009b) The expression and significance of HIF-1 α and GLUT-3 in glioma. *Brain Res* 1304:149–154.
- Livak KJ, Schmittgen TD (2001) Analysis of relative gene expression data using real-time quantitative PCR and the 2^{(-Delta Delta C(T))} Method. *Methods* 25:402–408.
- Loeck T, Rugi M, Todesca LM, Kalinowska P, Soret B, Neumann I, Schimmelpfennig S, Najder K, Pethő Z, Farfariello V, Prevarskaya N, Schwab A (2023) The context-dependent role of the Na⁺/Ca²⁺-exchanger (NCX) in pancreatic stellate cell migration. *Pflugers Arch* 475:1225–1240.
- Loeck T, Schwab A (2023) The role of the Na⁺/Ca²⁺-exchanger (NCX) in cancer-associated fibroblasts. *Biol Chem* 404:325–337.
- Long X, Nephew KP (2006) Fulvestrant (ICI 182,780)-dependent interacting proteins mediate immobilization and degradation of estrogen receptor- α . *J Biol Chem* 281:9607–9615.

- López-Anguila N, Gassaloglu SI, Stötzel M, Bolondi A, Conkar D, Typou M, Buschow R, Veenvliet JV, Bulut-Karslioglu A (2022) Hypoxia induces an early primitive streak signature, enhancing spontaneous elongation and lineage representation in gastruloids. *Development* 149:dev200679.
- Lopez-Charcas O, Poisson L, Benouna O, Lemoine R, Chadet S, Pétereau A, Lahlou W, Guyétant S, Ouaiissi M, Pukkanasut P, Dutta S, Velu SE, Besson P, Moussata D, Roger S (2022) Voltage-Gated Sodium Channel Nav1.5 Controls NHE-1-Dependent Invasive Properties in Colon Cancer Cells. *Cancers* 15 Available at: <http://dx.doi.org/10.3390/cancers15010046>.
- Lopez-Charcas O, Pukkanasut P, Velu SE, Brackenbury WJ, Hales TG, Besson P, Gomora JC, Roger S (2021) Pharmacological and nutritional targeting of voltage-gated sodium channels in the treatment of cancers. *ISCIENCE* 24:102270.
- Lorent J et al. (2019) Translational offsetting as a mode of estrogen receptor α -dependent regulation of gene expression. *EMBO J* 38:e101323.
- Love MI, Anders S, Huber W (2024) Analyzing RNA-seq data with DESeq2. Available at: <https://www.bioconductor.org/packages/release/bioc/vignettes/DESeq2/inst/doc/DESeq2.html#differential-expression-analysis> [Accessed August 5, 2024].
- Love MI, Huber W, Anders S (2014) Moderated estimation of fold change and dispersion for RNA-seq data with DESeq2. *Genome Biol* 15:550.
- Lucien F, Brochu-Gaudreau K, Arsenault D, Harper K, Dubois CM (2011) Hypoxia-induced invadopodia formation involves activation of NHE-1 by the p90 ribosomal S6 kinase (p90RSK). *PLoS One* 6:e28851.
- Łukasiewicz S, Czeczelewski M, Forma A, Baj J, Sitarz R, Stanisławek A (2021) Breast cancer-epidemiology, risk factors, classification, prognostic markers, and current treatment strategies-an updated review. *Cancers (Basel)* 13:4287.
- Luo Q, Wu T, Wu W, Chen G, Luo X, Jiang L, Tao H, Rong M, Kang S, Deng M (2020) The Functional Role of Voltage-Gated Sodium Channel Nav1.5 in Metastatic Breast Cancer. *Front Pharmacol* 11:1111.
- Lv C, Yang X, Yu B, Ma Q, Liu B, Liu Y (2012) Blocking the Na⁺/H⁺ exchanger 1 with cariporide (HOE642) reduces the hypoxia-induced invasion of human tongue squamous cell carcinoma. *Int J Oral Maxillofac Surg* 41:1206–1210.
- Ma S, Zhao Y, Lee WC, Ong L-T, Lee PL, Jiang Z, Oguz G, Niu Z, Liu M, Goh JY, Wang W, Bustos MA, Ehmsen S, Ramasamy A, Hoon DSB, Ditzel HJ, Tan EY, Chen Q, Yu Q (2022) Hypoxia induces HIF1 α -dependent epigenetic vulnerability in triple negative breast cancer to confer immune effector dysfunction and resistance to anti-PD-1 immunotherapy. *Nat Commun* 13:4118.
- Madak-Erdogan Z, Charn T-H, Jiang Y, Liu ET, Katzenellenbogen JA, Katzenellenbogen BS (2013) Integrative genomics of gene and metabolic regulation by estrogen receptors α and β , and their coregulators. *Mol Syst Biol* 9:676.

- Mader S, Kumar V, de Verneuil H, Chambon P (1989) Three amino acids of the oestrogen receptor are essential to its ability to distinguish an oestrogen from a glucocorticoid-responsive element. *Nature* 338:271–274.
- Maggi A (2011) Liganded and unliganded activation of estrogen receptor and hormone replacement therapies. *Biochim Biophys Acta* 1812:1054–1060.
- Mahalingaiah PKS, Ponnusamy L, Singh KP (2015) Chronic oxidative stress causes estrogen-independent aggressive phenotype, and epigenetic inactivation of estrogen receptor alpha in MCF-7 breast cancer cells. *Breast Cancer Res Treat* 153:41–56.
- Mahalingaiah PKS, Singh KP (2014) Chronic oxidative stress increases growth and tumorigenic potential of MCF-7 breast cancer cells. *PLoS One* 9:e87371.
- Malcolm JR, Bridge KS, Holding AN, Brackenbury WJ (2024) Identification of robust RT-qPCR reference genes for studying changes in gene expression in response to hypoxia in breast cancer cell lines. *bioRxiv:2024.08.02.606329* Available at: <https://www.biorxiv.org/content/10.1101/2024.08.02.606329v1.abstract> [Accessed August 7, 2024].
- Malcolm JR, Bridge KS, Holding AN, Brackenbury WJ (2025) Identification of robust RT-qPCR reference genes for studying changes in gene expression in response to hypoxia in breast cancer cell lines. *BMC Genomics* 26:59.
- Malcolm JR, Leese NK, Lamond-Warner PI, Brackenbury WJ, White RJ (2022) Widespread association of ER α with RMRP and tRNA genes in MCF-7 cells and breast cancers. *Gene* 821:146280.
- Malcolm JR, Sajjaboontawee N, Yerlikaya S, Plunkett-Jones C, Boxall PJ, Brackenbury WJ (2023) Voltage-gated sodium channels, sodium transport and progression of solid tumours. In: *Current Topics in Membranes*. Academic Press.
- Malcolm JR, White RJ (2022) Alternative isoforms of RNA polymerase III impact the non-coding RNA transcriptome, viability, proliferation and differentiation of prostate cancer cells. *Journal of Translational Genetics and Genomics* 6:126–133.
- Malhotra JD, Kazen-Gillespie K, Hortsch M, Isom LL (2000) Sodium channel beta subunits mediate homophilic cell adhesion and recruit ankyrin to points of cell-cell contact. *J Biol Chem* 275:11383–11388.
- Malhotra JD, Thyagarajan V, Chen C, Isom LL (2004) Tyrosine-phosphorylated and Nonphosphorylated Sodium Channel β 1 Subunits Are Differentially Localized in Cardiac Myocytes *. *J Biol Chem* 279:40748–40754.
- Mallikarjuna P, Raviprakash TS, Aripaka K, Ljungberg B, Landström M (2019) Interactions between TGF- β type I receptor and hypoxia-inducible factor- α mediates a synergistic crosstalk leading to poor prognosis for patients with clear cell renal cell carcinoma. *Cell Cycle* 18:2141–2156.
- Mamo M, Ye IC, DiGiacomo JW, Park JY, Downs B, Gilkes DM (2020) Hypoxia alters the response to anti-EGFR therapy by regulating EGFR expression

- and downstream signaling in a DNA methylation-specific and HIF-dependent manner. *Cancer Res* 80:4998–5010.
- Mantegazza M, Curia G, Biagini G, Ragsdale DS, Avoli M (2010) Voltage-gated sodium channels as therapeutic targets in epilepsy and other neurological disorders. *Lancet Neurol* 9:413–424.
- Martin AN, Li Y (2007) RNase MRP RNA and human genetic diseases. *Cell Res* 17:219–226.
- Martin TA, Ye L, Sanders AJ, Lane J, Jiang WG (2013) *Cancer Invasion and Metastasis: Molecular and Cellular Perspective*. Landes Bioscience.
- Mason CE, Shu F-J, Wang C, Session RM, Kallen RG, Sidell N, Yu T, Liu MH, Cheung E, Kallen CB (2010) Location analysis for the estrogen receptor- α reveals binding to diverse ERE sequences and widespread binding within repetitive DNA elements. *Nucleic Acids Res* 38:2355–2368.
- Masters JR, Thomson JA, Daly-Burns B, Reid YA, Dirks WG, Packer P, Toji LH, Ohno T, Tanabe H, Arlett CF, Kelland LR, Harrison M, Virmani A, Ward TH, Ayres KL, Debenham PG (2001) Short tandem repeat profiling provides an international reference standard for human cell lines. *Proc Natl Acad Sci U S A* 98:8012–8017.
- Mathews JC, Nadeem S, Levine AJ, Pouryahya M, Deasy JO, Tannenbaum A (2019) Robust and interpretable PAM50 reclassification exhibits survival advantage for myoepithelial and immune phenotypes. *NPJ Breast Cancer* 5:30.
- Mathieu V, Pirker C, Martin de Lassalle E, Vernier M, Mijatovic T, DeNeve N, Gaussin J-F, Dehoux M, Lefranc F, Berger W, Kiss R (2009) The sodium pump α 1 sub-unit: a disease progression-related target for metastatic melanoma treatment. *J Cell Mol Med* 13:3960–3972.
- Maxwell PH, Wiesener MS, Chang GW, Clifford SC, Vaux EC, Cockman ME, Wykoff CC, Pugh CW, Maher ER, Ratcliffe PJ (1999) The tumour suppressor protein VHL targets hypoxia-inducible factors for oxygen-dependent proteolysis. *Nature* 399:271–275.
- McDermott J, Sánchez G, Nangia AK, Blanco G (2015) Role of human Na,K-ATPase α 4 in sperm function, derived from studies in transgenic mice: HUMANNa,K-ATPase α 4INSPERMPHYSIOLOGY. *Mol Reprod Dev* 82:167–181.
- McEwen DP, Isom LL (2004) Heterophilic Interactions of Sodium Channel β 1 Subunits with Axonal and Glial Cell Adhesion Molecules. *Journal of Biological Chemistry* 279:52744–52752.
- Mercer RW, Biemesderfer D, Bliss DP Jr, Collins JH, Forbush B 3rd (1993) Molecular cloning and immunological characterization of the gamma polypeptide, a small protein associated with the Na,K-ATPase. *J Cell Biol* 121:579–586.
- Mertens C, Roeder RG (2008) Different functional modes of p300 in activation of RNA polymerase III transcription from chromatin templates. *Mol Cell Biol* 28:5764–5776.

- Meyer D, Kames J, Bar H, Komar AA, Alexaki A, Ibla J, Hunt RC, Santana-Quintero LV, Golikov A, DiCuccio M, Kimchi-Sarfaty C (2021) Distinct signatures of codon and codon pair usage in 32 primary tumor types in the novel database CancerCoCoPUTs for cancer-specific codon usage. *Genome Med* 13:122.
- Mijatovic T, Ingrassia L, Facchini V, Kiss R (2008) Na⁺/K⁺-ATPase alpha subunits as new targets in anticancer therapy. *Expert Opin Ther Targets* 12:1403–1417.
- Mills CN, Joshi SS, Niles RM (2009) Expression and function of hypoxia inducible factor-1 alpha in human melanoma under non-hypoxic conditions. *Mol Cancer* 8:104.
- Minor NT, Sha Q, Nichols CG, Mercer RW (1998) The gamma subunit of the Na,K-ATPase induces cation channel activity. *Proc Natl Acad Sci U S A* 95:6521–6525.
- Mirosevich J, Gao N, Matusik RJ (2005) Expression of Foxa transcription factors in the developing and adult murine prostate: Foxa Expression in the Murine Prostate. *Prostate* 62:339–352.
- Mishra D, Banerjee D (2023) Secretome of Stromal Cancer-Associated Fibroblasts (CAFs): Relevance in Cancer. *Cells* 12 Available at: <http://dx.doi.org/10.3390/cells12040628>.
- Mistry M, Khetani R, Piper M (2017) Gene-level differential expression analysis with DESeq2. Introduction to DGE - ARCHIVED Available at: https://hbctraining.github.io/DGE_workshop/lessons/05_DGE_DESeq2_analysis2.html [Accessed August 5, 2024].
- Mohammed FH, Khajah MA, Yang M, Brackenbury WJ, Luqmani YA (2016) Blockade of voltage-gated sodium channels inhibits invasion of endocrine-resistant breast cancer cells. *Int J Oncol* 48:73–83.
- Mohyeldin A, Garzón-Muvdi T, Quiñones-Hinojosa A (2010) Oxygen in stem cell biology: a critical component of the stem cell niche. *Cell Stem Cell* 7:150–161.
- Mole DR, Maxwell PH, Pugh CW, Ratcliffe PJ (2001) Regulation of HIF by the von Hippel-Lindau tumour suppressor: implications for cellular oxygen sensing. *IUBMB Life* 52:43–47.
- Mungall AJ et al. (2003) The DNA sequence and analysis of human chromosome 6. *Nature* 425:805–811.
- Murphy FV 4th, Ramakrishnan V (2004) Structure of a purine-purine wobble base pair in the decoding center of the ribosome. *Nat Struct Mol Biol* 11:1251–1252.
- Muz B, de la Puente P, Azab F, Azab AK (2015) The role of hypoxia in cancer progression, angiogenesis, metastasis, and resistance to therapy. *Hypoxia (Auckl)* 3:83–92.
- Nabet BY, Qiu Y, Shabason JE, Wu TJ, Yoon T, Kim BC, Benci JL, DeMichele AM, Tchou J, Marcotrigiano J, Minn AJ (2017) Exosome RNA Unshielding

Couples Stromal Activation to Pattern Recognition Receptor Signaling in Cancer. *Cell* 170:352-366.e13.

- Nadai T, Narumi K, Furugen A, Saito Y, Iseki K, Kobayashi M (2021) Pharmacological Inhibition of MCT4 Reduces 4-Hydroxytamoxifen Sensitivity by Increasing HIF-1 α Protein Expression in ER-Positive MCF-7 Breast Cancer Cells. *Biol Pharm Bull* 44:1247–1253.
- Nagaike T, Suzuki T, Tomari Y, Takemoto-Hori C, Negayama F, Watanabe K, Ueda T (2001) Identification and characterization of mammalian mitochondrial tRNA nucleotidyltransferases. *J Biol Chem* 276:40041–40049.
- Nakajima T, Kubota N, Tsutsumi T, Oguri A, Imuta H, Jo T, Oonuma H, Soma M, Meguro K, Takano H, Nagase T, Nagata T (2009) Eicosapentaenoic acid inhibits voltage-gated sodium channels and invasiveness in prostate cancer cells. *Br J Pharmacol* 156:420–431.
- Nakayama T, Okada N, Yoshikawa M, Asaka D, Kuboki A, Kojima H, Tanaka Y, Haruna S-I (2018) Assessment of suitable reference genes for RT-qPCR studies in chronic rhinosinusitis. *Sci Rep* 8:1568.
- Nardin S, Mora E, Varughese FM, D'Avanzo F, Vachanaram AR, Rossi V, Saggia C, Rubinelli S, Gennari A (2020) Breast Cancer Survivorship, Quality of Life, and Late Toxicities. *Front Oncol* 10:864.
- Neavin DR, Liu D, Ray B, Weinshilboum RM (2018) The role of the aryl hydrocarbon receptor (AHR) in immune and inflammatory diseases. *Int J Mol Sci* 19:3851.
- Nedeljković M, Damjanović A (2019) Mechanisms of chemotherapy resistance in triple-negative breast cancer-how we can rise to the challenge. *Cells* 8:957.
- Nelson M, Millican-Slater R, Forrest LC, Brackenbury WJ (2014) The sodium channel β 1 subunit mediates outgrowth of neurite-like processes on breast cancer cells and promotes tumour growth and metastasis. *Int J Cancer* 135:2338–2351.
- Nelson M, Yang M, Dowle AA, Thomas JR, Brackenbury WJ (2015a) The sodium channel-blocking antiepileptic drug phenytoin inhibits breast tumour growth and metastasis. *Mol Cancer* 14:13.
- Nelson M, Yang M, Millican-Slater R, Brackenbury WJ (2015b) Nav1.5 regulates breast tumor growth and metastatic dissemination in vivo. *Oncotarget* 6:32914–32929.
- Nicolau M, Levine AJ, Carlsson G (2011) Topology based data analysis identifies a subgroup of breast cancers with a unique mutational profile and excellent survival. *Proc Natl Acad Sci U S A* 108:7265–7270.
- Nicolini A, Rossi G, Ferrari P, Carpi A (2022) Minimal residual disease in advanced or metastatic solid cancers: The G0-G1 state and immunotherapy are key to unwinding cancer complexity. *Semin Cancer Biol* 79:68–82.
- Nielsen TO, Parker JS, Leung S, Voduc D, Ebbert M, Vickery T, Davies SR, Snider J, Stijleman IJ, Reed J, Cheang MCU, Mardis ER, Perou CM, Bernard PS, Ellis MJ (2010) A comparison of PAM50 intrinsic subtyping with

immunohistochemistry and clinical prognostic factors in tamoxifen-treated estrogen receptor-positive breast cancer. *Clin Cancer Res* 16:5222–5232.

Nilsson B, Mijatovic T, Mathieu A, Roland I, Van Quaquebeke E, Van Vynckt F, Darro F, Kiss R (2007) Targeting Na⁺/K⁺-ATPase in non-small cell lung cancer (NSCLC). *J Clin Oncol* 25:18144–18144.

Nishi H, Ono M, Ohno S, Yamanaka Z, Sasaki T, Ohyashiki K, Ohyashiki JH, Kuroda M (2023) Hypoxia-induced paclitaxel resistance in cervical cancer modulated by miR-100 targeting of USP15. *Gynecol Oncol Rep* 45:101138.

Nofech-Mozes I, Soave D, Awadalla P, Abelson S (2023) Pan-cancer classification of single cells in the tumour microenvironment. *Nat Commun* 14:1615.

Nordsmark M, Overgaard J (2004) Tumor hypoxia is independent of hemoglobin and prognostic for loco-regional tumor control after primary radiotherapy in advanced head and neck cancer. *Acta Oncol* 43:396–403.

Noreng S, Bharadwaj A, Posert R, Yoshioka C, Bacongus I (2018) Structure of the human epithelial sodium channel by cryo-electron microscopy. *Elife* 7 Available at: <https://elifesciences.org/articles/39340> [Accessed September 11, 2024].

Obidiro O, Battogtokh G, Akala EO (2023) Triple negative breast cancer treatment options and limitations: Future outlook. *Pharmaceutics* 15 Available at: <https://www.ncbi.nlm.nih.gov/pmc/articles/PMC10384267/> [Accessed September 19, 2024].

Obradovic M, Zafirovic S, Jovanovic A, Milovanovic ES, Mousa SA, Labudovic-Borovic M, Isenovic ER (2015) Effects of 17 β -estradiol on cardiac Na⁺/K⁺-ATPase in high fat diet fed rats. *Molecular and Cellular Endocrinology* 416:46–56.

Oda K, Iwamoto Y, Tsukada K (2016) Simultaneous mapping of unevenly distributed tissue hypoxia and vessel permeability in tumor microenvironment. *Biomed Phys Eng Express* 2:065017.

Ohira T, Suzuki T (2024) Transfer RNA modifications and cellular thermotolerance. *Mol Cell* 84:94–106.

Olde B, Leeb-Lundberg LMF (2009) GPR30/GPER1: searching for a role in estrogen physiology. *Trends Endocrinol Metab* 20:409–416.

O'Lone R, Frith MC, Karlsson EK, Hansen U (2004) Genomic targets of nuclear estrogen receptors. *Mol Endocrinol* 18:1859–1875.

Ong CHC, Lee DY, Lee B, Li H, Lim JCT, Lim JX, Yeong JPS, Lau HY, Thike AA, Tan PH, Iqbal J (2022) Hypoxia-regulated carbonic anhydrase IX (CAIX) protein is an independent prognostic indicator in triple negative breast cancer. *Breast Cancer Res* 24:38.

Ong HT, Prêle CM, Dilley RJ (2023) Using RNA-seq to identify suitable housekeeping genes for hypoxia studies in human adipose-derived stem cells. *BMC Mol Cell Biol* 24:16.

- Onitilo AA, Engel JM, Greenlee RT, Mukesh BN (2009) Breast cancer subtypes based on ER/PR and Her2 expression: comparison of clinicopathologic features and survival. *Clin Med Res* 7:4–13.
- Onkal R, Mattis JH, Fraser SP, Diss JKJ, Shao D, Okuse K, Djamgoz MBA (2008) Alternative splicing of Nav1.5: an electrophysiological comparison of “neonatal” and “adult” isoforms and critical involvement of a lysine residue. *J Cell Physiol* 216:716–726.
- Orioli A, Pascali C, Pagano A, Teichmann M, Dieci G (2012) RNA polymerase III transcription control elements: themes and variations. *Gene* 493:185–194.
- Orrantia-Borunda E, Anchondo-Nuñez P, Acuña-Aguilar LE, Gómez-Valles FO, Ramírez-Valdespino CA (2022) Subtypes of Breast Cancer. In: *Breast Cancer*, pp 31–42. Exon Publications.
- Ottaviano YL, Issa JP, Parl FF, Smith HS, Baylin SB, Davidson NE (1994) Methylation of the estrogen receptor gene CpG island marks loss of estrogen receptor expression in human breast cancer cells. *Cancer Res* 54:2552–2555.
- Ou S-W, Kameyama A, Hao L-Y, Horiuchi M, Minobe E, Wang W-Y, Makita N, Kameyama M (2005) Tetrodotoxin-resistant Na⁺ channels in human neuroblastoma cells are encoded by new variants of Nav1.5/SCN5A. *Eur J Neurosci* 22:793–801.
- Ou Y, Pan CX, Zuo J, van der Hoorn FA (2017) Ouabain affects cell migration via Na,K-ATPase-p130cas and via nucleus-centrosome association. *PLoS One* 12:e0183343.
- Ouwerkerk R, Bleich KB, Gillen JS, Pomper MG, Bottomley PA (2003) Tissue Sodium Concentration in Human Brain Tumors as Measured with ²³Na MR Imaging. *Radiology* 227:529–537.
- Ouwerkerk R, Jacobs MA, Macura KJ, Wolff AC, Stearns V, Mezban SD, Khouri NF, Bluemke DA, Bottomley PA (2007) Elevated tissue sodium concentration in malignant breast lesions detected with non-invasive ²³Na MRI. *Breast Cancer Res Treat* 106:151–160.
- Paakinaho V, Swinstead EE, Presman DM, Grøntved L, Hager GL (2019) Meta-analysis of Chromatin Programming by Steroid Receptors. *Cell Rep* 28:3523-3534.e2.
- Padró M, Louie RJ, Lananna BV, Krieg AJ, Timmerman LA, Chan DA (2017) Genome-independent hypoxic repression of estrogen receptor alpha in breast cancer cells. *BMC Cancer* 17:203.
- Pan H, Gray R, Braybrooke J, Davies C, Taylor C, McGale P, Peto R, Pritchard KI, Bergh J, Dowsett M, Hayes DF, EBCTCG (2017) 20-Year Risks of Breast-Cancer Recurrence after Stopping Endocrine Therapy at 5 Years. *N Engl J Med* 377:1836–1846.
- Pan T (2018) Modifications and functional genomics of human transfer RNA. *Cell Res* 28:395–404.

- Pan X, Li Z, Zhou Q, Shen H, Wu K, Huang X, Chen J, Zhang J, Zhu X, Lei J, Xiong W, Gong H, Xiao B, Yan N (2018) Structure of the human voltage-gated sodium channel Nav1.4 in complex with $\beta 1$. *Science* 362:eaau2486.
- Pancholi S, Leal MF, Ribas R, Simigdala N, Schuster E, Chateau-Joubert S, Zabaglo L, Hills M, Dodson A, Gao Q, Johnston SR, Dowsett M, Cosulich SC, Maragoni E, Martin L-A (2019) Combination of mTORC1/2 inhibitor vistusertib plus fulvestrant in vitro and in vivo targets oestrogen receptor-positive endocrine-resistant breast cancer. *Breast Cancer Res* 21:135.
- Pancholi S, Simigdala N, Ribas R, Schuster E, Leal MF, Nikitorowicz-Buniak J, Rega C, Bihani T, Patel H, Johnston SR, Dowsett M, Martin L-A (2022) Elacestrant demonstrates strong anti-estrogenic activity in PDX models of estrogen-receptor positive endocrine-resistant and fulvestrant-resistant breast cancer. *NPJ Breast Cancer* 8:125.
- Pancrazio J, Viglione M, Tabbara I, Kim YI (1989) Voltage-dependent ion channels in small-cell lung cancer cells. *Cancer Res* 49:5901–5906.
- Papachristou EK, Kishore K, Holding AN, Harvey K, Roumeliotis TI, Chilamakuri CSR, Omarjee S, Chia KM, Swarbrick A, Lim E, Markowitz F, Eldridge M, Siersbaek R, D'Santos CS, Carroll JS (2018) A quantitative mass spectrometry-based approach to monitor the dynamics of endogenous chromatin-associated protein complexes. *Nat Commun* 9:2311.
- Papi A, Ferreri AM, Guerra F, Orlandi M (2012) Anti-invasive effects and proapoptotic activity induction by the rexinoid IIF and valproic acid in combination on colon cancer cell lines. *Anticancer Res* 32:2855–2862.
- Park S, Koo JS, Kim MS, Park HS, Lee JS, Lee JS, Kim SI, Park B-W (2012) Characteristics and outcomes according to molecular subtypes of breast cancer as classified by a panel of four biomarkers using immunohistochemistry. *Breast* 21:50–57.
- Parker JS et al. (2009) Supervised risk predictor of breast cancer based on intrinsic subtypes. *J Clin Oncol* 27:1160–1167.
- Patino GA, Brackenbury WJ, Bao Y, Lopez-Santiago LF, O'Malley HA, Chen C, Calhoun JD, Lafrenière RG, Cossette P, Rouleau GA, Isom LL (2011) Voltage-gated Na⁺ channel $\beta 1B$: a secreted cell adhesion molecule involved in human epilepsy. *J Neurosci* 31:14577–14591.
- Patrone C, Gianazza E, Santagati S, Agrati P, Maggi A (1998) Divergent pathways regulate ligand-independent activation of ER alpha in SK-N-BE neuroblastoma and COS-1 renal carcinoma cells. *Mol Endocrinol* 12:835–841.
- Paudel P, McDonald FJ, Fronius M (2021) The δ subunit of epithelial sodium channel in humans—a potential player in vascular physiology. *Am J Physiol Heart Circ Physiol* 320:H487–H493.
- Paushkin SV, Patel M, Furia BS, Peltz SW, Trotta CR (2004) Identification of a human endonuclease complex reveals a link between tRNA splicing and pre-mRNA 3' end formation. *Cell* 117:311–321.

- Pavon-Eternod M, Gomes S, Geslain R, Dai Q, Rosner MR, Pan T (2009) tRNA over-expression in breast cancer and functional consequences. *Nucleic Acids Res* 37:7268–7280.
- Pavon-Eternod M, Gomes S, Rosner MR, Pan T (2013) Overexpression of initiator methionine tRNA leads to global reprogramming of tRNA expression and increased proliferation in human epithelial cells. *RNA Society* 19:461–466.
- Payandeh J, Scheuer T, Zheng N, Catterall WA (2011) The crystal structure of a voltage-gated sodium channel. *Nature* 475:353–358.
- Pedersen RN, Esen BÖ, Mellekjær L, Christiansen P, Ejlersen B, Lash TL, Nørgaard M, Cronin-Fenton D (2022) The incidence of breast cancer recurrence 10-32 years after primary diagnosis. *J Natl Cancer Inst* 114:391–399.
- Pedersen SF, Novak I, Alves F, Schwab A, Pardo LA (2017) Alternating pH landscapes shape epithelial cancer initiation and progression: Focus on pancreatic cancer. *Bioessays* 39 Available at: <http://dx.doi.org/10.1002/bies.201600253>.
- Pereira B et al. (2016) The somatic mutation profiles of 2,433 breast cancers refines their genomic and transcriptomic landscapes. *Nat Commun* 7:11479.
- Perou CM, Sørlie T, Eisen MB, van de Rijn M, Jeffrey SS, Rees CA, Pollack JR, Ross DT, Johnsen H, Akslén LA, Fluge O, Pergamenschikov A, Williams C, Zhu SX, Lønning PE, Børresen-Dale AL, Brown PO, Botstein D (2000) Molecular portraits of human breast tumours. *Nature* 406:747–752.
- Persi E, Duran-Frigola M, Damaghi M, Roush WR, Aloy P, Cleveland JL, Gillies RJ, Ruppin E (2018) Systems analysis of intracellular pH vulnerabilities for cancer therapy. *Nat Commun* 9:2997.
- Pethő Z, Najder K, Carvalho T, McMorrow R, Todesca LM, Rugi M, Bulk E, Chan A, Löwik CWGM, Reshkin SJ, Schwab A (2020) pH-Channeling in Cancer: How pH-Dependence of Cation Channels Shapes Cancer Pathophysiology. *Cancers* 12 Available at: <http://dx.doi.org/10.3390/cancers12092484>.
- Petrie JL, Swan C, Ingram RM, Frame FM, Collins AT, Dumay-Odelot H, Teichmann M, Maitland NJ, White RJ (2019) Effects on prostate cancer cells of targeting RNA polymerase III. *Nucleic Acids Res* 47:3937–3956.
- Petrova V, Annicchiarico-Petruzzelli M, Melino G, Amelio I (2018) The hypoxic tumour microenvironment. *Oncogenesis* 7:10.
- Pfaffl MW, Tichopad A, Prgomet C, Neuvians TP (2004) Determination of stable housekeeping genes, differentially regulated target genes and sample integrity: BestKeeper—Excel-based tool using pair-wise correlations. *Biotechnol Lett* 26:509–515.
- Philipson KD, Bersohn MM, Nishimoto AY (1982) Effects of pH on Na⁺-Ca²⁺ exchange in canine cardiac sarcolemmal vesicles. *Circ Res* 50:287–293.
- Phizicky EM, Alfonzo JD (2010) Do all modifications benefit all tRNAs? *FEBS Lett* 584:265–271.

- Pierandrei S, Truglio G, Ceci F, Del Porto P, Bruno SM, Castellani S, Conese M, Ascenzioni F, Lucarelli M (2021) DNA methylation patterns correlate with the expression of SCNN1A, SCNN1B, and SCNN1G (epithelial sodium channel, ENaC) genes. *Int J Mol Sci* 22:3754.
- Pimton P, Lecht S, Stabler CT, Johannes G, Schulman ES, Lelkes PI (2015) Hypoxia enhances differentiation of mouse embryonic stem cells into definitive endoderm and distal lung cells. *Stem Cells Dev* 24:663–676.
- Piryaei Z, Salehi Z, Ebrahimie E, Ebrahimi M, Kavousi K (2023) Meta-analysis of integrated ChIP-seq and transcriptome data revealed genomic regions affected by estrogen receptor alpha in breast cancer. *BMC Med Genomics* 16:219.
- Pistilli B, Lohrisch C, Sheade J, Fleming GF (2022) Personalizing adjuvant endocrine therapy for early-stage hormone receptor-positive breast cancer. *Am Soc Clin Oncol Educ Book* 42:1–13.
- Plant LD, Xiong D, Romero J, Dai H, Goldstein SAN (2020) Hypoxia Produces Pro-arrhythmic Late Sodium Current in Cardiac Myocytes by SUMOylation of Nav1.5 Channels. *Cell Rep* 30:2225-2236.e4.
- Pollard PJ, Spencer-Dene B, Shukla D, Howarth K, Nye E, El-Bahrawy M, Deheragoda M, Joannou M, McDonald S, Martin A, Igarashi P, Varsani-Brown S, Rosewell I, Poulson R, Maxwell P, Stamp GW, Tomlinson IPM (2007) Targeted inactivation of fh1 causes proliferative renal cyst development and activation of the hypoxia pathway. *Cancer Cell* 11:311–319.
- Prall OW, Sarcevic B, Musgrove EA, Watts CK, Sutherland RL (1997) Estrogen-induced activation of Cdk4 and Cdk2 during G1-S phase progression is accompanied by increased cyclin D1 expression and decreased cyclin-dependent kinase inhibitor association with cyclin E-Cdk2. *J Biol Chem* 272:10882–10894.
- Prat A, Perou CM (2011) Deconstructing the molecular portraits of breast cancer. *Mol Oncol* 5:5–23.
- Prevarskaya N, Skryma R, Shuba Y (2010) Ion channels and the hallmarks of cancer. *Trends Mol Med* 16:107–121.
- Prevarskaya N, Skryma R, Shuba Y (2018) Ion channels in cancer: Are cancer hallmarks oncochannelopathies? *Physiol Rev* 98:559–621.
- Pu J, Wang F, Ye P, Jiang X, Zhou W, Gu Y, Chen S (2022) Salt-inducible kinase 1 deficiency promotes vascular remodeling in pulmonary arterial hypertension via enhancement of yes-associated protein-mediated proliferation. *Heliyon* 8:e11016.
- Pu M, Messer K, Davies SR, Vickery TL, Pittman E, Parker BA, Ellis MJ, Flatt SW, Marinac CR, Nelson SH, Mardis ER, Pierce JP, Natarajan L (2020) Research-based PAM50 signature and long-term breast cancer survival. *Breast Cancer Res Treat* 179:197–206.
- Rafels-Ybern À, Torres AG, Grau-Bove X, Ruiz-Trillo I, Ribas de Pouplana L (2018) Codon adaptation to tRNAs with Inosine modification at position 34 is

widespread among Eukaryotes and present in two Bacterial phyla. *RNA Biol* 15:500–507.

- Rajasekaran SA, Ball WJ Jr, Bander NH, Liu H, Pardee JD, Rajasekaran AK (1999) Reduced expression of beta-subunit of Na,K-ATPase in human clear-cell renal cell carcinoma. *J Urol* 162:574–580.
- Ramachandran R, Ibragimova S, Woods LM, AlHouqani T, Gomez RL, Simeoni F, Hachim MY, Somerville TCP, Philpott A, Carroll JS, Ali FR (2024) Conserved role of FOXC1 in TNBC is parallel to FOXA1 in ER+ breast cancer. *iScience* 27:110500.
- Ramos EAS, Camargo AA, Braun K, Slowik R, Cavalli IJ, Ribeiro EMSF, Pedrosa F de O, de Souza EM, Costa FF, Klassen G (2010) Simultaneous CXCL12 and ESR1 CpG island hypermethylation correlates with poor prognosis in sporadic breast cancer. *BMC Cancer* 10:23.
- Ramsay EP, Abascal-Palacios G, Daiß JL, King H, Gouge J, Pilsel M, Beuron F, Morris E, Gunkel P, Engel C, Vannini A (2020) Structure of human RNA polymerase III. *Nat Commun* 11:6409.
- Ramsay EP, Vannini A (2018) Structural rearrangements of the RNA polymerase III machinery during tRNA transcription initiation. *Biochim Biophys Acta Gene Regul Mech* 1861:285–294.
- Raney BJ et al. (2024) The UCSC Genome Browser database: 2024 update. *Nucleic Acids Res* 52:D1082–D1088.
- Rangel N, Villegas VE, Rondón-Lagos M (2017) Profiling of gene expression regulated by 17 β -estradiol and tamoxifen in estrogen receptor-positive and estrogen receptor-negative human breast cancer cell lines. *Breast Cancer (Dove Med Press)* 9:537–550.
- Rankin EB, Nam J-M, Giaccia AJ (2016) Hypoxia: Signaling the Metastatic Cascade. *Trends Cancer Res* 2:295–304.
- Ratcliffe CF, Westenbroek RE, Curtis R, Catterall WA (2001) Sodium channel beta1 and beta3 subunits associate with neurofascin through their extracellular immunoglobulin-like domain. *J Cell Biol* 154:427–434.
- Rebouças E de L, Costa JJ do N, Passos MJ, Passos JR de S, van den Hurk R, Silva JRV (2013) Real time PCR and importance of housekeeping genes for normalization and quantification of mRNA expression in different tissues. *Braz Arch Biol Technol* 56:143–154.
- Reddy SM, Barcenas CH, Sinha AK, Hsu L, Moulder SL, Tripathy D, Hortobagyi GN, Valero V (2018) Long-term survival outcomes of triple-receptor negative breast cancer survivors who are disease free at 5 years and relationship with low hormone receptor positivity. *Br J Cancer* 118:17–23.
- Reese KA, Caldwell JH (1999) Immunocytochemical localization of NaCh6 in cultured spinal cord astrocytes. *Glia* 26:92–96.
- Reimand J, Isserlin R, Voisin V, Kucera M, Tannus-Lopes C, Rostamianfar A, Wadi L, Meyer M, Wong J, Xu C, Merico D, Bader GD (2019) Pathway enrichment

analysis and visualization of omics data using g:Profiler, GSEA, Cytoscape and EnrichmentMap. *Nat Protoc* 14:482–517.

- Renaud M, Praz V, Vieu E, Florens L, Washburn MP, l'Hôte P, Hernandez N (2014) Gene duplication and neofunctionalization: POLR3G and POLR3GL. *Genome Res* 24:37–51.
- Reshetnyak YK, Yao L, Zheng S, Kuznetsov S, Engelman DM, Andreev OA (2011) Measuring tumor aggressiveness and targeting metastatic lesions with fluorescent pHLIP. *Mol Imaging Biol* 13:1146–1156.
- Revankar CM, Cimino DF, Sklar LA, Arterburn JB, Prossnitz ER (2005) A transmembrane intracellular estrogen receptor mediates rapid cell signaling. *Science* 307:1625–1630.
- Rheinbay E et al. (2017) Recurrent and functional regulatory mutations in breast cancer. *Nature* 547:55–60.
- Rheinbay E et al. (2020) Analyses of non-coding somatic drivers in 2,658 cancer whole genomes. *Nature* 578:102–111.
- Ridanpää M, van Eenennaam H, Pelin K, Chadwick R, Johnson C, Yuan B, van Venrooij W, Pruijn G, Salmela R, Rockas S, Mäkitie O, Kaitila I, de la Chapelle A (2001) Mutations in the RNA component of RNase MRP cause a pleiotropic human disease, cartilage-hair hypoplasia. *Cell* 104:195–203.
- Rizaner N, Uzun S, Fraser SP, Djamgoz MBA, Altun S (2020) Riluzole: Anti-invasive effects on rat prostate cancer cells under normoxic and hypoxic conditions. *Basic Clin Pharmacol Toxicol* 127:254–264.
- Roger S, Besson P, Le Guennec J-Y (2003) Involvement of a novel fast inward sodium current in the invasion capacity of a breast cancer cell line. *Biochim Biophys Acta* 1616:107–111.
- Roger S, Gillet L, Le Guennec J-Y, Besson P (2015) Voltage-gated sodium channels and cancer: is excitability their primary role? *Front Pharmacol* 6:152.
- Roger S, Potier M, Vandier C, Besson P, Le Guennec J-Y (2006) Voltage-gated sodium channels: new targets in cancer therapy? *Curr Pharm Des* 12:3681–3695.
- Roger S, Rollin J, Barascu A, Besson P, Raynal P-I, Lochmann S, Lei M, Bougnoux P, Gruel Y, Le Guennec J-Y (2007) Voltage-gated sodium channels potentiate the invasive capacities of human non-small-cell lung cancer cell lines. *Int J Biochem Cell Biol* 39:774–786.
- Rooj AK, McNicholas CM, Bartoszewski R, Bebok Z, Benos DJ, Fuller CM (2012) Glioma-specific Cation Conductance Regulates Migration and Cell Cycle Progression. *Journal of Biological Chemistry* 287:4053–4065.
- Rosa P, Catacuzzeno L, Sforna L, Mangino G, Carlomagno S, Mincione G, Petrozza V, Ragona G, Franciolini F, Calogero A (2018) BK channels blockage inhibits hypoxia-induced migration and chemoresistance to cisplatin in human glioblastoma cells. *J Cell Physiol* 233:6866–6877.

- Rossi D, Zlotnik A (2000) The Biology of Chemokines and their Receptors. *Annu Rev Immunol* 18:217–242.
- Rossier BC, Baker ME, Studer RA (2015) Epithelial sodium transport and its control by aldosterone: the story of our internal environment revisited. *Physiol Rev* 95:297–340.
- Ross-Innes CS, Stark R, Teschendorff AE, Holmes KA, Ali HR, Dunning MJ, Brown GD, Gojis O, Ellis IO, Green AR, Ali S, Chin S-F, Palmieri C, Caldas C, Carroll JS (2012) Differential oestrogen receptor binding is associated with clinical outcome in breast cancer. *Nature* 481:389–393.
- Rusecka J, Kaliszewska M, Bartnik E, Tońska K (2018) Nuclear genes involved in mitochondrial diseases caused by instability of mitochondrial DNA. *J Appl Genet* 59:43–57.
- Russell J, Zomerdiijk JCBM (2005) RNA-polymerase-I-directed rDNA transcription, life and works. *Trends Biochem Sci* 30:87–96.
- Russell WC, Newman C, Williamson DH (1975) A simple cytochemical technique for demonstration of DNA in cells infected with mycoplasmas and viruses. *Nature* 253:461–462.
- Ryu K, Park C, Lee Y (2011) Hypoxia-inducible factor 1 alpha represses the transcription of the estrogen receptor alpha gene in human breast cancer cells. *Biochem Biophys Res Commun* 407:831–836.
- Sahai E et al. (2020) A framework for advancing our understanding of cancer-associated fibroblasts. *Nat Rev Cancer* 20:174–186.
- Sakai H, Suzuki T, Maeda M, Takahashi Y, Horikawa N, Minamimura T, Tsukada K, Takeguchi N (2004) Up-regulation of Na(+),K(+)-ATPase alpha 3-isoform and down-regulation of the alpha1-isoform in human colorectal cancer. *FEBS Lett* 563:151–154.
- Salceda S, Caro J (1997) Hypoxia-inducible factor 1alpha (HIF-1alpha) protein is rapidly degraded by the ubiquitin-proteasome system under normoxic conditions. Its stabilization by hypoxia depends on redox-induced changes. *J Biol Chem* 272:22642–22647.
- Samanta D, Gilkes DM, Chaturvedi P, Xiang L, Semenza GL (2014) Hypoxia-inducible factors are required for chemotherapy resistance of breast cancer stem cells. *Proc Natl Acad Sci U S A* 111:E5429-38.
- Samson J, Cronin S, Dean K (2018) BC200 (BCYRN1) - The shortest, long, non-coding RNA associated with cancer. *Noncoding RNA Res* 3:131–143.
- Sanchez-Sandoval AL, Hernández-Plata E, Gomora JC (2023) Voltage-gated sodium channels: from roles and mechanisms in the metastatic cell behavior to clinical potential as therapeutic targets. *Front Pharmacol* 14:1206136.
- Schneider C, Spaik H, Alexe G, Dharia NV, Meyer A, Merickel LA, Khalid D, Scheich S, Haupl B, Staudt LM, Oellerich T, Stegmaier K (2024) Targeting the sodium-potassium pump as a therapeutic strategy in acute myeloid leukemia. *Cancer Res* Available at: <https://aacrjournals.org/cancerres/article->

- Schoppmann SF, Birner P, Stöckl J, Kalt R, Ullrich R, Caucig C, Kriehuber E, Nagy K, Alitalo K, Kerjaschki D (2002) Tumor-associated macrophages express lymphatic endothelial growth factors and are related to peritumoral lymphangiogenesis. *Am J Pathol* 161:947–956.
- Schramm L, Hernandez N (2002) Recruitment of RNA polymerase III to its target promoters. *Genes Dev* 16:2593–2620.
- Schwabe JW, Chapman L, Finch JT, Rhodes D (1993) The crystal structure of the estrogen receptor DNA-binding domain bound to DNA: how receptors discriminate between their response elements. *Cell* 75:567–578.
- Seachrist DD, Anstine LJ, Keri RA (2021) FOXA1: A pioneer of nuclear receptor action in breast cancer. *Cancers (Basel)* 13:5205.
- Semenza GL, Wang GL (1992) A nuclear factor induced by hypoxia via de novo protein synthesis binds to the human erythropoietin gene enhancer at a site required for transcriptional activation. *Mol Cell Biol* 12:5447–5454.
- Sérandour AA, Avner S, Percevault F, Demay F, Bizot M, Lucchetti-Miganeh C, Barloy-Hubler F, Brown M, Lupien M, Métivier R, Salbert G, Eeckhoutte J (2011) Epigenetic switch involved in activation of pioneer factor FOXA1-dependent enhancers. *Genome Res* 21:555–565.
- Servais C, Erez N (2013) From sentinel cells to inflammatory culprits: cancer-associated fibroblasts in tumour-related inflammation. *J Pathol* 229:198–207.
- Shamis SAK, Quinn J, Mallon EEA, Edwards J, McMillan DC (2022) The Relationship Between the Tumor Cell Expression of Hypoxic Markers and Survival in Patients With ER-positive Invasive Ductal Breast Cancer. *J Histochem Cytochem* 70:479–494.
- Shan B, Dong M, Tang H, Wang N, Zhang J, Yan C, Jiao X, Zhang H, Wang C (2014) Voltage-gated sodium channels were differentially expressed in human normal prostate, benign prostatic hyperplasia and prostate cancer cells. *Oncol Lett* 8:345–350.
- Shandell MA, Capatina AL, Lawrence SM, Brackenbury WJ, Lagos D (2022) Inhibition of the Na⁺/K⁺-ATPase by cardiac glycosides suppresses expression of the IDO1 immune checkpoint in cancer cells by reducing STAT1 activation. *J Biol Chem* 298:101707.
- Shi Y, Chanana V, Watters JJ, Ferrazzano P, Sun D (2011) Role of sodium/hydrogen exchanger isoform 1 in microglial activation and proinflammatory responses in ischemic brains: Na⁺/H⁺ exchange in microglia. *J Neurochem* 119:124–135.
- Shiau AK, Barstad D, Loria PM, Cheng L, Kushner PJ, Agard DA, Greene GL (1998) The structural basis of estrogen receptor/coactivator recognition and the antagonism of this interaction by tamoxifen. *Cell* 95:927–937.
- Shibuya K, Fukuoka J, Fujii T, Shimoda E, Shimizu T, Sakai H, Tsukada K (2010) Increase in ouabain-sensitive K⁺-ATPase activity in hepatocellular

- carcinoma by overexpression of Na⁺, K⁺-ATPase alpha 3-isoform. *Eur J Pharmacol* 638:42–46.
- Shimoda LA, Fallon M, Pisarcik S, Wang J, Semenza GL (2006) HIF-1 regulates hypoxic induction of NHE1 expression and alkalization of intracellular pH in pulmonary arterial myocytes. *Am J Physiol Lung Cell Mol Physiol* 291:L941-9.
- Silva CI da, Gonçalves-de-Albuquerque CF, Moraes BPT de, Garcia DG, Burth P (2021) Na/K-ATPase: Their role in cell adhesion and migration in cancer. *Biochimie* 185:1–8.
- Silver N, Best S, Jiang J, Thein SL (2006) Selection of housekeeping genes for gene expression studies in human reticulocytes using real-time PCR. *BMC Mol Biol* 7:33.
- Singh JK, Simões BM, Howell SJ, Farnie G, Clarke RB (2013) Recent advances reveal IL-8 signaling as a potential key to targeting breast cancer stem cells. *Breast Cancer Res* 15:210.
- Singh R, Gupta SC, Peng W-X, Zhou N, Pochampally R, Atfi A, Watabe K, Lu Z, Mo Y-Y (2016) Regulation of alternative splicing of Bcl-x by BC200 contributes to breast cancer pathogenesis. *Cell Death Dis* 7:e2262.
- Sizer RE, Chahid N, Butterfield SP, Donze D, Bryant NJ, White RJ (2022) TFIIIC-based chromatin insulators through eukaryotic evolution. *Gene* 835:146533.
- Skou JC (1957) The influence of some cations on an adenosine triphosphatase from peripheral nerves. *Biochim Biophys Acta* 23:394–401.
- Skou JC, Esmann M (1992) The Na,K-ATPase. *J Bioenerg Biomembr* 24:249–261.
- Smith CL, Oñate SA, Tsai MJ, O'Malley BW (1996) CREB binding protein acts synergistically with steroid receptor coactivator-1 to enhance steroid receptor-dependent transcription. *Proc Natl Acad Sci U S A* 93:8884–8888.
- Smith IE, Dowsett M (2003) Aromatase inhibitors in breast cancer. *N Engl J Med* 348:2431–2442.
- Sørli T, Perou CM, Tibshirani R, Aas T, Geisler S, Johnsen H, Hastie T, Eisen MB, van de Rijn M, Jeffrey SS, Thorsen T, Quist H, Matese JC, Brown PO, Botstein D, Lønning PE, Børresen-Dale AL (2001) Gene expression patterns of breast carcinomas distinguish tumor subclasses with clinical implications. *Proc Natl Acad Sci U S A* 98:10869–10874.
- Soumoy L, Genbauffe A, Mouchart L, Sperone A, Trelcat A, Mukeba-Harchies L, Wells M, Blankert B, Najem A, Ghanem G, Saussez S, Journe F (2024) ATP1A1 is a promising new target for melanoma treatment and can be inhibited by its physiological ligand bufalin to restore targeted therapy efficacy. *Cancer Cell Int* 24:8.
- Sriskantheadavan-Pirahas S, Deshpande R, Lee B, Grewal SS (2018) Ras/ERK-signalling promotes tRNA synthesis and growth via the RNA polymerase III repressor Maf1 in *Drosophila*. *PLoS Genet* 14:e1007202.

- Stender JD, Kim K, Charn TH, Komm B, Chang KCN, Kraus WL, Benner C, Glass CK, Katzenellenbogen BS (2010) Genome-wide analysis of estrogen receptor alpha DNA binding and tethering mechanisms identifies Runx1 as a novel tethering factor in receptor-mediated transcriptional activation. *Mol Cell Biol* 30:3943–3955.
- Stoner M, Saville B, Wormke M, Dean D, Burghardt R, Safe S (2002) Hypoxia induces proteasome-dependent degradation of estrogen receptor alpha in ZR-75 breast cancer cells. *Mol Endocrinol* 16:2231–2242.
- Strazzullo P, Leclercq C (2014) Sodium. *Adv Nutr* 5:188–190.
- Subramanian A, Tamayo P, Mootha VK, Mukherjee S, Ebert BL, Gillette MA, Paulovich A, Pomeroy SL, Golub TR, Lander ES, Mesirov JP (2005) Gene set enrichment analysis: a knowledge-based approach for interpreting genome-wide expression profiles. *Proc Natl Acad Sci U S A* 102:15545–15550.
- Sudar E, Velebit J, Gluvic Z, Zakula Z, Lazic E, Vuksanovic-Topic L, Putnikovic B, Neskovic A, Isenovic ER (2008) Hypothetical mechanism of sodium pump regulation by estradiol under primary hypertension. *J Theor Biol* 251:584–592.
- Sui Q, Peng J, Han K, Lin J, Zhang R, Ou Q, Qin J, Deng Y, Zhou W, Kong L, Tang J, Xiao B, Li Y, Yu L, Fang Y, Ding P-R, Pan Z (2021) Voltage-gated sodium channel Nav1.5 promotes tumor progression and enhances chemosensitivity to 5-fluorouracil in colorectal cancer. *Cancer Lett* 500:119–131.
- Sun J, Nawaz Z, Slingerland JM (2007) Long-range activation of GREB1 by estrogen receptor via three distal consensus estrogen-responsive elements in breast cancer cells. *Mol Endocrinol* 21:2651–2662.
- Sun S, Ning X, Zhang Y, Lu Y, Nie Y, Han S, Liu L, Du R, Xia L, He L, Fan D (2009) Hypoxia-inducible factor-1alpha induces Twist expression in tubular epithelial cells subjected to hypoxia, leading to epithelial-to-mesenchymal transition. *Kidney Int* 75:1278–1287.
- Sun Z, Xu Y (2020) Nuclear receptor coactivators (NCOAs) and corepressors (NCORs) in the brain. *Endocrinology* 161 Available at: <https://www.ncbi.nlm.nih.gov/pmc/articles/PMC7351129/> [Accessed September 21, 2024].
- Suzuki T, Higgins PJ, Crawford DR (2000) Control selection for RNA quantitation. *Biotechniques* 29:332–337.
- Svastova E, WitarSKI W, Csaderova L, Kosik I, Skvarkova L, Hulikova A, Zatovicova M, Barathova M, Kopacek J, Pastorek J, Pastorekova S (2012) Carbonic anhydrase IX interacts with bicarbonate transporters in lamellipodia and increases cell migration via its catalytic domain. *J Biol Chem* 287:3392–3402.
- Swietach P, Vaughan-Jones RD, Harris AL, Hulikova A (2014) The chemistry, physiology and pathology of pH in cancer. *Philos Trans R Soc Lond B Biol Sci* 369:20130099.

- Swinstead EE, Miranda TB, Paakinaho V, Baek S, Goldstein I, Hawkins M, Karpova TS, Ball D, Mazza D, Lavis LD, Grimm JB, Morisaki T, Grøntved L, Presman DM, Hager GL (2016) Steroid Receptors Reprogram FoxA1 Occupancy through Dynamic Chromatin Transitions. *Cell* 165:593–605.
- Takatani-Nakase T, Matsui C, Hosotani M, Omura M, Takahashi K, Nakase I (2022) Hypoxia enhances motility and EMT through the Na⁺/H⁺ exchanger NHE-1 in MDA-MB-231 breast cancer cells. *Exp Cell Res* 412:113006.
- Tan G, Lenhard B (2016) TFBSTools: an R/bioconductor package for transcription factor binding site analysis. *Bioinformatics* 32:1555–1556.
- Tang D, Gao J, Wang S, Ye N, Chong Y, Huang Y, Wang J, Li B, Yin W, Wang D (2016) Cancer-associated fibroblasts promote angiogenesis in gastric cancer through galectin-1 expression. *Tumour Biol* 37:1889–1899.
- Tao L, Huang G, Song H, Chen Y, Chen L (2017) Cancer associated fibroblasts: An essential role in the tumor microenvironment. *Oncol Lett* 14:2611–2620.
- Taylor JMG, Simpson RU (1992) Inhibition of cancer cell growth by calcium channel antagonists in the athymic mouse. *Cancer Res* 52:2413–2418.
- Tewey KM, Chen GL, Nelson EM, Liu LF (1984) Intercalative antitumor drugs interfere with the breakage-reunion reaction of mammalian DNA topoisomerase II. *J Biol Chem* 259:9182–9187.
- Thiel CT, Horn D, Zabel B, Ekici AB, Salinas K, Gebhart E, Rüschemdorf F, Sticht H, Spranger J, Müller D, Zweier C, Schmitt ME, Reis A, Rauch A (2005) Severely incapacitating mutations in patients with extreme short stature identify RNA-processing endoribonuclease RMRP as an essential cell growth regulator. *Am J Hum Genet* 77:795–806.
- Tian H, McKnight SL, Russell DW (1997) Endothelial PAS domain protein 1 (EPAS1), a transcription factor selectively expressed in endothelial cells. *Genes Dev* 11:72–82.
- Tian J, Li X, Liang M, Liu L, Xie JX, Ye Q, Kometiani P, Tillekeratne M, Jin R, Xie Z (2009) Changes in sodium pump expression dictate the effects of ouabain on cell growth. *J Biol Chem* 284:14921–14929.
- Tian J-M, Ran B, Zhang C-L, Yan D-M, Li X-H (2018) Estrogen and progesterone promote breast cancer cell proliferation by inducing cyclin G1 expression. *Braz J Med Biol Res* 51:1–7.
- Tilli TM, Castro C da S, Tuszynski JA, Carels N (2016) A strategy to identify housekeeping genes suitable for analysis in breast cancer diseases. *BMC Genomics* 17:639.
- Tokhtaeva E, Munson K, Sachs G, Vagin O (2010) N-glycan-dependent quality control of the Na,K-ATPase beta(2) subunit. *Biochemistry* 49:3116–3128.
- Tolaney SM, Toi M, Neven P, Sohn J, Grischke E-M, Llombart-Cussac A, Soliman H, Wang H, Wijayawardana S, Jansen VM, Litchfield LM, Sledge GW (2022) Clinical significance of PIK3CA and ESR1 mutations in circulating tumor DNA: Analysis from the MONARCH 2 study of abemaciclib plus fulvestrant. *Clin Cancer Res* 28:1500–1506.

- Toni LS, Garcia AM, Jeffrey DA, Jiang X, Stauffer BL, Miyamoto SD, Sucharov CC (2018) Optimization of phenol-chloroform RNA extraction. *MethodsX* 5:599–608.
- Tricarico C, Pinzani P, Bianchi S, Paglierani M, Distante V, Pazzagli M, Bustin SA, Orlando C (2002) Quantitative real-time reverse transcription polymerase chain reaction: normalization to rRNA or single housekeeping genes is inappropriate for human tissue biopsies. *Anal Biochem* 309:293–300.
- Tsukamoto T, Chiba Y, Wakamori M, Yamada T, Tsunogae S, Cho Y, Sakakibara R, Imazu T, Tokoro S, Satake Y, Adachi M, Nishikawa T, Yotsu-Yamashita M, Konoki K (2017) Differential binding of tetrodotoxin and its derivatives to voltage-sensitive sodium channel subtypes (Nav 1.1 to Nav 1.7). *Br J Pharmacol* 174:3881–3892.
- Turner KJ, Crew JP, Wykoff CC, Watson PH, Poulsom R, Pastorek J, Ratcliffe PJ, Cranston D, Harris AL (2002) The hypoxia-inducible genes VEGF and CA9 are differentially regulated in superficial vs invasive bladder cancer. *Br J Cancer* 86:1276–1282.
- Turowski TW, Tollervey D (2016) Transcription by RNA polymerase III: insights into mechanism and regulation. *Biochem Soc Trans* 44:1367–1375.
- Tutzauer J, Sjöström M, Holmberg E, Karlsson P, Killander F, Leeb-Lundberg LMF, Malmström P, Niméus E, Fernö M, Jögi A (2022) Breast cancer hypoxia in relation to prognosis and benefit from radiotherapy after breast-conserving surgery in a large, randomised trial with long-term follow-up. *Br J Cancer* 126:1145–1156.
- Tzerpos P, Daniel B, Nagy L (2021) Global Run-on sequencing (GRO-Seq). *Methods Mol Biol* 2351:25–39.
- Ullah MS, Davies AJ, Halestrap AP (2006) The Plasma Membrane Lactate Transporter MCT4, but Not MCT1, Is Up-regulated by Hypoxia through a HIF-1 α -dependent Mechanism *. *J Biol Chem* 281:9030–9037.
- Ullu E, Tschudi C (1984) Alu sequences are processed 7SL RNA genes. *Nature* 312:171–172.
- Urbonavicius J, Qian Q, Durand JM, Hagervall TG, Björk GR (2001) Improvement of reading frame maintenance is a common function for several tRNA modifications. *EMBO J* 20:4863–4873.
- Vakkilainen S, Skoog T, Einarsdottir E, Middleton A, Pekkinen M, Öhman T, Katayama S, Krjutškov K, Kovanen PE, Varjosalo M, Lindqvist A, Kere J, Mäkitie O (2019) The human long non-coding RNA gene RMRP has pleiotropic effects and regulates cell-cycle progression at G2. *Sci Rep* 9:13758.
- Valente V, Teixeira SA, Neder L, Okamoto OK, Oba-Shinjo SM, Marie SKN, Scrideli CA, Paçó-Larson ML, Carlotti CG Jr (2009) Selection of suitable housekeeping genes for expression analysis in glioblastoma using quantitative RT-PCR. *BMC Mol Biol* 10:17.
- Van Bortle K, Marciano DP, Liu Q, Lipchik AM, Gollapudi S, Geller BS, Monte E, Kamakaka RT, Snyder MP (2021) A cancer-associated RNA polymerase III

identity drives robust transcription and expression of SNAR-A noncoding RNA. bioRxiv:2021.04.21.440535 Available at: <https://www.biorxiv.org/content/10.1101/2021.04.21.440535v1> [Accessed September 20, 2021].

- Van Bortle K, Phanstiel DH, Snyder MP (2017) Topological organization and dynamic regulation of human tRNA genes during macrophage differentiation. *Genome Biol* 18:180.
- Vandesompele J, De Preter K, Pattyn F, Poppe B, Van Roy N, De Paepe A, Speleman F (2002) Accurate normalization of real-time quantitative RT-PCR data by geometric averaging of multiple internal control genes. *Genome Biol* 3:RESEARCH0034.
- Vannini A, Cramer P (2012) Conservation between the RNA polymerase I, II, and III transcription initiation machineries. *Mol Cell* 45:439–446.
- Vanoye CG, Kunic JD, Ehring GR, George AL Jr (2013) Mechanism of sodium channel NaV1.9 potentiation by G-protein signaling. *J Gen Physiol* 141:193–202.
- Varlakhanova N, Snyder C, Jose S, Hahm JB, Privalsky ML (2010) Estrogen receptors recruit SMRT and N-CoR corepressors through newly recognized contacts between the corepressor N terminus and the receptor DNA binding domain. *Mol Cell Biol* 30:1434–1445.
- Vasconcelos I, Hussainzada A, Berger S, Fietze E, Linke J, Siedentopf F, Schoenegg W (2016) The St. Gallen surrogate classification for breast cancer subtypes successfully predicts tumor presenting features, nodal involvement, recurrence patterns and disease free survival. *Breast* 29:181–185.
- Vassilev PM, Scheuer T, Catterall WA (1988) Identification of an intracellular peptide segment involved in sodium channel inactivation. *Science* 241:1658–1661.
- Vaupel P, Höckel M, Mayer A (2007) Detection and characterization of tumor hypoxia using pO₂ histography. *Antioxid Redox Signal* 9:1221–1235.
- Vaziri-Gohar A et al. (2022) Limited nutrient availability in the tumor microenvironment renders pancreatic tumors sensitive to allosteric IDH1 inhibitors. *Nat Cancer* 3:852–865.
- Veras I, Rosen EM, Schramm L (2009) Inhibition of RNA polymerase III transcription by BRCA1. *J Mol Biol* 387:523–531.
- Vergote I, Abram P (2006) Fulvestrant, a new treatment option for advanced breast cancer: tolerability versus existing agents. *Ann Oncol* 17:200–204.
- Vermeulen A, McCallum SA, Pardi A (2005) Comparison of the global structure and dynamics of native and unmodified tRNA^{Val}. *Biochemistry* 44:6024–6033.
- Vesuna F, Lisok A, Kimble B, Domek J, Kato Y, van der Groep P, Artemov D, Kowalski J, Carraway H, van Diest P, Raman V (2012) Twist contributes to hormone resistance in breast cancer by downregulating estrogen receptor- α . *Oncogene* 31:3223–3234.

- Viviani B, Gardoni F, Marinovich M (2007) Cytokines and neuronal ion channels in health and disease. *Int Rev Neurobiol* 82:247–263.
- Vorländer MK, Jungblut A, Karius K, Baudin F, Grötsch H, Kosinski J, Müller CW (2020) Structure of the TFIIIC subcomplex τ A provides insights into RNA polymerase III pre-initiation complex formation. *Nat Commun* 11:4905.
- Waddell A, Mahmud I, Ding H, Huo Z, Liao D (2021) Pharmacological inhibition of CBP/p300 blocks estrogen receptor alpha (ER α) function through suppressing enhancer H3K27 acetylation in luminal breast cancer. *Cancers (Basel)* 13:2799.
- Wahl LM, Kleinman HK (1998) Tumor-associated macrophages as targets for cancer therapy. *J Natl Cancer Inst* 90:1583–1584.
- Waldmann R, Champigny G, Bassilana F, Voilley N, Lazdunski M (1995) Molecular cloning and functional expression of a novel amiloride-sensitive Na⁺ channel. *J Biol Chem* 270:27411–27414.
- Walisser JA, Glover E, Pande K, Liss AL, Bradfield CA (2005) Aryl hydrocarbon receptor-dependent liver development and hepatotoxicity are mediated by different cell types. *Proc Natl Acad Sci U S A* 102:17858–17863.
- Walter P, Blobel G (1982) Signal recognition particle contains a 7S RNA essential for protein translocation across the endoplasmic reticulum. *Nature* 299:691–698.
- Walter P, Green S, Greene G, Krust A, Bornert JM, Jeltsch JM, Staub A, Jensen E, Scrace G, Waterfield M (1985) Cloning of the human estrogen receptor cDNA. *Proc Natl Acad Sci U S A* 82:7889–7893.
- Wan H, Gao N, Lu W, Lu C, Chen J, Wang Y, Dong H (2022) NCX1 coupled with TRPC1 to promote gastric cancer via Ca²⁺/AKT/ β -catenin pathway. *Oncogene* 41:4169–4182.
- Wang C, Mayer JA, Mazumdar A, Fertuck K, Kim H, Brown M, Brown PH (2011) Estrogen induces c-myc gene expression via an upstream enhancer activated by the estrogen receptor and the AP-1 transcription factor. *Mol Endocrinol* 25:1527–1538.
- Wang GL, Jiang BH, Rue EA, Semenza GL (1995) Hypoxia-inducible factor 1 is a basic-helix-loop-helix-PAS heterodimer regulated by cellular O₂ tension. *Proc Natl Acad Sci U S A* 92:5510–5514.
- Wang GL, Semenza GL (1993) Characterization of hypoxia-inducible factor 1 and regulation of DNA binding activity by hypoxia. *J Biol Chem* 268:21513–21518.
- Wang H, Zhang C, Xu L, Zang K, Ning Z, Jiang F, Chi H, Zhu X, Meng Z (2016) Bufalin suppresses hepatocellular carcinoma invasion and metastasis by targeting HIF-1 α via the PI3K/AKT/mTOR pathway. *Oncotarget* 7:20193–20208.
- Wang J-G, Strong JA, Xie W, Yang R-H, Coyle DE, Wick DM, Dorsey ED, Zhang J-M (2008) The chemokine CXCL1/growth related oncogene increases sodium

- currents and neuronal excitability in small diameter sensory neurons. *Mol Pain* 4:38.
- Wang Q et al. (2018) Identification of a sodium pump Na⁺/K⁺ ATPase α 1-targeted peptide for PET imaging of breast cancer. *J Control Release* 281:178–188.
- Wang Q-S, Zheng Y-M, Dong L, Ho Y-S, Guo Z, Wang Y-X (2007) Role of mitochondrial reactive oxygen species in hypoxia-dependent increase in intracellular calcium in pulmonary artery myocytes. *Free Radic Biol Med* 42:642–653.
- Wang X et al. (2024) Cell-specific Nav1.6 knockdown reduced astrocyte-derived A β by reverse Na⁺-Ca²⁺ transporter-mediated autophagy in alzheimer-like mice. *J Adv Res* Available at: <http://dx.doi.org/10.1016/j.jare.2024.07.024> [Accessed September 3, 2024].
- Wang X, Gerber A, Chen W-Y, Roeder RG (2020) Functions of paralogous RNA polymerase III subunits POLR3G and POLR3GL in mouse development. *Proc Natl Acad Sci U S A* 117:15702–15711.
- Wang XT, Cheng K, Zhu L (2021) Hypoxia Accelerate β -Actin Expression through Transcriptional Activation of ACTB by Nuclear Respiratory Factor-1. *Mol Biol* 55:398–404.
- Ware AW, Harris JJ, Slatter TL, Cunliffe HE, McDonald FJ (2021) The epithelial sodium channel has a role in breast cancer cell proliferation. *Breast Cancer Res Treat* 187:31–43.
- Wärnmark A, Treuter E, Wright APH, Gustafsson J-A (2003) Activation functions 1 and 2 of nuclear receptors: molecular strategies for transcriptional activation. *Mol Endocrinol* 17:1901–1909.
- Watanabe H, Miki C, Okugawa Y, Toiyama Y, Inoue Y, Kusunoki M (2008) Decreased expression of monocyte chemoattractant protein-1 predicts poor prognosis following curative resection of colorectal cancer. *Dis Colon Rectum* 51:1800–1805.
- Wei J, Han B, Mao X-Y, Wei M-J, Yao F, Jin F (2012) Promoter methylation status and expression of estrogen receptor alpha in familial breast cancer patients. *Tumour Biol* 33:413–420.
- Westley BR, May FE (1987) Oestrogen regulates cathepsin D mRNA levels in oestrogen responsive human breast cancer cells. *Nucleic Acids Res* 15:3773–3786.
- White RJ (2004) RNA polymerase III transcription and cancer. *Oncogene* 23:3208–3216.
- White RJ (2005) RNA polymerases I and III, growth control and cancer. *Nat Rev Mol Cell Biol* 6:69–78.
- White RJ, Trouche D, Martin K, Jackson SP, Kouzarides T (1996) Repression of RNA polymerase III transcription by the retinoblastoma protein. *Nature* 382:88–90.

- Wickerham L (2002) Tamoxifen--an update on current data and where it can now be used. *Breast Cancer Res Treat* 75 Suppl 1:S7-12; discussion S33-5.
- Williams C, Edvardsson K, Lewandowski SA, Ström A, Gustafsson J-A (2008) A genome-wide study of the repressive effects of estrogen receptor beta on estrogen receptor alpha signaling in breast cancer cells. *Oncogene* 27:1019–1032.
- Woiwode A, Johnson SAS, Zhong S, Zhang C, Roeder RG, Teichmann M, Johnson DL (2008) PTEN represses RNA polymerase III-dependent transcription by targeting the TFIIIB complex. *Mol Cell Biol* 28:4204–4214.
- Wolff M, Kosyna FK, Dunst J, Jelkmann W, Depping R (2017) Impact of hypoxia inducible factors on estrogen receptor expression in breast cancer cells. *Arch Biochem Biophys* 613:23–30.
- Wong RC-B, Pollan S, Fong H, Ibrahim A, Smith EL, Ho M, Laslett AL, Donovan PJ (2011) A novel role for an RNA polymerase III subunit POLR3G in regulating pluripotency in human embryonic stem cells. *Stem Cells* 29:1517–1527.
- Woods L, Perez-Garcia V, Hemberger M (2018) Regulation of placental development and its impact on fetal growth—new insights from mouse models. *Front Endocrinol (Lausanne)* 9:416241.
- Wright K, Ly T, Kriet M, Czirok A, Thomas SM (2023) Cancer-associated fibroblasts: Master tumor microenvironment modifiers. *Cancers (Basel)* 15 Available at: <https://www.ncbi.nlm.nih.gov/pmc/articles/PMC10047485/> [Accessed September 18, 2024].
- Wykoff CC, Beasley NJ, Watson PH, Turner KJ, Pastorek J, Sibtain A, Wilson GD, Turley H, Talks KL, Maxwell PH, Pugh CW, Ratcliffe PJ, Harris AL (2000) Hypoxia-inducible expression of tumor-associated carbonic anhydrases. *Cancer Res* 60:7075–7083.
- Xia J, Huang N, Huang H, Sun L, Dong S, Su J, Zhang J, Wang L, Lin L, Shi M, Bin J, Liao Y, Li N, Liao W (2016) Voltage-gated sodium channel Nav 1.7 promotes gastric cancer progression through MACC1-mediated upregulation of NHE1. *Int J Cancer* 139:2553–2569.
- Xiao ZC, Ragsdale DS, Malhotra JD, Mattei LN, Braun PE, Schachner M, Isom LL (1999) Tenascin-R is a functional modulator of sodium channel beta subunits. *J Biol Chem* 274:26511–26517.
- Xie F, Wang J, Zhang B (2023) RefFinder: a web-based tool for comprehensively analyzing and identifying reference genes. *Funct Integr Genomics* 23:125.
- Xie F, Xiao P, Chen D, Xu L, Zhang B (2012) miRDeepFinder: a miRNA analysis tool for deep sequencing of plant small RNAs. *Plant Mol Biol* Available at: <http://dx.doi.org/10.1007/s11103-012-9885-2>.
- Xu J, Wu R-C, O'Malley BW (2009) Normal and cancer-related functions of the p160 steroid receptor co-activator (SRC) family. *Nat Rev Cancer* 9:615–630.
- Xu Y, Zou S-T, Zhu R, Li W, Gu C-W, Wei S-H, Xie J-M, Wu H-R (2013) Inhibition of proliferation of estrogen receptor-positive MCF-7 human breast cancer cells by tamoxifen through c-Jun transcription factors. *Mol Med Rep* 7:1283–1287.

- Yamaci RF, Fraser SP, Battaloglu E, Kaya H, Erguler K, Foster CS, Djamgoz MBA (2017) Neonatal Nav1.5 protein expression in normal adult human tissues and breast cancer. *Pathol Res Pract* 213:900–907.
- Yamamura H, Ugawa S, Ueda T, Shimada S (2008) Expression analysis of the epithelial Na⁺ channel delta subunit in human melanoma G-361 cells. *Biochem Biophys Res Commun* 366:489–492.
- Yamashita N, Hamada H, Tsuruo T, Ogata E (1987) Enhancement of voltage-gated Na⁺ channel current associated with multidrug resistance in human leukemia cells. *Cancer Res* 47:3736–3741.
- Yan F, Teng Y, Li X, Zhong Y, Li C, Yan F, He X (2024) Hypoxia promotes non-small cell lung cancer cell stemness, migration, and invasion via promoting glycolysis by lactylation of SOX9. *Cancer Biol Ther* 25:2304161.
- Yang M-H, Wu M-Z, Chiou S-H, Chen P-M, Chang S-Y, Liu C-J, Teng S-C, Wu K-J (2008a) Direct regulation of TWIST by HIF-1alpha promotes metastasis. *Nat Cell Biol* 10:295–305.
- Yang M-Q, Bai L-L, Wang Z, Lei L, Zheng Y-W, Li Z-H, Huang W-J, Liu C-C, Xu H-T (2021a) DEK is highly expressed in breast cancer and is associated with malignant phenotype and progression. *Oncol Lett* 21:440.
- Yang P, Chan D, Vijeswarapu M, Cartwright C, Cohen L, Meng Z, Liu L, Newman RA (2006) Anti-proliferative activity of Huachansu, a Bufo toad skin extract, against human malignant melanoma cells. *Cancer Res* 66:906–906.
- Yang S, Yang S, Zhang H, Hua H, Kong Q, Wang J, Jiang Y (2021b) Targeting Na⁺/K⁺ -ATPase by berbamine and ouabain synergizes with sorafenib to inhibit hepatocellular carcinoma. *Br J Pharmacol* 178:4389–4407.
- Yang Y, Fan W, Zhu L, Zhao T, Ma L, Wu Y, Ge R, Fan M (2008b) Effects of hypoxia on mRNA expression of housekeeping genes in rat brain tissue and primary cultured neural cells. *Front Med China* 2:239–243.
- Yarov-Yarovoy V, Baker D, Catterall WA (2006) Voltage sensor conformations in the open and closed states in ROSETTA structural models of K(+) channels. *Proc Natl Acad Sci U S A* 103:7292–7297.
- Ye IC, Fertig EJ, DiGiacomo JW, Considine M, Godet I, Gilkes DM (2018) Molecular Portrait of Hypoxia in Breast Cancer: A Prognostic Signature and Novel HIF-Regulated Genes. *Mol Cancer Res* 16:1889–1901.
- Yedjou CG, Sims JN, Miele L, Noubissi F, Lowe L, Fonseca DD, Alo RA, Payton M, Tchounwou PB (2019) Health and racial disparity in breast cancer. *Adv Exp Med Biol* 1152:31–49.
- Yeh JY, Huang WJ, Kan SF, Wang PS (2001) Inhibitory effects of digitalis on the proliferation of androgen dependent and independent prostate cancer cells. *J Urol* 166:1937–1942.
- Yeh W-L, Shioda K, Coser KR, Rivizzigno D, McSweeney KR, Shioda T (2013) Fulvestrant-induced cell death and proteasomal degradation of estrogen receptor α protein in MCF-7 cells require the CSK c-Src tyrosine kinase. *PLoS One* 8:e60889.

- Yong L, Tang S, Yu H, Zhang H, Zhang Y, Wan Y, Cai F (2022) The role of hypoxia-inducible factor-1 alpha in multidrug-resistant breast cancer. *Front Oncol* 12:964934.
- Yoshida T, Eguchi H, Nakachi K, Tanimoto K, Higashi Y, Suemasu K, Iino Y, Morishita Y, Hayashi S (2000) Distinct mechanisms of loss of estrogen receptor alpha gene expression in human breast cancer: methylation of the gene and alteration of trans-acting factors. *Carcinogenesis* 21:2193–2201.
- Yoshimura T, Li C, Wang Y, Matsukawa A (2023) The chemokine monocyte chemoattractant protein-1/CCL2 is a promoter of breast cancer metastasis. *Cell Mol Immunol* 20:714–738.
- Yu F, Zhang Y, Cheng C, Wang W, Zhou Z, Rang W, Yu H, Wei Y, Wu Q, Zhang Y (2020) Poly(A)-seq: A method for direct sequencing and analysis of the transcriptomic poly(A)-tails. *PLoS One* 15:e0234696.
- Yu G (2022) Chapter 5 Overview of enrichment analysis. Available at: <https://yulab-smu.top/biomedical-knowledge-mining-book/enrichment-overview.html#gsea-algorithm> [Accessed August 5, 2024].
- Yu G (04 / 24 / 2022) Chapter 6 GO enrichment analysis. Available at: <https://yulab-smu.top/biomedical-knowledge-mining-book/clusterProfiler-go.html#go-gene-set-enrichment-analysis> [Accessed August 5, 2024].
- Yu G, Wang L-G, Han Y, He Q-Y (2012) clusterProfiler: an R package for comparing biological themes among gene clusters. *OMICS* 16:284–287.
- Yu NY, Iftimi A, Yau C, Tobin NP, van 't Veer L, Hoadley KA, Benz CC, Nordenskjöld B, Fornander T, Stål O, Czene K, Esserman LJ, Lindström LS (2019) Assessment of long-term distant recurrence-free survival associated with tamoxifen therapy in postmenopausal patients with luminal A or luminal B breast cancer. *JAMA Oncol* 5:1304–1309.
- Yu S, Kim T, Yoo KH, Kang K (2017) The T47D cell line is an ideal experimental model to elucidate the progesterone-specific effects of a luminal A subtype of breast cancer. *Biochem Biophys Res Commun* 486:752–758.
- Zagami P, Carey LA (2022) Triple negative breast cancer: Pitfalls and progress. *NPJ Breast Cancer* 8:95.
- Zaric O, Pinker K, Zbyn S, Strasser B, Robinson S, Minarikova L, Gruber S, Farr A, Singer C, Helbich TH, Trattig S, Bogner W (2016) Quantitative sodium MR imaging at 7 T: Initial results and comparison with diffusion-weighted imaging in patients with breast tumors. *Radiology* 280:39–48.
- Zhang L, Huang G, Li X, Zhang Y, Jiang Y, Shen J, Liu J, Wang Q, Zhu J, Feng X, Dong J, Qian C (2013a) Hypoxia induces epithelial-mesenchymal transition via activation of SNAIL1 by hypoxia-inducible factor -1 α in hepatocellular carcinoma. *BMC Cancer* 13:108.
- Zhang Q, Jin J, Zhong Q, Yu X, Levy D, Zhong S (2013b) ER α mediates alcohol-induced deregulation of Pol III genes in breast cancer cells. *Carcinogenesis* 34:28–37.

- Zhang X-W, Qin X, Qin CY, Yin Y-L, Chen Y, Zhu H-L (2013c) Expression of monocyte chemoattractant protein-1 and CC chemokine receptor 2 in non-small cell lung cancer and its significance. *Cancer Immunol Immunother* 62:563–570.
- Zhang Y, Cai H, Liao Y, Zhu Y, Wang F, Hou J (2020) Activation of PGK1 under hypoxic conditions promotes glycolysis and increases stem cell-like properties and the epithelial-mesenchymal transition in oral squamous cell carcinoma cells via the AKT signalling pathway. *Int J Oncol* 57:743–755.
- Zhang Y, Fatima N, Dufau ML (2005) Coordinated changes in DNA methylation and histone modifications regulate silencing/derepression of luteinizing hormone receptor gene transcription. *Mol Cell Biol* 25:7929–7939.
- Zhang Z, Ye Y, Gong J, Ruan H, Liu C-J, Xiang Y, Cai C, Guo A-Y, Ling J, Diao L, Weinstein JN, Han L (2018) Global analysis of tRNA and translation factor expression reveals a dynamic landscape of translational regulation in human cancers. *Commun Biol* 1:234.
- Zhao C, Gao H, Liu Y, Papoutsi Z, Jaffrey S, Gustafsson J-A, Dahlman-Wright K (2010) Genome-wide mapping of estrogen receptor-beta-binding regions reveals extensive cross-talk with transcription factor activator protein-1. *Cancer Res* 70:5174–5183.
- Zheng L, Wu Y, Wang F, Shi H, Xu B, Yang A (2022) 6,7-Dimethoxycoumarin Influences the Erythroid Differentiation of Human Chronic Myelogenous Leukemia K562 Cells through Regulating FOXO3/p27 Signal Pathway. *J Oncol* 2022:1138851.
- Zhong H, De Marzo AM, Laughner E, Lim M, Hilton DA, Zagzag D, Buechler P, Isaacs WB, Semenza GL, Simons JW (1999) Overexpression of Hypoxia-inducible Factor 1 α in Common Human Cancers and Their Metastases. *Cancer Res* 59:5830–5835.
- Zhong Q, Shi G, Zhang Q, Lu L, Levy D, Zhong S (2014) Tamoxifen represses alcohol-induced transcription of RNA polymerase III-dependent genes in breast cancer cells. *Oncotarget* 5:12410–12417.
- Zhou L, Lim Q-E, Wan G, Too H-P (2010) Normalization with genes encoding ribosomal proteins but not GAPDH provides an accurate quantification of gene expressions in neuronal differentiation of PC12 cells. *BMC Genomics* 11:75.
- Zhou W, Dosey TL, Biechele T, Moon RT, Horwitz MS, Ruohola-Baker H (2011) Assessment of hypoxia inducible factor levels in cancer cell lines upon hypoxic induction using a novel reporter construct. *PLoS One* 6:e27460.
- Zhuang L, Xu L, Wang P, Jiang Y, Yong P, Zhang C, Zhang H, Meng Z, Yang P (2015) Na⁺/K⁺-ATPase α 1 subunit, a novel therapeutic target for hepatocellular carcinoma. *Oncotarget* 6:28183–28193.
- Zundel W, Schindler C, Haas-Kogan D, Koong A, Kaper F, Chen E, Gottschalk AR, Ryan HE, Johnson RS, Jefferson AB, Stokoe D, Giaccia AJ (2000) Loss of PTEN facilitates HIF-1-mediated gene expression. *Genes Dev* 14:391–396.

Zwart W, Theodorou V, Kok M, Canisius S, Linn S, Carroll JS (2011) Oestrogen receptor-co-factor-chromatin specificity in the transcriptional regulation of breast cancer. *EMBO J* 30:4764–4776.